DRAFT

Contract No. DTRS57-01-C-10044.

FINAL DRAFT

TECHNICAL SUPPORT DOCUMENT FOR A PROTOCOL TO ASSESS ASBESTOS-RELATED RISK

(Volume 1 of 2: Text)

Prepared for:

Mark Raney
Volpe Center
U.S. Department of Transportation
55 Broadway
Kendall Square
Cambridge MA 02142

and

Chris Weis
Paul Peronard
U.S. Environmental Protection Agency
Region 8
999 18th St., Suite 500
Denver, CO 80202

Prepared by:

D. Wayne Berman
Aeolus, Inc.
751 Taft St.
Albany, CA 94706

and

Kenny Crump
The KS Crump Group, Inc.
602 E. Georgia Ave
Ruston, LA 71270

September 4, 2001

ACKNOWLEDGMENTS

This technical support document was prepared by D. Wayne Berman of Aeolus, Inc., Albany, California and Kenny Crump, The KS Crump Group, Inc., Ruston, Louisiana under contract to the Volpe Center, Department of Transportation (Contract No. DTRS57-01-C-10044). The Technical Manager for this project is Mark Raney. The Contracting Officer is Linda Byrne. We also wish to acknowledge the guidance and support for this project provided by Chris Weis, Paul Peronard, and Peter Grevatt (U.S. EPA).

We wish to gratefully acknowledge the assistance of Nick DeKlerk, FDK Liddell, JC McDonald, and Terri Schnorr for graciously providing the raw epidemiology data from several key studies, without which we could not have completed our analysis.

We also wish to thank John Addison, John Dement, and Agnes Kane for their input and assistance.

Finally, we wish to acknowledge Eric Hack and Tammie Covington for their assistance with calculations and data management.

DISCLAIMER

This report was prepared under contract to the U.S. Department of Transportation for the U.S. Environmental Protection Agency. Such support, however, does not signify that the contents necessarily reflect the views and policies of either the Department of Transportation or the U.S. Environmental Protection Agency, nor does the mention of trade or commercial products constitute endorsement of recommendations for use.

TABLE OF CONTENTS

SECTION		PAGE
1	EXECUTIVE SUMMARY	1-0
2	INTRODUCTION	2-0
3	OVERVIEW	3-0
4	BACKGROUND	4-0
4.1	MINERALOGY OF ASBESTOS	4-3
4.2	MORPHOLOGY OF ASBESTOS DUSTS	4-4
4.3	CAPABILITIES OF ANALYTICAL TECHNIQUES AND METHODS USED TO MEASURE ASBESTOS	4-5
4.4	LUNG PHYSIOLOGY AND FUNCTION	4-13
5	THE ASBESTOS LITERATURE	5-0
5.1	EPIDEMIOLOGY STUDIES	5-2
5.2	HUMAN PATHOLOGY STUDIES	5-6
5.3	ANIMAL STUDIES	5-9
5.4	IN VITRO STUDIES	5-10
6	HUMAN HEALTH EFFECTS ASSOCIATED WITH OCCUPATIONAL EXPOSURE TO ASBESTOS	6-1
6.1	APPROACH FOR EVALUATING THE EPIDEMIOLOGY LITERATURE	6-2
6.2	LUNG CANCER	6-4
6.2.1	The Adequacy of the Current EPA Model for Lung Cancer	6-5
6.2.1.1	Time dependence	6-9
6.2.1.2	Comparison with biologically based model	6-19
6.2.2	Estimating K_L's from Published Epidemiology Studies	6-30
6.2.3	The Variation in K_L's Derived for Chrysotile Miners and Chrysotile Textile Workers	6-36

6.2.4 Evaluating Effects Associated with the Character of Exposure 6-45

6.2.4.1 Adjusting K_L's for size 6-46

6.2.4.2 Evaluating the implications of adjusting K_L's for size 6-53

6.3 Mesothelioma 6-65

6.3.1 The Adequacy of the Current EPA Model for Mesothelioma 6-66

6.3.1.1 Time dependence 6-70

6.3.1.2 Comparison with biologically based model 6-73

6.3.2 Estimating K_M's from Published Epidemiology Studies 6-79

6.3.3 Evaluating Effects Associated with the Character of Exposure 6-82

6.3.3.1 Adjusting K_M's for size 6-83

6.3.3.2 Evaluating the implications of adjusting K_M's for size 6-83

6.4 GENERAL CONCLUSIONS FROM HUMAN EPIDEMIOLOGY STUDIES 6-86

7 SUPPORTING EXPERIMENTAL STUDIES THAT CHARACTERIZE THE BIOLOGICAL ACTIVITY OF ASBESTOS 7-1

7.1 FACTORS AFFECTING RESPIRABILITY AND DEPOSITION 7-3

7.1.1 Respirability of Spherical Particles 7-4

7.1.2 Respirability of Fibrous Structures 7-7

7.1.3 Effects of Electrostatic Charage on Particle Respirability 7-12

7.1.4 General Conclusions Concerning Particle Respirability 7-13

7.2 FACTORS AFFECTING DEGRADATION, CLEARANCE AND TRANSLOCATION 7-14

7.2.1 Animal Retention Studies 7-18

7.2.1.1 Studies involving short-term exposure 7-19

7.2.1.2 Studies involving long-term exposure 7-32

7.2.2 Animal Histopathological Studies 7-41

7.2.3 Human Pathology Studies 7-47

7.2.4 Studies of Dissolution/Biodurability 7-53

7.2.5 Dynamic Models 7-58

7.2.6 General Conclusions Concerning Degradation, Clearance, and Translocation 7-62

7.3 FACTORS GOVERNING CELLULAR AND TISSUE RESPONSES 7-69

7.3.1 The Current Cancer Model 7-73

7.3.2 Evidence for Transformation 7-76

7.3.3 Evidence that Asbestos Acts as a Cancer Initiator 7-77

7.3.3.1 Interference with mitosis 7-78

7.3.3.2 Generation of reactive oxygen species 7-82

7.3.3.3 Generation of reactive nitrogen species 7-92

7.3.3.4 Conclusions concerning asbestos as a cancer initiator 7-96

7.3.4 Evidence that Asbestos Acts as a Cancer Promoter 7-97

7.3.4.1 Asbestos induced proliferation 7-98

7.3.4.2 Asbestos induced cell signaling 7-105

7.3.4.3 Asbestos induced apoptosis 7-119

7.3.4.4 Asbestos induced cytotoxicity 7-121

7.3.4.5 Association between fibrosis and carcinogenicity 7-125

7.3.4.6 Synergism between asbestos and smoking 7-126

7.3.4.7 Conclusions concerning asbestos as a cancer promoter 7-127

7.3.5 Evidence that Asbestos Induces an Inflammatory Response 7-128

7.3.6 Evidence that Asbestos Induces Fibrosis 7-128

7.3.7 Evidence that Asbestos Mediates Epithelial Permeability 7-128

7.3.8 Conclusions Regarding the Mechanisms of Asbestos-Associated Diseases 7-129

7.4 ANIMAL DOSE RESPONSE 7-131

7.4.1 Injection and Implantation Studies 7-131

7.4.2 Inhalation Studies 7-137

7.4.3 Supplemental Inhalation Study 7-140

7.4.4 Conclusions from Animal Dose-Response Studies 7-150

7.5 CONCLUSIONS FROM AN EVALUATION OF SUPPORTING STUDIES 7-151

8 DISCUSSION, CONCLUSIONS, AND RECOMMENDATIONS 8-1

8.1 DISCUSSION AND CONCLUSIONS 8-1

8.1.1 Addressing Issues 8-1

8.1.2 Comparison with Other, Recent Risk Reviews 8-5

8.2 RECOMMENDATIONS FOR ASSESSING ASBESTOS-RELATED RISKS 8-7

8.3 RECOMMENDATIONS FOR FURTHER STUDY 8-15

9 REFERENCES 9-1

APPENDIX A: UPDATE OF POTENCY FACTORS FOR LUNG CANCER (KL) AND MESOTHELIOMA (KM) A-1

APPENDIX B: BACKGROUND FOR DEVELOPMENT OF AN IMPROVED EXPOSURE INDEX FOR ASBESTOS B-1

APPENDIX C: COMPENDIUM OF MODEL FITS TO ANIMAL INHALATION DATA IN SUPPORT OF THE BERMAN ET AL. (1995) STUDY AND POST-STUDY WORK C-1

APPENDIX D: DERIVATION OF LIFETIME RISKS FOR LUNG CANCER AND MESOTHELIOMA FROM MODELS USING K_L AND K_M ESTIMATES FOR POTENCY D-1

LIST OF TABLES

Table No.	Title	Page
Table 4-1:	Capabilities and Limitations of Analytical Techniques Used for Asbestos Measurements	4-7
Table 4-2:	Comparison of Applicable Methods for Measuring Asbestos in Air	4-8
Table 6-1:	Fit of EPA Lung Cancer Model to Observed Mortality Among Wittenoom Miners Categorized by Cumulative Exposure	6-7
Table 6-2:	Fit of EPA Lung Cancer Model to Observed Mortality Among South Carolina Textile Workers Categorized by Cumulative Exposure	6-8
Table 6-3:	Fit of EPA Lung Cancer Model to Observed Mortality Among Wittenoom Miners Categorized by Time Since Last Exposure	6-11
Table 6-4:	Fit of EPA Lung Cancer Model to Observed Mortality Among Wittenoom Miners Categorized by Time Since Last Exposure with Cumulative Exposure Replaced by Internal Dose	6-12
Table 6-5:	Fit of EPA Lung Cancer Model to Observed Mortality Among South Carolina Textile Workers Categorized by Time Since Last Exposure	6-15
Table 6-6:	Fit of EPA Lung Cancer Model to Observed Mortality Among South Carolina Textile Workers Categorized by Time Since Last Exposure with Cumulative Exposure Replaced by Internal Dose	6-18
Table 6-7:	Results of Three Applications of the Two-Stage Model to the Lung Cancer Data from Wittenoom (Assumed Half-life: 20 yrs)	6-22
Table 6-8:	Results of Three Applications of the Two-Stage Model to the Lung Cancer Data from South Carolina (Assumed Half-life 0.5 yrs)	6-23

Table 6-9:	Fit of the Best-fitting Two-Stage Model to the Wittenoom Lung Cancer Data Categorized by Time Since Last Exposure (Assumed Half-life: 20 yrs)	6-25
Table 6-10:	Fit of the Best-fitting Two-Stage Model to the South Carolina Lung Cancer Data Categorized by Time Since Last Exposure (Assumed Half-life 0.5 yrs)	6-26
Table 6-11:	Fit of the Best-fitting Two-Stage Model to the Wittenoom Lung Cancer Data Categorized by Time Since Last Exposure (Assumed Half-life: 0.5 yrs)	6-28
Table 6-12:	Lung Cancer Dose-Response Coefficients (K_L's) and Mesothelioma Dose-Response Coefficients (K_M's) Derived from Published Epidemiology Studies	6-31
Table 6-13	Estimated Concentrations of Sized Fibers Observed in the Lungs of Thetford Miners and South Carolina Textile Workers	6-42
Table 6-14:	Correlation Between Published Quantitative Epidemiology Studies and Available TEM Fiber Size Distributions	6-48
Table 6-15:	Representative K_L and K_M Values Paired with Averaged TEM Fiber Size Distributions From Published Studies	6-51
Table 6-16:	Comparison of Original and Adjusted K_L and K_M Values	6-52
Table 6-17:	Estimated Uncertainty Assigned to Adjustment for Fiber Size	6-55
Table 6-18:	Comparison of Spread in Range of Original and Adjusted K_L and K_M Values for Specific Fiber Types	6-56
Table 6-19:	Results of an Analysis of the Combined Effects of Fiber Size and Type on the Original and Adjusted K_L values	6-59
Table 6-20:	Estimated Fraction of Amphiboles in Asbestos Dust	6-60
Table 6-21:	Comparison of Original and Size Adjusted Potency Factors with Simultaneous Consideration of Fiber Type and Uncertainty	6-64

Table 6-22:	Fit of EPA Mesothelioma Model to Observed Mortality Among Wittenoom Miners Categorized by Cumulative Exposure (Based on Averaged Exposure Level and Duration for each Category)	6-67
Table 6-23:	Fit of EPA Mesothelioma Model to Observed Mortality Among Wittenoom Miners Categorized by Cumulative Exposure (Based on Averaged Value of Integral for Each Category)	6-68
Table 6-24:	Fit of EPA Mesothelioma Model to Observed Mortality Among Wittenoom Miners Categorized by Time Since Last Exposure	6-71
Table 6-25:	Fit of EPA Mesothelioma Model to Observed Mortality Among Quebec Miners in Each of Three Mining Areas and Categorized by Time Since Last Exposure	6-72
Table 6-26:	Fit of EPA Mesothelioma Model to Observed Mortality Among South Carolina Textile Workers by Time Since Last Exposure	6-76
Table 6-27:	Results of Several Applications of the Two-Stage Model to the Mesothelioma Data from Wiittenoom	6-78
Table 6-28:	Fit of the Best-fitting Two-Stage Model to the Wittenoom Lung Cancer Data Categorized by Time Since Last Exposure (Assumed Infinite Half-life)	6-90
Table 6-29:	Optimized Risk Coefficients	6-90
Table 6-30:	Conservative Risk Coefficients	
Table 7-1:	Estimation of Lung Volume and Lung Surface Area Loading Rates for Rats and Humans	7-12
Table 7-2:	Clearance, Translocation, and Degradation Mechanisms Operating in the Lung and Their Relative Rates	7-15
Table 7-3:	Fraction of Fibers Retained Following Chronic Exposure	7-34
Table 7-4:	Measured In-Vitro Dissolution for Various Fiber Types	7-56
Table 7-5:	Putative Mechanisms by Which Asbestos May Interact With Lung Tissue Following Inhalation to Induce Disease	7-71

Table 7-6:	List of Chemical Species that Potentially Contribute to Asbestos-Related Disease, Their Sources and Effects	7-107
Table 7-7:	Summary Data for Animal Inhalation Experiments Conducted by Davis and Coworkers	7-142
Table 8-1	Additional Risks per One Hundred Thousand Persons From Lifetime, Continuous Exposure to 0.0005 TEM f/cc Longer than 5.0 μm and Thinner than 0.5 μm	8-10
	TABLES FROM APPENDIX A GO HERE	
Table B-1:	Estimated Tumor Incidence and PCME Dose (with Their Respective Confidence Bounds) for IP Injection Studies of Six Tremolite Samples of Varying Asbestiform Character	B-4
Table B-2:	Estimated Tumor Incidence and Dose Defined as Interim Index Structures (with Their Respective Confidence Bounds) for IP Injection Studies of Six Tremolite Samples of Varying Asbestiform Character	B-8

LIST OF FIGURES

Figure No.	Title	Page
Figure 4-1:	The Structure of Lung Parenchyma Showing Alveoli and Alveolar Ducts	4-15
Figure 4-2:	The Structure of Inter-Alveolar Septa	4-16
Figure 4-3:	The Detailed Structure of an Alveolar Wall that is Part of an Inter-Alveolar Septum	4-17
Figure 6-1:	Plot of $[(RR - \alpha)/(CE_{10})]$ vs. Time Since Last Exposure for Wittenoom Miners	6-13
Figure 6-2:	Plot of $[(RR - \alpha)/(CE_{10})]$ vs. Time Since Last Exposure for South Carolina Textile Workers	6-16
Figure 6-3:	Plot of Estimated K_L Values and Associated Confidence Intervals by Study Environment	6-33
Figure 6-4:	Plot of Adjusted K_L Values (K_L.'s) and Associated Confidence Intervals by Study Environment	6-54
Figure 6-5:	Plot of Estimated K_M Values and Associated Confidence Intervals by Study Environment	6-81
Figure 6-6:	Plot of Adjusted K_M Values (K_M.'s) and Associated Confidence Intervals by Study Environment	6-84
Figure 7-1:	Fractions of Respirable Particles Deposited in the Various Compartments of the Human Respiratory Tract as a Function of Aerodynamic Equivalent Diameter	7-6
Figure 7-2:	Fractions of Respirable Particles Deposited in the Various Compartments of the Human Respiratory Tract as a Function of the True Diameter of Asbestos Fibers	7-8
Figure 7-3:	Plot of Chrysotile Lung Burden/Aerosol Concentration vs. Time of Exposure	7-36
Figure 7-4:	Schematic Representation of Fate of Asbestos Fibers in the Lung and Surrounding Tissue	7-63

Figure 7-5: Fit of Model: Tumor Incidence vs. Structure Concentration by TEM. (Length Categories: 5 - 40 µm, > 40 µm, Width Categories: < 0.3 µm and ≥ 5 µm) 7-147

Figure 7-6: Fit of Model: Tumor Incidence vs. Structure Concentration by TEM. (Length Categories: 5 - 40 µm, > 40 µm, Width: < 0.4 µm) 7-149

FIGURES FROM APPENDIX A GO HERE

Figure B-1: Fit of Tumor Incidence vs. PCME Structures for Six Tremolite Samples of Varying Asbestiform Character B-6

Figure B-2: Fit of Tumor Incidence vs. Interim Index Structures for Six Tremolite Samples of Varying Asbestiform Character B-9

1.0 EXECUTIVE SUMMARY

The purpose of this report is to provide a firm basis for completing a state-of-the-art-protocol to assess potential human-health risks associated with exposure to asbestos. Such a protocol is intended specifically for use in performing risk assessments at Superfund sites, although it may be applicable to a broad range of situations.

The approach currently employed at the U.S. Environmental Protection Agency (U.S. EPA) to evaluate asbestos-related risks (IRIS 1988) is based primarily on a document completed in 1986 (U.S. EPA 1986) and has not been changed substantially in the past 15 years, despite substantial improvements in asbestos measurement techniques and in the understanding of the manner in which asbestos exposure contributes to disease. Therefore, this document provides an overview and evaluation of the more recent studies and presents proposed modifications to the protocol for assessing asbestos-related risks that can be justified based on the more recent work.

The studies relevant to developing a protocol are reviewed in this document and combined with supporting analysis to resolve issues and identify the best candidate procedures for assessing asbestos-related risks. Although the objective of this evaluation was to identify the single best procedures, when current knowledge is inadequate for distinguishing among alternatives, options are presented along with a discussion of their relative advantages and limitations. In a few cases, limited and focused additional research studies are recommended, which may enhance the current state of knowledge sufficiently to resolve one or more of the important, remaining issues.

Inhalation of asbestos dusts has been linked to several adverse health effects including primarily asbestosis, lung cancer, and mesothelioma (U.S. EPA 1986). Asbestosis, a chronic, degenerative lung disease, has been documented among asbestos workers from a wide variety of industries. Although asbestosis cases have been observed at some locations of current interest to the U.S. EPA, the disease is generally expected to be associated only with the higher levels of exposure commonly found in workplace settings and is not expected to contribute substantially to potential risks associated with environmental asbestos exposure. Therefore, asbestosis is only considered in this document to the extent required to address it's putative association with lung cancer. Overall, the majority of evidence indicates that lung cancer and mesothelioma are the most important sources of risk associated with exposure to low levels of asbestos.

A variety of human, animal, and tissue studies have provided insight into the nature of the relationship between asbestos exposure and disease. Ideally, human epidemiology

studies are employed to determine the quantitative dose/response relationships and the attendant risk coefficients for asbestos exposure. Risk coefficients have been estimated for asbestos from approximately 20 epidemiology studies for which adequate dose-response data exist. Such factors vary widely, however, and the observed variation has not been reconciled. Among the objectives addressed in this study is to evaluate and account for the sources of uncertainty that contribute to the variation among the risk coefficients derived from the literature so that these estimates can be reasonably interpreted and recommendations for their use in risk assessment developed.

Animal and tissue studies indicate that asbestos potency is a complex function of several characteristics of asbestos dusts including fiber size and fiber type (i.e., fiber mineralogy). Moreover, the influence of fiber size is a complex function of both diameter and length as critical parameters (among others). Therefore, whenever the goal is to compare across samples with differing characteristics, it is not sufficient to report asbestos concentrations simply as a function of mass (or any other single parameter) and this stands in stark contrast to the treatment of chemical toxins. It has generally been difficult to distinguish among the effects of fiber size and type in many studies because such effects are confounded and the materials studied have not been adequately characterized. However, several adequate studies do exist and these have been highlighted.

The influence of such effects cannot be adequately evaluated in the existing epidemiological studies because the analytical techniques used to monitor asbestos exposure in these studies are not capable of resolving all of the characteristics of asbestos dusts that other studies indicate are important. Moreover, the exposure indices (the range of structure sizes and shapes included in an analysis) that are employed in the existing epidemiology studies may not correspond precisely with the characteristics of asbestos that best relate to biological activity. This hinders the ability to compare the risk (dose-response) coefficients derived from the different studies. It also limits the confidence with which risk coefficients derived from the existing epidemiology studies can be applied to assess risks from asbestos exposure in other environments. Such limitations are explored in this study, along with potential remedies. At the same time, the existing epidemiology studies provide the most appropriate data from which to determine the relationship between asbestos dose and response in humans.

Briefly, the major kinds of limitations that potentially contribute to uncertainty in the available epidemiology studies (and the effect such limitations likely produce on trends in potency estimates) include:

- limitations in the manner that exposure concentrations were estimated (likely increases random variation across studies);

- limitations in the manner that the character of exposure (i.e. the mineralogical types of fibers and the range and distribution of fiber dimensions) was delineated (likely increases systematic variation between industry types and, potentially, between fiber types);

- limitations in the accuracy of mortality determinations or incompleteness in the extent of tracing of cohort members (likely increases random variation across studies);

- limitations in the adequacy of the match between cohort subjects and the selected control population (likely increases random variation across studies and may have a substantial effect on particular studies); and

- inadequate characterization of confounding factors, such as smoking histories for individual workers (likely increases random variation across studies and may have a substantial effect on particular studies).

Importantly, this new analysis of the epidemiology database differs from the evaluation conducted in the 1986 Health Effects Assessment Update (U.S. EPA 1986). Not only does it incorporate studies containing the latest available followup for the exposure settings previously evaluated and several additional studies addressing new exposure settings, but the manner in which the analysis was conducted incorporates important, new features including estimation of more realistic confidence bounds for the dose-response factors derived from each study.

Confidence bounds were adjusted to account for uncertainty contributed by the manner that exposure was estimated, by the manner that work histories were assigned, and by limitations in the degree of followup, in addition to the traditional practice of accounting for the statistical uncertainty associated with the observed incidence of disease mortality. Thus, most of the major contributors to the overall uncertainty of each study are now addressed, at least in qualitative fashion. By better accounting for overall uncertainty, we were better able to distinguish what can and cannot be reasonably concluded from the existing studies.

Separately, we also completed an evaluation to consider questions concerning the appropriateness of the range of fiber sizes characterized in the published epidemiology studies and whether adjusted exposure indices might improve the quality of asbestos

risk assessments. This was motivated by conclusions from our review of the supplemental literature, which indicate that the methods used to assess exposure in the existing epidemiology studies do not adequately reflect the characteristics of asbestos that determine biological activity.

Results from our evaluation of the available epidemiology studies indicate that:

(1) the results of individual epidemiology studies are uncertain, especially when one considers all of the major potential sources of uncertainty (rather than simply considering the statistical uncertainty associated with the number of deaths, as is traditionally done). However, more robust conclusions can be drawn from an analysis of the set of epidemiology studies taken as a whole than results derived from individual studies;

(2) by adjusting for fiber size and fiber type, the existing database of studies can be reconciled adequately to reasonably support risk assessment;

(3) the procedures recommended as a result of our analysis offer substantial improvement over EPA's current approach to evaluating asbestos-related risks;

(4) while there is some indication that the existing EPA models for lung cancer and, potentially, mesothelioma may not entirely reflect the time-dependence of disease at long times following cessation of exposure, such effects appear to be modest so that they are unlikely to adversely affect the proposed approach. Prudence dictates, however, that limited additional study may be warranted to adequately dismiss related concerns; and

(5) results from our review of the supplemental literature provide additional support for the approach recommended in this document and indicate additional, specific modifications that (if supported by limited additional study) could result in substantial improvement even over the approach currently recommended, which (in turn) provides substantial improvement over the current approach.

Based on our analysis, we recommend the following.

(1) Asbestos concentrations should be analyzed for structures that correspond to a new (interim) exposure index that is defined in this document. As previously indicated, an exposure index is a description of the sizes and shapes of fibers (and the relative weights to be assigned to each category of size and shape) that need to be counted in an analysis to determine asbestos concentrations.

(2) Because amphiboles, fiber-for-fiber, were found to be substantially more potent than chrysotile, the individual contributions from chrysotile and the combined amphiboles to any particular exposure need to be separately delineated and, because amphibole exposures are the primary drivers, the analytical sensitivity required for each particular study should be set based on amphiboles.

A set of new dose-response coefficients for chrysotile and the amphiboles are also recommended in this document, which indicate the relative potency of each toward the induction of lung cancer and mesothelioma, respectively.

Three options are presented in this document for incorporating the new exposure index, the new dose-response coefficients, and the other recommendations in this document into a general protocol for assessing asbestos-related risks:

- the first option involves performing lifetable analyses using the dose-response models that EPA currently recommends for lung cancer and mesothelioma. When sufficient data are available from a particular project to support this type of analysis, it should provide the best site-specific estimates of asbestos-related risks;

- the second option involves use of a risk table, which can be adapted to estimate risk for most cases of interest, even ones for which exposure estimates are crude and descriptions of the circumstances of exposure are sparse; and

- the third option involves development of a new unit risk factor for asbestos (based on the latest data presented in this document), which would replace the unit risk factor in current use.

A couple of focused, additional studies are also recommended in this document, due to a small number of important knowledge gaps that remain to be resolved, that can be resolved cost-effectively, and that, if resolved, can substantially increase both the overall confidence in the proposed approach and, potentially, improve the approach as well. Importantly, even without conducting the new studies, the approach currently recommended was shown in this document to provide substantial improvement in the ability to assess asbestos-related risks (in terms of reducing error) over the approach in current use. The objectives of the proposed studies are:

(1) to expand the test of the ability of the current EPA models to adequately track the time-dependence of disease; and

(2) to develop the supporting data needed to define adjustments for potency factors that will allow them to be used with an exposure index that even more closely captures the criteria that determine biological activity than the "interim" index recommended in this document.

2.0 INTRODUCTION

The purpose of this report is to provide a firm basis for completing a state-of-the-art-protocol to assess potential human-health risks associated with exposure to asbestos. Such a protocol is intended specifically for use in performing risk assessments at Superfund sites, although it may be applicable to a broad range of situations.

The approach currently employed at the U.S. Environmental Protection Agency (U.S. EPA) to evaluate asbestos-related risks (IRIS 1988) is based primarily on a document completed in 1986 (U.S. EPA 1986) and has not been changed substantially in the past 15 years, despite substantial improvements in asbestos measurement techniques and in the understanding of the manner in which asbestos exposure contributes to disease. Therefore, this document provides an overview and evaluation of the more recent studies and presents proposed modifications to the protocol for assessing asbestos-related risks that can be justified based on the more recent work.

In May, 2001, the U.S. EPA along with the California Environmental Protection Agency (Cal EPA), the National Institute for Occupational Safety and Health (NIOSH), the American Toxic Substances Disease Registry (ATSDR), and the Mine Safety and Health Administration (MSHA) hosted an international conference on asbestos in Oakland. The current state of knowledge (including, particularly, the status of knowledge gaps) was reviewed during this conference by many of the leading researchers. Consequently, several issues were raised concerning the state of knowledge of asbestos. To the extent that such issues are relevant to the assessment of asbestos-related risks, they are considered in this document.

Among the asbestos-related issues that have been the focus of recent attention:

- whether the dose-response models currently in use by the EPA for describing the incidence of asbestos-related diseases adequately reflect the time-dependence for the development of these diseases;

- whether the relative in-vivo durability of different asbestos mineral types affect their relative potency;

- whether the set of minerals included in the current definition of asbestos adequately covers the range of minerals that potentially contribute to asbestos-related diseases;

- whether the analytical techniques and methods currently used for determining asbestos concentrations adequately capture the biologically relevant characteristics of asbestos (particularly with regard to the sizes of the structures included in the various analyses) so that they can be used to support risk assessment; and

- whether reasonable confidence can be placed in the cross-study extrapolation of dose-response relationships that are required to assess asbestos-related risks in new environments of interest.

These and other asbestos-related issues are described in greater detail in Chapter 3 (Overview) and Chapter 4 (Background).

The studies relevant to developing a protocol are reviewed in this document and combined with supporting analysis to resolve issues and identify the best candidate procedures for assessing asbestos-related risks. Although the objective of this evaluation was to identify the single best procedures, when current knowledge is inadequate for distinguishing among alternatives, options are presented along with a discussion of their relative advantages and limitations. In a few cases, limited and focused additional research studies are recommended, which may enhance the current state of knowledge sufficiently to resolve one or more of the important, remaining issues.

This document is an update to a previous review (Berman and Crump 1999) and primarily incorporates information developed subsequent to the earlier review. It is also the last in a series of documents developed as part of a multi-task project to develop a set of mutually consistent methods for determining asbestos concentrations in a manner useful for assessing risk and a companion protocol for conducting such risk assessments. A method for the determination of asbestos in air (Chatfield and Berman 1990) and a companion technical background document (Berman and Chatfield 1990) were published by the U.S. EPA in 1990. The air method has since been superceded (improved) by the ISO Method (ISO 10312). A method for the determination of asbestos in soils and bulk materials (Berman and Kolk 1997) was also published by the U.S. EPA and the draft of an improved version was also recently completed (Berman and Kolk 2000). The recommendations in this document should serve as the basis for development of the companion risk-assessment protocol.

3.0 OVERVIEW

Inhalation of asbestos dusts has been linked to several adverse health effects including primarily asbestosis, lung cancer, and mesothelioma (U.S. EPA 1986). Asbestosis, a chronic, degenerative lung disease, has been documented among asbestos workers from a wide variety of industries. Although asbestosis cases have been observed at some locations of current interest to the U.S. EPA, the disease is generally expected to be associated only with the higher levels of exposure commonly found in workplace settings and is not expected to contribute substantially to potential risks associated with environmental asbestos exposure. Therefore, asbestosis is only considered in this document to the extent required to address it's putative association with lung cancer. Overall, the majority of evidence indicates that lung cancer and mesothelioma are the most important sources of risk associated with exposure to low levels of asbestos.

> Note that the primary route of exposure of concern in association with asbestos is inhalation. There is little evidence that ingestion of asbestos induces disease (see, for example, U.S. EPA 1986, IRIS 1988). Therefore, this study is focused on inhalation hazards and other routes of exposure are not addressed.

Gastrointestinal cancers and cancers of other organs (e.g. larynx, kidney, and ovaries) have also been linked with asbestos exposures (by inhalation) in some studies. However, such associations are not as compelling as those for the primary health effects listed above and the potential risks from asbestos exposures associated with these other cancers are much lower (U.S. EPA 1986). Consequently, this document is focused on risks associated with the induction of lung cancer and mesothelioma.

A variety of human, animal, and tissue studies have provided insight into the nature of the relationship between asbestos exposure and disease. Ideally, human epidemiology studies are employed to determine the quantitative dose/response relationships and the attendant risk coefficients for asbestos exposure. Risk coefficients have been estimated for asbestos from approximately 20 epidemiology studies for which adequate dose-response data exist. Such factors vary widely, however, and the observed variation has not been reconciled. Among the objectives addressed in this study is to evaluate and account for the sources of uncertainty that contribute to the variation among the risk coefficients derived from the literature so that these estimates can be reasonably interpreted and recommendations for their use in risk assessment developed.

Animal and tissue studies indicate that asbestos potency is a complex function of several characteristics of asbestos dusts including fiber size and fiber type (i.e., fiber

mineralogy). Moreover, the influence of fiber size is a complex function of both diameter and length as critical parameters (among others). Therefore, whenever the goal is to compare across samples with differing characteristics, it is not sufficient to report asbestos concentrations simply as a function of mass (or any other single parameter) and this stands in stark contrast to the treatment of chemical toxins. It has generally been difficult to distinguish among the effects of fiber size and type in many studies because such effects are confounded and the materials studied have not been adequately characterized. However, several adequate studies do exist and these have been highlighted.

The influence of such effects cannot be adequately evaluated in the existing epidemiological studies because the analytical techniques used to monitor asbestos exposure in these studies are not capable of resolving all of the characteristics of asbestos dusts that other studies indicate are important. Moreover, the exposure indices (the range of structure sizes and shapes included in an analysis) that are employed in the existing epidemiology studies may not correspond precisely with the characteristics of asbestos that best relate to biological activity. This hinders the ability to compare the risk (dose-response) coefficients derived from the different studies. It also limits the confidence with which risk coefficients derived from the existing epidemiology studies can be applied to assess risks from asbestos exposure in other environments. Such limitations are explored in this study, along with potential remedies.

Based on the approach developed for evaluating asbestos-related cancer risk by the U.S. EPA (1986), risk is estimated as the product of a risk coefficient and a mathematical function that depends on the level of exposure, the duration of exposure, and time. The risk coefficient for lung cancer is generally denoted, "K_L" and the one for mesothelioma is "K_M."

A detailed description of both the lung cancer and mesothelioma models is provided in Chapter 6. The models differ depending on whether lung cancer or mesothelioma is being considered.

For lung cancer, the model estimates *relative* risk, which means that the increase in lung cancer incidence that is attributable to asbestos exposure is proportional to the background lung cancer incidence in the exposed population. The background cancer incidence is the rate of lung cancer that would be expected to occur in the population in the absence of asbestos exposure. In other words, background lung cancer incidence is the lung cancer rate for the exposed population that is attributable to all causes other than asbestos.

The model for mesothelioma is an *absolute* risk model. This means that the increase in mesothelioma attributable to asbestos is independent of the background rate of mesothelioma, which is negligible in the general population.

Ideally, the risk coefficients derived from the existing epidemiology studies could be combined with measurements from other exposure settings (using the corresponding models) to estimate lung cancer and mesothelioma risks in these other exposure settings. However, such risk estimates are only valid if both of the following conditions are met:

(1) asbestos is measured in the exposure setting of interest in the identical manner in which it was measured in the study from which the corresponding risk coefficients are derived; and

(2) such measurements reflect the characteristics of asbestos exposures that determine risk.

A growing body of evidence indicates that the way in which asbestos concentrations were measured in the existing epidemiology studies do not reflect the characteristics of asbestos exposure that determine risk. Therefore, measuring asbestos concentrations in the same way in exposure settings of interest may not be sufficient to assure validity of risk estimates derived using the published risk coefficients (and the corresponding models). This is because the second of the above-listed conditions would not be satisfied.

Considerations necessary to compare risk coefficients derived in different exposure settings (or to apply a coefficient to predict risk in a setting different from the one in which the coefficient was derived) have been elucidated clearly in a mathematical model (Chesson et al 1989). The consequences of the model indicate that adjusting the existing risk coefficients so that they reflect asbestos characteristics that determine biological activity requires knowledge of the fiber size distributions of the dusts studied in the *original* epidemiology studies. To the extent they exist, such data may be used to normalize each of the published risk coefficients so that they relate to a common exposure index reflecting asbestos characteristics that determine biological activity.

Among the goals of this evaluation is to assess the relative importance of such limitations and to attempt to construct "fixes" as appropriate (within the confines of the current state of knowledge). Consequently, we explored the possibility of defining an improved exposure index (that better reflects biological activity) and of applying such an

improved index to the epidemiology data. We also evaluated improved ways of simultaneously accounting for the effects of both fiber size and type.

Unfortunately, some of the issues that need to be resolved to support development of a protocol for assessing asbestos-related risks cannot be entirely resolved with existing data. We have attempted to identify such issues, to assess their relative importance, and, when deemed appropriate, to propose limited and focused research projects designed to provide the data required to reduce the impacts of such knowledge gaps.

4.0 BACKGROUND

Asbestos is a term used to describe the fibrous habit of a family of hydrated metal silicate minerals. The most widely accepted definition of asbestos includes the fibrous habits of six of these minerals (IARC 1977). The most common type of asbestos is chrysotile, which is the fibrous habit of the mineral serpentine. The other five asbestos minerals are all amphiboles (i.e. all partially hydrolyzed, magnesium silicates). These are: fibrous reibeckite (crocidolite), fibrous grunerite (amosite), anthophyllite asbestos, tremolite asbestos, and actinolite asbestos.

All six of the minerals whose fibrous habits are termed asbestos occur most commonly in non-fibrous, massive habits. While unique names have been assigned to the asbestiform varieties of three of the six minerals (noted parenthetically above) to distinguish them from their massive forms, such nomenclature has not been developed for anthophyllite, tremolite, or actinolite. Therefore, when discussing these latter three minerals, it is important to specify whether a massive habit of the mineral or the fibrous (asbestiform) habit is intended.

Although other minerals may also occur in a fibrous habit, they are not generally included in the definition of asbestos either because they do not exhibit properties typically ascribed to asbestos (e.g. high tensile strength, the ability to be woven, heat stability, and resistence to attack by acid or alkali) or because they do not occur in sufficient quantities to be exploited commercially.

The first four of the six asbestos minerals listed above have been exploited commercially (IARC 1977). Of these, chrysotile alone accounts for more than 90% of the asbestos found in commercial products.

Importantly, it is neither clear whether the term asbestos maps reasonably onto the range of fibrous minerals that can contribute to asbestos-like health effects nor whether individual structures of the requisite mineralogy must formally be asbestiform to contribute to such health effects.

Regarding whether the term asbestos is a useful discriminator for health effects, it is well established that erionite (a fibrous zeolite not related to asbestos) is a potent inducer of mesothelioma (Baris et al. 1987), which is one of the two primary asbestos-induced cancers (see Chapter 3). It is therefore possible that the fibrous habits of at least some other minerals not formally included in the current definition of asbestos may contribute to the induction of asbestos-related diseases. Therefore, what needs to be

developed, is an efficient procedure for separating potentially hazardous materials from those that are most likely benign.

There are two issues related to the question of whether fibers must formally be asbestiform to contribute to health effects. The first involves the relationship between fiber structure and disease induction and the second involves measurement. Although the evidence is overwhelming that the size and shape of a fiber affects the degree to which it contributes to the induction of disease (see Chapter 7 and, specifically, Section 7.5), it does not appear that sizes inducing biological activity are well distinguished by criteria that define the asbestiform habit. For example, determining the concentration of a specific, common size range of structures was shown to adequately predict the observed tumorigenicity of six forms of tremolite (three asbestiform varieties and three non-asbestiform varieties) that were intrapleurally injected into rats (see Section Appendix B). Once again, therefore, what is needed is an efficient procedure for distinguishing between the potentially hazardous size range of fibrous structures and those that do not contribute to disease.

Importantly, depending on the definition employed for the fibers (or fibrous structures) that are counted during an analysis, it may or may not be necessary to distinguish formally between asbestiform and non-asbestiform structures for the concentrations derived from such a count to adequately reflect biological activity.

> Note, the dimensions of an asbestiform fiber are determined by the manner in which the fiber grows (Addison, J. private communication). In contrast, the massive forms of various minerals, when cleaved, also form elongated particles (termed "cleavage fragments") and, depending on the definition employed for fibrous structures during an analysis, such cleavage fragments may or may not be included along with asbestiform fibers in a count (see, Section 4.3). Although it is clear from the manner in which they are each formed that the surface properties of asbestiform fibers and cleavage fragments are likely to be very different (for example, the latter will have many "unsatisified" chemical bonds), the degree to which such differences affect potency for comparable sized structures is not currently known.

Although it is beyond the scope of this document to present a detailed treatise on asbestos mineralogy, the morphology of asbestos dusts, or the nature and limitations of analytical techniques and methods used to determine asbestos concentrations, a brief overview of these topics is presented in the following sections both to identify issues that need to be addressed as part of the development of an appropriate protocol for assessing asbestos risks and to provide the background required to facilitate evaluation

of the relevant issues. In that regard, a section on lung physiology and function is also provided.

4.1 THE MINERALOGY OF ASBESTOS

As previously indicated, the six asbestos minerals can be divided into two general classes.

Chrysotile is the fibrous habit of the mineral serpentine (Hodgson 1965). The smallest fibrils of chrysotile occur as rolled sheets or hollow tubules of this magnesium silicate mineral. The larger fibers of chrysotile form as tightly packed bundles of the unit fibrils.

Chrysotile fibrils typically range from 20 nm to approximately 300 or 400 nm (0.02 to 0.3 or 0.4 um) in diameter. Occasionally, structures up to 1000 nm (1 um) have been observed, but these are unusual. At some point the curvature induced by the mismatch between the magnesium and silicon layers of the fibril becomes thermodynamically unstable, so that production of thicker fibrils is prohibited (Addison, J. private communication).

Chrysotile bundles are held together primarily by Van der Waals forces and will readily disaggregate in aqueous solutions containing wetting agents (e.g. soap). They will also readily disaggregate in lung surfactant (Addision, J. private communication).

The general chemical composition of serpentine is reported as $Mg_3(Si_2O_5)(OH)_4$ (Hodgson 1965). However, the exact composition in any particular sample may vary somewhat from the general composition. For example, aluminum may occasionally replace silicon and iron, nickel, manganese, zinc or cobalt may occasionally replace magnesium in the crystal lattice of chrysotile (serpentine).

The five other common varieties of asbestos are all fibrous forms of amphibole minerals (Hodgson 1965). These are ferro-magnesium silicates of the general composition:

$$A_{2-3}B_5(Si,Al)_8O_{22}(OH)_2$$

where:

A = Mg, Fe, Ca, Na, or K; and
B = Mg, Fe, or Al.

Some of these elements may also be partially substituted by Mn, Cr, Li, Pb, Ti, or Zn.

The fibrous habits of the amphibole minerals tend to occur as extended chains of silica tetrahedra that are interconnected by bands of cations (Hodgson 1965). Each unit cell typically contains eight silica tetrahedra and the resulting fibers tend to be rhomboid in cross-section. Amphibole fibrils are generally thicker than chrysotile fibrils and may typically range from approximately 100 nm to 700 or 800 nm in diameter (Addison, J private communication). Substantially thicker fibrils have also been observed.

4.2 MORPHOLOGY OF ASBESTOS DUSTS

Structures comprising the fibrous habits of the asbestos minerals come in a variety of shapes and sizes. Not only do single, isolated fibers vary in length and thickness but such fibers may be found combined with other fibers to form bundles (aggregates of closely packed fibers arranged in parallel) or clusters (aggregates of randomly oriented fibers) or combined with equant particles to form matrices (asbestos fibers embedded in non-asbestos materials). Consequently, dusts (even of one mineral variety) are complex mixtures of structures. For precise definitions of the types of fibrous structures typically found in asbestos dusts, see Chatfield and Berman (1990).

Detailed descriptions of the characteristics of dusts typically encountered at environmental and occupational asbestos sites have been reported in the literature and the following summary is based on a previously published review (Berman and Chatfield 1990). Typically, the major components of the dust observed in most environments are non-fibrous, isometric particles. Fibrous structures consistently represent only a minor fraction of total dust. Asbestos structures represent a subset of the fibrous structures.

The magnitude of the fraction of total dust represented by fibers and the fraction of fibers composed of asbestos minerals vary from site to site. However, the fraction of asbestos in total dusts has been quantified only in a very limited number of occupational and environmental settings (see, for example, Lynch et al 1970 or Cherrie et al 1987).

The gross features of structure size distributions appear to be similar among asbestos dusts characterized to date (Berman and Chatfield 1990). The major asbestos fraction of all such dusts are small structures less than 5 µm in length. Length distributions generally exhibit a mode (maximum) between 0.8 and 1.5 µm with larger fibers occurring with decreasing frequency. Fibrous structures longer than 5 µm constitute no

more than approximately 25% of total asbestos structures in any particular dust and generally constitute less than 10%.

In some environments, the diameters of asbestos fibers exhibit a narrow distribution that is largely independent of length. In other environments, diameters appear to exhibit a narrow distribution about a mean for each specific length. In the latter case, both the mean and the spread of the diameter distribution increases as the length of the structures increase. The increase in diameter with length appears to be more pronounced for chrysotile than for the amphiboles, presumably due to an increase in the fraction of chrysotile bundles contributing to the overall distribution as length increases.

Only a few studies have been published that indicate the number of complex structures in asbestos size distributions. The limited data available indicate that complex structures may constitute a substantial fraction (up to one third) of total structures, at least for chrysotile dusts (see, for example, Sebastien et al 1984). Similar results were also obtained during a re-analysis of dusts generated from the asbestos samples evaluated in the animal inhalation studies conducted by Davis et al. (Berman et al. unpublished). This is the same re-analysis used to support a study to identify asbestos characteristics that promote biological activity (Berman et al. 1995), which is discussed further in Section 7.4.3.

Historically, fibrous structures have been arbitrarily defined as structures exhibiting aspect ratios (the ratio of length to width) greater than 3:1 to distinguish them from isometric particles (Walton, 1982). However, alternate definitions for fibers have also been proposed, which are believed to better relate to biological activity (see, for example, Wylie et al. 1993 or Berman et al. 1995). The degree to which fibers are combined within complex structures in a particular dust may also affect the biological activity of the dust (Berman et al. 1995). Therefore, proper characterization of asbestos exposure requires that the relative contributions from each of many components of exposure be simultaneously considered. Factors that need to be addressed include the distribution of structure sizes, shapes, and mineralogy in addition to the absolute concentration of structures. Such considerations are addressed further in Chapter 7. Thus, unlike the majority of other chemicals frequently monitored at hazardous wastes sites, asbestos exposures cannot be adequately characterized by a single concentration parameter.

4.3 CAPABILITIES OF ANALYTICAL TECHNIQUES USED TO MONITOR ASBESTOS

Due to a complex history, a range of analytical techniques and methods have been employed to measure asbestos in the various studies conducted over time (Walton 1982). Use of these various methods has affected the comparability of results across the relevant asbestos studies (Berman and Chatfield 1990). Therefore, the relative capabilities and limitations of the most important methods used to measure asbestos are summarized here. Later sections of this report incorporate attempts to reconcile effects that are attributable to the limitations of the different methods employed in the various studies evaluated.

Analytical techniques used to measure airborne asbestos concentrations vary greatly in their ability to fully characterize asbestos exposure. The capabilities and limitations of four analytical techniques (midget impinger, phase contrast microscopy, scanning electron microscopy, and transmission electron microscopy) need to be considered here.

Midget impinger (MI) and phase contrast microscopy (PCM) are the two analytical techniques used to derive exposure estimates in the majority of epidemiology studies from which the existing risk factors are derived. Scanning electron microscopy (SEM) is an analytical technique that has been employed in several key animal studies. Transmission electron microscopy (TEM) provokes interest because it is the only analytical technique that is potentially capable of distinguishing all of the characteristics of asbestos that potentially affect biological activity.

Although PCM is widely used to characterize occupational exposures, its inability to distinguish between asbestos and non-asbestos and its lack of sensitivity limits its usefulness in environmental settings (Berman and Chatfield 1990). In fact, PCM analyses and TEM analyses showed no correlation among measurements collected during the cleanup of the Oakland Hills fire (Berman, unpublished). Such lack of correlation is expected to be observed generally whenever measurements are collected at sites where no single, obvious source of asbestos is expected to dominate. Consequently, TEM is the technique that has been recommended for use at Superfund sites (Chatfield and Berman 1990 and Berman and Kolk 1997).

A general comparison of the relative capabilities and limitations of the analytical techniques introduced above is presented in Table 4-1.

Importantly, the physical limitations of the various analytical techniques is only part of the problem. To provide reproducible results that can be compared meaningfully to other analyses in other studies, one must also consider the choice of procedures

(methods) that address everything from sample collection and preparation to rules for counting and quantifying asbestos structures.

Multiple methods have been published for use in conjunction with several of the analytical techniques mentioned above (particularly TEM). Such methods differ in the procedures incorporated for sample preparation and for the manner in which asbestos structures are counted. The sample preparation requirements, conditions of analysis, and structure counting rules for several of the most commonly employed methods are presented in Table 4-2 to illustrate how the choice of method can result in substantially different measurements (even on duplicate or split samples).

Table 4-1:
Capabilities and Limitations of Analytical Techniques Used for Asbestos Measurements[1]

Parameter	Midget Impinger	Phase Contrast Microscopy	Scanning Electron Microscopy	Transmission Electron Microscopy
Range of Magnification	100	400	2,000 - 10,000	5,000 - 20,000
Particles Counted	All	Fibrous Structures[2]	Fibrous Structures[2]	Fibrous Structures[2,3]
Minimum Diameter (size) Visible	1 µm	0.3 µm	0.1 µm	< 0.01 µm
Resolve Internal Structure	No	No	Maybe	Yes
Distinguish Mineralogy[4]	No	No	Yes	Yes

1. The capabilities and limitations in this table are based primarily on the physical constraints of the indicated instrumentation. Differences attributable to the associated procedures and practices of methods in common use over the last 25 years are highlighted in Table 4-2.

2. Fibrous structures are defined here as particles exhibiting aspect ratios (the ratio of length to width) greater than 3 (see Walton 1982).

3. TEM counts frequently resolve individual fibrous structures within larger, complex structures. Based on internal structure, several different counting rules have been developed for handling complex structures. See the discussion of methods presented below.

4. Most SEM and TEM instruments are equipped with the capability to record selected area electron diffraction (SAED) spectra and perform energy dispersive X-ray analysis (EDXA), which are used to distinguish the mineralogy of structures observed.

The second column of Table 4-2 describes the specifications of the PCM method currently mandated by the Occupational Safety and Health Agency (OSHA) for characterizing asbestos exposure in occupational settings. Although this method is in common use today, several alternate methods for counting fibrous structures by PCM

Table 4-2: Comparison of Applicable Methods For Measuring Asbestos In Air

	NIOSH 7400[1]	NIOSH 7402[2]	YAMATE[3]	AHERA[4]	ISO[5,6]
Analytical Technique	PCM[7]	TEM	TEM	TEM	TEM
Preparation Methodology	Direct (no transfer)	Direct	Direct (Indirect Optional)	Direct	Direct (Indirect Optional)
Magnification	450x	10,000x	20,000x	15,000x - 20,000x	20,000x (total structures) 10,000x (structures longer than 5 µm)
Dimensions Counted					
Length (L):	L > 5 µm	L > 1 µm	L > 0.06 µm	L > 0.5 µm	L > 0.5 µm total structures L > 5 µm long structures
Width (W):	W > 0.25 µm	3.0 > W > 0.04 µm	W > 0.02 µm	W > 0.02 µm	W < 3.0 µm (respirability)
Aspect Ratio (AR):	AR > 3	AR > 3	AR > 3	AR > 5	AR > 5
Sensitivity:					
s/cm²				0.005	Adjustable
s/mm²				70	10 for total structures 0.1 for long structures
Mineralogy Determined	No	Yes	Yes, except matrix particles	Yes, except matrix particles	Yes
Maximum Number Counted	100 structures	100 structures	100 structures	50 structures	100 total structures 100 long structures
Maximum Area Scanned	100 fields	100 grid openings	10 grid openings	Blanks: 10 openings Samples: 10 openings (assuming defined sensitivity is achieved with the collected air volumes).	Adjustable

Table 2 (Page 2)

	NIOSH 7400	NIOSH 7402	YAMATE	AHERA	ISO
Statistically Based Counting[7]	No	No	No	No	Yes
Counting Rules					
Structures	Count all structures exhibiting L > 5 µm, W < 3.0 µm, and AR > 3.	Count all structures exhibiting L > 1 µm, W < 3.0 µm, and AR > 3. Note PCME[8] fraction within count.	Count all structures exhibiting an AR > 3.	Count all structures with L > 0.5 µm exhibiting an AR > 5. Record individual fibers within all groupings with fewer than 3 intersections. Count structures with L > 5 µm separately (PCME[8]).	Count all structures with L > 0.5 µm or containing components with L > 0.5 µm that also exhibit an AR > 5. Separately identifiable components of parent structures that satisfy dimensional criteria are also separately enumerated. Conduct a similar count to that indicated above for structures with L > 5 µm.
Bundles	Bundles meeting overall dimensional criteria generally counted as single fibers unless up to 10 individual fiber ends can be distinguished within the bundle (representing 5 individual fibers).	Bundles meeting overall dimensional criteria generally counted as single fibers.	Bundles meeting overall dimensional criteria generally counted as single entities and noted as bundles on the count sheet.	Bundles of 3 or more fibers that meet the overall dimensional criteria are counted as single entities and noted as bundles on the count sheet.	Count parent bundles with L > 0.5 µm containing at least one component fiber that exhibits an AR > 5. Qualifying bundles that are components of other parent structures are also separately enumerated. For counts of structures with L > 5 µm, include only bundles longer than 5 µm.
Clusters	Within a cluster, count up to 10 individual fiber ends from (up to 5) fibers that meet the overall dimensional criteria. Otherwise, count a cluster as a single entity.	Within a cluster, count up to 3 individual fibers that meet the overall dimensional criteria. Otherwise, clusters that contain more than 3 fibers that meet the overall dimensional criteria are counted as single clusters.	Within a cluster, count up to 3 individual fibers that meet the overall dimensional criteria. Otherwise, clusters that contain more than 3 fibers that meet the overall dimensional criteria are counted as single clusters.	A collection of fibers with more than 2 intersections where at least one individual projection meets the overall dimensional criteria is counted as a single cluster.	Distinguish "dispersed" and "compact" clusters. Count all clusters containing at least one component fiber or bundle satisfying appropriate dimensional criteria. Separately enumerate up to 10 component structures satisfying appropriate dimensional criteria.

Table 2 (Page 3)

	NIOSH 7400	NIOSH 7402	YAMATE	AHERA	ISO
Matrices	Count up to 5 fibers emanating from a clump (matrix). Each individual fiber must meet the dimensional criteria.	Count individually identifiable fibers within a matrix. Fibers must individually meet the dimensional criteria.	Count as a single matrix, all matrices with at least one protruding or embedded fiber that meets the dimensional criteria.	Count as a single matrix, all matrices with at least one protruding fiber such that the protruding section meets the dimensional criteria.	Distinguish "dispersed" and "compact" matrices. Count all matrices containing at least one component fiber or bundle satisfying appropriate dimensional criteria. Separately enumerate up to 10 component structures satisfying appropriate dimensional criteria.

1. National Institute for Occupational Safety and Health (1985). *Method for Determination of Asbestos in Air Using Positive Phase Contrast Microscopy.* NIOSH Method 7400. NIOSH, Cincinnati, Ohio, U.S.A.

2. National Institute for Occupational Safety and Health (1986). *Method for Determination of Asbestos in Air Using Transmission Electron Microscopy.* NIOSH Method 7402. NIOSH, Cincinnati, Ohio, U.S.A.

3. Yamate, G., Agarwal, S.C., and Gibbons, R.D. (1984). *Methodology for the Measurement of Airborne Asbestos by Electron Microscopy.* U.S. EPA Report No. 68-02-3266. U.S. Environmental Protection Agency, Washington, D.C., U.S.A.

4. U.S. Environmental Protection Agency (1987). *Asbestos Hazard Emergency Response Act: Asbestos-Containing Materials in Schools.* Final Rule and Notice (Appendix A: AHERA Method). Federal Register, 40 CFR 763, Vol. 52, No. 2, pp. 41826-41903, October.

5. Chatfield, E.J. (1993). *Ambient Air: Determination of Asbestos Fibres, Direct Transfer Transmission Electron Microscopy Procedure.* Submitted to the International Standards Organization: ISO/TC 146/SC 3. **Note: I need to check this number, I think it is incorrect.**

6. Note that the ISO Method is a successor to the Interim Superfund Method: Chatfield, E.J. and Berman, D.W. (1990). *Superfund Method for the Determination of Asbestos in Ambient Air. Part 1: Method Interim Version..* Prepared for the U.S. Environmental Protection Agency, Office of Emergency and Remedial Response, Washington, D.C. EPA/540-2-90/005a. May.

7. Statistically balanced counting is a procedure incorporated into some asbestos methods (e.g. the Superfund Methods and the ISO Methods) in which long structures (typically longer than 5 µm) are counted separately during a lower magnification scan than used to count total structures (which are predominantly short). This procedure assures that the relatively rare longer structures are enumerated with comparable precision to that of the shorter structures.

8. PCME stands for phase contrast microscope equivalent and indicates the fraction of structures observed by transmission electron micrscopy that would also be visible by phase contrast microscopy.

Table 4-2, Page 3

have also been used historically. Therefore, PCM measurements reported in earlier studies (including the available epidemiology studies) may not be comparable to PCM results collected today.

The last four columns of Table 4-2 describe TEM methods that are in current use. Comparison across these methods indicates:

- the shortest lengths included in counts using these methods vary between 0.06 and 1 μm. Given that structures shorter than 1 μm represent a substantial fraction of total asbestos structures in almost any environment (Section 4.2), this difference alone contributes substantially to variation in measurement results across methods;

- the definitions and procedures for counting complex structures (i.e. bundles, clusters, and matrices) vary substantially across methods, which further contribute to variation in measurement results. For example, the ISO Method requires that component fibers of clusters and matrices be counted separately, if they can be readily distinguished. In contrast, clusters are counted as single structures under the AHERA Method; and

- although all of the methods listed incorporate sample preparation by a direct transfer process, several of the methods have also been paired with an optional indirect transfer process. Measurements derived from split samples that are prepared, respectively, by direct and indirect transfer, can vary by factors as large as several 100 (Berman and Chatfield 1990). More typically, however, counts of asbestos structures on samples prepared by an indirect transfer procedure are greater than those derived from directly prepared samples by factors of between 5 and 50.

Given the combined effects from the physical limitations of the various techniques employed to analyze for asbestos and the varying attributes of the methods developed to guide use of these techniques, the relative capabilities and limitations of asbestos measurements derived, respectively, from paired methods and techniques in common use can be summarized as follows:

- all four techniques are particle counting techniques;

- neither MI nor PCM are capable of distinguishing asbestos from non-asbestos (i.e. they are incapable of determining structure mineralogy);

- counting rules used in conjunction with MI do not distinguish isometric particles from fibers;
- counting rules used in conjunction with PCM limits counting to fibrous structures longer than 5 μm with aspect ratios greater than 3:1;
- the range of visibility associated with PCM limits counting to fibers thicker than approximately 0.3 μm;
- under conditions typically employed for asbestos analysis, the range of visibility associated with SEM limits counting to fibers thicker than approximately 0.1 μm, which is only marginally better than PCM;
- SEM is capable of distinguishing asbestos structures from non-asbestos structures;
- TEM is capable of resolving asbestos structures over their entire size range (down to thicknesses of 0.01 μm);
- TEM is capable of distinguishing the internal components of complex asbestos structures; and
- TEM is capable of distinguishing asbestos structures from non-asbestos structures.

More detailed treatments of the similarities and differences between asbestos techniques and methods can also be found in the literature (see, for example, Berman and Chatfield 1990).

Due to the differences indicated, measurements from a particular environment (even from duplicate samples) that are derived using different analytical techniques and methods can vary substantially and are not comparable. In fact, results can differ by two or three orders of magnitude (Berman and Chatfield 1990). More importantly, because the relative distributions of structure sizes and shapes vary from environment to environment, measurements derived using different analytical techniques and methods do not even remain proportional from one environment to the next. Therefore, the results from multiple asbestos studies can only be meaningfully compared if the effects that are attributable to use of differing analytical techniques and methods can be quantified and reconciled. To complicate the situation, however, few of

the existing studies document analytical procedures in sufficient detail to reconstruct exactly what was done.

4.4 THE STRUCTURE AND FUNCTION OF THE HUMAN LUNG

4.4.1 Lung Structure

The lungs are the organs of the body in which gas exchange occurs to replenish the supply of oxygen and eliminate carbon dioxide. To reach the gas exchange regions of the lung, inhaled air (and any associated toxins) must first traverse the proximal conducting (non-respiratory) airways of the body and the lung including the nose (or mouth), pharynx, larynx, trachea, and the various branching bronchi of the lungs down to the smallest (non-respiratory) bronchioles. Air then enters the distal (respiratory) portion of the lung, where gas exchange occurs.

In humans, the respiratory portion of the lungs are composed of the respiratory or aveolarized bronchioles, the alveolar ducts, and the alveoli (or alveolar sacs). There are approximately 3×10^8 alveoli in human lungs (about 20 per alveolar duct) with a cumulative volume of 3.9×10^3 cm^3 (Yeh and Harkema 1993). This represents approximately 65% of the total volume capacity of human lungs at full inspiration.

Yeh and Harkema also report that the ratio of lung volume to body weight is approximately constant across a broad range of mammals (from a shrew - 0.007 kg to a horse - 500 kg). Human lung volumes average a little more than 5 L.

Each human alveolus has a diameter of approximately 0.03 cm (300 µm) and a length of 0.025 cm (Yeh and Herkema 1993). The typical path length from the trachea to an alveolus is approximately 25 cm. The bronchi leading to each alveolus have branched an average of 16 times from the trachea (with a range of 9 to 22 branches). Importantly, the mean path length, the number of branches between trachea and alveolus, and the detailed architecture (branching pattern) of the respiratory region of the lung vary across mammalian species. For example, rats and mice lack respiratory bronchioles while macaque monkeys exhibit similar numbers of respiratory bronchiole generations as humans (Nikula et al. 1997). Furthermore, branching in humans tends to be symmetric (each daughter branch being approximately the same size and the angle of branching for each is similar but not quite equal) while rodents tend to exhibit

monopodal branching in which smaller branches tend to come off at angles from a main trunk (Lippmann and Schlesinger 1984).

The gas exchange regions of the lung are contained within the lung parenchyma, which constitute approximately 82% of the total volume of the lungs (Gehr et al. 1993). Importantly, the lung parenchyma is not a "portion" of the lung; it fills virtually the entire volume of the organ traditionally visualized as the "whole" lung. Embedded within the parenchyma are the larger conducting airways of the lungs and the conducting blood vessels that transport blood to and from the capillaries that are associated with each alveolus. In the human lung, approximately 213 ml of blood are distributed over 143 m^2 of gas-exchange (alveolar) surface area (about the size of a tennis court). The gas-exchange surface area of lungs scale linearly with body weight over most mammalian species. The slope of the line is 0.95. Figure 4-1 is a photomicrograph showing two views of a portion of lung parenchyma in the vicinity of a terminal bronchiole and an alveolar duct, which are labeled. The circular spaces in the left portion of the figure and the cavities in the right portion of the figure are alveoli. Note the thinness of the walls (septa) separating alveoli.

Alveoli are separated from each other by alveolar septa that average only a few micrometers in thickness (Gehr et al. 1993). Gas-exchange capillaries run within these septa and the air-blood barrier, which averages only 0.62 μm in thickness, is composed of three layers: the alveolar epithelium, the interstitium, and endothelium. The epithelium is described in detail below. The interstitium is primarily composed of a collagenous, extracellular matrix, which constitute about two-thirds of the volume with a collection of fibroblasts, macrophages, and other cells interspersed within the matrix (Miller et al. 1993). The cells of the interstitium constitute about one third of its volume. The endothelial layer is composed of the smooth muscle cells and connective tissue that constitute the walls of vascular capillaries. The amount of connective tissue in the septa between alveoli also varies between animal species; small rodents have less and primates more (Nikula et al. 1997).

Figures 4-2 and 4-3 show, respectively, a typical alveolar septum and a closeup of one portion of such a septum. In Figure 4-2, one can see that the septa themselves are thin and are filled almost entirely with capillaries. Figure 4-3 shows that the epithelial lining of an alveolus is no more than 1 μm thick, that the underlying interstitium is no thicker, and that the endothelium of the adjacent capillary is similarly thin. These three layers constitute the major tissues of the air-blood barrier (the rest of the barrier includes the limited quantity of blood plasma between the endothelial wall of a capillary and a red blood cell and the outer membrane of the red blood cell itself).

Gehr et al. (1993) also report that interalveolar septa constitute approximately 14% of the volume of the gas-exchange region of the lung (i.e. the lung parenchyma). Of this tissue mass, approximately 20% is endothelium, 55% is interstitium, and the rest is composed of cells associated with the alveolar epithelium. The remainder of the gas-exchange region is air space. Gehr et al. also report that the interalveolar septa fold to accommodate changes in lung volume during respiration, although the major contribution to lung volume changes (over the range of normal inspiration) appears to be the collapsing (folding) of alveolar ducts (Mercer and Crapo 1993).

Figure 4-1:
The Structure of Lung Parenchyma Showing Alveoli and Alveolar Ducts

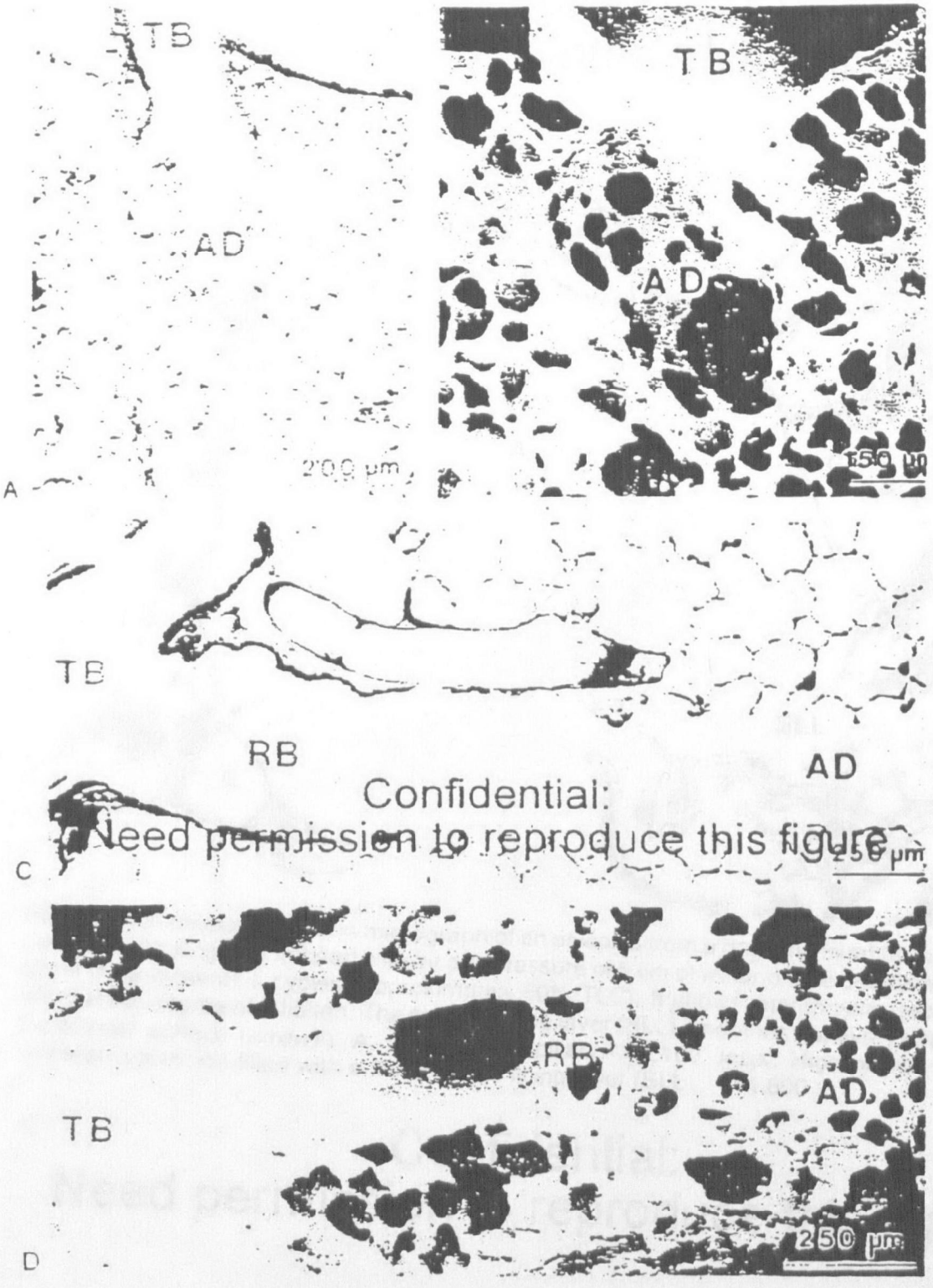

Confidential:
Need permission to reproduce this figure

FIG. 10. LM and SEM comparison of the centriacinar region with two different organization and B. The short or poorly developed respiratory bronchiole of the rat; C and D, the v alveolarized respiratory bronchiole of the cat. Terminal bronchiole (TB), respiratory bronch (RB), and alveolar duct (AD). For details see ref. 106.

Figure 4-2:
The Structure of the Inter-Alveolar Septa

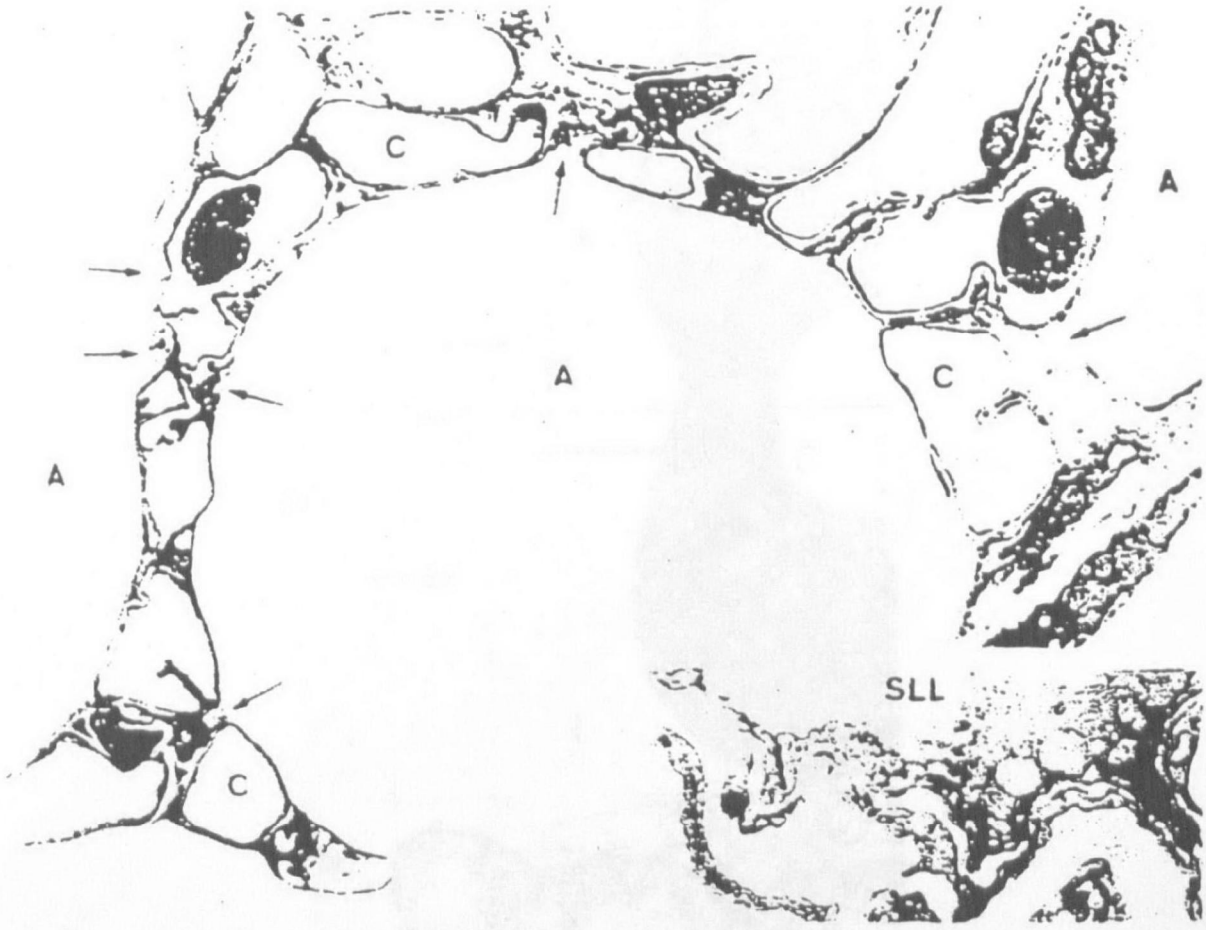

FIG. 10. Transmission electron micrograph of an alveolus from a dog lung fixed by intravascular perfusion. The lung was inflated with air at a pressure of 5 cm of water on the deflation limb of the last of three hysteresis cycles (approximately 60% TLC). It shows interalveolar septa that are folded at this degree of inflation. The surface lining layer (SLL) smoothes out every depression of the alveolar surface (*arrows*). A, alveoli; C, capillary. × 2,100. *Inset*: High power view of an epithelial depression filled with a fluid surface lining layer (SLL). × 14,600.

Confidential:
Need permission to reproduce this figure

Figure 4-2:
The Detailed Structure of an Alveolar Wall that is Part of an Inter-Alveolar Septum

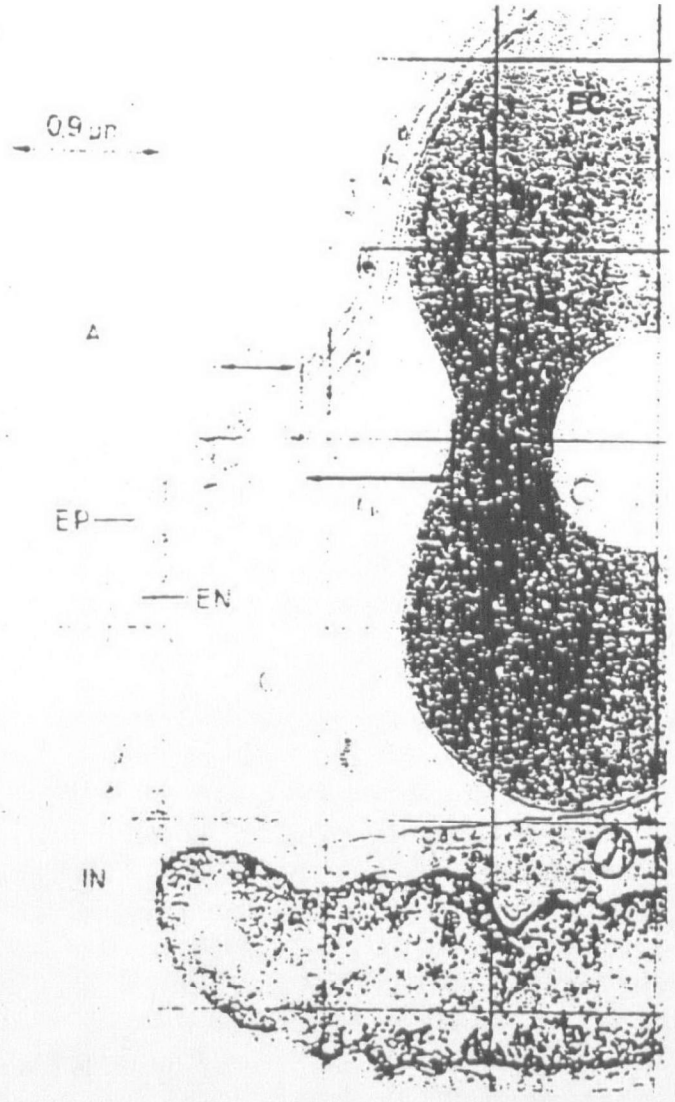

FIG. 19. Fraction of square lattice test grid superimposed on alveolar capillary to measure intercept lengths in tissue (T) and plasma (P) for the calculation of the harmonic mean barrier thickness. Note the erythrocyte (EC) in capillary (C) and that the barrier separating blood from alveolar air (A) is made of the [illegible] epithelium (EP), endothelium (EN), and interstitium (IN). ×29,000. (Reproduced at [illegible])

Confidential:
Need permission to reproduce this figure

Figure 4-3

According to Gehr et al. (1993), human alveoli contain approximately 380 cells and the total number reportedly increases as a power function with body mass for other mammals. In humans, this includes approximately 12 alveolar macrophages (although this number is larger in smokers, apparently due to chronic inflammation), 40 Type I epithelial cells, 67 Type II epithelial cells, 106 interstitial cells, and 148 endothelial cells.

The relative number of the various types of cells associated with alveoli varies across mammalian species (Gehr et al. 1993). In the rat, for example, Type I epithelium is approximately 20% of the total (rather than 12% in humans) with less interstitium and more endothelium.

According to Gehr et al. (1993), Type I epithelial cells, which constitute approximately 95% of the surface area of alveolar epithelium, are flat and platy (squamous), and average less than 1 μm in thickness (except where cell nuclei exist, which are approximately 7.5 μm in diameter and protrude into the alveolar space). Type II epithelial cells, which are cuboidal, constitute no more than 5% of the epithelial surface. Despite the small fraction of surface that they occupy, Type II cells serve to maintain the integrity of the overall epithelial lining so that, for example, they limit the tissue's permeability and control/prevent transport of macromolecules from the interstitium to the alveolar space, or the reverse (Leikauf and Driscoll 1993). Type II cells also secrete lung surfactant. The basement membrane of alveolar epithelium is a collagenous structure.

In contrast, the epithelial cells lining the trachea and bronchi (including the respiratory bronchioles) are ciliated and columnar and averages between 10 and 15 μm in thickness (based on photomicrographs presented in St. George et al. 1993). Tracheobronchial epithelium reportedly contains at least 8 distinct cell types (St. George et al. 1993): ciliated epithelium, basal cells (small flat cells situated along the basal lamina and not reaching the luminal surface), mucous goblet cells, serous cells, nonciliated bronchiolar (clara) cells, small mucous granule (SMG) cells, brush cells, and neuroendocrine cells. The relative abundance of the various cells varies across mammalian species as well as across the various airway generations (branches) and even the opposing sides of specific airways. The number of cells per length of basal lamina also varies across mammalian species.

4.4.2 The Structure of the Mesothelium

The mesothelium is a double layered membrane and each layer is a single-cell thick. The two layers of the mesothelium are separated by a space (e.g. the pleural space), which contains extracellular fluid and free macrophages (Kane and McDonald 1993).

The pleural space is drained at fixed locations by lymphatic ducts. Each layer of the mesothelium overlies a collagenous basement membrane containing dispersed spindle cells. Depending on the location of the mesothelium, the basement membrane may overlie the skeletal muscle of the diaphragm or the rib cage (in the case of the parietal pleura, which is the outer layer). For the inner layer or visceral pleura, the basement membrane overlies visceral organs (including the lungs) within the rib cage. Healthy mesothelium is quiescent, meaning that cells are not actively dividing.

The relative size and thickness of mesothelial tissue varies across mammalian species (Nikula et al. 1997). For example, rats have relatively thin pleura with limited lymphatic ducts. In contrast, nonhuman primates have thicker pleura with greater lymphatic drainage than rats and humans have even thicker pleura and relatively abundant lymphatic ducts.

4.4.3 Cytology

Alveolar Epithelium. In the respiratory region of the lung, Type II epithelial cells are progenitor cells for Type I epithelium (Leikauf and Driscoll 1993). Type I epithelial cells are not proliferation competent (Nehls et al. 1997). After injury to Type I cells, Type II cells proliferate and reestablish the continuous epithelial surface. Type II cells also secrete surfactant. It appears that the identity and location of the progenitor cells for Type II epithelial cells are not currently known.

Injury or alteration of Type II cell function are associated with several diseases included idiopathic pulmonary fibrosis (Leikauf and Driscoll 1993). Also, crystalline silica and other toxic agents have been shown to directly modify Type II cellular activity. For example, crystalline silica (at sub-cytotoxic levels, < 100 µg/ml) stimulates Type II proliferation in tissue culture. In contrast, neither titanium dioxide nor aluminum coated silica induce proliferation at corresponding concentrations.

In culture, Type II epithelial cells transform slowly into Type I cells and thus have limited population doubling capacity (Leikauf and Driscoll 1993). Rarely can the number of Type II cells expand past three to 10 passages (20-30 doublings). During this time, cells terminally differentiate, develop cross-linked envelopes, and appear squamous, enlarged, and multinucleated. The process is noted to be accelerated by the presence of transforming growith factor beta (TGF-β).

Macrophages. Alveolar macrophages (the largest population of macrophages in the lung) are mobile, avidly phagocytic, present antigens, and release cytokines that trigger various other immune responses (Leikauf and Driscoll 1993). They also initiate

inflammatory responses and other repair mechanisms that are designed to restore tissue homeostasis.

The next largest population of macrophages in the lung are the interstitial macrophages (Leikauf and Driscoll 1993). These are localized in the peribronchial and perivascular spaces, the interstitial spaces of the lung parenchyma, the lymphatic channels, and the visceral pleura. The various populations of macrophages in the lung express different surface proteins, show different proliferative capacity, and show differences in metabolism.

The sizes of alveolar macrophages varies substantially across mammalian species (Krombach et al. 1997). Krombach and co-workers provide a table summary of the relative sizes across several species of interest:

Animal	Mean diameter (um)	Mean Volume (um^3)
Rats	13.1 +/-0.2	1166 +/-42
Syrian Golden Hamsters	13.6 +/-0.4	1328 +/-123
Cyanomolgus Monkeys	15.3 +/-0.5	
Healthy Humans	21.2 +/-0.3	4990 +/-174

As indicated later (Section 7.2), the relative size of various macrophages has direct implications regarding the dependence of clearance mechanisms on fiber size.

Mesothelium. Importantly, mesothelial cells are proliferation competent and may be their own progenitor cells (Kane and McDonald 1993). It is also possible, however, that as yet to be identified progenitor cells are located along opposite walls of pleura or at other locations within the pleural space.

Tracheo-bronchiolar epithelium. As previously indicated, tracheo-bronchiolar (i.e. non-respiratory) epithelium is composed primarily of ciliated, columnar cells that are 10 to 15 μm thick. Although some report that Clara cells serve as progenitor cells for tracheo-bronchiolar epithelium (Finkelstein et al. 1997), others report that both Clara cells and bronchiolar epithelium are proliferation competent (Nehls et al. 1997). It appears that the identity and location of the progenitor cells for Clara cells are not currently known.

4.4.4 Implications

The potential implications of the above observations concerning lung structure and cytology are:

- that the thicknesses of Type I epithelial cells, endothelial cells, and the interstitium in the alveolar septa are all very small relative to the lengths of the putative asbestos fibers that contribute to disease;

- that an entire alveolus is only 300 μm across and a typical Type I cell is 46 μm in radius by < 1 μm thick;

- that distances across alveolar septa are only on the order of a few μm and such septa contain both the endothelium and the interstitum. Thus, the distances that have to be traversed to get to these structures are also small relative even to the length of a fiber;

- that the alveolar septa and the walls of the alveolar ducts fold during respiration, which may provide mechanical forces that facilitate movement of fibers into and through the alveolar epithelium;

- that Type I epithelium do not proliferate so they cannot be the cells that lead to cancer. It is the Type II epithelial cells (and potentially macrophages, basal cells, or endothelial cells) that contribute to cancer in the pulmonary portion of the lung. Type II cells eventually terminally differentiate to Type I cells;

- that other cells in the lung that have variously been reported to be proliferation competent (so that they potentially serve as target cells for the induction of cancer) include Clara cells and bronchiolar epithelial cells;

- that the distance from the most distal airways and alveoli to the pleura is small relative to the lengths of a fiber; and

- that mesothelial cells are proliferation competent and thus serve as potential targets for the induction of cancer;

5.0 THE ASBESTOS LITERATURE

This is a description of the common types of studies in the asbestos literature and an overview of the sources of potential uncertainty typically associated with each. Such limitations must be considered when drawing conclusions from these studies and, more importantly, when comparing inferences across studies. Throughout this document, we have endeavored to identify the major sources of uncertainty in the studies we examined and have endeavored to account for such uncertainties during our evaluation and interpretation of study results.

The types of studies available for examining relationships between risk and asbestos exposure include human epidemiology studies, human pathology studies, a broad variety of animal studies, and a broad variety of in-vitro studies in both tissue cultures and cell-free systems. To properly compare and contrast the results from such studies:

- the method(s) employed for asbestos characterization in each study need to be reconciled;
- the procedures employed for evaluating study end points need to be compared and contrasted;
- the relationship between the route of exposure employed in each type of study and the exposure route of interest (i.e. human inhalation) needs to be examined; and
- other major, study-specific sources of uncertainty need to identified and addressed.

Among study conditions and procedures that must be considered before evaluating study conclusions, it is particularly important to address the analytical methodologies employed to characterize the nature of exposures (or doses) in each study and such considerations are common to virtually all of the various types of studies of interest.

As indicated in Section 4.3, the only instrument capable of completely delineating asbestos structure size distributions is TEM (or TEM combined with other techniques). Thus, for example, conclusions regarding variations in biological effects due to differences in such things as fiber size must be viewed with caution when fiber sizes are characterized using only PCM, SEM, or other, cruder analytical techniques. Similarly, the ability to adequately determine fiber mineralogy (fiber type), particularly of what may be minor constituents of various dusts or bulk materials, also depends strongly on the

instrumentation employed for analysis as well as the strategy for sampling and for conducting the actual structure count. All of these factors must be considered.

Not only does the specific instrumentation (analytical technique) that is employed in an asbestos measurement affect the outcome of that measurement, but the particular method employed to guide the measurement affects the outcome. As previously indicated (Section 4.3), details concerning the definition of structures to be included in a count, the strategy for counting, and the minimum number of specific types of structures to be included in a count (all features that vary across analytical methods) affect the precision with which fiber concentrations (particularly of longer and thinner fibers) are delineated. It is not uncommon, for example, that asbestos concentrations measured in the same sample may vary by several orders of magnitude, due simply to a difference in the analytical method employed for the analysis (even when the same analytical technique is employed, see Section 4.3).

Other important sources of uncertainty tend to be study-type specific and are thus addressed separately below.

5.1 HUMAN EPIDEMIOLOGY STUDIES

A good overview of the kinds of limitations that contribute to uncertainty in the available epidemiology studies was presented in the Health Effects Assessment Update (U.S. EPA 1986). As described in Appendix A of this document, while evaluating dose-response factors derived from the human epidemiology studies, we tried to address most of the major sources of uncertainty commonly associated with such studies, which are described briefly below.

Epidemiology studies, which track the incidence of disease (or mortality) within a defined group (cohort) sharing comparable exposures, have been performed on cohorts of workers exposed to asbestos and other mineral fibers in a variety of occupational and environmental settings. Among these, studies that include quantification of exposures are particularly useful for evaluating dose/response relationships and deriving risk factors.

Generally, the most severe limitations in an epidemiology study involve the exposure data. Both estimates of the level of exposure and determination of the character of exposure are affected by such limitations. Regarding the character of exposure, because exposure measurements from most of the available quantitative epidemiology studies are based on midget impinger measurements or PCM measurements, detailed characterization of the size distribution or the mineral type of fibrous structures

(particularly of minor constituents) that contributed to exposure in such studies is generally lacking (Section 4.3). This is particularly important because of the evidence that neither midget impinger or PCM are capable of providing measurements that remain proportional (across study environments) to the biologically-relevant characteristics of an asbestos dust (see Section 7.5 and Appendix B). This limits the ability both to compare results across the existing studies and to extrapolate such results to new environments for which risks need to be estimated. At the same time, effects on the ability to observe dose-response trends within a single study are not typically impaired.

Samples collected prior to the mid-1960s were often analyzed by measuring total dust in units of millions of particles per cubic foot (MPCF) using impingers or thermal precipitators. A description of the relative strengths and weaknesses of these techniques is provided in Section 4.3. The fibrous portion of the dust was not monitored. Impinger measurements are sometimes related to fiber counts (based on PCM) using side-by-side measurements of total dust and fiber counts collected during a relatively brief period of time (e.g., McDonald et al, 1980b, Dement et al, 1983a). However, the correlation between fiber counts and total dust is sometimes poor within a plant and generally poor between plants (see, for example, U.S. EPA 1986). Thus, conversions based on limited sets of paired measurements are of questionable validity. In some studies (e.g., McDonald et al, 1983b) the only available measurements are impinger measurements in MPCF and these have been related to f/ml by PCM using conversion factors derived in other plants, which raises further questions concerning validity.

Even conversion to PCM may not be adequate for assessing risk in a manner that allows extrapolation across exposure environments or studies. As indicated in Section 7.5, comparing dose-response factors derived in different exposure environments (or extrapolating to new environments to predict risk) requires that asbestos measurements reflect the characteristics of asbestos structures (size, shape, mineralogy) that determine biological activity. If surrogate measures are employed (e.g. measures of asbestos structures displaying characteristics other than those that determine biological activity), there is no guarantee that concentrations of such surrogate measures and the true biologically active structures will remain proportional from one environment to the next. As a consequence, the relationship between exposure (measured by surrogate) and risk may not remain constant from one environment to the next. Importantly, several studies suggest that PCM may, at best, be no more than a surrogate measure (see, for example, Berman et al. 1995). Moreover, the technique was adapted to asbestos in an ad hoc fashion with only limited thought given to biological relevance (Walton 1982).

Use of surrogate measures of asbestos exposure may be less of a problem within a single exposure environment (where airborne asbestos structures likely have been generated in a similar manner from similar source material). Thus, surrogate measures of asbestos exposure may remain approximately proportional to the true biologically active structures, which suggests why monotonically increasing dose-response relationships have likely been observed with PCM-measured concentrations *in single exposure environments.* In different exposure environments, however, airborne asbestos structures likely are generated in different processes from different source material. There is thus little reason to expect surrogate measures of exposure to remain proportional across such environments.

None of the published epidemiology studies incorporate TEM measurements of asbestos and such measurements are not widely available in occupational settings (Section 6.2.4). However, TEM is the method currently used (and recommended) to assess exposure in environmental settings (due both to questions concerning biological relevance (Section 7.5) and to problems with measuring environmental asbestos concentrations by PCM (Section 4.3 and Appendix B).

In some cases, the limited exposure characterization presented in specific epidemiology studies can be augmented by pairing such studies with published TEM characterizations of dusts from the same or similar exposure settings, to the extent the appropriate supplemental studies are available. In fact, this is the procedure adopted in this document to adjust the existing risk factors to exposure indices that are thought to better relate to biological activity (Sections 6.2.4 and 6.3.3). Such an approach is limited, however, to the extent that the published asbestos characterizations actually represent exposure conditions in the corresponding epidemiology studies. To the extent reasonable, the limitations of this approach have been addressed in this study by assigning and incorporating additional factors into the calculation of the confidence intervals associated with the adjusted potency factors (Sections 6.2.4 and 6.3.3).

Regarding levels of exposure in the epidemiology studies, in most cases, air measurements were collected only at limited points in time and measurements may be entirely lacking from the earliest time periods, when exposures may have been heaviest. In such cases, exposures are typically estimated either by extrapolation from periods when measurements are available or by expert judgement based on personal accounts and records of changes in plant operations, industrial hygiene procedures, air standards, etc. Moreover, the majority of exposure measurements used in these studies are based on area (ambient) rather than personal samples. Typically, only a few areas of a plant have been sampled so that levels in other areas must be approximated using expert judgement by persons familiar with operations at the plant.

It is difficult to judge the degree that available asbestos concentration measurements are representative of actual exposures in the existing studies. In some cases, it seems likely that operations were shut down or otherwise modified in preparation for sampling. Likewise, in some operations there are brief episodes of very intense exposure and it is questionable whether such episodes are adequately represented in the available data.

Most of the asbestos measurements used in the published epidemiology studies were collected for insurance or compliance purposes. They were not intended to provide representative estimates of the direct level of exposure to workers. Some of the published epidemiology studies lack any direct exposure data. For example, exposures were estimated for the cohort studied by Seidman (1984) based on conditions simulated many years later in a similar plant to the one from which Seidman studied the original cohort. In fact, the equipment in the plant from which Seidman obtained exposure estimates came originally from the plant where Seidman studied the workers; it was purchased and moved. Recently, an epidemiology study was also completed for a cohort working at that new plant (Levin et al. 1998).

In addition to problems with the actual analysis of asbestos concentrations, individual exposures are generally estimated in the existing epidemiology studies by relating ambient asbestos measurements to job descriptions and integrating the duration of exposure over the recorded time that each worker spent in each job category. However, sometimes there are no records of specific areas in which an employee worked, so that work areas must be assumed based on job title. Some types of workers (e.g., maintenance workers) may have spent time in many different areas of a plant so their exposure varies from what might otherwise be assumed.

Although the greatest problems with the data in existing epidemiology studies likely lies within the estimates of exposure, problems with disease-response data also exist. Mesothelioma is rare and this disease may have been under-reported as a cause of death in older studies. This is probably less of a problem in more recent studies, since the association of mesothelioma with asbestos exposure is now well known. In fact, the opposite tendency (over-reporting) may now be occurring because an asbestos worker with mesothelioma is probably eligible for compensation. Some studies have re-diagnosed causes of death from all of the available data (e.g., Selikoff et al, 1979); however, this creates the problem of lack of comparability to control populations (for which such re-diagnosis is not generally performed).

The choice of an appropriate control population is also an important consideration. Local cancer rates may differ substantially from regional or national rates and the choice of an appropriate control is not always clear. A related problem is the lack of

smoking data in many of the studies. Because of the interrelation between smoking and asbestos in lung cancer, errors could occur in lung cancer risk estimates if the smoking patterns of the cohort are substantially different from those of the control population.

In some of the studies, a substantial portion of the population is lost to follow-up (e.g., Armstrong 1988), and this adds additional uncertainty to the analysis. Also, the effect of exposure may be inaccurately evaluated if the follow-up of the population is too brief. This may be a limitation, for example, of the Levin et al. (1998) study.

Another problem frequently associated with these studies is that available data are not reported in a form that is well-suited to risk assessment. The EPA lung cancer model, for example, requires that exposure be estimated as cumulative exposure in f/ml·years excluding the most recent 10 years (Section 6.2); generally the data are not published in this form. The data are also frequently not available in a form that permits study of the shape of the lung cancer dose/response curve, so it is not possible to determine how well the EPA model describes the data. The form of the data for mesothelioma is generally even less appropriate for risk assessment. Ideally, what is needed is the incidence of mesothelioma subdivided according to exposure level, age at beginning of exposure, and duration of exposure (Section 6.3). Such data are almost never available in published studies and crude approximations must be made to account for this lack.

It is important to appreciate the type and magnitude of effect that each of these sources of uncertainties are likely to have on the distribution of potency estimates derived from the set of available studies for lung cancer and mesothelioma, respectively. Some of the above-described limitations likely introduce random errors that simply decrease the overall precision of a potency estimate. However, other types of limitations may cause systematic errors in particular studies, which potentially biases the potency estimate either high or low. Some of the limitations may only affect between-study differences and some may introduce a systematic bias between either industry types or fiber types. Examples of some of these types of variation are provided in Section 6.1.

We also note that, although individual estimates of potency factors from individual studies may be highly uncertain, by combining results across multiple studies while properly addressing such uncertainties, it may be possible to draw conclusions with greater precision than reasonable for any individual study. This is the essential advantage of the type of meta analysis discussed in Section 6.2.4 for lung cancer and 6.3.3 for mesothelioma.

5.2 HUMAN PATHOLOGY STUDIES

Human pathology studies provide a characterization of disease morphology and correlations between causes of death and the types of asbestos fibers retained in the lungs and other bodily tissues. These studies generally involve microscopic examination of tissue samples for indications of morphologic changes characteristic of disease and/or microscopic examination of digested tissue specimens to characterize the mineral fibers extracted from such tissue.

The results of human pathology studies need to be evaluated carefully by addressing effects that are attributable to:

- the way that tissue samples are fixed for preservation;
- the way that tissue samples are prepared for analysis (e.g. ashing, bleach digestion, digestion in alkali, or some combination);
- the choice of methods employed for characterization of asbestos; and
- the choice of locations within tissues from which samples are collected for analysis.

Because tissue samples obtained from deceased individuals are typically stored for long periods of time before they may be analyzed as part of a human pathology study, such samples are commonly fixed by treatment with chemical preservatives prior to storage. However, Law et al. (1991) studied the effects of two common fixatives (Karnovsky's fixative and formalin fixative) on asbestos fibers and concluded that such fixatives degrade and dissolve asbestos fibers (including both chrysotile and crocidolite) at measurable rates (Section 7.2.4). Therefore, particularly for samples that are stored "wet" (as opposed, for example, to storage in paraffin blocks), the concentrations and character of the tissue burden of asbestos may be altered during storage. Even for studies in which relative (as opposed) to absolute concentrations are being compared, alterations associated with preservation may limit the ability to make such comparisons, particularly among samples stored for widely disparate periods of time or stored using widely disparate procedures.

Fiber concentrations in tissue samples have also been shown to vary as a function of the method employed for preparing such samples for analysis. Historically, samples that are digested in bleach or alkali have tended to exhibit lower recovery of asbestos fibers than samples that are ashed (REF). However, more recent studies suggest that

improving technique has narrowed these differences so that this is no longer a major consideration (**REF**). Thus, when comparing results across studies, due consideration needs to be given for the time frame during which such studies were conducted and the comparability/differences in the techniques employed for tissue sample preparation.

Once prepared, both the character and the concentration of the tissue burden measured in a tissue sample will also depend heavily on the particular analytical method employed to characterize asbestos and differences attributable to such techniques must be reconciled before measurements across samples or conclusions across studies can be reasonably compared. A more detailed description of the effects attributable to asbestos measurement was presented in the previous section on human epidemiology studies (Section 5.1) and the same issues obtain for human pathology studies. Unless measurements are made using comparable instrumentation with comparable methodology, comparisons across such measurements can be very misleading.

Perhaps the biggest limitation hindering the kinds of evaluation that can be conducted based on human pathology studies is that due to the strong dependence of asbestos concentrations on the specific location within a tissue from which a sample is obtained. Numerous authors have reported that asbestos is non-uniformly distributed in lung parenchyma and other tissues following exposure (see, for example: Davis et al. 1986a, Bignon et al. 1979, or Pooley 1982). The incidence of lesions and other pathological effects attributed to asbestos exposure correspondingly exhibit a non-uniform distribution.

For lung tissue samples (which tend to be among the primary interests in human pathology studies) the relationship between sample location and asbestos concentration is particularly important. To sample deep lung tissue reproducibly, it has been shown necessary to select a specific section of lung parenchyma from a defined portion of the bronchio-alveolar tree. Pinkerton et al. (1986) showed that the deposition of asbestos in the lungs is an inverse function both of the pathlength and the number of bifurcations between the trachea and the site. Thus, analyses of samples from different animals of the same species can only be compared meaningfully if the samples are collected from identical locations in the bronchio-alveolar tree. Similar, nonuniform depositional patterns have also been observed in humans (Raabe 1984). Futhermore, due to the complex branching and folding pattern of the lung, adjacent sections of lung parenchyma frequently represent disparate portions of the bronchio-alveolar tree (**REF**). Consequently, lung burdens derived even from adjacent samples of lung parenchyma can show broadly varying concentrations (dffering by orders of magnitude).

Unfortunately, however, tissue samples that are available for analysis in support of a human pathology study are typically "opportunistic" samples, which means that they were selected and stored for an entirely different purpose, usually with little or no thought given to the specific location from which they were collected (except in the most general way). It is therefore seldom possible to address the effects of sample location directly. Consequently, comparisons of tissue burden concentrations across samples from different individuals in a human pathology study are at best qualitative and may only be useful when averaged over large numbers of individuals and only when large differences in concentrations (several orders of magnitude) are being distinguished. Moreover, because the parts of a tissue that undergoes morphologic changes induced by asbestos typically corresponds to the parts of a tissue where asbestos burdens are the highest, even comparison of morphologic effects across tissue samples requires proper consideration of the effects of the locations from which such tissue samples were derived.

5.3 ANIMAL STUDIES

In animal studies, various species are exposed to measured doses of size-selected mineral fibers and the resultant biological responses are monitored. Animals may be dosed either by inhalation, intratracheal installation, implantation, or injection (U.S. EPA 1986). Such studies are conducted for several purposes. As with human pathology studies, animal pathology studies are those in which the transport of asbestos structures is tracked through the various organs and tissues of the animal and the attendent cellular and molecular changes are characterized. In parallel with quantitative epidemiology studies, animal dose/response studies track the incidence of disease among a population that has been exposed in a controlled manner. One of the advantages of animal dose/response studies over epidemiology studies is that exposures are controlled and can be well characterized. The major disadvantage is that there are many uncertainties introduced when extrapolating the results of animal data to predict effects in humans. Therefore, attempts to adapt such things as animal derived dose-response factors to humans are not generally recommended.

As with human epidemiology and pathology studies, the validity of conclusions drawn from animal studies depends strongly on the techniques and methods used to characterize and quantify asbestos structures either in the delivered dose or in the tissues of the dosed animals (see Section 5.1). The ability to reconcile conclusions derived from many animal studies with the rest of the asbestos literature is limited because SEM was commonly employed to measure asbestos in animal studies but not other kinds of studies. Even many of those studies in which TEM was employed for asbestos analysis suffer from use of non-standard methods that cannot be easily

reconciled with the more traditional TEM methods, particularly because such specialized methods are seldom adequately documented to allow comparison.

As with human pathology studies, the location of a tissue sample excised for analysis is a critical factor that also governs the quality of an animal pathology study (Section 5.2). However, one potential advantage frequently available in animal pathology studies over human studies is the ability to carefully identify and select the precise tissue samples to be analyzed. The extent that a particular animal pathology study exploits this capability can affect the overall utility of the study. Thus, such issues need to be addressed carefully when evaluating and comparing the results across animal pathology studies.

The route of exposure employed in a particular animal study is also important to consider. Each of the routes of exposure commonly employed in these studies (inhalation, intratracheal installation, and injection or implantation) delivers different size fractions of asbestos to a target tissue with varying efficiencies. For example, injection or implantation studies deliver 100% of all size categories of structures to the target tissue. However, the efficiency that each size category is delivered by inhalation is a function of the aerodynamic properties of the asbestos structures and the air flow characteristics of the lungs (Section 7.1). Thus, the relationship between dose and exposure depends upon the route of exposure employed. Importantly, because the ultimate goal is to understand the effects that inhaled fibers have on humans, differences between the character of the delivered dose in an animal study and the character that such a dose would have, had it originally been inhaled, typically need to be addressed.

Regarding the measurement of health effects, many of the results in animal studies suffer from a lack of statistical significance because of small numbers of observed tumors. Consequently, trends cannot be established conclusively. Interestingly, several studies draw conclusions regarding the relative potency of different sample types when variations within the dose/response trend of a single sample type is larger than observed differences between types (**REFERENCE**).

For animal inhalation studies, meaningful comparison of the relative deposition of asbestos dusts across species is not direct. To extrapolate results across species, the detailed differences in the physiology of the respiratory tracts between the species need to be addressed (Sections 4.4 and 7.1). However, if measurements are available for both species, differences in physiology are addressed, and the manner in which tissue burdens are analyzed is considered, it may be possible to compare relative tissue doses (mass of asbestos per mass of tissue) across species.

5.4 IN-VITRO STUDIES

A broad range of in-vitro studies provide useful insight on the effects of asbestos. These include, for example, studies in cell-free systems (which have been used to evaluate such things as asbestos dissolution rates or the kinetics of free radical formation on the surface of asbestos fibers) and studies of the effects of asbestos on cultures of a broad variety of cell types and tissues.

As with other studies, the potential limitations and sources of uncertainty associated with in-vitro studies need to be considered when evaluating the validity of study results or comparing such results to those of other studies, particular studies of varying type. Also, as with other studies, among the primary sources of uncertainty that need to be addressed for in-vitro studies is the manner in which asbestos doses are characterized and quantified (Section 5.1). For in-vitro studies (as with animal studies dosed by routes other than inhalation), this also extends to the need to consider the relationship between the character of the asbestos dose applied in vitro and the character that a similar exposure might possess following inhalation exposure in vivo (Section 5.3). This can be particularly problematic for studies in tissue cultures because it is not clear how the application of a suspension of fibers (with known concentration) to a dish containing cultured cells can be related to doses that reach corresponding tissues following administration to whole animals.

In-vitro studies, of necessity, represent isolated components of living systems observed under conditions that may vary radically from those under which such components operate in vivo. Consequently, the behavior of such components may also vary radically from the behavior of the same components in vivo. Therefore, additional study-specific considerations (concerning the design of a study and the conditions under which a study is conducted) also need to be addressed before evaluating the validity or relevance of the results from an in-vitro study to what might otherwise be observed in a whole animals. Examples of such considerations include:

- for cell-free systems:
  - whether conditions under which the study is conducted are sufficiently similar to conditions in vivo to expect that the observed effect is likely to occur in vivo; and
  - if the observed variables describing the nature or magnitude of the effect are also likely to reflect what may occur in vivo;

– for tissue cultures:

- whether conditions under which the study is conducted are sufficiently similar to conditions in vivo to expect that the observed effect is likely to occur in vivo;

- whether responses by specific tissues or cells in culture are likely to behave similarly in vivo where their behavior may be suppressed, enhanced, or modified in some other manner due to additional stimuli provided by responses of other tissues and cells that are components of a complete organism but that may be lacking in culture; and

- whether the conditions required to establish and maintain a tissue culture for experimentation sufficiently alters the characteristics and behavior of the cells being studied to minimize the relevance of results from such a study to conditions in vivo.

Among the most important examples of the last consideration relates to the general need to create immortalized cells to maintain tissue cultures. Thus, questions must always be raised concerning whether the alterations required to create immortalized cells for culture (from what are normally mortal cells in vivo) also alter the nature of the responses being studied.

Note, many studies in the current literature also incorporate combined aspects of several of the four general study types described in this chapter. For these studies, a corresponding combination of the considerations described must therefore be addressed when evaluating such studies and comparing their results with inferences derived from the rest of the literature.

6.0 EPIDEMIOLOGY STUDIES

The existing epidemiology studies provide the most appropriate data from which to determine the relationship between asbestos dose and response in humans. As previously indicated, however, due to a variety of methodological limitations (Section 5.1), the ability to compare and contrast results across studies needs to be evaluated to determine the confidence with which risk may be predicted by extrapolating from the "reference" epidemiology studies to new environments where risk needs to be assessed. This requires both that the uncertainties contributed by such methodological limitations and that several ancillary issues (identified in Chapter 2) be adequately addressed.

A detailed discussion of the methodological limitations inherent to the available epidemiology studies was provided in the Health Effects Assessment Update (U.S. EPA 1986) and additional perspectives are provided in this document (Section 5.1). The manner in which the uncertainties associated with these limitations are addressed in this document are described in Appendix A. As previously indicated (Chapter 2), the ancillary issues that need to be addressed include:

- whether the models currently employed to assess asbestos-related risk adequately predict the time-dependence of disease;
- whether the relative in-vivo durability of different asbestos mineral types affect their relative potency;
- whether the set of minerals included in the current definition for asbestos adequately covers the range of minerals that potentially contribute to asbestos-related diseases; and
- whether the analytical techniques and methods used to characterize exposures in the available epidemiology studies adequately capture the characteristics of exposure that affect biological activity.

All but the third of the above issues are addressed in this Chapter. Currently, the third issue can best be addressed by evaluating inferences from the broader literature (see Chapter 7). The remaining issues are addressed separately for lung cancer and mesothelioma following a brief overview of the approach adopted for evaluating the epidemiology literature.

6.1 APPROACH FOR EVALUATING THE EPIDEMIOLOGY LITERATURE

To develop dose/response relationships (and corresponding risk coefficients) for use in risk assessment from epidemiological data, two basic types of information are necessary: information on disease mortality in the study population (cohort) and information on the asbestos exposure experienced by each member of the cohort. So that disease mortality attributable to asbestos can be distinguished from other (background) causes of death, it is also necessary to have knowledge of the rates of mortality that would be expected in the study population, absent exposure. Normally, such information must be determined based on a "reference" or "control" population.

Ideally, one would like to have complete knowledge of exposure at any period of time for each individual in the cohort and complete access to the data in order to fit different types of dose/response models to the data so that the approach for evaluating the relationship between dose and response can be optimized. In most instances, unfortunately, the data suffer from multiple limitations (see Section 5.1 and Appendix A) and the epidemiologist is further constrained by less than complete access to the data.

Briefly, the major kinds of limitations that potentially contribute to uncertainty in the available epidemiology studies (and the effect such limitations likely produce on trends in potency estimates) include:

- limitations in the manner that exposure concentrations were estimated (likely increases random variation across studies);
- limitations in the manner that the character of exposure (i.e. the mineralogical types of fibers and the range and distribution of fiber dimensions) was delineated (likely increases systematic variation between industry types and, potentially, between fiber types);
- limitations in the accuracy of mortality determinations or incompleteness in the extent of tracing of cohort members (likely increases random variation across studies);
- limitations in the adequacy of the match between cohort subjects and the selected control population (likely increases random variation across studies and may have a substantial effect on particular studies); and

- inadequate characterization of confounding factors, such as smoking histories for individual workers (likely increases random variation across studies and may have a substantial effect on particular studies).

More detailed discussion of the above limitations is provided in Section 5.1. The manner in which these limitations are being addressed in this evaluation are described briefly below and in more detail in Appendix A.

The existing asbestos epidemiology database consists of approximately 150 studies of which approximately 35 contain exposure data sufficient to derive quantitative dose/response relationships. A detailed evaluation of 20 of the most recent of these studies, which includes the most recent followup for all of the cohorts evaluated in the 35 studies, based on the considerations presented in this overview, is provided in Appendix A.

Importantly, this new analysis of the epidemiology database differs from the evaluation conducted in the 1986 Health Effects Assessment Update (U.S. EPA 1986). Not only does it incorporate studies containing the latest available followup for the exposure settings previously evaluated and several additional studies addressing new exposure settings, but the manner in which the analysis was conducted incorporates important, new features. These new features include:

- estimation of more realistic confidence bounds for the dose-response factors derived from each study; and

- for the lung cancer model, introducing a parameter, "α", which represents the ratio of the background rate of lung cancer in the cohort relative to the control population.

Confidence bounds were adjusted to account for uncertainty contributed by the manner that exposure was estimated, by the manner that work histories were assigned, and by limitations in the degree of followup, in addition to the traditional practice of accounting for the statistical uncertainty associated with the observed incidence of disease mortality. Thus, most of the major contributors to the overall uncertainty of each study are now addressed, at least in qualitative fashion. A detailed description of how the new confidence bounds were constructed is provided in Appendix A.

Note, in the text of this Chapter, we occasionally refer to significant differences between certain measured or estimated values. When such differences are determined informally (for example, by comparing confidence intervals) they are simply referred to

as "significant." When they are determined formally (by statistical test), they are denoted as "statistically significant."

In this analysis, dose-response coefficients were estimated for each cohort both by requiring that $\alpha = 1$ (the traditional approach) and by allowing α to vary while optimizing the fit of the data. Allowing α to vary addresses such potential problems as differences in the relative fraction of smokers among cohort and controls, respectively, or differences in background cancer rates due to lack of the appropriateness of the selected control population for the cohort. As indicated in Appendix A, such adjustments have a substantial effect on the fit of the EPA model to the data for several specific cohorts and a corresponding effect on the estimates of the lung cancer dose-response coefficients for those cohorts.

To better evaluate the sources of variation in estimated dose-response coefficients observed across the available studies and potentially reconcile such variation so that the precision of asbestos risk assessments might be improved (Sections 6.2 and 6.3), we were also able to obtain the original, raw data for selected cohorts from a limited number of some of the most important of the published epidemiology studies. This allowed us to more formally evaluate the appropriateness of the existing U.S. EPA models for lung cancer and mesothelioma, respectively, and to evaluate the effects of such things as fiber biodurability. The models were evaluated by determining the fit of the models to various representations of the time-dependence of mortality observed in these raw data sets. A biologically based model, the two-stage model developed by Moolgavkar et al. (Moolgavkar and Luebeck 1990) was also fit to the observed time-dependence and contrasted with results from the U.S. EPA models.

Separately, we also completed an evaluation to consider questions concerning the appropriateness of the range of fiber sizes characterized in the published epidemiology studies and whether adjusted exposure indices might improve the quality of asbestos risk assessments.

6.2 LUNG CANCER

The Airborne Health Effects Assessment Update (U.S. EPA 1986) utilizes a model for lung cancer in which the asbestos-related age-specific incidence of lung cancer, "t" years from onset of exposure, is proportional to cumulative asbestos exposure at time t-10 years, multiplied by the age and calendar year incidence of lung cancer in the absence of asbestos exposure. A linear relationship between cumulative dose and response was assumed based on the ten epidemiology studies identified (in the 1986

EPA document) as containing sufficient information to establish a dose/response curve for asbestos induced lung cancer:

$$I_L = I_E[1+K_L \cdot f \cdot d_{(t-10)}] \qquad (6.1)$$

where:

"I_L" is the overall incidence of lung cancer (expected new cancers per year per person) adjusted for age and calendar year;

"I_E" is the corresponding cancer incidence in a population not exposed to asbestos;

"f" is the concentration of asbestos (expressed as PCM fibers longer than 5 µm in the existing evaluations of the published epidemiology data);

"t" is the time since onset of exposure in years;

"$d_{(t-10)}$" is the duration of exposure excluding the most recent 10 years; and

"K_L" is the proportionality constant between dose and response. This is the risk coefficient that represents the potency of asbestos.

The above model is a relative risk model in that it assumes that the excess incidence of lung cancer from asbestos is proportional to the incidence in an unexposed population. Since smokers have a much higher incidence of lung cancer, if smoking-specific incidence rates are applied, the model predicts a higher excess incidence of asbestos-related lung cancer in smokers than in non-smokers. This is consistent with the multiplicative relationship between smoking and asbestos that has been observed in epidemiological studies (see, for example, Hammond et al. 1979). Note that the K_L in the model pertains to an occupational pattern of exposure (e.g., 8 hours per day, 240 days per year) and must be modified before application to environmental exposure patterns.

Equation 6.1 is generally written as follows to indicate that K_L is a proportionality constant between dose and response:

$$K_L(f)(d') = RR-1 \qquad (6.2)$$

where:

"RR" is the relative risk and is equal to (I_L/I_E) and d' is now the duration excluding the final 10 years before observation of total lung cancer deaths.

6.2.1 The Adequacy of the Current EPA Model for Lung Cancer

Access to the raw epidemiology data from a small number of key studies allowed us to evaluate the adequacy of the EPA model for describing the time-dependence for lung cancer in asbestos exposed cohorts. For this analysis, the raw data for the cohort of crocidolite miners in Whittenoom, Australia was graciously provided by Nick DeKlerk (unpublished) and the raw data for the cohort of chrysotile textile workers (described by Dement et al. 1994) was graciously provided by Terri Schnorr of NIOSH. The Whittenoom cohort was originally described by Armstrong et al. (1988), but the data provided by DeKlerk included additional followup through 1999.

The EPA lung cancer model was fit to the raw data from both South Carolina and Wittenoom. In these analyses, each person-year of followup was categorized by cumulative exposure defined using a lag of 10 years, in accordance with the EPA lung cancer model. The data were then grouped into a set of cumulative exposure categories and the observed and expected numbers of lung cancers were computed for each category. For South Carolina, expected numbers were based on sex-race-age- and calendar-year-specific U.S. rates and separate analyses were conducted for white males, black males, and white females, as well as for the combined group. For Wittenoom expected rates were based on age- and calendar-year-specific rates for Australian men. These data were also categorized by cumulative exposure lagged 10 years. The resulting fit of the EPA model to the data from Wittenoom and South Carolina are presented in Tables 6-1 and 6-2, respectively.

The data in these tables were fit assuming that the observed cancers in each cumulative exposure category had a Poisson distribution with mean response equal to the expected response in the comparison population times α $(1 + K_L{*}CE_{10})$, where the linear slope, K_L, is the "lung cancer potency factor" in the EPA lung cancer model, and CE_{10} is the mean cumulative exposure for a category computed using a lag of 10 years.

For the Wittenoom data (Table 6-1), the fit with $\alpha = 1$ is poor ($p < 0.0001$), as the model overpredicts the number of cancers in the highest exposure category and greatly underpredicts at lower exposures. By contrast the fit of the model with α variable is adequate ($p = 0.1$). This model predicts a high background of lung cancer in this cohort ($\alpha = 2.1$) and a fairly shallow slope, with the relative risk increasing only from 2.1 at background to 3.6 in the highest exposure category. A test of the hypothesis that $\alpha = 1$

for this cohort is rejected ($P < 0.01$) and the model fit to the data (with α variable) predicts $K_L = 0.0047$.

The fit of the EPA model to the South Carolina lung cancer data categorized by cumulative exposure is shown in Table 6-2. The model with $\alpha = 1$ cannot be rejected both when the model is applied to white males only ($p = 0.54$) or with all data combined ($p = 0.92$). Since the values α and K_L estimated from white males only are similar to those estimated using the complete cohort (black and white males and white females), the fit to the complete data is emphasized in this analysis. This model fit to the data predicts $\alpha = 1.2$ and $K_L = 0.021$ $(f/ml\text{-}y)^{-1}$. A test of the hypothesis that $\alpha = 1$ for this cohort cannot be rejected ($P = 0.21$).

Table 6-1

Table 6-1:
Fit of EPA Lung Cancer Model to Observed Mortality Among Wittenoom Miners Categorized by Cumulative Exposure

Mean Cumulative Exposure Lagged 10 years (f· yr)/cc	Cases		Predicted		Log Likelihood
	Observed	Expected	(α = 1)	(α variable)	
0	5	4.6	4.6	9.8	-3.8
0.193	27	7.9	8.0	17.0	-4.1
0.692	11	8.2	8.3	17.6	-4.4
1.59	22	11.6	12.1	24.9	-3.1
3.27	28	12.9	14.0	27.9	-2.7
6.19	38	14.3	16.7	31.4	-3.0
11.8	31	13.2	17.4	29.8	-2.6
21.5	21	9.2	14.5	21.6	-2.5
41.1	25	11.6	24.5	29.6	-2.7
142	43	11.6	56.5	41.6	-6.4
Totals	251	105.1	176.6	251.0	-35.1
Goodness of Fit P-value			1.3316E-13	0.10	

Test of H_0: α=1
$p < 0.01$

Estimates of K_L $((f\text{-}yr)/cc)^{-1}$
(α = 1)
$K_L = 0.027$
90% CI = (0.020, 0.035)

(α variable)
$K_L = 0.0047$
90% CI = (0.0017, 0.0087)

Table 6-2:
Fit of EPA Lung Cancer Model to Observed Mortality Among South Carolina Textile Workers Categorized by Cumulative Exposure

Cumulative Exposure Lagged 10 years (f-yr)/cc		Cases		Predicted		Log
Mean	Range	Observed	Expected	($\alpha = 1$)	(α variable)	Likelihood
0.00	0	0	0.88	0.88	1.06	-1.06
0.35	[0.0, 0.5)	4	2.64	2.67	3.23	-1.72
0.75	[0.5, 1.0)	7	5.51	5.63	6.78	-1.91
1.66	[1.0, 2.5)	10	9.66	10.12	12.11	-2.27
3.37	[2.5, 4.5)	13	7.89	8.65	10.23	-2.55
6.23	[4.5, 8.5)	11	7.69	9.05	10.53	-2.14
11.80	[8.5, 16)	11	7.20	9.61	10.86	-2.13
21.28	[16, 28)	8	5.26	8.43	9.20	-2.05
41.49	[28, 60)	14	6.34	13.80	14.33	-2.25
69.17	[60, 80)	9	3.03	8.98	8.97	-2.03
93.28	[80, 110)	10	2.95	10.76	10.53	-2.09
173.36	(>= 110)	25	4.32	25.56	24.17	-2.55
Totals		122	63.36	114.14	122.00	
Goodness of Fit P-value				0.92	0.96	

Test of H_0: α=1
p = 0.21

Estimates of K_L ((f-yr)/cc)$^{-1}$
($\alpha = 1$)
K_L = 0.028
90% CI = (0.021, 0.037)

(α variable)
K_L = 0.021
90% CI = (0.012, 0.034)

Table 6-2

6.2.1.1 Time Dependence

The EPA model was next evaluated to determine whether it adequately describes the time-dependence of the mortality observed in the Wittenoom and South Carolina cohorts. The model predicts that relative risk will remain constant following 10 years from the time of last exposure.

Table 6-3, shows the fit of the EPA model to the Wittenoom data categorized by time since last exposure. In each category of time since last exposure, the number of lung cancer deaths are predicted by the EPA model using the parameter values calculated in Table 6-1, based on the expected cancers and the average cumulative exposure for each category. This categorization allows investigation of the assumption inherent in the EPA model that the relative risk remains constant following 10 years from last exposure. The Wittenoom data appear to be consistent with this assumption, as the excess relative risk per f/ml-y of cumulative exposure varies only between 0.059 and 0.073 for categories representing more than ten years from last exposure.

The conclusion that relative risk remains constant following 10 years from last exposure among Wittenoom miners is further illustrated in Figure 6-1. Figure 6-1 is a plot of the quantity: (relative risk - α)/(cumulative exposure) versus time since last exposure. Based on the modified form of the EPA model (in which α is allowed to vary), this quantity, $(RR-\alpha)/(CE_{10})$, should be constant and equal to $\alpha^{*}K_L$ (beyond 10 years from last exposure). Figure 6-1 demonstrates that this is exactly the behavior observed among Wittenoom miners, where the value of the quantity plotted on the Y-axis rises rapidly until 10 years after exposure ends and then remains constant for all longer times. Moreover, a test of the hypothesis that the slope of the data depicted in Figure 6-1 (beyond 10 years after the end of exposure) differs from zero cannot be rejected

Because it has been reported that asbestos fibers (especially chrysotile but including amphiboles) dissolve in biological fluids and that animal studies suggest that the tumorigenicity of fibers is proportional to in-vivo durability (Section 7.2.4), the Wittenoom data categorized by time since last exposure was also fit to a modification of the EPA lung cancer model in which the cumulative exposure variable is replaced by an estimate of internal dose derived assuming first-order clearance of fibers. Results are presented in Table 6-4

In developing Table 6-4, a preliminary investigation, based upon an "exact" likelihood that did not involve categorization of exposures, indicated that this model provided a best fit using a half-life of 11 years and a lag of 12 years. As this table indicates,

despite optimizing the model with respect to the lag and half-life, it did not fit the data as well as the standard EPA model based upon cumulative number of inhaled fibers. Thus, there is no evidence from the Wittenoom data that crocidolite fibers degrade (or

Table 6-3

Table 6-3:
Fit of EPA Lung Cancer Model to Observed Mortality Among Wittenoom Miners Categorized by Time Since Last Exposure

Time Since Last Exposure		Cumulative Exposure Lagged			Predicted		Excess relative risk per
Mean (Yrs)	Range (Yrs)	10 years (f-Yr)/cc	Cases	Expected	(α = 1)	(α variable)	f/ml-y
0.267	[0 - 1]	1.18	0	0.64	0.658	1.368	-0.8505
3.01	[1 - 5]	1.23	1	1.60	1.652	3.432	-0.3042
7.49	[5 - 10]	7.68	8	3.93	4.750	8.698	0.1347
14.9	[10 - 20]	24.43	45	18.39	30.557	43.792	0.0592
24.7	[20 - 30]	22.48	96	36.41	58.584	86.002	0.0728
34.0	[30 - 40]	21.12	81	34.20	53.766	80.306	0.0648
43.6	[40 - 1000]	16.62	20	9.91	14.376	22.828	0.0612
Totals			251	105.08	164.342	246.427	
Goodness of Fit				**Chi sq**	43.2811	6.7165	
				P value	3.24E-08	0.152	

Using Australian Mortality Rates

Table 6-4:

Fit of EPA Lung Cancer Model to Observed Mortality Among Wittenoom Miners Categorized by Time Since Last Exposure with Cumulative Exposure Replace by Internal Dose

Time Since Last Exposure (Yrs)	Internal Dose	Cases			EPA model (α variable)	Log Likelihood
		Observed	Expected	Predicted		
0	15.8	0	0.5	1.2	1.4	-1.16
(0 - 5)	18.4	0	1.5	3.8	3.4	-3.82
[5 - 10)	19.9	5	3.6	9.7	8.7	-3.13
[10 - 20)	9.1	42	17.5	41.3	43.8	-2.80
[20 - 30)	6.4	91	35.7	81.6	86.0	-3.69
[30 - 40)	4.2	88	35.4	79.0	80.3	-3.65
[40 - 100)	1.7	25	11.0	23.7	22.8	-2.57
Totals		251	105.1	240.3		-20.81
Goodness of Fit			**Chi sq**	14.83	6.72	
			***P* value**	0.01	0.15	

Figure 6-1:
Plot of [(RR - alpha)/(CE10)] vs. Time Since Last Exposure for Wittenoom Miners

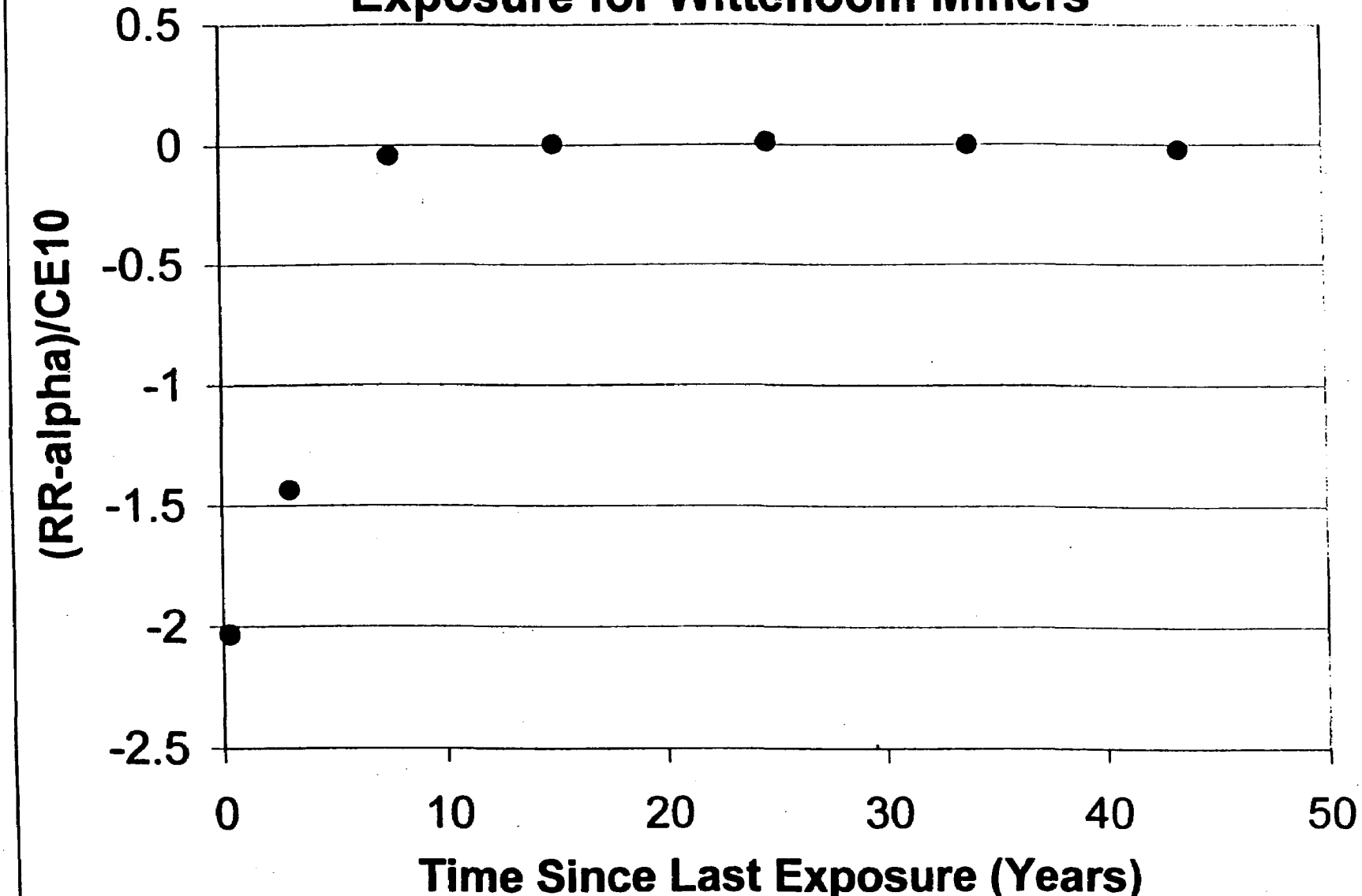

that the effects of crocidolite fibers are diminished) in vivo over time scales that are short relative to a human life time and this is consistent with the data presented in Section 7.2.4 that suggest crocidolite fibers likely last many decades in human lungs, at a minimum. It is also consistent with the appearance of Figure 6-1, which shows no decrease in the effect of crocidolite following cessation of exposure.

Table 6-5 shows the fit of the EPA model to the South Carolina data categorized by time since last exposure. This table was constructed in the same manner as Table 6-3. In contrast to the data from Wittenoom, the time dependence of the South Carolina data cannot be adequately fit with the EPA model, whether α is held equal to one ($P < 0.0001$) or allowed to vary ($P < 0.0007$). A plot of $(RR-\alpha)/CE_{10}$ versus time (Figure 6-2) indicates why.

In Figure 6-2 (as with the Wittenoom data), the quantity plotted on the Y-axis increases sharply to a maximum at approximately 10 years following the end of exposure. In contrast to what is observed for Wittenoom, however, the value of this quantity decreases with time beyond the first 10 years following the end of exposure. This decrease is clear from the figure, despite some scatter in the data. Thus, in contrast to the assumption inherent to the EPA model, relative risk decreases precipitously in this cohort after 10 years following the cessation of exposure. This suggests that the effects of chrysotile are somehow diminished after long periods of time.

There are several reasonable hypotheses that might explain the decrease in relative risk with time within the South Carolina cohort. Among those that have attracted interest is the possibility that risk is a function of biodurability (for example, see Section 7.2.4). We therefore decided to explore this possibility.

Given that the expected lifetime for respirable chrysotile fibers in biological fluids is anticipated to be only on the order of a year (see Section 7.2.4), further analysis of the decreasing trend observed in Figure 6-2 is warranted. Therefore, the South Carolina data were also fit using the modified form of the EPA model that accounts for internal dose (rather than cumulative exposure). In this model, as indicated above, the internal dose is derived from cumulative exposure, except it is assumed that, from the moment that a fiber is deposited in the lung, it dissolves by a first order process. Actually, the best analysis of the dissolution process indicates that it is likely zero order, but the first order decay (see Section 7.2.4) is assumed as an approximation because this provides an easier description of the lifetime of the material.

Table 6-5

Table 6-5:
Fit of EPA Lung Cancer Model to Observed Mortality Among South Carolina Textile Workers Categorized by Time Since Last Exposure

Time Since Last Exposure		Cumulative Exposure Lagged			Predicted		Log Likelihood		Excess relative risk per
Mean (Yrs)	Range (Yrs)	10 Years (f-yr)/cc	Cases	Expected	($\alpha = 1$)	(α variable)	($\alpha = 1$)	(α variable)	(f-yr)/cc
0.06	[0 - 1)	21.97	15	4.1	6.7	7.2	-6.1	-5.4	0.12
3.00	[1 - 5)	14.73	7	2.2	3.1	3.5	-3.7	-3.3	0.15
7.50	[5 - 10)	18.51	14	3.5	5.4	6.0	-7.0	-6.2	0.16
14.84	[10 - 20)	16.38	11	7.4	10.9	12.1	-2.1	-2.2	0.03
24.60	[20 - 30)	11.05	28	12.2	16.1	18.2	-6.2	-4.8	0.12
34.65	[30 - 40)	8.93	28	20.0	25.1	28.8	-2.8	-2.6	0.04
43.49	[40 - 100)	7.32	19	13.8	16.7	19.3	-2.5	-2.4	0.05
Totals			122	63.4	84.0	95.1	-30.4	-26.9	
Goodness of fit				Chi sq	28.5	21.5			
				P value	0.0001	0.0007			

Figure 6-2:
Plot of [(RR-alpha)/(CE10)] vs. Time Since Last Exposure for South Carolina Textile Workers

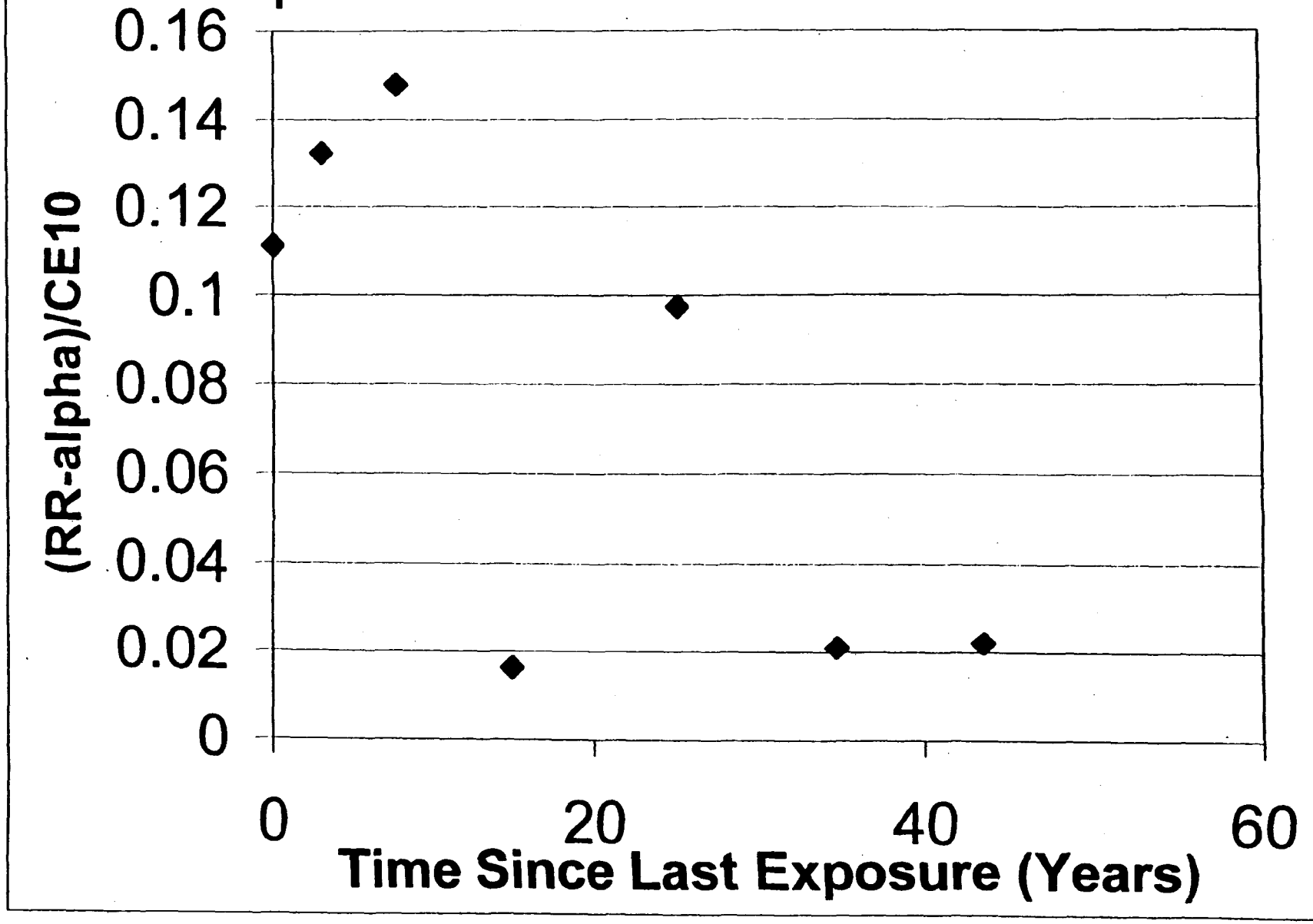

Figure 6-2

Table 6-6 shows the fit to the South Carolina data to the EPA model using internal dose. This Table was derived from the South Carolina data in the same manner that Table 6-4 was derived from the Wittenoom data. Since data appeared to be about equally consistent with a range of lags and half-lives, for consistency, the same values were used as with the Wittenoom data. This table indicates that this model provides an adequate fit to the South Carolina data (P = 0.16).

Assuming a first order decay process, the best fit trend line to the data beyond 10 years following cessation of exposure in Figure 6-2 suggests a half-life for chrysotile of approximately 20 years. A similar analysis of the Whittenoom data suggests a half-life for crocidolite that is > 700 years, which is no different than infinity.

Although this is in stark contrast to the dissolution half-life for chrysotile fibers estimated based on in-vitro data, these results may not be inconsistent. There are at least two reasonable explanations for this apparent discrepancy. First, the data in Figure 6-2 track the risk attributable to the presence of chrysotile, not the presence of chrysotile itself. It is therefore reasonable that, even if the chrysotile fibers disappear readily, the risk from their initial presence may decay only much more slowly; the biological changes induced by the initial presence of the fibers may persist.

Second, as indicated in the in-vitro studies (see Section 7.2.4), the dissolution rate of chrysotile is limited by the rate at which fluid flows past the material. The maximum dissolution rate (i.e. the rate reported in the in-vitro studies) is observed only when flow is adequate. Otherwise, partial saturation of the solution surrounding the chrysotile fibers will slow the dissolution rate until it is only a fraction of what is observed in the optimally designed studies. Therefore, that a slower dissolution rate is suggested by the South Carolina data may simply indicate that the various biological compartments in which the biologically active fibers are located do not allow for adequate flow of an adequate reservoir of biological fluids to maintain the dissolution rate at its theoretical maximum.

An alternate hypothesis is that the fibers are not dissolving at all but are simply being sequestered in some manner that reduces their biological activity with time. Such a hypothesis, however, does not appear consistent with the animal data that suggests that tumorigenicity is indeed a function of the in-vivo durability of fibrous materials (see Section 7.2.4). However, other hypotheses may also reasonably explain the data. Therefore, although relative risk clearly decreases with time after cessation of exposure among the South Carolina workers and such observations are not inconsistent with the possibility that this is an effect of biodurability, it is premature to conclude such a link without further study.

Table 6-6:

Fit of EPA Lung Cancer Model to Observed Mortality Among South Carolina Textile Workers Categorized by Time Since Last Exposure with Cumulative Exposure Replace by Internal Dose

Time Since Last Exposure		Internal	Cases			EPA model	Log
Mean (Yrs)	Range (Yrs)	Dose	Observed	Expected	Predicted	(α variable)	Likelihood
0	0	16.4	12	3.8	8.6	7.2	-2.77
3	(0 - 5)	18.9	10	2.1	5.1	3.5	-3.95
7	[5 - 10)	20.8	11	3.4	8.4	6.0	-2.48
14	[10 - 20)	15.1	13	7.5	16.4	12.1	-2.59
25	[20 - 30)	10.8	25	11.9	23.1	18.2	-2.61
35	[30 - 40)	5.9	27	19.9	33.5	26.8	-3.24
45	[40 - 100)	4.7	23	14.8	23.9	19.3	-2.51
Totals			121	63.5	119.0	95.1	-20.14
Goodness of Fit				**Chi sq**	7.94	21.5	
				P value	0.16	0.0007	

Importantly, the time-dependent behavior described above for crocidolite and chrysotile are each based on analysis of data from only a single study. Thus, although such trends are also consistent with additional evidence from animal studies and other implications from the literature, it would be useful to confirm these observations by analyzing additional raw epidemiology data sets. If they can be acquired, the raw data from Libby may serve as a second example for amphiboles and the lung cancer data from Quebec may serve as a second example for chrysotile.

6.2.1.2 Comparison with biologically-based model

To further evaluate the behavior of the EPA model, results were compared with those of a biologically based (two-stage) model.

Definition of the two-stage model. The two-stage model of cancer implemented in this report (Moolgavkar and Luebeck, 1990) assumes that there is a population of normal cells under homeostatic control whose size remains fixed at X. A normal cell mutates at a given rate to an intermediate cell. (Mathematically, intermediate cells are generated according to a non-homogeneous Poisson process with intensity v, which implies that the per-cell mutation rate is v/X. For a given value of v the hazard function does not depend upon X and, without loss of generality, X was fixed at 10^7 cells.) An intermediate cell divides into two intermediate cells at a rate α, dies at a rate β, and divides into one intermediate and one malignant cell at a rate μ. (Mathematically, a clone of intermediate cells is a non-homogeneous birth, death and mutation process.) Importantly, the "α" in this model is in no way related to the "α" variable used to adjust for background mortality in the EPA lung cancer model and the two should not be confused.

The mortality hazard function (rate of dying of cancer at age t among persons who survive to that age) is assumed to be the hazard for the occurrence of the first malignant cell, with a delay of L years. That is, the mortality hazard at t years of age is assumed to be h(t-L), where h is the hazard for the occurrence of the first malignant cell. Thus, L represents the delay between the occurrence of the first malignant cell and the subsequent death from the resulting cancer. Following the assumption of Doll and Peto (1978) and Moolgavkar *et al.* (1993), a lag of L = 4 years was generally assumed. We note that the lag in this model is conceptually different from the lag of ten years used in the EPA models. Whereas the lags in the latter model were empirically derived based on goodness of fit, the lag in the two-stage model has a mechanistic interpretation and, consequently, should not necessarily have the same value.

To introduce the effect of exposure to asbestos into the model, one or more of the parameters ν, α, β or μ were assumed to be linear functions of the instantaneous whole-body fiber burden, d(t), where t indicates age:

$$\nu(t) = \nu_0 + \nu_1 * d(t),$$

$$\alpha(t) = \alpha_0 + \alpha_1 * d(t),$$

$$\beta(t) = \beta_0 + \beta_1 * d(t),$$

$$\mu(t) = \mu_0 + \mu_1 * d(t).$$

The hazard function, h(t) and the corresponding survival function (probability of surviving to age t without death from lung cancer in the absence of competing causes of death), $S(t) = \exp(-\int_0 h(s)ds$, predicted by this model, although mathematically complex, can be solved for explicitly whenever the parameters are piecewise constant (Moolgavkar and Luebeck, 1990; Heidenreich *et al.*, 1997).

In application of this model to lung cancer (and mesothelioma) data from Wittenoom, South Carolina, and Quebec: the fiber body burden, d(t), was computed (up to a multiplicative constant) from a subject's exposure pattern, assuming a first-order elimination process with an elimination rate of r (half-life of -Ln(.5)/r). In these calculations, an average exposure rate during work hours was computed for each year of work. Based on the first-order assumption, the body burden at time t resulting from exposure to an average of f f/ml during the year between s and s+1 is

$$\begin{aligned} d(t) &= (f/r)[1 - \exp(-r(t-s)] && \text{for } t \le s+1 \\ &= (f/r)[1 - \exp(-r)]\exp[-r(t-s-1)] && \text{for } t > s+1. \end{aligned}$$

This expression does not include the multiplicative constant needed to convert from the air concentration of asbestos to internal deposition rate, but without loss of generality is assumed to be included in the parameters μ_1, α_1, β_1, and ν_1.

The average body burden between t and t+1 years due to exposure between s and s+1 years was computed by integrating this expression from t to t+1. The average body burden during each year was then computed by summing the contributions to the average from each year (by summing over $s \le t$). The body burden d(t) was approximated by the step function formed by these yearly average body burdens. With this approximation the two-stage parameters $\nu(t)$, $\alpha(t)$, $\beta(t)$ and $\mu(t)$ are piecewise constant and the exact solution to the two-stage model for this case (Heidenreich *et al.*,

1997) was used to calculate the hazard, h(t) and survival function, S(t). This calculation was made using a FORTRAN subroutine kindly provided by Drs. Suresh Moolgavkar and Georg Luebeck.
This model was fit to the raw lung cancer and mesothelioma data from Wittenoom and South Carolina, and to the raw mesothelioma data from Quebec using the method of maximum likelihood. The contribution to the likelihood for a subject who began work at age t_0 and died of cancer at age t_1 was $h(t_1)*S(t_1)/S(t_0)$, and the corresponding expression for a subject whose followup ended at t_1 without resulting in death from cancer was $S(t_1)/S(t_0)$. The complete likelihood was computed as the product of these individual contributions. The software program, MINUIT, developed by CERN in Geneva, was used to maximize the log-likelihood.

The full two-stage model described above has eight parameters (nine if the elimination rate, r, is included), which is too many to be estimated reliably using the epidemiologic data available. Moreover, the general model is not fully identifiable, as different combinations of parameters can lead to the same hazard (Heidenreich *et al.*, 1997). Accordingly, in applications of this model, not all of the parameters were estimated independently. For example, in most cases only one of the two-stage parameters (v, α, β, μ) was allowed to be dose-related. Also, to reduce the number of estimated parameters, in most cases either α or β was fixed at zero, because, when the mortality rate is low, h(t) is practically a function of the difference between these two parameters. Also, the elimination rate, r, was not estimated from the epidemiologic data, but was determined from evidence on the durability of different types of asbestos fibers (see Section 7.2.4).

Although the parameters in the two-stage model at least nominally represent physiological phenomena, it must be realized that the model is, at best, likely to be a highly idealized representation of a very complex process (see Section 7.3.1). Accordingly, the results from this model are probably best used to investigate the relative contributions to risk from exposures at different ages (e.g., if the model predicts that v is dose-related, then earlier exposures are more important in determining risk, whereas if the model predicts that μ is dose-related, then more recent exposures are more important). Moreover, if the model predicts that v is dose-related, the offending toxic substance can be considered to be acting as a classical initiator; if α (or, more precisely, α - β) is dose-related, the toxic substance is more likely a promoter. If μ is dose related, the toxin is likely a late-stage actor, which also would present different behavior than an initiator. An important advantage of the two-stage model is that, since it models risk as a function of internal dose, it can naturally incorporate consideration of fiber clearance.

Applying the two-stage model to lung cancer. Table 6-7 summarizes the results of three applications of the two-stage model to the lung cancer data from Wittenoom, and

Table 6-8 summarizes a similar application of the model to the South Carolina lung cancer data. With each set of data, the model is fit allowing either ν, α, or μ to be a linear function of the fiber body burden. In keeping with the half-life estimates based on the durability of chrysotile and amphibole fibers in Section 7.2.4, for the South

Table 6-7:
Results of Three Applications of the Two-Stage Model to the Lung Cancer Data from Wittenoom (Assumed Half-life: 20 yrs)

Parameter	Application 1		Application 2		Application 3	
	Fitted Value	Standard Error	Fitted Value	Standard Error	Fitted Value	Standard Error
$\alpha 0$	0.106	0.00535	0.345	0.0071	0.338	0.00782
$\alpha 1$	0	fixed	0.000754	0.000301	0	fixed
$\beta 0$	0	fixed	0	fixed	0	fixed
$\beta 1$	0	fixed	0	fixed	0	fixed
$\nu 0$	2.03	0.304	0.00669	0.000682	0.00744	0.000774
$\nu 1$	0.474	0.223	0	fixed	0	fixed
$\mu 0$	2.03E-07	3.04E-08	6.69E-10	6.82E-11	7.44E-10	7.74E-11
$\mu 1$	0	fixed	0	fixed	2.57E-11	1.76E-11
X	1.00E+07	fixed	1.00E+07	fixed	1.00E+07	fixed
Log Likelihood	-1669.29		-1642.19		-1642.33	
Predicted Cancers	235.6		240.9		240.7	

Table 6-8:
Results of Three Applications of the Two-Stage Model to the Lung Cancer Data from South Carolina (Assumed Half-life: 0.5 yrs)

Parameter	Application 1		Application 2		Application 3	
	Fitted Value	Standard Error	Fitted Value	Standard Error	Fitted Value	Standard Error
$\alpha 0$	0.100	0.00815	0.0964	0.00725	0.107	0.00795
$\alpha 1$	0	fixed	0.00610	0.00115	0	fixed
$\beta 0$	0	fixed	0	fixed	0	fixed
$\beta 1$	0	fixed	0	fixed	0	fixed
$v0$	1.63	0.385	2.07	0.418	1.61	0.375
$v1$	20.3	5.77	0	fixed	0	fixed
$\mu 0$	1.63E-07	3.85E-08	2.07E-07	4.18E-08	1.61E-07	3.75E-08
$\mu 1$	0	fixed	0	fixed	8.13E-08	3.05E-08
X	1.000E+07	fixed	1.000E+07	fixed	1.000E+07	fixed
Log Likelihood	-825.4		-830.9		-832.9	
Predicted Cancers	114.8		113.9		115.3	

Carolina data, the half-life of internally deposited fibers was assumed to be 0.5 years (r = -ln(0.5)/20 = 1.39/year) and, for the Wittenoom data, the half-life was assumed to be 20 years (r = 0.035/year).

Note that these analyses were completed before the analysis of the time-dependence of the data using the EPA model, so that we did not have the opportunity to go back and run this biological model using half-lives that might better represent what has been observed with the time-dependence of the Wittenoom and South Carolina data (Section 6.2.1.1). However, now that we have developed an approach that allows evaluation of the time-dependence of lung cancer mortality based on estimates of internal dose using the EPA model, further analysis using the two-stage model may not be warranted (see Section 6.3.1).

When applied to the Wittenoom data the model provided comparable descriptions of the data (i.e., similar likelihoods) when either the proliferation rate of intermediate cells, α, or the mutation rate of intermediate cells, μ, was assumed to be dose related. These models provided a much larger likelihood than the model in which the mutation rate of normal cells, ν, was assumed to be dose-related. Note that the "likelihoods" reported in the table are "negative likelihoods" so that the smaller the number in the table, the larger the actual likelihood.

Table 6-9 shows the fit of the best-fitting 2-stage model to the Wittenoom data categorized by time since last exposure, compared to the fit of the EPA lung cancer model. As this Table shows, the simpler EPA model fits these data better than the 2-stage model, although the fit of both models is adequate (lack of fit p-value = 0.12 for 2-stage model and 0.35 for EPA model).

The above indicates that the best-fitting model runs for Wittenoom adequately describe the time-dependence for lung cancer and further indicate that asbestos primarily affects α (and potentially μ). This suggests that crocidolite may be acting primarily as a promoter (or at least a late-stage actor) rather than an initiator toward the induction of lung cancer, which is consistent with inferences from several recent in-vitro studies (Section 7.3.3.4 and 7.3.4.7) and a recent retrospective cohort study of retired workers (Sanden et al. 1992).

Table 6-10 shows the fit of the 2-stage model (in which ν, the mutation rate from normal to intermediate cells is dose-related, i.e. the best-fitting model) to the totality of the South Carolina data categorized by time since last exposure, compared to the fit of the EPA model. Although the 2-stage model fits the data only marginally well ($p = 0.05$), it fits the data much better than the EPA model ($p < 0.001$). The EPA model underpredicts the number of cases for short times since end of exposure.

Table 6-9:

Fit of the Best-fitting Two-Stage Model to the Wittenoom Lung Cancer Data Categorized by Time Since Last Exposure (Assumed Half-life: 20 yrs)

Time Since Last Exposure		Hazard	Cases		EPA	Log	EPA Log
Mean (Yrs)	Range (Yrs)		Observed	Predicted	(α variable)	Likelihood	Likelihood
0.3	[0 - 1)	0.00013	0	1.3	1.4	-1.35	-1.37
3.0	[1 - 5)	0.00016	1	3.3	3.4	-2.13	-2.20
7.5	[5 - 10)	0.00035	8	8.6	8.7	-2.01	-2.00
14.9	[10 - 20)	0.00092	45	41.7	43.8	-2.95	-2.84
24.7	[20 - 30)	0.0024	96	88.5	86.0	-3.51	-3.76
34.0	[30 - 40)	0.0047	81	91.4	80.3	-3.73	-3.12
43.6	[40 - 100)	0.0084	20	21.6	22.8	-2.48	-2.60
Totals			251	258.7	246.9	-18.16	-17.89
Goodness of Fit		**Chi sq**		7.26	6.72		
		P value		0.12	0.35		

Table 6-10:

Fit of the Best-fitting Two-Stage Model to the South Carolina Lung Cancer Data Categorized by Time Since Last Exposure (Assumed Half-life: 0.5 yrs)

Time Since Last Exposure			Cases		EPA	Log	EPA Log
Mean (Yrs)	Range (Yrs)	Hazard	Observed	Predicted	(α variable)	Likelihood	Likelihood
0.06	[0 - 1)	0.00055	15	12.9	7.2	-2.43	-5.43
3.0	[1 - 5)	0.00060	7	6.1	3.5	-1.97	-3.25
7.5	[5 - 10)	0.00080	14	9.7	6.0	-3.06	-6.17
14.8	[10 - 20)	0.00089	11	19.3	12.1	-4.23	-2.18
24.8	[20 - 30)	0.0012	28	21.4	18.2	-3.51	-4.83
34.6	[30 - 40)	0.0024	28	30.7	28.8	-2.71	-2.60
43.5	[40 - 100)	0.0044	19	24.0	19.3	-2.96	-2.40
Totals			122	124.2	95.1	-20.88	-26.86
Goodness of Fit			**Chi sq**	9.52	21.47		
			P value	0.05	0.0015		

The results with the South Carolina data provide a stark contrast to the Wittenoom results. With the South Carolina data, the model with v dose-related provided the best fit. Thus, the results from South Carolina suggest that chrysotile may be acting primarily as an initiator. Such an interpretation must be tempered, however, by several inconsistencies and potential problems with the South Carolina fits that may be attributed, among other possibilities, to the short half-lives assumed for chrysotile.

The two fits (for South Carolina and Wittenoom) also provide very different estimates of the background parameters (ν_0, α_0 and μ_0). The μ_0 and ν_0 estimated from the South Carolina data both are about 250 times larger than those estimated from the Wittenoom data. Although these rates could differ somewhat in these cohorts, owing to different lifestyles and genetic traits in the two populations, these differences appear too large to be attributable to such causes.

Due to the apparently conflicting results from the analyses of the lung cancer data from Wittenoom and South Carolina, we conducted several additional analyses to attempt to identify the source of the apparent conflict. We initially explored the possibility that the assumed half-life for crocidolite was too long and completed additional model runs assuming a 0.5 yr half-life (identical to what was assumed for South Carolina) and these results are described below. Subsequently, we discovered during our analysis of time-dependence using the EPA model (see Section 6.2.1.1), that the half-lives measured in vitro for these fibers are likely much too short, which suggests a solution to the apparent conflict and this is also described below. Unfortunately, however, this revelation came too late to allow additional, confirmatory runs with the two-stage model to be completed in time for this report. Therefore, the apparent conflict between the Wittenoom and South Carolina results (at least with regard to the two-stage model) remains to be definitively resolved.

The results of the two-stage model are based on the assumption that one of the two-stage parameters is a linear function of the instantaneous body burden predicted by a first order retention model that relies on dissolution lifetimes for the asbestos fibers that are observed in vitro (Section 7.2.4). Alternately, it could be the case that an inhaled fiber is soon neutralized in some manner (e.g. by some type of sequestration mechanism) so that any contribution to cancer induction must occur soon after exposure. To explore this possibility, the two-stage model was also fit to the Wittenoom data assuming a half-life of only 0.5 year (the same value used for the South Carolina cohort) and results are indicated in Table 6-11.

When the Wittenoom data are evaluated assuming a fiber half-life of 0.5 yrs, as was the case using a 20-year half life, the best-fitting of the three submodels considered was the one with α dose-related. This fit using this submodel was not appreciably worse than that obtained assuming a 20-year half life (difference in likelihoods of 1.16).

Table 6-11

Table 6-11:
Results of Three Applications of the Two-Stage Model to the Lung Cancer Data from Wittenoom (Assumed Half-life: 0.5 yrs)

Parameter	Application 1		Application 2		Application 3	
	Fitted Value	Standard Error	Fitted Value	Standard Error	Fitted Value	Standard Error
$\alpha 0$	0.106	0.00533	0.342	0.00739	0.349	0.00730
$\alpha 1$	0	fixed	0.00856	0.00439	0	fixed
$\beta 0$	0	fixed	0	fixed	0	fixed
$\beta 1$	0	fixed	0	fixed	0	fixed
$\nu 0$	2.01	0.302	0.00717	0.000731	0.00692	0.000707
$\nu 1$	4.66	2.21	0	fixed	0	fixed
$\mu 0$	2.01E-07	3.02E-08	7.17E-10	7.31E-11	6.92E-10	7.07E-11
$\mu 1$	0	fixed	0	fixed	0.00E+00	1.49E-11
X	1.00E+07	fixed	1.00E+07	fixed	1.00E+07	fixed
Log Likelihood	-1669.40		-1643.36		-1647.27	
Predicted Cancers	235.6		240.9		241.1	

However, with a 0.5-year half-life, the fit of the model that assumed μ was dose-related was appreciably worse than the comparable model assuming a 20-year half life (change in likelihoods of 5). As this analysis demonstrates, choice of an appropriate internal dose can be confounded with selection of the appropriate two-stage parameter that is affected by that dose. The analysis also implies that, due to the number of variables that can be optimized, the two-stage model does not appear to be a good discriminator for evaluating the biodurability of fibers.

These results do not suggest that asbestos acts at short times and is then sequestered. However, they do suggest that favored dose-dependent variables may be strong functions of other constraints placed on the model (such as the assumed half-life of the fibers). This further implies that the South Carolina results reported above might be anomalous, due to the assumption of a half-life that is short relative to the actual rate at which risk is observed to decrease for this cohort (based on the results from the analysis using the EPA model, Section 6.2.1.1).

It is unfortunate that it now appears that we may have evaluated these data using the wrong estimates of dissolution half-lives (which were, nevertheless, based on the best estimates from the literature). Our analysis of the time-dependence of the data using the EPA model (Section 6.2.1.1) suggests that both crocidolite and chyrsotile dissolve in vivo much more slowly than in vitro studies suggest and that this should not be surprising given that such materials only dissolve at their optimum rates when the fluid they are dissolving in is rapidly and continually renewed. Fluid flow rates in most compartments of the lung may simply not be adequate to facilitate dissolution of asbestos at the maximum rate.

It would be interesting to rerun the Moolgavkar model using half-lives based on what was observed with the analyses using the EPA model (approximately 20 years for chrysotile and > 700 yrs or virtually infinite for crocidolite). The goal would be to determine whether the fitting the South Carolina data might then show that chrysotile also acts primarily as a promoter (in agreement both with what is observed for Wittenoom and with what is indicated by the most current mechanism studies, see Sections 7.3.3.4 and 7.3.4.7).

That the two-stage model with v dose-dependent only marginally fits the time-dependence of the South Carolina data, may further reflect the inadequacy of this model (because the assumed half-life for asbestos is much too short). Incorporating a longer half life may improve this fit. In contrast, model fits for Wittenoom in which longer half-lives were assumed (although still short based on observations reported from our analysis using the EPA model), do adequately describe the time-dependence for lung cancer mortality observed in that cohort. As previously indicated, however, the marginal benefit derived from the two-stage model in this application may not be

justified compared to the cost and effort that may be required to obtain the new results. Especially given that we can now address questions concerning bio-durability with the adaptation we developed for the EPA lung cancer model (Section 6.2.1.1).

6.2.2 Estimating K_L's from the Published Epidemiology Studies

The EPA model for lung cancer (described in Section 6.2.1.1) was applied to each of the available epidemiology data sets to obtain study-specific estimates for the lung cancer risk coefficient, K_L. Based on the results presented in Section 6.2.1.1, there is no indication that the current model does not provide an adequate description of lung cancer mortality, at least in association with exposure to amphiboles. There is some indication that the current model may not provide an adequate description of the time-dependence of mortality following exposure to chrysotile. However, it is believed that the effect that such deviations might have on estimates of K_L derived using the model are likely to be small, except in rare cases when studies incorporate long periods of followup after cessation of exposure. It will be prudent to evaluate the observed deviations further (if additional raw data sets can be obtained) and to adapt the current model to account for the observed effect, should it be confirmed in other studies. However, at this point in time, we see no reason not to proceed with the analysis of published studies using the existing model.

The set of K_L values derived from available epidemiology studies are presented in Table 6-12. Note that this table is a reproduction of Table A-1 in Appendix A.

In Table 6-12, Column 1 lists the fiber types for the various studies, Column 2 lists the exposure settings (industry type), and Column 3 indicates the specific locations studied. Column 4 presents the best estimate of each K_L value derived for studies, as reported in the original 1986 Health Effects Update and Column 5 presents the reference for each respective study. Columns 6, 7, and 8 present, respectively: the best-estimates for the K_L values derived for all of the studies currently available (including studies corresponding to those in the original Health Effects Update); the estimated lower and upper bounds for each K_L value (derived as described in Appendix A); and the reference for the respective study from which the data were derived. To assure comparability across studies, values for all studies (even those that have not been updated since their inclusion in the 1986 Health Effects Update) were re-derived using the modified procedures described in Appendix A. The remaining columns of the table present information relevant to risk coefficients for mesothelioma and are discussed in Section 6.3.2.

The K_L values derived in this study and the corresponding values derived in the original 1986 Health Effects Update generally agree; most vary be no more than a factor of 2, a couple vary by a factor of 3, and one varies by a factor of about 5. In no case,

however, are the differences significant (based on visual comparison of confidence intervals).

Table 6-12

Table 8-12:

Lung Cancer Dose-Response Coefficients (K_L's) and Mesothelioma Dose-Response Coefficients (K_M's) Derived from Published Epidemiology Studies

			EPA (1986)		This update			EPA (1986)		This update	
Fiber Type	Operation	Cohort	K_Lx100	Reference	K_Lx100	Range	Reference	K_Mx10^6	Reference	K_Mx10^6	Range	Reference
Chrysotile	Mining and Milling	Quebec mines and mills	0.06	McDonald et al., (1980)	0.029	(0.0065, 0.11)	Liddell et al. (1997)					
			0.17	Nicholson et al., (1979)								
		Asbestos, Quebec Thedford Mines, Quebec								0.013	(0.003, 0.049)	Liddell et al. (1997) (raw data)
										0.021	(0.0065, 0.065)	Liddell et al. (1997) (raw data)
		Italian mine and mill	0.081	Piolatto et al. (1990)	0.035	(0, 1.1)	Piolatto et al. (1990)					
	Friction Products	Connecticut plant	0.01	McDonald et al., (1984)	0	(0, 2.2)	McDonald et al. (1984)			0	(0, 0.9)	McDonald et al. (1984)
	Cement manufacture	New Orleans plants			0.4	(0, 1.6)	Hughes et al. (1987)			0.2	(0.028, 1.4)	Hughes et al. (1987)
	Textiles	South Carolina plant	2.8	Dement et al., (1983)	2.4	(0.81, 5.6)	Dement et al. (1994 raw data)			0.11	(0.037, 0.25)	per. comm. Dement (2001)
			2.5	McDonald et al., (1983a)	1.15	(0.22, 4.9)	McDonald et al. (1983a)			0.068	(0.002, 1.6)	McDonald et al. (1983a)
Crocidolite	Mining and Milling	Whitenoom, Australia			0.47	(0.06, 6.9)	DeKlerk, unpublished data			7.9	(3.5, 18)	DeKlerk, unpublished data
Amosite	Insulation Manufacture	Patterson, NJ factory	4.3	Seidman (1984)	2.6	(0.17, 27)	Seidman (1988)	3.2	Seidman (1984)	3.9	(0.74, 20)	Seidman (1988)
		Tyler, Texas factory			0.13	(0, 6.6)	Levin et al. (1998)					
Tremolite	Vermiculite mines & mills	Libby, Montana			0.61	(0.04, 5.3)	Amandus and Wheeler (1987)					
					0.64	(0.025, 4.7)	McDonald et al. (1986)					
Mixed	Friction Products	British factory	0.058	Berry and Newhouse (1983)	0.058	(0, 2.4)	Berry and Newhouse (1983)					
	Cement manufacture	Ontario factory	4.8	Finkelstein (1983)	1.2	(0, 29)	Finkelstein (1984)	12	Finkelstein (1983)	18	(2.1, 149)	Finkelstein (1984)
		New Orleans plants	0.53	Weill et al., (1979); Weill (1984)	0.4	(0, 1.6)	Hughes et al. (1987)			0.3	(0.062, 1.4)	Hughes et al. (1987)
		Swedish plant			0.07	(0, 25.9)	Albin et al. (1990)					
		Belgium factory			0	(0, 0.84)	Laquet et al. (1980)					
	Factory workers	U.S. retirees	0.49	Henderson and Enterline (1979)	0.15	(0.011, 1)	Enterline et al. (1986)					
		Asbestos, Quebec								0.092	(0.02, 0.35)	Liddell et al. (1997) (raw data)
	Insulation application	U.S. insulation workers	0.75	Selikoff et al., (1979)	0.4	(0.012, 5.1)	Selikoff and Seidman (1991)	1.5	Selikoff et al (1979)	1.3	(0.25, 6.5)	Selikoff and Seidman (1991)
	Textiles	Pennsylvania plant	1.4	McDonald et al., (1983b)	1.8	(0.073, 16.5)	McDonald et al. (1983b)			1.1	(0.13, 8.8)	McDonald et al. (1983b)
		Rochedale, England plant	1.1	Peto (1980)	0.9	(0.16, 5)	Peto (1985)	1	Peto(1980), Peto et al (1982)	1.31	(0.28, 5.6)	Peto (1985)

Perhaps the most interesting of the changes between the 1986 K_L value estimates and the current K_L value estimates involves the friction products plant in Connecticut (McDonald et al. 1984). Although a relatively small, positive dose-response was estimated from this study in the 1986 Health Effects Update, the best current estimate is that this is essentially a negative study (no excess risk attributable to asbestos). The difference derives primarily from allowing α to vary in the current analysis. The exposure groups in this cohort do not exhibit a monotonically increasing dose-response relationship and, in fact, the highest response is observed among the group with the lowest overall exposure. Thus, the most likely explanation for the observed relative risk in this cohort is that there is poor agreement in the background cancer rates between the study cohort and the control population. As indicated in Appendix A, lack of a monotonically increasing dose-response relationship is a problem observed in several of the studies evaluated.

Among the K_L values derived in the current study, the lowest and highest of the best-estimate values differ by a factor of 90 (excluding the two negative studies, which would make the spread even larger) and several of the pair-wise comparisons across this spectrum are significant (based on a comparison of their confidence intervals). For example, the K_L value derived for the chrysotile miners in Quebec is significantly smaller than the K_L values derived for chrysotile textile workers (in either of the two studies for South Carolina, which are of highly redundant cohorts in the same plant), for textile workers in the Roachdale, UK plant, and amosite insulation manufacturers (in the Seidman study).

The K_L values and the associated confidence bounds derived in the current study are plotted in Figure 6-3. Each exposure environment is plotted along the X-axis of the figure and is labeled with a four-digit code that indicates fiber type (chrysotile, mixed, crocidolite, or tremolite), industry (mining, friction products, asbestos-cement pipe, textiles, insulation manufacturing, or insulation application); and a two-digit numerical value indicating the study from which the data were derived. A key is also provided. In the Figure, the chrysotile studies are grouped on the left, amphibole studies are grouped on the right, and mixed studies are in the middle. Note also that studies conducted in the same facility (generally among highly overlapping cohorts), such as the Dement et al. (1994) and the McDonald et al. (1983a) studies of the same South Carolina textile facility, are combined (averaged) and presented as a single entry in the Figure. The two Libby Vermiculite studies were similarly combined.

Figure 6-3

Figure 6-3:
Plot of Estimated KL Values and Associated Confidence Intervals by Study Environment

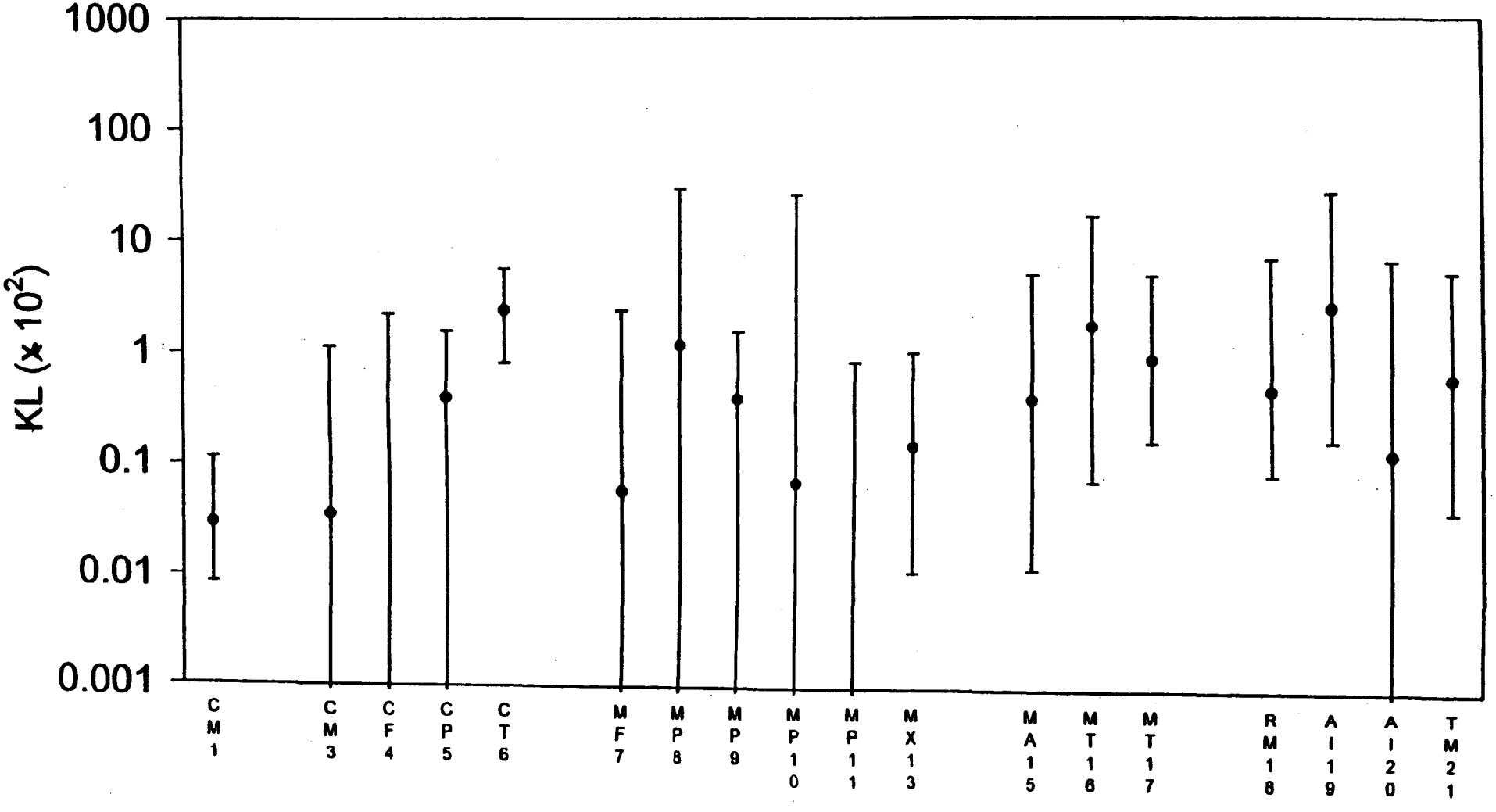

Key for Figure 6-3 Code

Fiber Types (First Digit of Code)	Study Environment (Second Digit of Code)
A = amosite	A = insulation application
C = chrysotile	F = friction products manufacturing
M = mixed fibers	I = insulation manufacturing
R = crocidolite	M = mining
T = tremolite (in vermiculite)	P = ac pipe manufacturing
	T = textile manufacturing
	X = misc. products manufacturing

Study Cohorts
(Last 2 digits)

1 = Quebec miners (Liddell et al. 1997)
2 = Quebec miners (Liddell et al. 1997, raw data)
3 = Italian miners
4 = Connecticut friction product workers (McDonald et al. 1984)
5 = New Orleans ac pipe manufacturers (Hughs et al. 1987)
6 = South Carolina textile manufacturers (Dement et al. 1994,raw data)
7 = British friction product manufacturers (Berry and Newhouse 1983)
8 = Ontario ac pipe manufacturers (Finkelstein 1984)
9 = New Orleans ac pipe manufacturers (Hughes et al. 1987)
10 = Swedish ac pipe manufacturers (Albin et al. 1990)
11 = Belgium ac pipe manufacturers (Laque et al. 1980)
13 = Retired factory workers (Enterline et al. 1986)
14 = Factory workers (Liddell et al. 1997)
15 = Insulation appliers (Selikoff and Seidman 1991)
16 = Pennsylvania textile workers (Mcdonald et al. 1983b)
17 = British textile workers (Peto 1985)
18 = Australian crocidolite miners (DeKlerk, unpublished, raw data)
19 = New Jersey insulation manufacturers (Seidman 1986)
20 = Texas insulation manufacturers (Levine et al. 1998)
21 = Libby vermiculite miners (Amandus and Wheeler 1987)

Key for Figure 6-3

Comparisons of K_L values across the available studies are instructive. Within chrysotile studies alone, lowest and highest K_L values vary by approximately a factor of 80 (again, excluding the negative friction products study), which is little different than the range observed across all studies. Moreover, as indicated above, the differences between the lowest (non-zero) value (for Quebec miners) and the highest value (textile workers) is significant. Differences between the negative friction product study and the other K_L estimates for chrysotile are not significant, primarily due to the wide confidence interval associated with the negative study.

Among the apparent variations, differences in lung cancer potency observed among Quebec miners versus that observed among South Carolina textile workers has been the subject of much discussion and evaluation, which is worthy of review (Section 6.2.3). In fact, the inability to reconcile these differences, appears to be among the biggest obstacles to reliably estimating an overall chyrsotile potency factor for lung cancer.

Among "pure" amphibole studies, the lowest and highest of the best-estimate K_L values vary by a factor of approximately 20 and, interestingly, the two extremes both derive from within the same industry (amosite insulation). However, these two estimates for amosite insulation are not significantly different (based on a comparison of their confidence intervals) Taking the arithmetic mean of the values for the two amosite insulation studies, results indicate that K_L values estimated, respectively, for crocidolite mining, amosite insulation manufacture, and mining of vermiculite contaminated with tremolite vary by less than a factor of 3, which constitutes stellar agreement (given the magnitude of the associated confidence intervals, as shown in Figure 6-3), if this is indeed the appropriate interpretation. However, alternate interpretations cannot be excluded.

As indicated in Section 6.2.3, for example, it is possible that mining studies tend to exhibit low K_L values relative to studies of asbestos products industries. As indicated in that section, this may be due to the presence of large numbers of cleavage fragments in the dusts, which may not contribute to biological activity (because the majority of these may not exhibit the requisite size to be biologically active) but which, nevertheless, are included in estimates of asbestos concentrations in the original epidemiology studies. Under this interpretation, the K_L estimates for Libby and for Wittenoom might both be raised substantially, if they could be adjusted for similar effects, so that they are closer in value to that obtained from the Seidman study. Then the "outlier" Levin study might be re-evaluated to see if inadequate consideration of lag, the relatively young age of the cohort studied, or other factors might contribute to a low K_L estimate for this study. As indicated in Section 6.2.3, such considerations have implications both for identifying appropriate size ranges of structures to be included in the analysis of asbestos and for evaluating the relative potency of chrysotile and the

amphiboles. Of course, because the difference between the K_L values from the Levin et al. study and the Seidman study do not appear significant, such differences may simply be due to unavoidable statistical variation.

It is also instructive to compare variation within and between industries. Within industries (especially for a single fiber type), the data are limited. The studies from the two chrysotile mines (Quebec and Italy) show remarkably close agreement, varying by less than about 20%. However, the studies of the two amosite insulation plants (Paterson, New Jersey and Tyler, Texas) show K_L values that vary by a factor of 20; due primarily to the uncertainty of the K_L value for the Tyler facility; these differences are not significant. As previously mentioned, the same equipment (literally) was used at both of these insulation plants and the sources of asbestos were also apparently similar, although the cohorts at the two plants are entirely independent.

The differences between the K_L values from the New Jersey and Texas facilities may represent the practical limit to agreement within industries that can be expected. However, it is also possible that an "explanation" for the difference may eventually present itself.

Across all asbestos types (including mixed), the asbestos-cement pipe industry shows the greatest variation, including a negative study (best estimate $K_L = 0$) and three positive studies with K_L values that range amongst themselves by a factor of 17. The friction products industry includes one negative and one positive study. Better agreement is observed among textiles. The two mixed textile plants show K_L values that vary by no more than a factor of 2.5 from each other and from the pure chrysotile textile plant value. However, given the variation observed within other industry groups, such agreement may be fortuitous.

K_L estimates within the mining industry (but between fiber types) range over a factor of 20, from a low of 0.029 for Quebec miners to a high of 0.62 for tremolite in vermiculite miners. Based on inspection of confidence intervals, however, none of the pairwise differences within this industry appear significant.

6.2.3 The Variation in K_L's Derived for Chrysotile Miners and Chrysotile Textile Workers

The difference between the observed risk of lung cancer for comparable levels of chrysotile exposure among Quebec miners (most recent followup: Liddell et al. 1997) and South Carolina textile workers (McDonald et al. 1983a and Dement et al. 1994) has been the focus of much attention. Although the discrepancy in lung cancer risk between Connecticut friction products workers (McDonald et al. 1984) and South Carolina textile workers is potentially even greater (Table 6-12), the large uncertainties

associated with the risk estimate in the friction products study make comparisons with friction products more difficult to evaluate (Section 6.2.2). Moreover, reasonably good agreement between results from the Quebec studies and another study of chrysotile miners in Italy (Piolatto et al. 1990) coupled with reasonably good agreement between results from the South Carolina Plant and results from two other textile plants: one in Mannheim, Pennsylvania (McDonald et al. 1983b)and one in Roachdale, England (Peto 1980), suggest that the difference between Quebec and South Carolina may reflect a general difference between the two industries, rather than specific locations (see Table 6-12 and Section 6.2.2). This appears true despite the fact, for example, that cohorts at the two other textile plants may have been exposed to mixed fiber types (amphiboles as well as chrysotile), see Appendix A and Section 6.2.2. Importantly, this "discrepancy" has been recognized as an issue for lung cancer only, the differences in mesothelioma rates observed in the Quebec mines and the South Carolina textile plant are not widely disparate (see Table 6-12).

Three main hypotheses have been advanced to explain the difference in the risk per unit exposure observed among miners and textile workers (see, for example, Sebastien et al. 1989). These are:

(1) the low reliability of exposure estimates in the various studies;

(2) differences in fiber size distributions in the two industries (with textile-related exposures presumably involving greater fractions of longer fibers); or

(3) simultaneous exposure to a co-carcinogen (oil that may have been sprayed on the asbestos fibers) in the textile industry.

It has also been proposed that differences in the concentration of long tremolite (amphibole) fibers in dusts from each of the two industries might represent an explanatory factor (see, for example, McDonald 1998b). However, this would also require a large relative difference between the potencies of tremolite (amphiboles) and chrysotile toward the induction of lung cancer. This latter issue is addressed further in Section 6.2.4. McDonald (1998b) also presents an overview of the current status of each of the hypotheses described above.

In an attempt to distinguish among the above-listed hypotheses, Sebastien et al. (1989) conducted a study to determine lung fiber concentrations in tissue samples from deceased members of the cohorts studied from both the Quebec mines (specifically, from the Thetford mine) and the South Carolina textile plant. These researchers ultimately analyzed tissue samples from 72 members of the South Carolina cohort and 89 members of the Thetford (Quebec) cohort. Because the tissue samples came from cohort members, they could be matched with estimates of the exposure experienced by

each of the individuals as well as details concerning the age at first employment, the age at death, the years of employment, and the number of years following employment until death.

In the Sebastien et al. study, tissue samples were obtained in formalin-fixed or paraffin blocks, which were then digested in bleach, filtered, and analyzed by TEM. Tissue samples were apparently "opportunistic." Only fibers longer than 5 µm with an aspect ratio greater than 3:1 were included in the count. For consideration of the limitations associated with such preparations, see Section 5.2.

Results from matching of tissue samples with the histories of corresponding cohort members indicate that tissue samples obtained from each cohort covered a broad range of exposure levels, duration of exposure, and years since the end of exposure. They also indicate that South Carolina cohort members included in the Sebastien et al. study experienced, on average, 13.5 years of exposure with 18.1 years between the end of exposure and death. In contrast, Thetford workers included in this study experienced an average of 32.6 years of exposure with only 11.6 years between the end of exposure and death. Corresponding to differences in exposure levels observed across the two cohorts in the original epidemiology studies, mean exposure levels experienced by Thetford cohort members included in this study were about 10 times mean exposure levels experienced by South Carolina workers (19.5 mpcf vs. 1.9 mpcf).

Because Sebastien and coworkers recognized the general lack of a good model describing the retention and clearance of asbestos fibers in the lungs at the time their study was conducted, they performed most of their analyses either on pairs of members (one from each cohort) matched for duration of exposure and time since end of exposure or on groups of members from each cohort similarly stratified by duration of exposure and time since end of exposure.

Results from their study indicate that, overall, lung burdens observed among Thetford cohort members are substantially higher than those observed among South Carolina cohort members. Geometric mean lung chrysotile concentrations are reported to be 5.3 and 0.63 fibers/µg dry lung tissue in Thetford workers and South Carolina workers, respectively. Furthermore, despite tremolite representing only a minor contaminant in the chrysotile from Quebec and the dusts to which the miners were exposed (Sebastien et al. 1986), the majority of fibers observed in the lungs of Thetford miners were in fact tremolite (mean concentration 18.4 f/µg dry lung). Since the raw material used in the South Carolina plant came largely from Quebec, tremolite was also expected to be a minor contaminant in the dusts to which textile workers were exposed. Yet among these workers also, tremolite represented a substantial fraction of the lung fibers observed (mean concentration 0.36 f/µg). Thus, the ratio of tremolite concentrations

observed among Thetford miners and that observed among South Carolina workers (18.4:0.36 or 51) is even more extreme than the ratio observed for chrysotile (8.4).

To evaluate the first of the above-listed hypotheses, it is instructive to compare the ratios of chrysotile or tremolite fibers observed in the lungs of deceased workers from Thetford and South Carolina, respectively, with the overall exposures that each received. A rough estimate of cumulative exposure for each set of workers in the Sebastien et al. (1989) study representing each cohort can be derived as the product of the mean duration of exposure and the mean intensity of exposure. Thus, for example, mean cumulative exposure in Thetford was 32.6 years x 19.5 mpcf or 635.7 mpcf-yrs. Similarly, for South Carolina, mean cumulative exposure was 25.65 mpcf-yrs, which gives a Thetford/South Carolina ratio of 24.8. This presumably represents the relative cumulative exposure to chrysotile. For tremolite, Sebastien et al. report that, based on a regression analysis, air concentrations of tremolite were likely only 0.4 times as much in South Carolina than in Thetford (where they likely averaged 1% of total fibers). Therefore, the ratio of cumulative exposures to tremolite for the sets of cohort members studied by Sebastien is likely 62.

Comparing the ratio of Thetford:South Carolina lung burden estimates with the ratios of the corresponding cumulative exposures, it appears that the chrysotile lung burden ratio (8.4) is only a third of the ratio predicted based on cumulative exposure (24.8). However, the ratio of lung tremolite concentrations (51) is much closer to the corresponding cumulative exposure ratio (62). It thus appears that, although, airborne concentrations may not closely track the exposures that led to the observed lung burdens, the overall trend in exposures predicted by airborne measurements is approximately correct. It is therefore likely that overall exposure concentrations in Thetford were in fact substantially higher than in South Carolina (in agreement with airborne measurements). Thus, we concur with Sebastien et al. that the unreliability of exposure estimates in these two cohorts is unlikely to explain the observed difference in the risk per unit of exposure observed for each cohort.

Importantly, although the general trend in relative overall exposure levels predicted by airborne measurements between Thetford and South Carolina appear to have been confirmed by mean lung fiber concentrations in the Sebastien et al. (1989) study, estimated exposures appear to do a very poor job of predicting lung burdens for any particular individual. To demonstrate this, we analyzed the Thetford: South Carolina ratios of lung chrysotile concentrations and, separately, lung tremolite concentrations reported by Sebastien et al. for their set of 32 matched pairs of cohort workers to determine whether trends in these ratios adequately matched trends in the corresponding estimated airborne exposure level ratios for the same matched pairs. To do this, we subjected the ratios presented in Table 7 of the Sebastien et al. (1989) study to a Rank Von Neuman test (Gilbert 1987). Results indicate that trends in

neither lung chrysotile concentration ratios nor lung tremolite concentration ratios can be predicted by the observed trend in the estimated airborne concentration ratios among these 32 matched pairs.

There are numerous sources of potential uncertainty that may mask the relationship between airborne exposure estimates and resulting lung burdens (Section 5.2). Potentially the largest of these is the variation expected among lung burden estimates derived from use of "opportunistic" tissue samples, which are not controlled for the portion of the respiratory tree represented by the sample. Even for samples collected from adjacent locations in lung parenchyma, observed fiber concentrations may vary substantially and such variation is magnified between samples taken from different individuals at locations in the lung that may not in any way correspond to their relative position in the respiratory tree.

Other potentially important sources of variation that may mask the relationship between airborne exposure concentrations and resulting lung burden estimates may primarily involve limitations in the degree to which the airborne estimates from an epidemiology study represent actual exposures to the individual members of a study cohort (Section 5.1). Thus, such things as: potential differences between individual exposures versus area concentrations (which are what is typically measured), the adequacy of extrapolation to the earliest exposures in a cohort (when measurements were generally not available), or the adequacy of estimating job x time matrices for individual workers that can then be integrated with work area exposure estimates to derive individual exposure estimates may all contribute to the uncertainty of exposure estimates.

The second of the above-listed hypotheses, involves potential differences in the size of structures that may have been present in the airborne concentrations in Thetford and South Carolina, which may not have been adequately represented by the exposure measurements. More generally, this is a question of the degree to which measured exposures in the two environments adequately reflect potential differences in the character of exposure that relate to biological activity.

Sebastien et al. (1989) considered this second hypothesis by generating and comparing size distributions for the fibers observed in the lungs of workers from Thetford and, separately, South Carolina. Importantly, the size distributions for each cohort were generated by including the first five fibers observed from every member of that cohort, without regard to the duration of exposure, level of exposure, or time since exposure experienced by each cohort member. Therefore, the size distributions obtained are "averaged" over very different time frames during which differing degrees of fiber retention and clearance will have taken place, each of which potentially alters the distributions of fiber sizes (Section 7.2). Thus, the two distributions generated are each actually collections of samples from multiple, varied size distributions (rather than

single distributions) and this likely masks distinctions between the two work environments. It is therefore not surprising that the authors found relatively little differences in the two size distributions.

The portion of the generated size distributions that are least likely to have been affected by the limitations due to the manner in which they are generated (as Sebastien et al. suggest) is the fraction of tremolite (amphibole) fibers longer than 20 µm. This is because (1) tremolite fibers (unlike chrysotile) are biodurable and (2) biodurable fibers longer than approximately 20 µm have been shown to clear from the lung only very slowly, if at all (Section 7.2). Thus, the Thetford:South Carolina ratio of long tremolite fibers may provide the best indication of the relative size distributions in the two environments.

Table 6-13 presents a table of the estimated, relative concentrations of specific lengths of fibers observed in lung tissue among Thetford miners and South Carolina workers, respectively. The length category for various fibers is presented in the last column of the table. The estimated concentrations, presented in Columns 2 (for Thetford) and 3 (for South Carolina) of this table were derived as follows. For the first length category (L > 5 µm), concentrations are taken directly from Table 5 of the Sebastien et al. paper (the geometric means are presented). Concentrations for the remaining length categories were estimated by multiplying the concentrations for this first length category by the fraction of the size distribution represented by each succeeding length category (as provided in Table 4 of the Sebastien et al. paper). So that the relative precision of these concentration estimates can be evaluated, an estimate of the numbers of fibers included in each length category (from the total used to derive the size distribution in Table 4 of Sebastien et al.) are provided in Columns 6 (for Thetford) and 7 (for South Carolina), respectively. The Thetford:South Carolina ratios of the concentrations of fibers in each length category (for each fiber type) are provided in Column 5 of the table.

It is instructive to compare the ratios presented in Table 6-13 to the Thetford:South Carolina ratios of mean cumulative exposures estimated above for chrysotile and tremolite among the cohort members included in the Sebastien et al. study (24.8 and 62, respectively). As indicated in Table 6-13, for chrysotile, the ratio remains approximately constant at about 9 (varying only between 8.4 and 10) for all of the size ranges reported except the longest. For the longest category (L > 20), however, the ratio drops to 5. Because fibers longer than 20 µm are expected to be the most persistent in the body (Section 7.2), it may be that the ratio of 5 best represents the relative concentration of long chrysotile structures among the two sets of cohort members.

Because this ratio (for the long fibers found in the lung) is only approximately one fifth of the estimated ratio for the cumulative exposure to chrysotile (24.8), this suggests that the South Carolina cohort may indeed have been exposed to dusts enriched in long fibers relative to dusts experienced at Thetford. Because the estimate of this ratio is based on counts of at least 11 fibers from Thetford and South Carolina, respectively, it is unlikely that this ratio will vary by more than a factor of two or three (the 95% confidence interval around 11 fibers, based on a Poisson distribution is 6 to 19).

Table 6-13

Table 6-13:
Estimated Concentrations of Sized Fibers Observed in the Lungs of Thetford Miners and South Carolina Textile Workers[1]

Fiber Type	MEAN LUNG CONCENTRATION Thetford	South Carolina	Units	Ratio: Th/SC	NUMBER OF FIBERS Thetford	South Carolina	Size Range of Fibers
Chrys	5.3	0.63	f/µg lung	8.41	371	226	Length > 5 µm
Trem	18.4	0.38	f/µg lung	48.42	405	175	
Chrys	1.73	0.17	f/µg lung	10.00	121	62	Length > 8 µm
Trem	3.90	0.091	f/µg lung	42.95	86	42	
Chrys	0.59	0.070	f/µg lung	8.41	41	25	Length > 13µm
Trem	0.72	0.024	f/µg lung	30.46	16	11	
Chrys	0.16	0.031	f/µg lung	5.15	11	11	Length > 20 µm
Trem	0.037	0.008	f/µg lung	4.40	1	4	

[1] Derived from data presented in Tables 4 and 5 of Sebastien et al. 1989

The trend with tremolite is even more striking. Moreover, as previously indicated, because tremolite fibers are biodurable, it is the tremolite fibers longer than 20 µm that may best represent the ratio of long fibers to which these two groups of cohort members were exposed. The ratios observed among tremolite fibers steadily decrease from approximately 50 for fibers longer than 5 µm to 4.4 for fibers longer than 20 µm, although this last value is uncertain (due to it being based on only 1 fiber observed among Thetford-derived lungs and only 4 fibers among South Carolina-derived lungs). In fact these data are statistically consistent even with a ratio considerably less than one, (i.e., with a considerably higher concentration of long tremolite fibers in South Carolina than in Quebec). Given that the ratio of the original cumulative exposures for tremolite was estimated to be 62, that the ratio of long tremolite fibers is only 4.4 suggests that dusts in South Carolina may have been highly enriched in long fibers.

Observations that the fibers to which textile workers were exposed were longer and thinner than those found in mining are further supported by various published size distributions of fibers determined in air samples collected in these environments (see, for example, Gibbs and Hwang 1975, 1980). Also, as noted in Curmp et al. (1985), the raw fiber purchased by textile plants was commonly described as the longest grade of product (see Table 22 of Crump et al.) Size issues are addressed further in Section 6.2.4.

At this point it is worth mentioning some of the potential differences in the characteristics of mining dusts and textile mill dusts that may affect biological activity, but that may not be adequately delineated when measuring exposures by PCM (in f/ml) and almost certainly not delineated when exposures are measured by midget impinger (in mpcf), see Section 4.3. During the mining of asbestos, only a small fraction of the rock (generally no more than 10%) that is mined is typically composed of the fibers of interest.

While the host rock in a mine may be of similar chemical composition, it generally represents an entirely different crystalline habit. Nevertheless, a large fraction of the dust that is created during mining is likely composed of fragments from the host rock and many of these fragments will be of a size that would be included in the particles counted by midget impinger. Furthermore, at least some fraction of the fragments created by the crushing and cutting of the host rock will be elongated "cleavage" fragments (Section 4.0) so that at least some fraction of these may be included even in PCM counts, despite many of them being either too thick to be respirable or too short or thick to be biologically active (see Section 7.2). Note, although Sebastien et al. employed TEM to characterize fibers in their 1989 study, they apparently employed a fiber definition that was sufficiently broad that they too would have counted large numbers of structures that may not contribute to biological activity.

In comparison, the dusts created in a textile factory are likely composed almost exclusively of true asbestos fibers. The raw material received by the factory will already have been milled and beneficiated to remove the vast majority of non-fibrous material. It is therefore, much less likely that extraneous fragments (even cleavage fragments) exist that might be counted either by midget impinger or PCM. We make this point because, if this represents the true situation, it would be expected that risk per unit exposure estimates (i.e. dose-response factors) derived from any mining site, may be smaller than estimates derived for the same fiber type in occupational environments where only finished fiber is used. Thus, another interpretation of the variation observed among estimated K_L and K_M values for amphiboles (reported in Section 6.2.2 and Section 6.3.2, respectively) is that the mining values are somewhat low. The implications of this possibility are discussed further in each respective section.

Note, although the Sebastien et al. paper suggests that (mpcf) exposure estimates from Thetford and South Carolina grossly suggest the relative range of lung burdens observed, there is too much scatter in the data to determine how closely the air ratios track the lung burden ratios. For example, ratios derived from arithmetic means (rather than the geometric means) for the Sebastien et al. data are substantially different. Moreover, as indicated above, there may be substantially different size distributions in the two environments, which might at least in part be explained by the inclusion of large numbers of cleavage fragments (with dimensions inappropriate for biological activity) in the mining environment.

Although the third of the above-listed hypotheses was not addressed by Sebastien and coworkers, the question of whether a co-carcinogen contributes to the overall observed lung cancer rate among textile workers has been considered by several other researchers. To test the hypothesis of whether oils potentially contributed to disease in South Carolina, Dement and Brown (1994) performed a nested case-control study among a subset of the cohort members previously studied by Dement et al. (most recent update, 1994). In this analysis, Dement and Brown qualitatively assessed the probability of mineral oil exposure for cases and controls based on knowledge of historic descriptions of mineral oil use. The extent of such exposure was then further categorized into three strata: none or little, moderate, or heavy, based on where each worker was longest employed. Cases and controls were then further categorized based on years at risk and level of asbestos exposure. Results from this nested analysis indicated no significant change in the estimated exposure-response slope for asbestos after adjusting for mineral oil exposure.

Additional, albeit qualitative, evidence that oils may not represent an adequate explanation for the relative lung cancer risks observed in mining and textiles is provided by McDonald (1998b). McDonald suggests that oils were not used in the Roachdale plant until 1974. Therefore, due to latency, it is unlikely that the use of such oils would

have had a substantial impact on the observed lung cancer cases at the point in time that the study was conducted (Peto 1980).

Taken as a whole, the evidence presented in this Section suggests that the relative distribution of fiber sizes found in dusts in the textile industry and the mining industry, respectively, may be the leading hypothesis for explaining the observed differences in lung cancer risk per unit of exposure between these two industries.

6.2.4 Evaluating Effects Associated with the Character of Exposure

As indicated in Chapter 3(Overview), valid extrapolation of risk coefficients derived from a reference site for use at a new site (to predict risk) requires that both of the following two conditions be satisfied:

(1) that asbestos be measured in both environments in an identical manner; and

(2) that such measurements reflect (or at least remain proportional to) the characteristics of asbestos exposure that determine biological activity.

Because there is mounting evidence that the manner in which asbestos was measured in the available epidemiology studies may not adequately reflect the characteristics that relate to biological activity (Section 7.4 and 7.5), the second of the above two criteria may not be satisfied when dose-response factors (i.e. K_L's and K_M's) derived from these studies are used to predict risk in new environments, without first applying some type of adjustment. Therefore, we explored the possibility that an improved index of exposure could be identified and that dose-response factors from the available human epidemiology studies could be adjusted so that they could be matched with measurements based on an improved exposure index to predict risk.

Based on an extensive evaluation of the broader literature and the results from a series of supplemental studies (Chapter 7), the primary features required of an improved index of exposure were identified and an "optimum" exposure index was defined. As indicated below, however, compromises were required to adapt the risk coefficients derived from human epidemiology studies to match measurements using the improved index. Due to the limitations of the data available for adjusting the existing K_L's and K_M's, an improved, but less than optimum exposure index was defined, which nevertheless represents the best of adjustments that can be justified, based on existing data.

Following a description of the procedures employed to adjust the existing K_L's and K_M's, the effects of such adjustments and their appurtenant implications for risk assessment are explored.

6.2.4.1 Adjusting K_i's for size

As previously indicated, considerations necessary to compare risk coefficients derived in different exposure settings (or to apply a coefficient to predict risk in a setting different from the one in which the coefficient was derived) have been elucidated clearly in a mathematical model (Chesson et al 1989). The consequences of the model indicate that adjusting the existing risk coefficients so that they reflect asbestos characteristics that determine biological activity requires knowledge of the fiber size distributions of the dusts studied in the *original* epidemiology studies. To the extent they exist, such data may be used to normalize each of the published risk coefficients so that they relate to a common exposure index reflecting asbestos characteristics that determine biological activity.

Adjustment of the existing risk coefficients is necessary because they have all been derived based primarily on PCM and MI measurements and neither PCM nor MI measurements relate adequately to biological activity (Section 7.5). Thus, analytical techniques employed at the time these studies were conducted were not capable of providing asbestos measurements that directly reflect biological activity.

Ideally, the existing risk coefficients should be adjusted so that they are all normalized to an exposure index such as that defined by Equation 7.12, which has been shown to adequately reflect the characteristics of asbestos that determine biological activity (Section 7.5). However, as indicated below, the database available for describing structure-size distributions for exposures in the original epidemiology studies do not contain sufficient information to individually characterize frequencies for structures in separate length categories longer than approximately 10 μm, while Equation 7.12 requires that fibers longer than 40 μm be separately enumerated. Therefore, an ad hoc exposure index is presented, which represents a compromise between theoretical needs defined in Chapter 7 (Section 7.5) and the limitations of the available data.

Importantly, the conclusions that can be drawn from a review of the general asbestos literature (Section 7.5) is that the asbestos fibers that drive risk are almost certainly longer than 10 μm with potency likely increasing for longer structures, at least up to a length of 20 μm. Therefore, due to the fact that structures longer than 20 μm have not been adequately characterized in any of the epidemiologically studied environments, it is not possible to test optimal exposure indices such as the one defined in the earlier analysis of animal inhalation studies (Berman et al. 1995). At the same time, it is apparent that an exposure index focusing on structures longer than 10 μm as the

primary contributors to risk should be superior to the arbitrary index originally defined for PCM analysis and employed in the original epidemiology studies. Moreover, the new index proposed here is also limited to structures that are clearly respirable and includes counting of even the thinnest of respirable structures while the index defined for PCM does neither (Appendix B).

In the remainder of this section, the K_L's derived in Section 6.2.2 (and summarized in Table 6-12) are normalized (using a series of published size distributions derived from TEM measurements) to an exposure index that is expected to better reflect biological activity. The distributions are defined for exposure settings that correspond to several of the settings evaluated in the epidemiology studies from which the published risk coefficients were derived. The coefficients are then combined with the asbestos risk models presented previously (U.S. EPA 1986) and evaluated above (Section 6.2.1) to derive a set of adjusted K_L values (K_L's), which are appropriately matched for use with the proposed, new exposure index. The proposed, new index is also defined below.

For the lung cancer model and the associated risk coefficient, "K_L," to be applicable generally, the asbestos concentration, "f," needs to be expressed in an exposure index that incorporates the characteristics of asbestos that determine risk. Correspondingly, the risk coefficient, "K_L" needs to be normalized to a model in which "f" is properly expressed.

As indicated previously, published structure size distributions derived from TEM measurements are used to adjust the existing K_L's by normalizing them to an exposure index that is expected to better relate to biological activity than the measurements in the epidemiology studies from which the K_L's were obtained.

Assuming that the available TEM size distributions are representative of dust characteristics for the exposure settings (industries) studied, these were paired with corresponding epidemiology studies. The TEM size distributions are then used to convert the exposure measurements used in the epidemiology studies to the new exposure index that is potentially more characteristic of biological activity. Studies were paired as indicated in Table 6-14

Only a subset of the TEM size distributions listed in Table 6-14 were actually employed in the effort to normalize K_L values. To minimize uncertainty introduced by between-study variability, it was decided to employ distributions from common studies, to the extent that this could be accomplished without reducing the number of "size-distribution -- K_L" pairs available for inclusion in the analysis. Also, studies containing the best documented procedures were favored over those in which the limitations of the distributions were less clear. Ultimately, the size distributions selected for use (with one exception) came from only two studies, which were reported in three publications:

Dement and Harris (1979), Gibbs and Hwang (1980), and Hwang and Gibbs (1981). In the case of the one exception, size distributions for Libby (tremolite asbestos in vermiculite) were derived from TEM data recently acquired directly from the site.

Table 6-14

Table 6-15 presents bivariate fiber size distributions derived from the published TEM data that are paired with representative K_L values from the corresponding epidemiology studies. These data were used to adjust K_L values in the manner described below.

The procedure for adjusting risk coefficients is straightforward. First, Equation 6.2 is re-written to reflect the fact that the fiber concentrations, "f," in the original epidemiology studies were typically measured by PCM:

$$K_L(C_{PCM})(d') = RR - 1 \qquad 6.3$$

where:

"C_{PCM}" is the concentration of asbestos structures that are typically included in a PCM measurement (Section 4.3); and

all other parameters have been previously defined.

The left side of Equation 6.3 is then multiplied by one (expressed as a product of reciprocal ratios):

$$\left[K_L\left(\frac{f_{PCME} * C_{tot}}{f_{Opt} * C_{tot}}\right)\right]\left(\frac{f_{Opt} * C_{tot}}{f_{PCME} * C_{tot}}\right)(C_{PCM})(d') = RR - 1 \qquad 6.4$$

where:

"f_{PCME}" is the fraction of asbestos structures in the published size distribution that are typically included in PCM measurements;

"f_{opt}" is the fraction of asbestos structures in the published size distribution that represent the optimal exposure index (i.e. the index of exposure that determines biological activity); and

"C_{tot}" is the concentration of total structures from which the fractions derive.

Remembering that the product of any fraction and the total concentration of a distribution is equal to the concentration of that fraction and that C_{PCME} is supposed to equal C_{PCM} (Section 4.3) and canceling terms accordingly, one is left with a new equation for risk in which asbestos concentrations are expressed in terms of the optimal exposure index:

$$K_{L*}(C_{Opt})(d') = RR - 1 \qquad 6.5$$

TABLE 6-14:
CORRELATION BETWEEN PUBLISHED QUANTITATIVE EPIDEMIOLOGY STUDIES AND AVAILABLE TEM FIBER SIZE DISTRIBUTIONS

Fiber Type	Exposure Setting	Distribution Reference	Epidemiology Reference
Chrysotile	Textiles	Dement and Harris 1979	Dement et al. 1994, 1983b
		Cherrie et al. 1979	McDonald et al. 1983a, b
			Peto 1980 and 1985
	Friction Products	Dement and Harris 1979	Berry and Newhouse 1983
		Marconi et al. 1984	McDonald et al. 1984
		Winer and Cossett 1979	
		Roberts and Zumwalde 1982	
		Rood and Scott 1989	
	Mining and Milling	Gibbs and Hwang 1980	Liddell et al. 1997
		Winer and Cossett 1979	McDonald et al. 1980
			Nicholson et al. 1979
			Piolatto et al. 1990
	Asbestos Cement Manu.	Dement and Harris 1979	Hughs et al. 1987
		Snyder et al. 1987	
		Winer and Cossett 1979	
Chrysotile and Crocidolite	Asbestos Cement Manu.	Hwang and Gibbs 1981	Finkelstein 1984
			Finkelstein 1983
			Hughs et al. 1987
			Weill et al. 1979
			Weill et al. 1984
			Albin et al. 1990
Crocidolite	Mining and Milling	Gibbs and Hwang 1980	Armstrong et al. 1988
		Hwang and Gibbs 1981	DeKlerk, unpublished
Amosite	Insulation Manu.	Dement and Harris 1979	Levine et al. 1990
			Seidman 1986
			Seidman 1984
	Insulation Application		Selikoff et al. 1979
	Insulation Clearance	Snyder et al. 1987	
		Cherrie et al. 1979	
Tremolite	Vermiculite Mining	EPA, unpublished	McDonald et al. 1986
			Amandus and Wheeler 1987

where:

"K_L." is now the adjusted risk coefficient, defined (and derived) as described in Equation 6.6:

$$K_{L\bullet} = K_L\left(\frac{C_{PCME}}{C_{Opt}}\right) \qquad 6.6$$

where all terms have been previously defined.

The adjusted risk coefficients, the "K_Ls", derived from the data provided in Table 6-15 in the manner described above are presented in Table 6-16. Adjusted risk coefficients for mesothelioma, "K_M's", are also provided. K_M's and K_L's are derived in precisely the same manner. The model adopted for mesothelioma risk is described in the next section.

Ideally, C_{opt} would be set equal to the concentration of asbestos structures defined as described in Equation 7.12. However, as previously described, published size distributions cannot be used to adjust risk coefficients to be consistent with the exposure index described by Equation 7.12. This is because the longest size category individually represented in the published distributions is for all structures longer than 10 µm and the exposure index described by Equation 7.12 requires that structures longer than 40 µm be individually enumerated. Therefore, Equation 7.12 was modified in an ad hoc fashion to generate the exposure index that is evaluated in this document:

$$C_{asb} = 0.003C_S + 0.997C_L \qquad 6.7$$

where:

"C_{asb}" is the concentration of asbestos to be used to estimate risk;

"C_S" is the concentration of asbestos structures between 5 and 10 µm in length that are also thinner than 0.5 µm; and

"C_L" is the concentration of asbestos structures longer than 10 µm that are also thinner than 0.5 µm.

Although not optimized, as previously indicated, this index is nevertheless expected to represent a substantial improvement over the PCM-related index in current use,

because it reflects more of the general criteria for biological activity defined in Section 7.5.

Table 6-15:

Represntative KL and KM Values Paired with Averaged TEM Fiber Size Distributions From Published Papers

Environment	Study Code	KL	KM	Size Distributions: PCME	w < 0.2 L < 5 5 < L < 10	w < 0.2 10 < L	w < 0.3 L < 5 5 < L < 10	w < 0.3 10 < L	w < 0.4 L < 5 5 < L < 10	w < 0.4 10 < L	w > 0.3 L < 5 5 < L < 10	w > 0.3 10 < L	w > 0.4 L < 5 5 < L < 10	w > 0.4 10 < L	Total L < 5 5 < L < 10	Total 10 < L	Size Reference
Quebec mines and mills	CM1	0.029		0.014	0.93545	0.00955	0.0023	0.954	0.0113	0.0031	0.013221	0.00372	0.0189	0.00915	0.0023	(0.4 NOT AVAILABLE IN DIST)	0.9729	0.02045	0.0054	G&H 1980
Quebec mines	CM1		0.0165	0.014	0.93545	0.00955	0.0023	0.954	0.0113	0.0031	0.013221	0.00372	0.0189	0.00915	0.0023	(0.4 NOT AVAILABLE IN DIST)	0.9729-	0.02045	0.0054	G&H 1980
Italian mine and mill	CM2	0.035		0.014	0.93545	0.00955	0.0023	0.954	0.0113	0.0031	0.013221	0.00372	0.0189	0.00915	0.0023	(0.4 NOT AVAILABLE IN DIST)	0.9729	0.02045	0.0054	G&H 1980
Connecticut plant	CF3	0	0	0.072352	0.763588	0.026133	0.018745	0.828041	0.034278	0.027062	0.849385	0.039022	0.031229	0.054729	0.020207	0.035685	0.033385	0.015461	0.031518	0.86277	0.054483	0.062747	D&H 1979
New Orleans plants	CP4	0.4	0.2	0.05071	0.774687	0.022829	0.015743	0.859923	0.030691	0.020432	0.886635	0.036762	0.023435	0.050795	0.01767	0.020489	0.024083	0.011599	0.017486	0.910718	0.048361	0.040921	D&H 1979
South Carolina plant	CT5	2.4	0.25	0.129625	0.656293	0.030243	0.027099	0.740474	0.043327	0.039829	0.767104	0.04959	0.048795	0.072558	0.039205	0.064606	0.045929	0.032942	0.05564	0.813033	0.082532	0.104435	D&H 1979
Wittenoom, Australia	RM14	0.47	7.9	0.011667	0.890167	0.026567	0.005033	0.937733	0.033033	0.006167	0.950433	0.0351	0.0063	0.018933	0.003567	0.0005	0.006233	0.0015	0.000367	0.956667	0.0366	0.006667	H&G 1981
Patterson, NJ factory	AI15	2.6	3.9	0.351981	0.171093	0.028721	0.007167	0.300525	0.060177	0.030991	0.377358	0.091114	0.052598	0.311607	0.134634	0.162068	0.234773	0.103698	0.14046	0.612131	0.19481	0.193059	D&H 1979
Tyler, Texas factory	AI16	0.13		0.351981	0.171093	0.028721	0.007167	0.300525	0.060177	0.030991	0.377358	0.091114	0.052598	0.311607	0.134634	0.162068	0.234773	0.103698	0.14046	0.612131	0.19481	0.193059	D&H 1979
Libby, Montana	TM17	0.81		4								1	1										2001 Libby sampling
British factory	MF5.5	0.058		0.072352	0.763588	0.026133	0.018745	0.828041	0.034278	0.027062	0.849385	0.039022	0.031229	0.054729	0.020207	0.035685	0.033385	0.015461	0.031518	0.86277	0.054483	0.062747	D&H 1979
Ontario factory	MP6	1.2	18	0.00755	0.93345	0.01125	0.00155	0.954025	0.013775	0.00215	0.9746	0.0163	0.00275	0.025725	0.002975	0.00145	0.00515	0.00045	0.00065	0.97975	0.01675	0.0036	H&G 1981
New Orleans plants	MP7	0.4	0.3	0.00755	0.93345	0.01125	0.00155	0.954025	0.013775	0.00215	0.9746	0.0163	0.00275	0.025725	0.002975	0.00145	0.00515	0.00045	0.00065	0.97975	0.01675	0.0036	H&G 1981
Swedish plant	MI8	0.07		0.00755	0.93345	0.01125	0.00155	0.954025	0.013775	0.00215	0.9746	0.0163	0.00275	0.025725	0.002975	0.00145	0.00515	0.00045	0.00065	0.97975	0.01675	0.0036	H&G 1981
Belgium factory	MI9	0																					
U.S. retirees	MI10	0.15																					
Asbestos, Quebec	MF		0.092																				
U.S Insulation workers	MI11	0.4	1.3	0.327511	0.117904	0.021834	0	0.270742	0.061135	0.004367	0.344978	0.087336	0.017467	0.379913	0.144105	0.139738	0.305677	0.117904	0.126638	0.650655	0.20524	0.144105	D&H 1979
Pennsylvania plant	MT12	1.8	1.1	0.129625	0.656293	0.030243	0.027099	0.740474	0.043327	0.039829	0.767104	0.04959	0.048795	0.072558	0.039205	0.064606	0.045929	0.032942	0.05564	0.813033	0.082532	0.104435	D&H 1979
Rochedale, England plant	MT13	0.9	1.31	0.129625	0.656293	0.030243	0.027099	0.740474	0.043327	0.039829	0.767104	0.04959	0.048795	0.072558	0.039205	0.064606	0.045929	0.032942	0.05564	0.813033	0.082532	0.104435	D&H 1979

Table 6-16:
Comparison of Original and Adjusted KL and KM Values

Environment	Study Code	KL Reference	KM reference	KL	KM	KL*	KM*
Quebec mines and mills	CM1	Liddell et al. (1997)		0.029		0.11	
Quebec mines	CM1		Liddell et al. (1997) (raw data)		0.017		0.062
Italian mine and mill	CM2	Piolatto et al. (1990)		0.035		0.13	
Connecticut plant	CF3	McDonald et al. (1984)	McDonald et al. (1984)	0	0	0	0
New Orleans plants	CP4	Hughes et al. (1987)	Hughes et al. (1987)	0.4	0.2	0.86	0.43
South Carolina plant	CT5	Dement et al. (1994 raw da	per. comm. Dement (2001)	2.4	0.25	6.4	0.66
Wittenoom, Australia	RM14	DeKlerk, unpublished data	DeKlerk, unpublished data	0.47	7.9	0.87	14
Patterson, NJ factory	AI15	Seidman (1986)	Seidman (1986)	2.6	3.9	17.4	26
Tyler, Texas factory	AI16	Levin et al. (1998)		0.13		0.87	
Libby, Montana	TM17	Amandus and Wheeler (1987)		0.61		2.4	
British factory	MF5.5	Berry and Newhouse (1983)		0.058		0.13	
Ontario factory	MP6	Finkelstein (1984)	Finkelstein (1984)	1.2	18	3.2	49
New Orleans plants	MP7	Hughes et al. (1987)	Hughes et al. (1987)	0.4	0.3	1.1	0.81
Swedish plant	M8	Albin et al. (1990)		0.07		0.19	
Belgium factory	M9	Laquet et al. (1980)		0			
U.S. retirees	M10	Enterline et al. (1986)		0.15			
Asbestos, Quebec	MF		Liddell et al. (1997)(raw data)		0.092		
U.S. insulation workers	MI11	Selikoff and Seidman (199	Selikoff and Seidman (1991)	0.4	1.3	7.4	24
Pennsylvania plant	MT12	McDonald et al. (1983b)	McDonald et al. (1983b)	1.8	1.1	4.8	2.9
Rochedale, England plant	MT13	Peto (1985)	Peto (1985)	0.9	1.31	2.4	3.5

The justification for selecting the above exposure index and the potential limitations associated with its use are described in Appendix B. Until such time that a study is completed in which size distributions are generated that allows use of an exposure index incorporating consideration of longer structures (such as that defined by Equation 7.12), it is recommended that asbestos concentrations be defined in terms of the exposure index defined by Equation 6.7 when evaluating asbestos risks. We therefore recommend that this index be incorporated into an interim protocol for conducting asbestos risk assessments.

6.2.4.2 Evaluating the implications of adjusting K_L's for size

To compare the effects of adjusting K_L values for fiber size, the adjusted values (the K_L's), are plotted (along with their associated confidence intervals) in Figure 6-4, which exhibits a format identical to that of Figure 6-3, to facilitate direct comparison. The "key" provided in Figure 6-3 is also directly transferable to Figure 6-4.

At first glance, the two figures look quite similar. However, closer inspection indicates that: (1) two of the points plotted in Figure 6-3 (for MP11 and MX13) are missing in Figure 6-4; (2) the confidence intervals are larger in Figure 6-4 than in Figure 6-3; and (3) the relative location of the best estimate values (central points within each confidence interval) have changed slightly relative to one another. The implications of these observations are discussed below.

Regarding Figure 6-4, the two points missing (for MP11 and MX13) were omitted because it was felt that none of the available size distributions used for adjusting the K_L values were suitably applicable for these study sites, so no conversions were possible. The confidence intervals are larger in Figure 6-4 because, as previously indicated, we have attempted throughout our analysis of the epidemiology data to account for major sources of uncertainty. Thus, the confidence intervals depicted in Figure 6-4 are modified from those depicted in Figure 6-3 to account for the uncertainty of making the adjustment for fiber size using paired data from published size distributions. The intervals were adjusted by multiplying the upper bound and dividing the lower bound by a factor thought to represent the relative contribution to uncertainty contributed by the need to match data from separate studies to perform the conversions. The factors employed are provided in Table 6-17.

The visual impressions from a comparison between Figures 6-3 and 6-4 regarding changes in the relative locations of the central values (best estimate) K_L and adjusted K_L values are subtle. Thus, numerical representations are provided in Table 6-18.

Figure 6-4

Figure 6-4:
Plot of Adjusted KL Values (KL*'s) and Associated Confidence Intervals by Study Environment

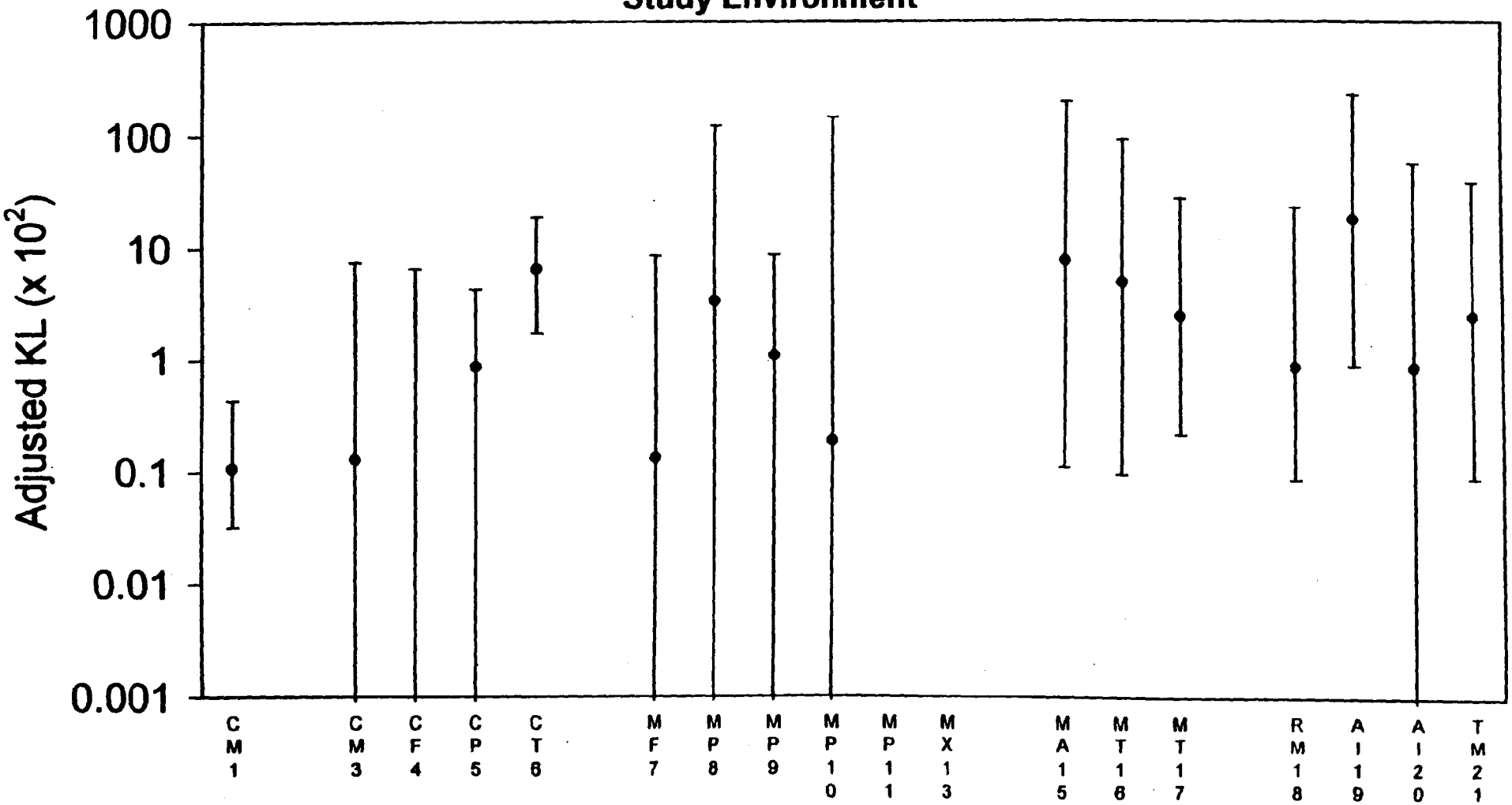

Table 6-17:
Estimated Uncertainty Assigned to Adjustment for Fiber Size

Study Location	Study Code	Estimated Uncertainty Factor	Explanation	KL Reference	KM reference
Quebec mines and mills	CM1	1	Location common to epidemiology study and size study	Liddell et al. (1997)	
Quebec mines	CM2	1	Location common to epidemiology study and size study		Liddell et al. (1997) (raw data Loc.
Italian mine and mill	CM3	1.75	Same industry, separate locations for epidemiology and size studies	Piolatto et al. (1990)	
Connecticut plant	CF4	1.25	Epidemiology location one of several combined for size study	McDonald et al. (1984)	McDonald et al. (1984)
New Orleans plants	CP5	1.25	Epidemiology location one of several combined for size study	Hughes et al. (1987)	Hughes et al. (1987)
South Carolina plant	CT6	1.25	Epidemiology location one of several combined for size study	Dement et al. (1994 raw data)	per. comm. Dement (2001)
British factory	MF7	1.5	Same industry, separate locations for epidemiology and size studies	Berry and Newhouse (1983)	
Ontario factory	MP8	1.5	Epidemiology location probably one of several combined for size study	Finkelstein (1984)	Finkelstein (1984)
New Orleans plants	MP9	2	Same industry, separate locations, mixed exposures	Hughes et al. (1987)	Hughes et al. (1987)
Swedish plant	MP10	2	Same industry, separate locations, mixed exposures	Albin et al. (1990)	
Belgium factory	MF11			Laquet et al. (1980)	
U.S. retirees	MF13			Enterline et al. (1986)	
Asbestos, Quebec	MF14				Liddell et al. (1997)(raw data)
U.S. insulation workers	MI15	2	Generally similar industries studied for epidemiology and size	Selikoff and Seidman (1991)	Selikoff and Seidman (1991)
Pennsylvania plant	MT16	2	Same industry, separate locations, mixed exposures	McDonald et al. (1983b)	McDonald et al. (1983b)
Rochedale, England plant	MT17	2	Same industry, separate locations, mixed exposures	Peto (1985)	Peto (1985)
Whitenoom, Australia	RM18	1.75	Same industry, separate locations for epidemiology and size studies	DeKlerk, unpublished data	DeKlerk, unpublished data
Patterson, NJ factory	AI19	1.25	Epidemiology location one of several combined for size study	Seidman (1986)	Seidman (1986)
Tyler, Texas factory	AI20	1.25	Epidemiology location one of several combined for size study	Levin et al. (1998)	
Libby, Montana	TM21	1.75	Extrapolated from limited, marginally associated air data	Amandus and Wheeler (1987)	

TABLE 6-18:
COMPARISON OF SPREAD IN RANGE OF ORIGINAL AND ADJUSTED K_L AND K_M VALUES FOR SPECIFIC FIBER TYPES

Fiber Type	Ranges of Values					
	Number in K_L, K_L. Sets	K_L	K_L.	Number in K_M, K_M. Sets	K_M	K_M.
All fiber types combined	15	90	160	10	1089	789
Chrysotile only (excluding mixed)	4	83	59	3	15	11
Chrysotile and mixed settings	11	83	68	8	1089	789
Amphibole and mixed settings	11	90	160	7	1089	789
Amphiboles only (excluding mixed)	4	20	20	2	2	2

Table 6-18 presents the magnitude of the spread in the range of original and adjusted K_L values (and also original and adjusted K_M values) estimated as the quotient of the maximum and minimum values of each range. Note that, of necessity, such an analysis requires that the zero values obtained for the Connecticut friction products plant (CF4) be omitted. Note further that the data sets evaluated in Table 6-18 for the original and adjusted values are identical (i.e., the two studies for which no suitable conversion factor could be found were excluded).

In Table 6-18, it is apparent that the spread in values among "pure" fiber types (i.e. chrysotile only or amphibole only) are both smaller than those for mixed data sets (containing both fiber types). This suggests that there may be differences in the potencies of each fiber type toward each respective disease (lung cancer and mesothelioma). In fact, the effect appears to be even more extreme among mesothelioma values than among lung cancer values (discussed further in Section 6.3.3.2). Moreover, that the spread in adjusted values for the data sets containing only the pure fiber types are smaller than for the unadjusted values, but (at least for lung cancer) larger than the unadjusted values for mixed data sets suggests that the effects from adjusting the K_L (and K_M) values for fiber size may be confounded with differences in the potency of fiber types. Therefore, we endeavored to develop a procedure for evaluating these data that would simultaneously account for both fiber size and type.

To address these issues, we considered that the mixed exposure environments represent situations in which there would be combined contributions to risk from both amphiboles and chrysotile. It is also known that chrysotile from the Quebec mines contains small amounts of tremolite (amphibole) asbestos (Sebastien et al. 1986). We therefore set up the following formalism to separate the effects of chrysotile asbestos from the effects of the amphiboles. Note, based on results of a previous study (Berman et al. 1995) and lack of compelling evidence elsewhere in the literature (assuming that size effects are adequately addressed, see Chapter 7), we assume in this formalism that all similarly-sized amphibole fibers are equipotent.

We start by defining potency factors for truly pure fiber types: K_{La} for pure amphiboles and K_{lc} for pure chrysotile. Next we define the relative potency of chrysotile, "RPC" as the ratio of these factors. Thus:

$$K_{Lc} = RPC * K_{La} \qquad 6.8$$

If one then knows the fraction of amphibole asbestos, f_{amph} in an exposure setting, the relationship between the observed, overall potency factors (e.g. the K_L's) and these fiber-specific factors is given by:

$$K_L = K_{La}*f_{amph} + RPC*K_{La}*(1-f_{amph}) \qquad 6.9$$

Note that, if RPC = 1 then Equation 6.9 reduces to the identity $K_L = K_{La}$ and Equation 6.8 reduces to $K_{Lc} = K_{La}$, meaning that all fibers are equipotent and there is no distinction for fiber type. Also, if RPC = 0, then chrysotile is non-potent and Equation 6.9 reduces to $K_L = K_{La}*f_{amph}$. Moreover, because f_{amph} is always less than one, this latter equation means that the true potency of the amphibole fibers is greater than would be indicated by the overall K_L in a study (whenever RPC = 0).

Finally, solving Equation 6.9 for K_{La} yields:

$$K_{La} = \frac{K_L}{[f_{amph} + RPC*(1 - f_{amph})]} \qquad 6.10$$

and we further define the denominator on the right side of Equation 6.10 as the function "Q".

Because the value for K_{La} should be constant across all study environments, if we also know the fraction of exposure in each environment contributed by amphiboles, we can apply Equation 6.10 to each of the available K_L's and search for the value of RPC that minimizes the spread in the resulting K_{La} values. Furthermore, by applying this same procedure both to the original K_L values and to the size adjusted K_L values (the K_L's) allows simultaneous consideration of fiber size and type. Results of applying this analysis are presented in Table 6-19.

The results provided in Table 6-19 are based on the estimates of the fraction of exposures in each environment that is represented by amphiboles presented in Table 6-20. In Table 6-20, the best estimate of the fraction of amphiboles is provided in Column 3 along with an estimate of the range (in Column 4), which indicates the degree of uncertainty that should be associated with each estimate of the fraction of amphiboles. The source of information from which each estimate was derived is provided in Column 5. Note that, depending on the particular study environment, such fractions either represent a time/operations average (e.g. commercial amphiboles were employed in a certain fraction of the plant for a certain period of time) or a composition average (e.g. tremolite constitutes some defined fraction of the chrysotile used).

Table 6-19:
Results of an Analysis of the Combined Effects of Fiber Size and Type on the Original and Adjusted K_L values[1]

Data Sets	Number of Studies	Optimum Value for RPC	Range Max/Min of K_x Values at Optimum RPC	Ratio K_x/K_{x*} at Optimum RPC	Ratio K_x/K_{x*} at RPC = 1	Studies Representing Max:Min K_x Values at Optimum RPC
Among K_{La} Values	15	0.5	83	0.98	1.8	CT6:CM1
Among K_{La*} Values	15	0.35	59	0.72		CT6:CM1
Among K_{Ha} Values	10	< 0.00001	36	0.72	0.72	MP8:CM1
Among K_{Ha*} Values	10	< 0.00001	26	0.72		MP8:CM1

[1] Excluding "zero" value for Connecticut friction products (CF4)

Table 6-20:

Estimated Fraction of Amphiboles in Asbestos Dusts

Study Location	Study Code	Fraction of Amphiboles: Best Estimate (%)	Fraction of Amphiboles: Estimated Range (%)	Source of Estimate	KL Reference	KM reference
Quebec mines and mills	CM1	1	0 - 4	Sebastien et al. (1986), Extrapolated from air data	Liddell et al. (1997)	
Quebec mines	CM2	1	0 - 4	Sebastien et al. (1986), Extrapolated from air data		Liddell et al. (1997) (raw data Loc. 1,3,4))
Italian mine and mill	CM3	0.3	0.1 - 0.5	CHECK THIS	Piolatto et al. (1990)	
Connecticut plant	CF4	0.5	0 - 2	McDonald et al. (1984), Extrapolated from planty history	McDonald et al. (1984)	McDonald et al. (1984)
New Orleans plants	CP5	1	0 - 2	Hughs et al. (1987), Extrapolated from plant history.	Hughes et al. (1987)	Hughes et al. (1987)
South Carolina plant	CT6	0.5	0 - 2	Extrapolated from Quebec source material: Based on Sebastien et al. (1989)	Dement et al. (1994 raw data)	per. comm. Dement (2001)
British factory	MF7	0.5	0 - 2	Berry and Newhouse, Extrapolated from plant history	Berry and Newhouse (1983)	
Ontario factory	MP8	30	10 - 50	Finkelstein (1984), Extrapolated from plant history	Finkelstein (1984)	Finkelstein (1984)
New Orleans plants	MP9	5	2 - 15	Hughes et al. (1987), Extrapolated from plant history	Hughes et al. (1987)	Hughes et al. (1987)
Swedish plant	MP10	3	0 - 6	Albin et al. (1990), Extrapolated from plant history	Albin et al. (1990)	
Belgium factory	MF11				Lequet et al. (1980)	
U.S. retirees	MF13				Enterline et al. (1986)	
Asbestos, Quebec	MF14					Liddell et al. (1997)(raw data)
U.S. insulation workers	MI15	50	25 - 75	Guesstimate for broad industry	Selikoff and Seidman (1991)	Selikoff and Seidman (1991)
Pennsylvania plant	MT16	8	3 - 15	McDonald et al. (1983b), Extrapolated from plant history	McDonald et al. (1983b)	McDonald et al. (1983b)
Rochedale, England plant	MT17	5	2.5 - 15	Peto (1985), Extrapolated from plant history	Peto (1985)	Peto (1985)
Whitenoom, Australia	RM18	97	95 - 100	General Estimate*	DeKlerk, unpublished data	DeKlerk, unpublished data
Patterson, NJ factory	AI19	97	95 - 100	General Estimate*	Seidman (1986)	Seidman (1986)
Tyler, Texas factory	AI20	97	95 - 100	General Estimate*	Levin et al. (1998)	
Libby, Montana	TM21	95	90 - 100	General Estimate*	Amandus and Wheeler (1987)	

* Allows for the possibility of some foreign material. Practical effect for the analysis is nil. Might just as well assume 100%.

In Table 6-19, the different data sets evaluated (i.e. the K_{Ls}'s, K_{Ls}*'s. K_{Ms}'s, and K_{Ms}*'s) are identified in Column 1. The number of studies included in each data set is listed in Column 2. Column 3 presents the values of the optimized RPC's (the RPC's for which the spread in K_{xs} values across each data set is smallest). Column 4 presents the minimized (optimum) range in the corresponding K_{xs} values for each data set (expressed as the ratio of the maximum/minimum values). Column 5 presents the corresponding ratio of the original and adjusted K_{xs} values. Column 6 presents this same ratio of original and adjusted K_{xs} values with RPC held fixed at one, and Column 7 indicates which study environments represent the maximum and minimum values for the optimized range of each data set.

Several conclusions can be drawn from the data presented in Table 6-19. First, it appears that, for both lung cancer and mesothelioma, the best estimate is that there is a difference in potency between chrysotile and amphiboles. For lung cancer, chrysotile may only be one third to one half as potent as the amphiboles, depending on whether one also adjusts risk factors for fiber size. For mesothelioma, no matter whether risk factors are adjusted for fiber size or not, it appears that chrysotile is much less potent than amphiboles and, in fact, may be non-potent. However, because improvement in the reconciliation of potency estimates across studies becomes marginal for RPC's smaller than about 1/1000 (and changes are no longer noticeable for RPC's smaller than about 1/10,000), a conservative estimate suggests that, at most, chrysotile is no more than about 1/1000 as potent as amphiboles toward the induction of mesothelioma. Other inferences concerning mesothelioma are addressed further in Section 6.3.3.2.

Although the improvements in reconciliation across potency estimates for the different studies are modest when one adjusts for fiber size (the ranges are decreased by about 30%), these reductions are based on spreads over the entire, available data sets (15 studies for lung cancer and 10 studies for mesothelioma). Moreover, such reductions are achieved using the relatively crude procedure of matching published size distributions to published epidemiology studies (rather than by obtaining true study-specific size distributions). Thus, combined with the strong inferences from the rest of the literature (see Chapter 7) that such size adjustments better reflect the characteristics of biological activity, adjusting values for fiber size is well justified and will improve the confidence with which risks can be extrapolated to new sites.

In this analysis, the range in lung cancer potency estimates is reduced from about a factor of 90 (when data are neither adjusted for fiber size or type, Table 6-18) to 59 (when data are adjusted for both fiber size and type). Interestingly, the extremes of this range are contributed by South Carolina textiles (CT6 - the maximum value) and Quebec mining (CM1 - the minimum value). Once adjusted for fiber size and type, the lung cancer potency estimates from all other studies (including those both for mixed

exposures and for nominally pure amphibole exposures) falls between these two extremes. As previously indicated (Section 6.2.3) the differences in potency estimates in these two environments has been the focus of much attention. Based on the analysis presented in Section 6.2.3, the best of candidate explanations for the differences between mining and textile production is the range of sizes of fibers in these two environments. Further evidence that this is the case is apparent from Table 6-19. As indicated from a comparison of the range in K_L and K_L. values in the table, adjusting values for fiber size (even given the crude approach currently available for making such adjustments) already reduces the difference in the potency estimates from these two environments by about 30%.

Although useful, the above analysis of ranges is potentially limited by the need to exclude the nominally zero value from the Connecticut friction products plant (CF4) and the lack of formal consideration of uncertainty. Therefore, an additional analysis was conducted in which uncertainty is addressed formally and the value from the Connecticut study was included.

In this analysis, we assumed that the log of the measured K_L values (or K_L., K_M, K_M. values) were normally distributed with mean $Ln\{K_{La}*[f_{amph} + rpc*(1-f_{amph})\}$, where K_{La}, RPC, and f_{amph} were all as previously defined. The variance of K_L was assumed to be composed of two or three independent components. The first component, σ_i, was assumed to be equal to one-half of the difference between the log transforms of the upper limit of the confidence interval and the point estimate of K_L (see Table 6-12). This variance was assumed to represent statistical uncertainty in response and exposure measurements (i.e, uncertainty that the confidence intervals were designed to represent, see Appendix A). Note that these values represent the irreducible fraction of uncertainty in the potency estimates.

A second component, σ, of the standard deviation was assumed to be constant for all studies, and may be thought of as representing the uncertainty in the estimate resulting from differences in exposure conditions, such as fiber size distributions, which are not represented in the σ_i. The overall standard deviation of the K_L from study i was assumed to be $(\sigma_i^2 + \sigma^2)^{1/2}$. As an alternate approach, the uncertainty in f_{amphi} was incorporated by adding a third independent component of exposure, σ_{ai}, given by one-half of the difference between the log transforms of the upper limit of the confidence interval for f_{amphi} and the best estimate of f_{amphi} (see Table 6-20). Thus, when the uncertainty in f_{amph} was accounted for, the overall standard deviation of the K_L from study i was $(\sigma_i^2 + \sigma^2 + \sigma_{ai}^2)^{1/2}$.

Using this model, a likelihood test was applied to estimate the parameters, Ln (K_{La}), RPC, and σ, and to conduct likelihood tests of the hypotheses that chrysotile was non-potent (RPC=0) or equally potent (RPC = 1) with amphibole. The same test was

applied to the K_L*, K_M, and K_M* values. When applied to the adjusted (starred) variables, the uncertainty in the fiber size distribution data was not accounted for so that the relative effect of adjusting for fiber size could be evaluated.

In this approach, the overall likelihood is estimated as the product of a series of terms that each represent the likelihood of obtaining a K_L value equal to that obtained from one of each of the available studies, given that they are derived from a common normal distribution with mean, K_{L_e} and standard deviation $(\sigma_i^2 + \sigma^2)^{1/2}$, as indicated above. The optimized (best estimate values) for K_{L_e} and σ are those for which the overall likelihood is maximized. Results from the analysis with the two parameter standard deviation are summarized in Table 6-21.

In Table 6-21, the first and fifth columns identify the specific data set being considered and the size of each data set is also presented. Columns 2 and 6 indicate the specific variables estimated. Columns 3 and 7 indicate the values for the estimated parameters with the value for RPC optimized. Columns 4 and 8 indicate the values for the estimated parameters with the value for RPC fixed at 1 and Columns 5 and 9 indicate the values for the estimated parameters with the values for RPC fixed at 0.

The results presented in Table 6-21 closely parallel the results obtained from the analysis of the range of values presented in Table 6-19. The best estimated value of relative potency for lung cancer indicates that chrysotile is only between a fifth and a half as potent as the amphiboles toward the induction of lung cancer, depending on whether potency factors are adjusted for fiber size. The results of a hypothesis test indicate that this is not significantly different from the hypothesis that chrysotile and amphiboles are equipotent (in either the original or the size-adjusted data sets). However, the hypothesis that chrysotile is non-potent toward the induction of lung cancer is clearly rejected. Size-adjusting the potency values provides a small improvement (reduction) in the overall variance of the data set of about 3% (although substantially larger improvements are noted for mesothelioma). Assuming the optimal difference in potency for the different fiber types, best estimate K_L and K_L* values for chrysotile and amphiboles are also presented in Rows 8 and 9, respectively, of the table. Although the data are not shown, the analysis using the three parameter estimate of standard deviation gave entirely comparable results.

Discussion of the results from the analysis of the mesothelioma values (also presented in the table) is provided in Section 6.3.3.2. Based on this analysis and the rest of the evaluation described in this chapter, a recommended set of lung cancer (and mesothelioma) potency factors has been developed and is presented in Section 6.4.

Table 6-21

Table 6-21:
Comparison of Original and Size Adjusted Potency Factors with Simultaneous Consideration of Fiber Type and Uncertainty
[Standard Deviation = $(\sigma_i^2 + \sigma^2)^{1/2}$]

Data Set	Variable	Optimized Values	RPC =1	RPC = 0	Data Set	Variable	Optimized Values	RPC =1	RPC = 0
K_L					$K_{L'}$				
(N = 16)	RPC	0.407	1	0	(N = 16)	RPC	0.179	1	0
	$Ln(K_{Le})$	-0.206	-0.836	1.806		$Ln(K_{Le'})$	1.549	0.378	3.087
	σ	1.076	1.085	1.806		σ	1.041	1.106	1.619
	LL	-17.6182	-17.9464	-22.2693		LL	-17.518	-18.6264	-21.1145
	P value		0.42	0.002		P value		0.14	0.007
	$100*K_{Le}$	0.81				$100*K_{Le'}$	4.71		
	$100*K_{Lc}$	0.33				$100*K_{Lc'}$	0.84		
K_M					$K_{M'}$				
(N = 11)	RPC	0.0040	1	0	(N = 11)	RPC	0.0017	1	0
	$Ln(K_{Me})$	2.084	-0.234	2.234		$Ln(K_{Me'})$	3.358	1.004	3.431
	σ	0.8123	1.817	0.846		σ	0.6561	1.925	0.672
	LL	-10.1285	-15.9751	-10.3145		LL	-8.854	-16.638	-8.916
	P value		0.0006	0.54		P value		< 0.0001	0.72
	10^6*K_{Me}	8.04				$10^6*K_{Me'}$	28.7		
	10^6*K_{Mc}	0.032				$10^6*K_{Mc'}$	0.050		

6.3 MESOTHELIOMA

The EPA model used to describe the incidence of mesothelioma in relation to asbestos exposure is the model proposed in the Airborne Health Assessment Update (U.S. EPA 1986). This model assumes that the incidence of asbestos induced mesothelioma is independent of age at first exposure and increases according to a power of time from onset of exposure, as described in the following relationship:

$$I_M = K_M \cdot f \cdot [(T-10)^3 - (T-10-d)^3] \quad \text{for } T > 10+d \quad (6.11)$$

$$= K_M \cdot f \cdot (T-10)^3 \quad \text{for } 10+d > T > 10$$

$$= 0 \quad \text{for } 10 > T$$

where:

"I_M" is the mesothelioma mortality observed at "T" years from onset of exposure to asbestos for duration "d" and concentration "f";

"K_M" is the proportionality constant between dose and mesothelioma response and represents the potency of asbestos; and

all other factors have been previously defined.

This is an absolute risk model, which means that the incidence of mesothelioma predicted by the model is a direct function of asbestos exposure that does not depend on the background incidence of the disease. Background mesothelioma cases are rare in the general population in any case.

The EPA model for mesothelioma is the solution to the following integral equation, assuming that exposure remains constant:

$$I_M = 3K_M \int_0^t C_{(x)} (t - 10 - x)^2 dx \quad (6\text{-}12)$$

This expression is more general than Equation 6.11, as it applies to both constant and variable exposures (see Appendix A).

6.3.1 The Adequacy of the Current EPA Model for Mesothelioma

Access to the raw epidemiology data from a small number of key studies allowed us to evaluate the adequacy of the EPA model for describing the time-dependence for mesothelioma in asbestos exposed cohorts. For this analysis, the raw data for the cohorts for the chrysotile miners in Quebec was graciously provided by Drs. Liddell and McDonald (described in Liddell et al. 1997), the raw data for the cohort of crocidolite miners in Whittenoom, Australia was graciously provided by Nick DeKlerk (unpublished) and the raw data for the cohort of chrysotile textile workers (described by Dement et al. 1994) was graciously provided by Terri Schnorr of NIOSH. The Whittenoom cohort was originally described by Armstrong et al. (1988), but the data provided by DeKlerk included additional followup through 1999.

To identify potential effects due to varying procedures, different methods for fitting the EPA mesothelioma model to epidemiological data were evaluated. In this evaluation, three methods were used to fit the EPA mesothelioma model to data from Wittenoom.

In the first approach the data were categorized in a manner often available in published form, so this method mimics the method generally used when raw data are not available. The observed mesotheliomas and person years of observation were categorized by time since first exposure, and the mean exposure level and duration of exposure were calculated for each such category. The EPA model is then applied to such data using the approach for the typical situation (as described in Appendix A) and results for the Wittenoom cohort are presented in Table 6-22. The K_M value estimated for Wittenoom using this approach is 7.15E-8 (90% CI: 6.27, 8.11). The fit of this model to data categorized by time since first exposure is good ($p = 0.65$).

Note that, for most of the published epidemiology data sets, the average level and duration of exposure are not available so that these have to be estimated from cruder data, such as cohort-wide averages.

A second approach to fitting the EPA model to epidemiology data, exploits the fact that the mesothelioma model (Equation 6-12) expresses the mesothelioma mortality rate as the product of K_M and an integral involving the exposure pattern, the time of observation, and the ten-year time lag, but not any variable parameters. The value of this integral was calculated for each year of followup of each subject. Person-years of followup and mesothelioma deaths were then categorized according to the values of the integral, and the average value of the integral determined for each category. Results are presented in Table 6-23.

Table 6-22:
Fit of EPA Mesothelioma Model to Observed Mortality Among Wittenoom Miners

Time Since First Exposure Range (Yrs)	Mean (Yrs)	Duration	Concentration	Cases	Predicted	Log Likelihood
[0, 5)	2.5	0.6	30.2	0	0	0.00
[5, 10)	7.4	0.9	30.2	0	0	0.00
[10, 15)	12.4	1	30	1	0.6	-1.14
[15, 20)	17.4	1	29.7	5	6.6	-1.95
[20, 25)	22.4	1	29.5	20	17.6	-2.58
[25, 30)	27.4	1	29.3	25	30.1	-2.99
[30, 40)	34.1	1	29	90	78.1	-4.04
[40, 100)	43.6	1.1	28.1	23	31.1	-3.65
Totals				164	164	-16.35

Goodness of Fit

Chi sq	5.95
P value	0.65

$K_M \times 10^6$

7.15

90% Confidence Interval

(6.27, 8.11)

Table 6-23:

Fit of EPA Mesothelioma Model to Observed Mortality Among Wittenoom Miners Categorized by Cumulative Exposure (Based on Averaged Value of Integral for Each Category)

Average Value of Integral	Cases	Predicted	Log Likelihood
0	0	0	0.00
28.4	0	0	-0.03
206.3	1	0.3	-1.56
732.3	4	1	-4.15
2038.1	10	2.9	-7.27
5153.7	23	6.8	-14.20
12385.8	32	13.8	-11.40
30639.7	27	25.8	-2.60
144801	67	113.3	-14.14
Totals	164	164	-55.35

Goodness of Fit	ChiSq	79.8
	P Value	1.5E-14

$K_M \times 10^5$	9.00
90% Confidence Interval	(7.89, 10.2)

K_M was estimated by maximum likelihood from Table 6-23 assuming that the observed numbers of cancer deaths were independently Poisson distributed with a mean equal to the mean value of the integral for that category times K_M. The value of K_M obtained in this fashion was K_M = 9.00E-8 (90% CI: 7.89, 10.2). The fit of the model to data categorized by the integral is not good ($P < 0.00001$), as the model predicts too few mesotheliomas for small values of the integral and too many mesotheliomas for large values of the integral. However, the estimates for K_M obtained from applying the model in this manner are still very similar to those obtained using the exact method (described below).

A third method of estimating K_M (termed the "exact method") employs a likelihood that does not involve any categorization of data. With this method, the hazard function, $h(t) = I_M(t)$ and the corresponding survival function (probability of surviving to age t without death from mesothelioma in the absence of competing causes of death), $S(t) = \exp(-\int_0^t h(s)ds$, are computed for time at the end of followup. The contribution to the likelihood of a subject who died of mesothelioma t_1 years after beginning of followup is $h(t_1)*S(t_1)$, and the contribution of a subject whose followup was not terminated by death from mesothelioma is $S(t_1)$. The complete likelihood is the product of such terms over all members of the cohort. The estimate of K_M obtained by maximizing the logarithm of this likelihood was 7.95E-8 (90% CI: 7.0, 9.0).

We consider the exact method of computing K_M to be the most accurate and results from this method are reported in the summary tables (see, for example, Table 6-12). The Quebec and South Carolina data sets were thus evaluated using the exact method. However, it is noteworthy that the two other methods described above, one of which is often applied to published data, give similar estimates of K_M, at least for this data set.

The Quebec cohort was subdivided into three subcohorts, believed to correspond to differing amounts of amphibole exposure due to tremolite contamination within the chrysotile (Liddell et al. 1997). Location I consisted of workers at the mine at Asbestos where the ore reportedly had less tremolite contamination. Locations 3 and 4 consisted of workers at the large central mine and at smaller mines, respectively, near Thedford, where the ore was more heavily contaminated with tremolite. Location 2 consisted of workers at an asbestos products factory at Asbestos, which processed some commercial amphibole fibers in addition to chrysotile. The exact method of calculating K_M produced the following estimates: Location 1 (8 cases): K_M = 1.3E-10 (90% CI: 0.3E-10, 4.9E-10); Location 2 (5 cases): 9.2E-10, (90% CI: 2.0E-10, 35E-10); Locations 3 and 4 (22 cases): K_M = 2.1E-10 (95% CI: 0.65E-10, 6.5E-10. The relative magnitudes of these estimates track with the relative amounts of amphibole exposure estimated for these locations (Liddell et al. 1997), which is consistent with the hypothesis that the mesothelioma risk in this cohort is due, at least in large measure, to exposure to amphiboles.

There were only two confirmed mesothelioma deaths in the South Carolina cohort and four additional suspected deaths. These were too few to permit detailed analysis. Based on both confirmed and suspected mesothelioma deaths, the exact method of analysis gave an estimate for K_M of $K_M = 0.43 \times 10^{-8}$, 90% CI: ($0.20 \times 10^{-8}$, 0.79×10^{-8}). Using only the two confirmed mesotheliomas, the same analysis yielded $K_M = 0.14 \times 10^{-8}$, 90% CI: ($0.034 \times 10^{-8}$, 0.38×10^{-8}). The same estimates were obtained by estimating K_M from data categorized by time since first exposure and fitting a linear model to the categorized value of the integral in the definition of the EPA model. Thus, for this cohort (in parallel with the cohort from Wittenoom) comparable K_M values are estimated no matter which of the three methods described above are used for fitting the EPA mesothelioma model to the epidemiology data.

6.3.1.1 Time dependence

The EPA mesothelioma model was next evaluated to determine whether it adequately describes the time-dependence of mesothelioma mortality following cessation of exposure in the Wittenoom and Quebec cohorts. The small number of mesotheliomas observed among the South Carolina cohort precluded our completing this analysis for that cohort. The model predicts that risk rises as the difference between the third power of time since the start of exposure and the third power of time since the cessation of exposure (both lagged by 10 years).

Table 6-24 shows the fit of the EPA mesothelioma model to Wittenoom data characterized by time since last exposure, based on the K_M estimated from the exact analysis. Although this fit appears adequate (P = 0.21), there appears to be a slight tendency for the EPA model to under-predict the mesothelioma rate at long times following cessation of exposure. However, given that the EPA model does not appear to under-predict the mesothelioma rate at long times for the other two cohorts evaluated (see below), it is not clear that this is a real limitation in the model. At the same time, the number of mesotheliomas in the other two cohorts are relatively small. Moreover, both of these other cohorts nominally involve chrysotile exposure (as opposed to crocidolite). Therefore, it may prove useful to obtain additional cohorts (preferably with relatively large numbers of mesotheliomas and preferably involving amphibole exposure) before concluding definitively whether the current EPA mesothelioma model adequately describes the time dependence for mesothelioma.

Table 6-25 shows the observed and expected mesotheliomas in the three separate locations at Quebec, categorized by time since last exposure, and computed using the K_M values obtained using the exact fitting method. Although the small numbers of mesotheliomas make it difficult to draw definite conclusions about the adequacy of the model, there is little evidence that the model under or over-predicts the numbers of mesotheliomas at long periods after the end of exposure.

Table 6-25:
Fit of EPA Mesothelioma Model to Observed Mortality Among Quebec Miners in Each of Three Mining Areas and

Time Since Last Exposure Range (Yrs)	Predicted	Cases	Averaged Value of the Integral	Relative Risk	Rate	Log Likelihood	K_M	Goodness of Fit ChiSq	Goodness of Fit P-value
Location 1									
[0, 10)	3.1	3	94267.5	0.98	3.90E-05	-1.50	1.34E-10	4.83	0.44
[10, 20)	1.4	2	119190	1.47	7.30E-05	-1.44			
[20, 30)	1.2	0	119971	0	0.00E+00	-1.15			
[30, 40)	1.4	1	181470	0.72	5.50E-05	-1.06			
[40, 50)	1.4	2	278118	1.44	1.70E-04	-1.43			
50+	1.0	0	339160	0	0.00E+00	-0.95			
30+	3.7	3		0.80429					
Totals	9.3	8		0.860215		-7.52			
Location 2									
[0, 10)	2.6	0	56377.5	0	0.00E+00	-2.55	9.55E-10	12.33	0.03
[10, 20)	0.8	2	56445.7	2.44	4.10E-04	-1.91			
[20, 30)	0.7	0	58307.7	0	0.00E+00	-0.70			
[30, 40)	0.7	2	78685.8	2.71	6.40E-04	-2.04			
[40, 50)	0.5	0	88541.2	0	0.00E+00	-0.49			
50+	0.1	1	59590.4	7.03	1.30E-03	-2.09			
30+	1.4	3		2.189781					
Totals	5.4	5		0.919118		-9.78			
Location 3&4									
[0, 10)	12.7	13	194913	1.02	1.40E-04	-2.21	2.18E-10	13.34	0.02
[10, 20)	4.3	5	262898	1.16	2.10E-04	-1.79			
[20, 30)	2.3	0	179052	0	0.00E+00	-2.30			
[30, 40)	2.5	0	251766	0	0.00E+00	-2.47			
[40, 50)	2.1	1	348264	0.48	1.10E-04	-1.36			
50+	0.9	3	298743	3.29	6.70E-04	-2.98			
30+	5.5	4		0.729927					
Totals	24.8	22		0.886739		-13.12			

Table 6-24:

Fit of EPA Mesothelioma Model to Observed Mortality Among Wittenoom Miners Categorized by Time Since Last Exposure

Time Since Last Exposure Range (Yrs)	Time Since Last Exposure Mean (Yrs)	Predicted	Cases	Average Value of Integral	Relative Risk	Log Likelihood
[0, 1)	0.3	0.0	0	35	0	-0.03
[1, 5)	3.0	0.1	0	72	0	-0.12
[5, 10)	7.5	0.6	0	327	0	-0.64
[10, 20)	14.9	14.5	10	4025	0.7	-2.85
[20, 30)	24.7	52.9	58	18058	1.1	-3.19
[30, 40)	34.0	81.3	79	39802	1.3	-5.44
40+	43.6	15.5	17	57952	1.1	-2.41
30+		76.8	96.0		1.3	
Totals		144.9	164			-14.68

Goodness of Fit		
	ChiSq	8.41
	P value	0.21

Table 6-26 similarly shows the fit of the EPA model to the South Carolina mesothelioma data (including all four suspected mesotheliomas as real). As with the Quebec cohort, there is little evidence from this cohort that the model under or over-predicts the number of mesotheliomas at long times following the end of exposure. Particularly with this cohort, however, conclusions must be drawn with caution due to the very small number of mesotheliomas observed.

Based on the analysis performed, we see marginal evidence that the current EPA model for mesothelioma may not provide an adequate description of the long term risk of mesothelioma in cohorts exposed to asbestos (even for extended periods of time following cessation of exposure); the fit of the model to the Wittenoom cohort is adequate, despite the small apparent discrepancy at long times. There also appears to be little evidence that there is a difference in the time development of mesothelioma between the Wittenoom and Quebec cohorts, although it is acknowledged that the data from the Quebec cohorts were divided into sets containing only small numbers of mesotheliomas. This latter observation contrasts with what was observed for the lung cancer model, where there is evidence that the effect that chrysotile has on relative risk appears to decrease with time following cessation of exposure while the effects of crocidolite appear to remain constant (Section 6.2.1.1).

If the observed difference in the time dependence for *lung cancer* risk observed for chrysotile (among South Carolina textile workers and Quebec miners) and crocidolite (among Wittenoom miners) is indeed due to fiber type, that a similar effect is not observed for mesothelioma suggests, among other possibilities, that similar fiber types may be primarily responsible for driving mesothelioma risk. This provides further, albeit circumstantial, support for the "amphibole hypothesis" (that amphiboles are primarily responsible for the induction of mesothelioma, even when present as minor contaminants in chrysotile).

Given the importance of these two issues: (1) the relative potencies of chrysotile and the amphiboles and (2) the adequacy of EPA models for predicting the time dependence of disease, limited analysis of raw data from a small number of additional cohorts is warranted. Such recommendations are discussed further in the conclusions to this Chapter (Section 6.4).

6.3.1.2 Comparison with a biologically based model

Definition of the two-stage model. The two-stage model of cancer implemented in this report (Moolgavkar and Luebeck, 1990) was previously described (Section 6.2.1.2).

Table 6-26

Table 6-26:
Fit of EPA Mesothelioma Model to Observed Mortality Among South Carolina Textile Workers

Time Since Last Exposure		Predicted	Cases	Averaged Value of the Integral	Relative Risk	Rate	Log Likelihood
Range (Yrs)	Mean (Yrs)						
[0, 1)	0.08	11.9	1	118165	0.08	0.00004	-9.40
[1, 5)	3.00	2.1	2	47292	0.97	0.0002	-1.31
[5, 10)	7.50	2.4	0	46052	0	0	-2.42
[10, 20)	14.84	3.7	2	40029	0.54	0.00009	-1.78
[20, 30)	24.80	2.7	1	35825	0.37	0.00006	-1.70
[30, 40)	34.65	1.9	0	35224	0	0	-1.94
40+	43.49	0.8	0	33443.5	0	0	-0.79
30+		2.7	0		0	0	
Totals		25.5	6				-19.33

Goodness of Fit	ChiSq	29.44
	P value	5.0E-05

Applying the two-stage model to mesothelioma. The 2-stage model was fit to the mesothelioma data using the same general approach applied to the lung cancer data and described earlier (Section 6.2.1.2). Since the background risk of mesothelioma is very small, the first stage mutation rate, ν_0, was fixed at zero in these analyses. Also, the death rate for intermediate cells, β_0, was likewise fixed at zero. (This is not expected to affect the range of hazards predicted by the model, since so long as the hazard is small, it is approximately a function of the difference $\alpha - \beta$.). Four situations were modeled:

(1) assuming only the mutation rate of normal cells into intermediate cells is dose-related [$\nu = \nu_1 d(t)$, $\alpha = \alpha_0$, $\mu = \mu_0$];

(2) assuming both the mutation rate of normal cells and the proliferation rate of intermediate cells are dose-related [$\nu = \nu_1 d(t)$, $\alpha = \alpha_0 + \alpha_1 d(t)$, $\mu = \mu_0$];

(3) assuming both mutation rates are dose-related [$\nu = \nu_1 d(t)$, $\alpha = \alpha_0$, $\mu = \mu_0 + \mu_1 d(t)$]; and

(4) assuming that both mutation rates are dose-related and equal on a per-cell basis [$\nu = \mu X = \nu_1 d(t)$, $\alpha = \alpha_0$, where $X = 10^7$ is the assumed number of normal cells].

The two-stage model was fit to the mesothelioma data from both Wittenoom and Quebec in a variety of situations. Table 6-27 shows results of fitting the two-stage model to the Wittenoom mesothelioma data assuming either an infinite half-life of internally deposited fibers ($r = 0$) or a ten-year half-life ($r = 0.069$). This Table shows the results of fitting allowing each one of the four parameters α, β, ν, and μ individually to be related to internal exposure (Model 1-4) and allowing all four simultaneously to be exposure-related (Models 5,6). The best fit (largest likelihood) using a single exposure-related parameter came from allowing ν to depend upon exposure. This was true when either an infinite half-life or a ten-year half-life was assumed. The likelihoods from the two assumed half-lives were similar. The estimated parameters were also similar, except for ν_1, which was larger using to ten-year half life in order to compensate for the smaller estimated exposures in this case.

The fit with an infinite half-life allowing all four parameters to be exposure-related (Model 5) did not improve the fit, even though parameter estimates differed considerably. This suggests that the likelihood is quite flat and diverse parameter estimates can provide comparable fits. However, the differences $\alpha_0 - \beta_0$ are nearly constant, which is consistent with the observation by Moolgavkar *et al.* (1988) that in many cases the model depends upon these parameters mainly through their difference.

Table 6-27

Table 6-27:
Results of Several Applications of the Two-Stage Model to the Mesothelioma Data from Wittenoom

	Parameter	MODEL 1 Fitted Value	MODEL 1 Standard Error	MODEL 2 Fitted Value	MODEL 2 Standard Error	MODEL 3 Fitted Value	MODEL 3 Standard Error	MODEL 4 Fitted Value	MODEL 4 Standard Error	MODEL 5 Fitted Value	MODEL 5 Standard Error	MODEL 6 Fitted Value	MODEL 6 Standard Error
INFINITE HALFLIFE	$\alpha 0$	1.42E+01	2.78E-01	1.42E+01	4.57E-02	1.42E+01	3.00E-02	2.26E-01	2.51E-02	4.98E-01	1.16E-01	5.50E-01	1.01E-01
	$\alpha 1$	1.31E-03	3.47E-04	0	fixed	0	fixed	0	fixed	1.49E-01	6.19E-02	1.26E-01	2.45E-03
	$\beta 0$	1.40E+01	2.79E-01	1.39E+01	4.58E-02	1.41E+01	2.99E-02	1.44E-09	9.13E-01	1.13E-02	1.81E-01	5.94E-02	9.92E-02
	$\beta 1$	0	fixed	-1.27E-03	3.29E-04	0	fixed	0	fixed	1.50E-01	6.19E-02	1.27E-01	2.44E-03
	$\nu 0$	2.66E-01	6.12E-02	2.66E-01	5.88E-02	1.05E+00	2.63E-01	5.05E-03	7.52E-04	7.36E-05	7.24E-05	0	fixed
	$\nu 1$	0	fixed	0	fixed	2.95E+00	6.33E-01	0	fixed	2.78E-03	6.06E-04	2.24E-03	4.23E-04
	$\mu 0$	2.66E-08	6.12E-09	2.66E-08	5.88E-09	1.05E-07	2.63E-08	5.05E-10	7.52E-11	7.36E-12	7.24E-12	0	fixed
	$\mu 1$	0	fixed	0	fixed	0	fixed	1.29E-07	1.22E-07	1.08E-07	9.76E-08	2.66E-07	1.80E-07
	Log Likelihood	-1149.6		-1149.9		-1131.7		-1144.8		-1098.4		-1101.8	
10 YEAR HALFLIFE	$\alpha 0$	1.47E+01	4.16E-02	1.47E+01	1.39E+00	1.47E+01	2.97E-02	1.48E+01	4.36E-02	5.74E-01	1.49E-01	5.97E-01	1.48E-01
	$\alpha 1$	1.79E-03	4.39E-04	0	fixed	0	fixed	0	fixed	3.73E-01	1.13E-01	2.75E-01	1.01E-01
	$\beta 0$	1.45E+01	4.16E-02	1.45E+01	1.39E+00	1.46E+01	2.88E-02	1.45E+01	4.37E-02	7.68E-02	1.47E-01	9.96E-02	1.48E-01
	$\beta 1$	0	fixed	3.44E-13	2.90E-05	0	fixed	0	fixed	3.76E-01	1.13E-01	2.78E-01	1.01E-01
	$\nu 0$	3.44E-01	7.72E-02	2.77E-01	6.30E-02	9.68E-01	2.42E-01	2.89E-01	6.52E-02	4.58E-05	4.50E-05	0	fixed
	$\nu 1$	0	fixed	0	fixed	4.60E+00	1.01E+00	0	fixed	7.24E-03	1.85E-03	5.13E-03	1.50E-03
	$\mu 0$	3.44E-08	7.72E-09	2.77E-08	6.30E-09	9.68E-08	2.42E-08	2.89E-08	6.52E-09	4.58E-12	4.50E-12	0	fixed
	$\mu 1$	0	fixed	0	fixed	0	fixed	2.91E-10	8.06E-10	3.13E-07	2.41E-07	4.84E-07	3.09E-07
	Log Likelihood	-1157.3		-1171.7		-1132.1		-1171.6		-1091.7		-1094.3	

Allowing each of the parameters to be exposure-related did significantly improve the fit of the model assuming a ten-year half life over that obtained by assuming any one of the parameters to be exposure-related, based on the improvement in the log-likelihood.

The model assuming an infinite half-life and all four two-stage parameters dose-related predicts that the background hazard increases sharply between age 50 and 60 and reaches a plateau of about $7x10^{-5}$ per year from age 60 onward. This seems somewhat implausible given the low mortality rate for mesothelioma in persons without asbestos exposure. Consequently, this model was refit with the background mesothelioma risk of zero, by assuming both ν_0 and μ_0 were fixed at zero (Model 6). This model, although being perhaps more realistic, gave a poorer fit ($p = 0.03$ for infinite half-life and $p=0.08$ for ten-year half-life, based on likelihood ratio test) than the model with the high background.

That the highest likelihoods for the Wittenoom data arise when the mutation rate from normal to intermediate cells (ν) is dose related, suggests that asbestos is acting as an initiator for mesothelioma. That the fit improves when either the proliferation rate or the mutation rate of intermediate cells is also allowed to vary with dose suggests that asbestos may also be serving as either a promoter or a late-stage actor for mesothelioma. This contrasts with the two-stage model results for lung cancer, in which having ν dose dependent did not improve the fits. Given the apparent limitations of the two-stage model, the interpretation of such results needs to be taken with great caution. However, the implication that asbestos serve primarily as a promoter (or late stage actor) toward lung cancer but also acts as an initiator toward mesothelioma is consistent with inferences from the broader literature (see Section 7.3).

Table 6-28 shows the fit of the two-stage model with an an infinite half-life and without background ($\nu_0 = \mu_0 = 0$) to the Wittnoom data categorized as to time since end of exposure. The fit of these data to the two-stage model is poor ($P = 0.03$). For comparison purposes the fit of the EPA mesothelioma model to the same data is also provided. The EPA model provides an adequate fit ($p = 0.21$), which is the same as previously indicated (Table 6-24).

Based on this limited exploration of the application of the two-stage model to the Wittenoom data, as well as the Quebec data (not shown), the decision has been reached that this model is probably not suitable for routine use in asbestos risk assessment. There are several reasons for this conclusion. The two-stage model was originally considered because there was some evidence from the literature that the mesothelioma risk did not continue to rise after the end of exposure, as predicted by the EPA model. The hazard function from the two-stage model predicts that risk will eventually fall back to baseline after exposure ceases, and consequently can predict

Table 6-28

Table 6-28:
Fit of the Best-fitting Two-Stage Model to the Wittenoom Mesothelioma Data

Time Since Last Exposure		Cases	Predicted	EPA Prediction	Log Likelihood	EPA Log Likelihood
Range (Yrs)	Mean (Yrs)					
[0, 1)	0.27	0	0.1	0.0	-0.05	-0.03
[1, 5)	3.01	0	0.2	0.1	-0.15	-0.12
[5, 10)	7.49	0	0.7	0.6	-0.65	-0.64
[10, 20)	14.89	10	10.9	14.5	-2.12	-2.85
[20, 30)	24.74	58	68.2	52.9	-3.76	-3.19
[30, 40)	33.95	79	74.0	61.3	-3.27	-5.44
>= 40	43.55	17	13.1	15.5	-2.86	-2.41
Total		164	167.1	144.9	-12.85	-14.68

		Two-Stage	EPA
Goodness of Fit	ChiSq	4.75	8.41
	P-value	0.03	0.21

this behavior. However, a detailed analysis of the mesothelioma data from both Wittnoom and Quebec indicates that neither demonstrates such behavior (Section 6.3.1.1). In fact, if anything, the EPA model may tend to under-predict the risk at the longest time periods following cessation of exposure (based on the Wittenoom data), although the results with the other two cohorts may not support this observation (see Tables 6-24, 6-25, and 6-26).

Although the two-stage model has been shown to be a useful research tool, some of its features make it less suitable for routine use in risk assessment. The model is complex and would be more difficult to comprehend by stakeholders in an asbestos risk assessment. Because of the numerous parameters in the model, numerical calculations are time-consuming and the results are sometimes problematic. Data are sometimes compatible with a range of possible outcomes under this model (e.g., exposure affecting either the first mutation rate or the cell death rate); currently the mechanism of mesothelioma causation is not well enough understood to permit choice among these possibilities with any degree of confidence, although our findings are not inconsistent with inferences from the literature (see Section 7.3). Moreover, the absence of a single "potency parameter" in the two-stage model would complicate simple comparisons of potency across studies or environments. For these reasons, the decision was reached to not pursue the two-stage model further in this project, but instead to consider simple modifications to the existing EPA model for cases in which this model was not adequate (Section 6.2.1.1).

An advantage of the two-stage model is that, since it models risk as a function of internal dose, it can naturally incorporate effects of fiber clearance.[1] However, we found that, due to the complexity of the model, it was neither particularly useful at predicting fiber half-lives nor distinguishing among assumed half-lives. We also found it possible to develop simpler adaptations to the EPA model that could reasonably address this consideration (Section 6.2.1.1) and found this latter approach more fruitful.

6.3.2 Estimating K_M's from Published Epidemiology Studies

At the time that the Health Effects Update was published (U.S. EPA 1986), four studies were found to provide suitable quantitative data for estimating a value for K_M and six additional studies provide corroborative support for the mesothelioma model applied. Currently, there are 14 published studies with adequate data for deriving an estimate of K_M (including updates to all four of the quantitative studies evaluated in 1986).

The EPA mesothelioma model described at the beginning of Section 6.3 was applied to each of these data sets to obtain study-specific estimates for the mesothelioma risk coefficient, K_M. The resulting set of K_M values are presented in Table 6-12 (which has been previously described, Section 6.2.2. In Table 6-12, Columns 9 and 10 list,

respectively, the best estimate of each K_M value derived for studies reported in the original 1986 Health Effects Update and the reference for each respective study. Columns 11, 12, and 13 present, respectively: the best-estimates for the K_M values derived for all of the studies currently available (including studies corresponding to those in the original Health Effects Update); the estimated lower and upper bounds for each K_M value (derived as described in Appendix A); and the reference for the respective study from which the data were obtained. To assure comparability across studies, values for all studies (even those that have not been updated since their inclusion in the 1986 Health Effects Update) were re-derived using the modified procedures described in Appendix A.

The K_M values derived in this study and the corresponding values derived in the original 1986 Health Effects Update are in close agreement, none vary by more than a factor of 2 and none of the differences appear significant (based on a comparison of their relative confidence intervals).

Among the K_M values derived in the current study, the lowest and highest of the best-estimate values differ by a factor of approximately 1400 (excluding the one negative study) and many of the pair-wise comparisons across this spectrum appear significant (because their confidence intervals do not overlap). For example, none of the confidence intervals for the K_M values derived for any of the environments involving exposure to chrysotile overlap the confidence intervals associated with the K_M values derived for either crocidolite mining or asbestos-cement manufacture using mxed fibers at the Ontario plant (Finkelstein 1984). Furthermore, neither of the confidence intervals for the K_M values derived for each of the two sets of chrysotile mines in Quebec (Asbestos and Thetford) overlap the intervals around K_M values for any of the amphibole environments or any of the mixed environments, except the Quebec factory that is associated with the Asbestos mine (Liddell et al. 1997).

The K_M values and the associated confidence bounds derived in the current study are plotted in Figure 6-5. Each exposure environment is plotted along the X-axis of the figure and is labeled with a four-digit code that indicates fiber type (chrysotile, mixed, crocidolite, or tremolite), industry (mining, friction products, asbestos-cement pipe, textiles, insulation manufacturing, or insulation application); and a two-digit numerical value indicating the study from which the data were derived. The same key provided for Figure 6-3 also applies to this figure. In the Figure, the chrysotile studies are grouped on the left, amphibole studies are grouped on the right, and mixed studies are in the middle. Note also that studies conducted in the same facility (generally among highly overlapping cohorts), such as the Dement et al. (1994) and the McDonald et al. (1983a) studies of the same South Carolina textile facility, are combined as a single entry in the Figure. The cohorts from Asbestos Quebec and Thetford are also combined in the Figure.

Figure 6-5:
Plot of Estimated KM Values and Associated Confidence Intervals by Study Environment

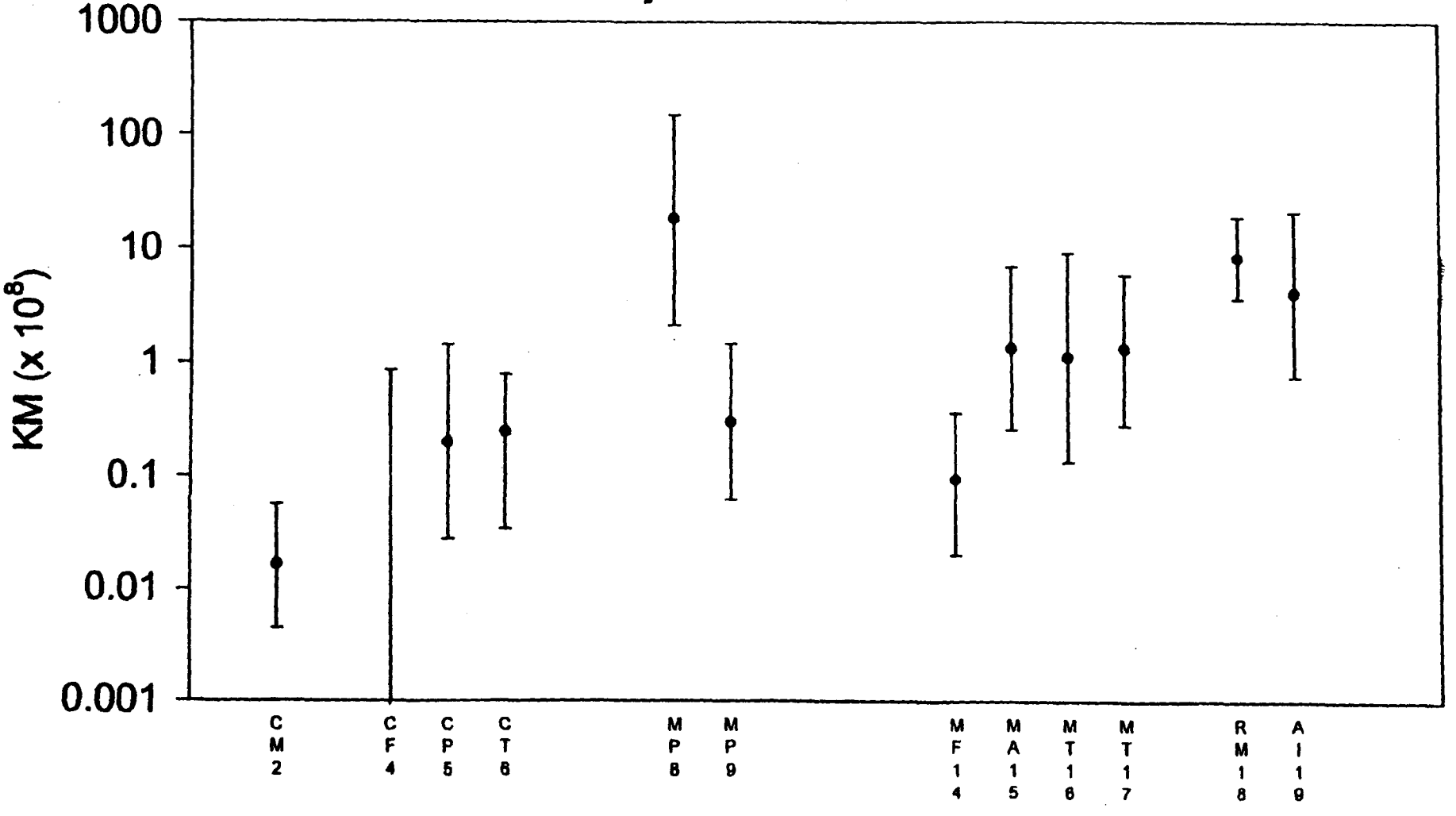

Figure 6-5

As with the K_L values, comparison of K_M values across the available studies are instructive. Within chrysotile studies alone, lowest and highest K_M values vary by approximately a factor of 15 (again, excluding the negative friction products study), which is minimal variation relative to the spread across the values from all of the studies in the table. Based on the overlap of their confidence intervals, none of these differences appear to be significant.

The K_M values for the two "pure" amphibole studies (crocidolite mining and amosite manufacturing) agree to within a factor of 2 and, with the exception of the value from the Ontario asbestos-cement plant (Study No. 8 in the Figure) and the factory plant associated with the Asbestos, Quebec mines (Study No. 14), the mixed exposures fall in between the high values for the "pure" amphibole exposures and the lower values reported for all of the chrysotile sites. Although the K_M value for the asbestos-cement plant (Study No. 8) appears high, it does not appear to be significantly different than the values from either of the "pure" amphibole studies or values for many of the other mixed exposures (based on the degree of overlap of their respective confidence intervals). The K_M value reported for the factory associated with the Asbestos, Quebec mine (Study No. 14) is the lowest of those reported for mixed exposures, but (again based on the overlap of confidence intervals) it does not appear to differ significantly from values for several of the other mixed exposures nor the highest values among the chrysotile studies.

As with K_L values, the asbestos-cement pipe industry shows the greatest variation in K_M values across all asbestos types, with a range that varies over a factor of 90. Moreover, the difference between the highest and lowest values in this industry may be significant (due to the lack of overlap of their intervals). Within the textile industry, the K_M value for the South Carolina chrysotile plant is only a tenth of the values reported for the two textile plants using mixed fibers, but these differences do not appear to be pairwise significant. The potential sources of variation across all of the K_M values are likely attributable to the same sources of variation identified for the K_L values and previously described in detail (Section 6.22).

6.3.3 Evaluating Effects Associated with the Character of Exposure

To evaluate the effects of fiber size on the K_M values listed in Table 6-12 (in parallel with the manner in which the K_L values were evaluated) K_M values were also adjusted to match them to the improved exposure index defined in Equation 6.7 and the implications of these adjustments were evaluated (in a manner entirely analogous to that described in Section 6.2.4.2). The justification for the development of the improved exposure index is provided in Appendix B.

6.3.3.1 Adjusting K_M's for size

The K_M values were adjusted for size in the same manner described in Section 6.2.4.1 for the K_L values. To accomplish this, the same, published fiber size distributions were matched to the same epidemiology studies (Table 6-14) and the conversions performed as described by Equations 6.4 to 6.6 using the data presented in Table 6-15. The resulting adjusted values, the K_M's are listed in Table 6-16.

6.3.3.2 Evaluating the implications of adjusting K_M's for size

To compare the effects of adjusting K_M values for fiber size, the adjusted values (the K_M's), are plotted (along with their associated confidence intervals) in Figure 6-6, which exhibits a format identical to that of Figure 6-5. In fact, the formats of Figures 6-3 (unadjusted K_L's), 6-4 (the adjusted, K_L's), 6-5 (unadjusted K_M's), and Figure 6-6 (adjusted, K_M's) are also designed for direct comparison. The "key" provided for Figure 6-3 is also directly transferable to all of the figures, including Figure 6-6.

Although Figures 6-5 and 6-6 may look similar at first glance, there are several differences. First, the value for study MF14 had to be omitted from Figure 6-6 because no suitable size distribution is available to allow the potency factor from this study to be adjusted. The confidence intervals presented in Figure 6-6 are also larger than those depicted in Figure 6-5. This is because the one's depicted in Figure 6-6 incorporate an additional factor to account for the uncertainty of adjusting for fiber size using paired data from published size distributions. Table 6-17 lists the factors by which the upper bounds are multiplied and lower bounds are divided to derive the confidence intervals depicted in Figure 6-6.

The most important differences between Figures 6-5 and 6-6 are the changes in the relative positions of the central value estimates for the potency factors depicted. Therefore, numerical representations of these changes are provided in Table 6-18.

Table 6-18 presents the magnitude of the spread in the range of original and adjusted K_M values (original and adjusted K_L values are also presented, see Section 6.2.4.2). Such spreads are estimated as the quotient of the maximum and minimum values of each range. As previously indicated, this type of analysis (of necessity) requires that the zero value obtained for the Connecticut friction products plant study (CF4) be omitted. The one study for which no suitable conversion factor could be found for the corresponding K_M, (Study No. MF14) was also omitted.

Figure 6-6

Table 6-6:
Plot of Adjiusted KM Values (KM*'s) and Associated Confidence Intervals by Study Environment

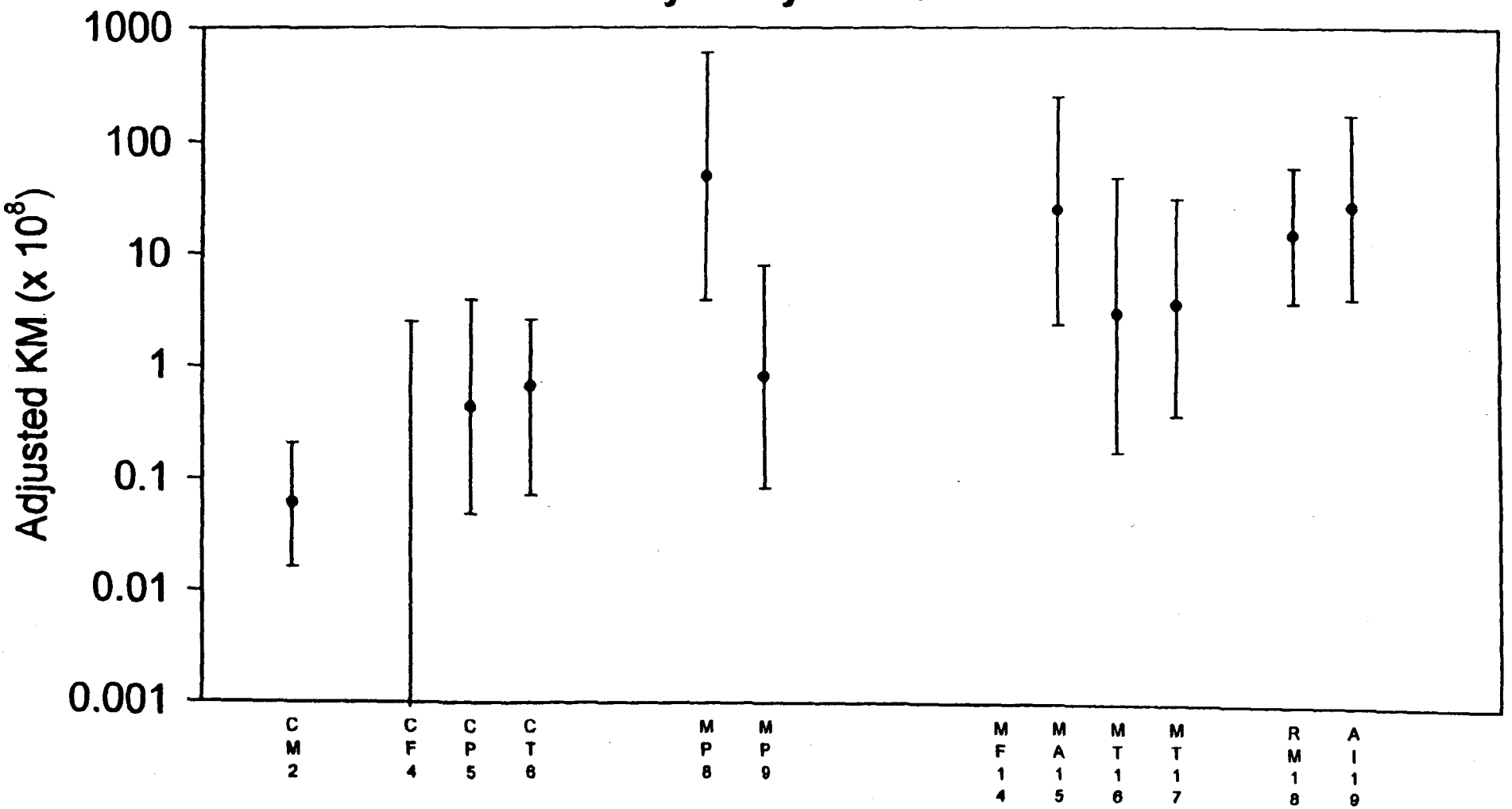

The trends apparent in Table 6-18 that were described for a comparison between K_L and K_L. values are similar but exaggerated between the K_M and K_M. values. Briefly, the spread in values among "pure"fiber types (i.e. chrysotile or amphiboles only) are much smaller than the spread observed over all values (or over data sets that include mixed exposures) and this is true for both the adjusted and unadjusted K_M values. This suggests that chrysotile and the amphiboles exhibit different potencies toward the induction of mesothelioma. Also, the spreads for all of the data sets presented in Table 6-18 (except the one for pure amphiboles, which is already minuscule) are reduced when values are adjusted for fiber size. However, even for adjusted values, the spreads in data sets including mixed exposures are still rather large. As for lung cancer, this implies that the effects of fiber type and fiber size are also confounded for mesothelioma. Therefore, an evaluation similar to that conducted for lung cancer potency factors was also conducted for mesothelioma potency factors to simultaneously address the effects of fiber size and fiber type. The manner in which the evaluation was conducted is described in Section 6.2.4.2.

Table 6-19 presents the results of the analysis in which the K_M estimates are adjusted both for fiber size and for the fraction of the exposures in each environment contributed by amphiboles. As previously described, K_{MA} values are the estimated potencies of pure amphiboles, K_{MA}.'s are the estimated potency of pure amphiboles adjusted for fiber size, and RPC is the ratio of the potency of pure chrysotile to pure amphibole toward the induction of mesothelioma, in this case (see Section 6.2.4.2). In the analysis, the spread of the range in values for each data set was minimized by optimizing the value for RPC.

That the optimum values for RPC (presented in Column 3 of Table 6-19) are substantially smaller than one for both the unadjusted K_{MA} values and the K_{MA}. values (which are adjusted for fiber size) suggests that chrysotile is substantially less potent toward the induction of mesothelioma than amphiboles and may be non-potent. However, because improvement (reduction) in the spread in values for these data sets becomes marginal for values of RPC less than about 1/1000, a conservative estimate suggests that, at most, chrysotile is no more than 1/1000 as potent as amphiboles toward the induction of mesothelioma.

Based on a comparison of the magnitude of the spreads in range for each data set (listed in Column 4), adjusting mesothelioma potency factors for fiber size results in a 30% improvement in agreement across estimated values. Moreover, simultaneously accounting for the effects of fiber type and fiber size results in very effective reconciliation of potency estimates for mesothelioma. Once adjusted in ths manner, the spread in potency estimates across all 10 of the studies available for this analysis is only a factor of 26 (only a little larger than an order of magnitude). This should provide

reasonable confidence that a representative value for amphibole potency that might be selected from this range can be applied to new environments to estimate risk.

As with lung cancer, a more sophisticated analysis of mesothelioma potency values was also completed, which incorporates formal consideration of uncertainty and (due to the manner in which the analysis is performed) allows us to include the nominally zero value from the Connecticut friction products plant (Study No. CF4). The details of the analysis are provided in Section 6.2.4.2. Results are provided in Table 6-21.

As with lung cancer, the results of this more formal analysis of mesothelioma potency factors closely parallels the results described in the above analysis. The best estimated values of the relative potency of chrysotile toward mesothelioma lies between 1/250th (0.004) and 1/570th (0.002) of that for the amphiboles and these values are not statistically different from an estimate of zero potency for chrysotile (P = 0.54 for the unadjusted data set and P = 0.72 for the size adjusted data set).

Adjusting the mesothelioma potency factors for fiber size results in an about a 23% improvement in the overall agreement among values (determined by comparing the relative magnitudes of the optimized "σ" estimated for the size adjusted data set (0.6561) and the unadjusted data sets (0.8123), respectively. Thus, even using the relatively crude procedure of adjusting K_M values based on published (rather than study-specific) size distributions, results in moderate improvement in the agreement in values across studies.

6.4 GENERAL CONCLUSIONS FROM HUMAN EPIDEMIOLOGY STUDIES

Results from our evaluation of the available epidemiology studies indicate that:

(1) the results of individual epidemiology studies are uncertain, especially when one considers all of the major potential sources of uncertainty (rather than simply considering the statistical uncertainty associated with the number of deaths, as is traditionally done). However, more robust conclusions can be drawn from an analysis of the set of epidemiology studies taken as a whole than results derived from individual studies;

(2) by adjusting for fiber size and fiber type, the existing database of studies can be reconciled adequately to reasonably support risk assessment;

(3) the procedures recommended as a result of our analysis offer substantial improvement over EPA's current approach to evaluating asbestos-related risks;

(4) while there is some indication that the existing EPA models for lung cancer and, potentially, mesothelioma may not entirely reflect the time-dependence of disease at long times following cessation of exposure, such effects appear to be modest so that they are unlikely to adversely affect the proposed approach. Prudence dictates, however, that limited additional study may be warranted to adequately dismiss related concerns; and

(5) results from our review of the supplemental literature provide additional support for the approach recommended in this chapter and indicate additional, specific modifications that (if supported by limited additional study) could result in substantial improvement even over the approach currently recommended, which (in turn) provides substantial improvement over the current approach.

More detailed conclusions and recommendations are described below.

Conclusions and Recommendations For Lung Cancer

Without adjustments, the K_L values estimated from the 18 existing studies vary by a factor of 90 and pairwise differences between several individual studies are likely significant (based on a comparison of their associated confidence intervals). By simultaneously adjusting these values for fiber size and type, variation across the 16 studies (for which data are available to make the required adjustments) is reduced to a factor of about 60.

Especially given the crude manner available for performing size adjustments coupled with the very consistent picture that such adjustments improve matters and that there is a strong theoretical basis for expecting that such adjustments should improve cross-study comparison or extrapolation, we believe that such adjustments increase overall confidence in cross-study comparison/extrapolation. We therefore recommend their use.

The maximum and minimum values driving the factor of 60 come from cohorts of South Carolina textile workers and Quebec miners, respectively, and the difference in the lung cancer potency estimated between these studies has long been the subject of much attention. A detailed evaluation of the studies addressing this difference, the results of our analysis of the overall epidemiology literature, and implications from the broader literature, indicate that the most likely cause of the difference between these studies is the relative distribution of fiber sizes in the two study environments. It is therefore likely that the variation between these studies can be further reduced by implementing one or a combination of the following:

- deriving improved characterizations of the exposures experienced by cohort members in each, respective environment based on study-specific size distributions (instead of relying on the cruder use of published distributions, as currently required);

- deriving improved characterization of the exposures experienced by cohort members in each, respective environment based on improved analysis of relevant material (instead of relying on the existing, published distributions, which are insufficiently detailed to capture all of the biologically-relevant aspects of size distributions);

- from a selected subset of key studies, developing the improved characterization data required to allow the existing lung cancer potency factors to be adjusted to an exposure index that is even closer to an optimized index than the one recommended in this document;

- procedures for accomplishing some or all of the these objectives are described below.

Importantly, the exposure index recommended in this document (and used throughout this analysis), while not perfect, when coupled with the recommended adjustments for fiber type, already provides substantial improvement over EPA's current approach to evaluating asbestos-related risks. This is evident, for example, if one compares certain values of the variance (σ) provided in Table 6-21. Because, under the current approach, chrysotile and amphiboles are considered equipotent and lung cancer and mesothelioma risks are combined, the overall variance estimated for the unadjusted K_M values with RPC =1 (1.817) should be compared with the variance estimated for adjusted K_M values with RPC optimized (0.6561), which represents the recommended approach. Thus, the new approach reduces variance by approximately a factor of three over the current approach. Actually, the improvement is even larger because the K_M values employed in our analysis include a greater number of studies than available to the U.S. EPA in 1986. Therefore, despite our recommendations below to conduct limited, additional study that may lead to further improvements, there is no reason not to implement the recommendations from our current analysis now.

Although the EPA lung cancer model appears to adequately describe the time dependence of disease for amphiboles, it may not adequately describe risks for chrysotile at long times following cessation of exposure. In contrast to predictions from the model (potentially due to the observed, lower biodurability of chrysotile), lung cancer risks from chrysotile decrease with time following cessation of exposure. Thus, if the model is applied to any new site to predict risks, if anything, risk estimates will be conservative. However, particularly for studies with long followup times after cessation

of exposure, the K_L's estimated from existing studies (using the EPA model) may be underestimated. Importantly, these conclusions are based on raw observations from only one chrysotile and one amphibole study. Thus, it may be prudent to evaluate raw data from a minimum of one additional chrysotile study and one additional amphibole study to confirm that such observations are indeed general. However, it is likely that these time-dependent effects are relatively small.

Conclusions and Recommendations For Mesothelioma

Without adjustments, the K_M values estimated from the 12 existing studies vary by more than a factor of 1000 and pairwise differences between several individual studies are likely significant (based on a comparison of their associated confidence intervals). By simultaneously adjusting these values for fiber size and type, variation across the 11 studies (for which data are available to make the required adjustments) is reduced to a factor of about 26. Given that this is little larger than an order of magnitude, it appears that we have essentially reconciled the mesothelioma studies.

Although the EPA mesothelioma model appears to adequately describe the time dependence of disease in general, there was some indication that it may under estimate risks at long times following cessation of exposure for amphiboles. Therefore, as part of the analysis recommended for further testing the time dependence of the lung cancer model, it may also be prudent to further evaluate the behavior of the mesothelioma model.

Conclusions and Recommendations for Risk Assessment

Based on our analysis, we recommend the following.

(1) Asbestos concentrations should be analyzed for structures that correspond to the exposure index defined in Equation 6.7. Thus, count only structures longer than 5 μm and thinner than 0.5 μm with structures longer than 10 μm weighted as indicated in Equation 6.7. Further, count both parent fibers and bundles and fibers and bundles that are components of more complex structures, but that individually satisfy the above-defined dimensional criteria. Importantly, analysis needs to be performed by TEM following preparation by a direct-transfer procedure.

(2) When mixed, the individual contributions from chrysotile and the combined amphiboles to any particular exposure need to be separately delineated and, because amphibole exposures are the primary drivers, the analytical sensitivity required for each particular study should be set based on amphiboles.

(3) Combine such counts with the matched potency factors for lung cancer and mesothelioma described in Tables 6-29 or 6-30 below using the appropriate EPA model for each disease.

Based on our analysis, the optimized potency coefficients that are adjusted for size (so that they are appropriately matched to the exposure index defined above) are obtained from Table 6-21 and reproduced here:

Table 6-29:
Optimized Risk Coefficients
for Pure Fiber Types

Fiber Type	$K_L \cdot$ x 100	$K_M \cdot$ x 10^8
Chrysotile	0.85	0.05
Amphiboles	4.5	30

In keeping with the tradition of incorporating conservative estimates to minimize the chance of under-estimating risks, conservative estimates for the potency factors listed in Table 6-29 are derived by up-adjusting the amphibole potency values for both lung cancer and mesothelioma so that they match the largest value from the set of available studies and adjusting the chrysotile values proportionally. Results from this calculation are presented in Table 6-30.

Table 6-30:
Conservative Risk Coefficients
for Pure Fiber Types

Fiber Type	$K_L \cdot$ x 100	$K_M \cdot$ x 10^8
Chrysotile	3.0	0.1
Amphiboles	15	50

We leave it as an option for deciding which values to employ. Interestingly, however, due to the great degree of reconciliation among the disparate values for the potency estimates already achieved in this document, the ratio of the conservative and optimum $K_L \cdot$ estimates is only a little larger than a factor of 3 while the conservative and optimum $K_M \cdot$ values vary by less than a factor of 2.

Recommendations for Limited, Further Study

The two major objectives identified above for further study are:

(1) to expand the test of the ability of the current EPA models to adequately track the time-dependence of disease; and

(2) to develop the supporting data needed to define adjustments for potency factors that will allow them to be used with an exposure index that even more closely captures the criteria that determine biological activity (see Section 7.5). Among other things, this may ultimately provide the data allowing complete reconciliation of the potency factors derived for Quebec miners and South Carolina textile workers, one of the major outstanding issues identified among asbestos researchers.

The first of the above objectives requires that we gain access to raw data from a small number of selected, additional epidemiology studies. The best candidate studies include: (for chrysotile) the lung cancer data from Quebec (best) or, potentially, from the New Orleans asbestos-cement pipe plant studied by Hughes et al. For amphiboles, the best candidate studies include: the lung cancer and *newest* mesothelioma data from Libby (best), or, potentially the lung cancer and mesothelioma data from the Paterson, New Jersey insulation manufacturing plant studied by Seidman. The possibility of obtaining some or all of these data sets needs to be further explored.

The second of the above objectives requires more detailed size characterization data for the environments of interest. Although archived air samples do not appear to be available from any of the study locations of interest, we believe that suitable data can be developed from appropriate bulk samples. Thus, for example, it would be useful to obtain samples of the raw ore from Libby, Wittenoom, and Quebec and the textile, asbestos-cement pipe, and friction-product grade products from Quebec. We have already approached individuals who can provide access to these materials and they have all expressed interest in collaborating.

Results from our review of the supporting literature suggest that the optimum cutoff for increased potency occurs at a length that is closer to 20 μm than10 μm, (the latter of which is the cutoff in the exposure index provided in this study). Data do not currently exist to improve on this latter cutoff. However, provided that study-specific size distribution data could be obtained as indicated above, with the appropriate analyses, it will be possible to develop the size distributions necessary to evaluate a range of considerations including:

- delineation of size fractions among individual length categories out to lengths as long as 30 or 40 μm;

- determination of the relative presence and importance of cleavage fragments (of non-biologically relevant sizes) in mine ores vs. finished fibers; and

- the relative fraction of fibrous material vs. non-fibrous particles in the various exposure dusts of interest.

7.0 SUPPORTING EXPERIMENTAL STUDIES

To evaluate the plausibility of cancer risk models for asbestos it is useful to examine what is currently known (and what is not known) about (1) the mechanisms that facilitate the transport of asbestos to the various target tissues of interest (in the lungs and mesothelium) and (2) the mechanisms that contribute to the development of cancer in these target tissues. Accordingly, a detailed review of the relevant literature is provided in this Chapter.

Although much progress has been made over the last decade toward elucidating the fiber/particle mechanisms that contribute to transport and subsequent cancer induction, at least two critical data gaps remain:

- no one has yet been able to track a specific lesion induced by asbestos in a specific cell through to the development of a specific tumor. There have been experiments that show altered DNA and other types of cellular and tissue damage that are produced in association with exposure to asbestos and other studies demonstrating that various tumors of the kinds that result from asbestos exposure exhibit specific patterns of DNA alteration or other damage. There are also studies that show that exposure to asbestos can lead ultimately to development of tumors. However, these types of studies have yet to be linked; and

- although the target tissues in which asbestos-induced cancers develop have generally been identified, the specific target cells that serve as precursors to these tumors are not known with certainty.

Because of the first of the above limitations, researchers have tended to report on a broad range of tissue and cellular effects induced by asbestos that may lead generally to various kinds of cellular damage or injury. Direct cytotoxicity, for example, is one of the end points typically tracked as a marker for asbestos-induced injury. However, not all of these effects necessarily contribute (either directly or indirectly) to the development of cancer. Therefore, one of the goals of the following discussion is to distinguish (within the limitations of the current state of knowledge) among effects that likely contribute to the development of cancer from those that are less likely or unlikely to contribute.

In addition, because the relative effects of fiber size, shape, and mineralogy need to be elucidated to better indicate how asbestos concentrations should be characterized to support risk assessment, studies that address these topics are highlighted. Of

particular interest are studies that contrast the effects of different sized fibers or the effects of fibers from the effects of non-fibrous particles of similar mineralogy and studies that contrast the effects of fibers of comparable morphology (size and shape) but differing mineralogy.

The types of studies that have contributed to the state of knowledge of the effects of asbestos (in addition to the human epidemiology studies previously reviewed, see Chapter 6) include:

- whole animal inhalation studies;
- whole animal instillation studies;
- whole animal injection, implantation studies;
- human pathological studies;
- in-vitro studies in cell cultures; and
- in-vitro studies in cell-free systems.

Note, depending on the outcome(s) monitored, the animal studies may alternately be categorized as retention studies, histopathology studies, or dose-response studies.

Each type of study possesses certain advantages and exhibits certain limitations, which have previously been described (Chapter 5) along with descriptions of the nature of each of these study types. In addition to the advantages and limitations that are attributable to the type of study, the quality of the characterization of asbestos (or other particulate matter) determines the utility of the study for addressing issues associated with fiber morphology and mineralogy. Unfortunately, for many published studies, both the characterization of the asbestos (or other particulate matter) and descriptions of the manner in which such materials were handled are insufficient to establish the detailed morphology or mineralogy. Thus, such limitations need to be considered when comparing across study results or evaluating the validity of study conclusions.

As previously indicated (Chapter 3), the primary route of asbestos exposure of concern for humans is inhalation. Moreover, the biological activity of inhaled asbestos depends on the following factors:

- the extent that asbestos structures are respirable and the pattern of deposition of inhaled structures;

- the extent that deposited structures are subsequently cleared or degraded;

- the extent that deposited structures are transported or migrate to the various target tissues; and

- the extent that retained structures induce a biological response in each target tissue.

7.1 FACTORS AFFECTING RESPIRABILITY AND DEPOSITION

Discounting systemic affects resulting from other forms of exposure, factors affecting respirability are common to all of the toxic end points associated with asbestos exposure considered in this study (asbestosis, pulmonary carcinomas, and mesothelioma). Moreover, respirability is common to the factors affecting the toxicity of inhaled, insoluble particles in general. To be respirable, an inhaled particle must pass the blocking hairs and tortuous passageways of the nose and throat and be deposited in the lungs. Particles deposited in the naso-pharyngeal portion of the respiratory tract are not considered respirable.

Not all of the inhaled particles that reach the lungs will be deposited. Small particles may not impact lung surfaces during inhalation and are subsequently exhaled. Once a particle impacts on a surface, however, it is likely to remain because the surfaces of the lungs are wetted with a surfactant (Raabe 1984).

Adverse health effects potentially result when particles are deposited in the lungs and remain in contact with tissue within the lungs for a sufficient period of time to provoke a biological response. To affect the mesothelium, an offending particle may also need to migrate or be transported from the lung to this surrounding tissue. However, due to the proximity of the mesothelium to peripheral portions of the lung parenchyma (which include locations where particles are typically deposited), it is also possible that diffusable molecules produced in lung tissue in response to deposited particles can have an adverse effect on the mesothelium (see, for example, Adamson 1997). Such effects are considered among the mechanisms of disease induction addressed in the discussion of biological responses (Section 7.3).

It is long-term retention of particles in the respiratory tract that potentially leads to adverse health effects. Consequently, the interplay between deposition and removal (clearance) is an important determinant of biological activity and separating the impact of these two processes is difficult. The term "retention" is used here to represent the fraction of particles remaining in the lungs beyond the time frame over which only the

most rapid removal processes are active (i.e. muco-ciliary clearance). The factors affecting retention are addressed further in Section 7.2.

Published inhalation studies divide the respiratory tract into three units (see, for example, Raabe 1984). The naso-pharyngeal portion of the respiratory tract extends from the nares in the nose through the entrance to the trachea. The tracheo-bronchial portion of the respiratory tract includes the trachea and all of the branching bronchi down to the terminal bronchioles. The respiratory bronchioles and the alveoli, which are collectively referred to as the "deep lung", are the bronchio-alveolar (or pulmonary) portion of the respiratory tract. For a more detailed description of the features of the respiratory tract, see Section 4.4.

The dimensional requirements for respirability have been studied and reviewed by several authors (see, for example, Raabe or 1984 or U.S. EPA 1986). A more recent review is also presented by Stober et al. (1993). Much of the data reviewed by these authors is based on earlier studies in which researchers exposed animals or human volunteers to a series of monodisperse spherical particles (although Stober et al. also reviews fiber experiments). In this manner, the impact of the diameter of spherical particles on respirability was elucidated. The respirability of fibrous materials (such as asbestos) tends to be described in terms closely associated with those employed for spherical particles, but with adjustments for density and shape. Importantly, because respirability is a mechanical process: the size, shape, and density of a particle (or fiber) determine its respirability along with the morphometry of the airways through which the particle passes (Stober et al. 1993). Other than affecting the particle's density or the distribution of fiber shapes, the chemical composition (mineralogy) of a particle (or fiber) does not influence respirability.

The respirability of particles and fibers by humans and a variety of other mammals of experimental interest has also been the subject of increasingly sophisticated modeling efforts (Stober et al. 1993). The latest refinements of such models predict particle deposition with a degree of accuracy that is beyond what can be validated with existing, experimental data. The application of several of these models to asbestos (and other fibrous materials) are considered throughout this chapter. However, a detailed overview of the state of the art of such modeling is beyond the scope of this document. Such an overview is presented by Stober et al. (1993).

7.1.1 Respirability of Spherical Particles

Spherical particles larger than 10 μm in diameter are considered non-respirable because virtually all particles in this size range are trapped in naso-pharyngeal

passageways and blocked from entering the lungs. As the diameter of the particles fall, an increasing fraction traverses the nose and throat and may be deposited in the lungs. About half of particles 5 μm in diameter are blocked before entering the lungs. Virtually all particles smaller than 1 μm enter the lungs, although other factors determine whether they are in fact deposited or simply exhaled. Figure 7-1 (Source: Raabe 1984) is a representation of the relative deposition in the various compartments of the respiratory tract as a function of particle diameter.

Within the lungs (Figure 7-1), the greatest fraction of respirable particles (over the entire range of diameters down to less than 0.01 μm) are deposited in the deep lung (the broncho-alveolar portion of the respiratory tract), primarily at alveolar duct bifurcations (see, for example, Brody et al. 1981, Davis et al. 1987, Johnson 1987, and Sussman et al. 1991a). These studies also indicate that biological responses appear to be initiated where deposition is heaviest. Generally, the fraction of particles deposited in the deep lung increases regularly with decreasing diameter until a maximum of 60% deposition in the deep lung is reached at about 0.1 μm diameter.

As indicated in Figure 7-1, a transition occurs at particle diameters between 0.5 and 1 μm. For particles in this range and smaller, deposition in the deep lung competes primarily with deposition in the tracheo-bronchial tree and with exhalation; smaller particles have an increasing probability of being exhaled without ever impacting the surface of an air passageway. For particles larger than this transition range, broncho-alveolar deposition is limited chiefly by the fraction of particles that are removed from the air stream prior to reaching the deep lung (either by deposition in the naso-pharyngeal or the tracheo-bronchial portions of the respiratory tract).

The transition between naso-pharyngeal competition with deep-lung deposition and competition from other removal processes is important because, during mouth breathing, a process that bypasses the tortuous pathways of the nose and throat, it has been observed that larger particles (up to several micrometers in diameter) may be deposited in the deep lung (Raabe 1984). Studies of the effects of mouth breathing are also reviewed by Stober et al. (1993). Because most people spend at least small amounts of time mouth breathing, especially during exertion or during snoring, this mechanism for allowing larger particles to settle in the deep lung should not be ignored.

A diameter of 0.5 μm also happens to represent the transition between the regime where inertial flow and the regime where diffusional flow becomes the major factor controlling deposition in the lungs. Below the 0.5 μm transition, the diffusional diameter becomes more important in determining deposition than the aerodynamic equivalent diameter (defined below).

Figure 7-1. OLD Figure 5-1

NEED TO GET PERMISSION TO REPRODUCE FIGURE AND NEED TO DEVELOP FIGURE.

Figure 7-1:
FRACTIONS OF RESPIRABLE PARTICLES DEPOSITED IN THE VARIOUS COMPARTMENTS OF THE HUMAN RESPIRATORY TRACT AS A FUNCTION OF AERODYNAMIC EQUIVALENT DIAMETER[a,b]

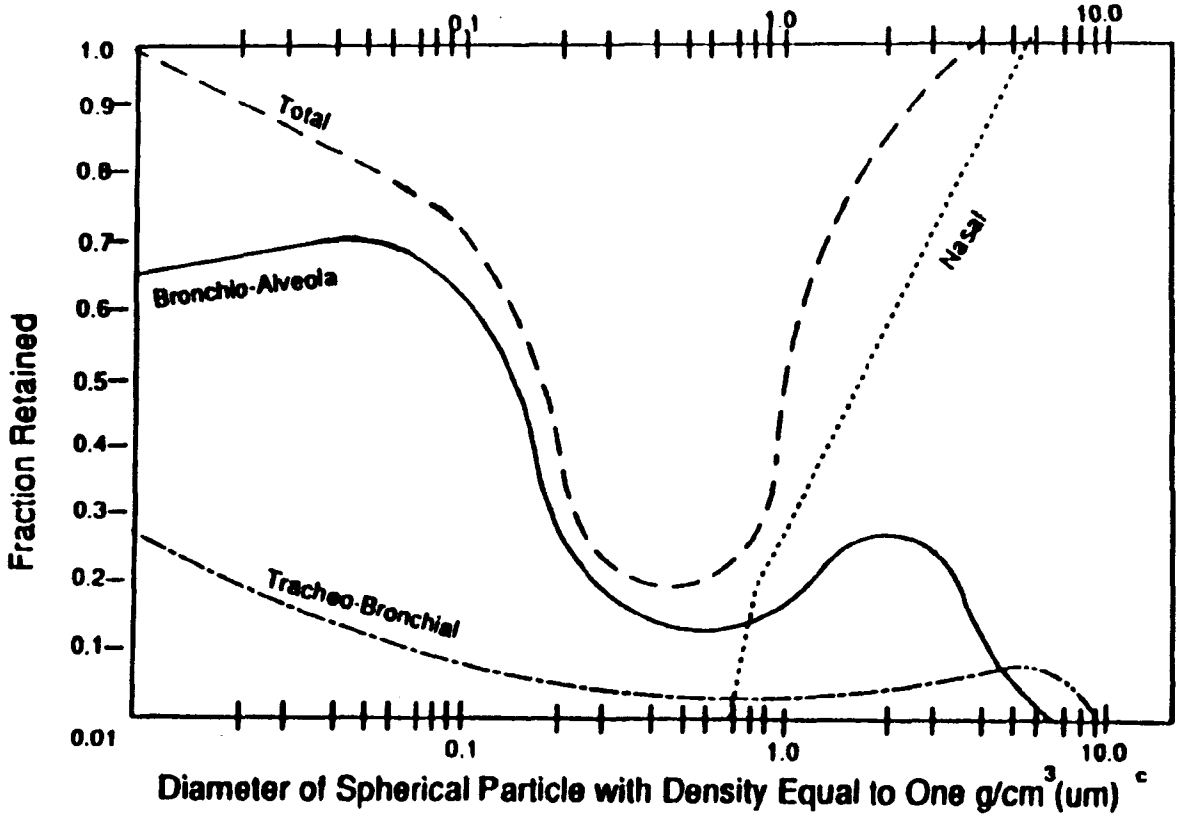

[a] Source: Raabe 1984.

[b] Assumes a typical tidal value of 1450 cm^3 and a rate of 15 breaths per minute.

[c] Aerodynamic equivalent diameter.

Confidential:
Need permission to reproduce this figure

7.1.2 Respirability of Fibrous Structures

Several authors have investigated the effect of the shape of non-spherical particles (including fibers) on respirability and deposition (see, for example, Harris and Timbrell 1977, Sussman et al. 1991a and b, Strom and Yu 1994, or Yu et al. 1995a and b). It has been found that the behavior of non-spherical particles can be related to the behavior of spherical particles by introducing a concept known as the aerodynamic equivalent diameter. The aerodynamic equivalent diameter is the diameter of a hypothetical spherical particle of unit density that would exhibit the same settling velocities and aerodynamic behavior as the real, non-spherical particle of interest. Factors that affect the aerodynamic equivalent diameter are density, true diameter, true length (for elongated particles such as fibers) and the regularity of the particle shape.

Harris and Timbrell Findings

Because fibrous particles tend to align primarily along the axis of travel under the flow conditions found in the lungs, respirability is predominantly a function of the diameter of a fiber and the effect of length is secondary (Harris and Timbrell 1977). Fibrous structures (of unit density) with aspect ratios greater than 3:1 behave like spherical particles with diameters up to 3 times larger (the aerodynamic equivalent diameter) and exhibit only a very weak dependence on length. This is demonstrated in Figure 7-2 where the true diameter of a fiber is graphed on the top horizontal axis against spherical (aerodynamic equivalent) diameters on the bottom horizontal axis. Figure 7-2 is an overlay of Figure 7-1. Note that, to adjust for the density of asbestos, the true diameters listed in the figure have been shifted to the right of where they would appear if the relationship was exactly one third of the aerodynamic equivalent diameter. Two vertical dashed lines in Figure 7-2 represent effective limits to the range of respirable asbestos. The left line in the figure represents the limiting diameter of the smallest chrysotile fibril (about 0.02 μm true diameter) and thus represents a lower limit to the deposition chart that is of concern when considering asbestos. The right vertical line represents the cutoff where deposition in the deep lung becomes unimportant due to removal of such particles by the naso-pharyngeal passageways. This latter cutoff corresponds to a true fiber diameter of 2.0 μm, which theoretically represents the upper limit to the size of asbestos that is respirable. As indicated in the figure, however, deposition in the deep lung drops precipitously for fibers thicker than about 0.7 μm so that no more than a few percent of asbestos fibers thicker than approximately 1 μm actually reach the deep lung.

Figure 7-2.

FRACTIONS OF RESPIRABLE PARTICLES DEPOSITED IN THE VARIOUS COMPARTMENTS OF THE HUMAN RESPIRATORY TRACT AS A FUNCTION OF THE TRUE DIAMETER OF ASBESTOS FIBERS[a,b,c]

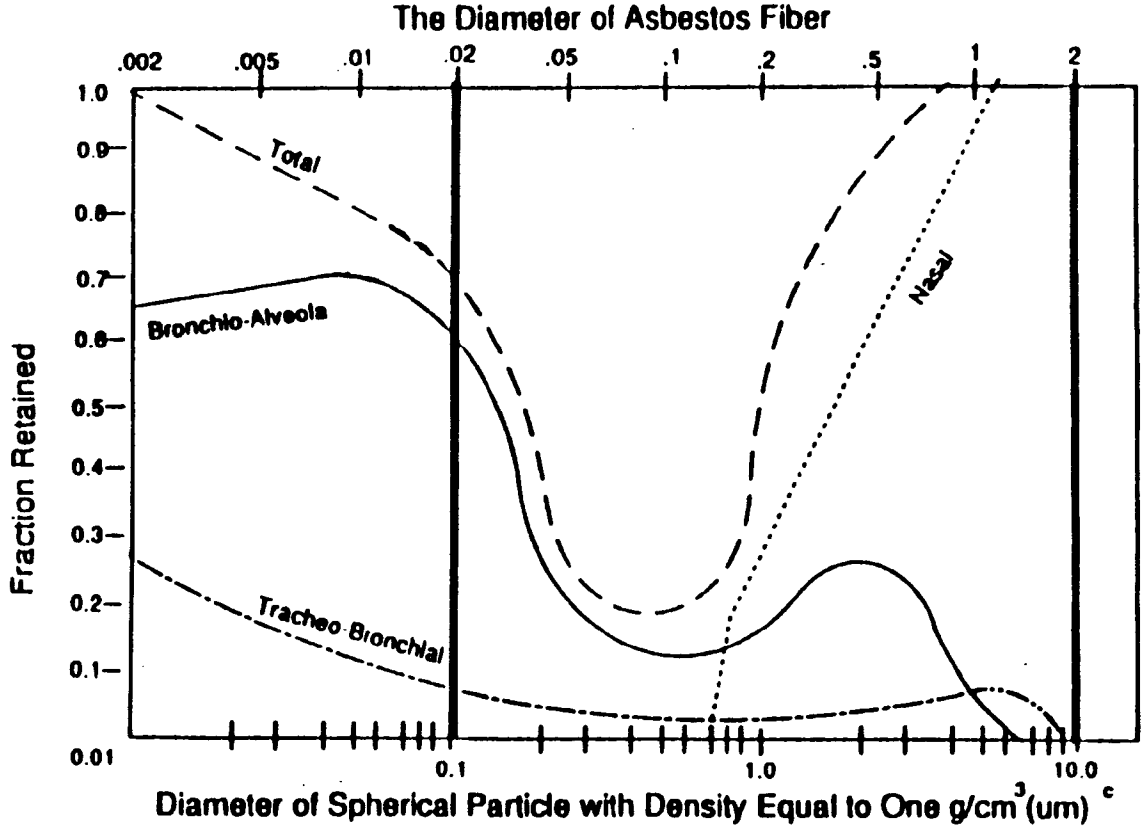

[a] Source of original: Raabe 1984.

[b] Assumes a typical tidal value of 1450 cm^3 and a rate of 15 breaths per minute.

[c] The relationship between true diameters and aerodynamic equivalent diameters derived from Harris & Timbrell (1977). Diameters adjusted for shape and density of asbestos fibers.

[d] Aerodynamic equivalent diameter.

Confidential:
Need permission to reproduce this figure

Figure 7-2 (old Figure 5-2)

Harris and Timbrell (1977) also evaluated the relationship between the overall shape of a particle and the extent of deposition. Over the range of diameters that potentially represent the range of asbestos fibers likely to be encountered, pulmonary deposition decreases with increasing complexity of shape beyond simple cylinders (such as clusters and matrices) at the expense of increasing naso-pharyngeal or tracheo-bronchial deposition. This change also becomes increasingly important as the length of the structure increases.

For structures less than 25 µm in length, the difference in deposition between simple fibers and complex clusters or matrices may vary by up to a factor of 2 with the complex structures being more likely to be removed in the naso-pharyngeal portion of the respiratory tract and the fibers more likely to be deposited in the deep lung. At 100 µm lengths, the fraction of complex structures that survive passage through the nose and throat in comparison with simple fibers may vary by a factor of five. This means that large structures become relatively less respirable as their complexity increases. However, during mouth breathing large clusters and matrices may enter the deep lung.

When all of the factors that Harris and Timbrell (1977) addressed are considered, the efficiency of the deposition of asbestos structures in the deep lung is maximal for short, thin, single fibers (less than 10 µm in length with a true diameter less than 0.7 µm). The efficiency decreases slowly with increasing length (up to an effective limit of 200 µm), moderately with increasing complexity of shape, and rapidly with increasing diameter (up to an effective limit of 2.0 µm, true diameter). Thinner fibers, down to the lower limit of the range for asbestos fibers (0.02 µm, true diameter), are deposited with roughly the same efficiency. Approximately 20 to 25% of the fibers between 0.7 and 0.02 µm in diameter (and less than 10 µm in length) are deposited in the deep lung.

Sussman et al. Findings

Based on a series of experiments on human tracheal bronchial casts, Sussman et al. (1991a and b), also developed models of fiber deposition in the human lung. Such experiments are in fact illustrative of several research groups who have developed deposition models based on results from experiments on airway casts (for a review, see Stober et al. 1993).

The results reported by Sussman et al. (1991a and b) appear to be generally consistent with the results reported by Harris and Timbrell (above) and Yu and coworkers (below), although the manner in which their results are reported make them somewhat less directly comparable. Briefly, Sussman et al. report that deposition increases along most generations of the bronchial tree with increasing fiber length and increasing airflow rate

for any fixed aerodynamic diameter. This increased deposition efficiency is demonstrated for airway generations at least through the ninth bifurcation and is implied to continue through to airway generations that would be representative of the respiratory (pulmonary) portion of the lung (i.e. airway bifurcations greater than approximately 16 to 22). For definitions and a description of airway generations, see Section 4.4.

Findings of Yu and Coworkers

In a series of studies, Yu and coworkers combined an improved model of human lung physiology (Asgharian and Yu 1988) with a series of more rigorous equations to describe fiber mobility (Chen 1992) and used these to evaluate the deposition of various types of fibrous materials in the lung. The trends indicated in their studies show general agreement with those reported by Harris and Timbrell, but with several notable refinements.

In a study of refractory ceramic fibers (Yu et al. 1995a), a maximum deposition efficiency of 15% is reported for fibers that are approximately 6 μm long and approximately 1 μm in diameter. This is close to the fiber size at which maximal deposition is reported by Harris and Timbrell (1977). As with Harris and Timbrell, Yu et al. also report that deposition efficiency decreases precipitously for thicker structures and more slowly for thinner structures. For thinner structures, deposition efficiency increases with both decreasing width and length. As fibers get longer, optimum deposition occurs with decreasing thickness. Thus, for example, a maximum deposition rate of 10% occurs for fibers that are 20 μm long at a thickness of 0.8 μm.

In a study of silicon-carbide whiskers (Strom and Yu 1994), the deposition model is extended to fiber widths as narrow as 0.01 μm. Results from this study indicate that fibers between 0.01 and 0.1 μm in thickness are deposited with a minimum efficiency of 5% up to lengths of approximately 40 μm before efficiency drops below 5%. For thin fibers (thinner than 0.5 μm), shorter fibers tend to be deposited in the deep lung much more efficiently than longer fibers. More than 25% of thin fibers shorter than 1 μm are deposited in the deep lung following inhalation. Strom and Yu also report that the efficiency of deposition in the deep lung of long structures increases substantially during mouth breathing.

Comparing the results reported for refractory ceramic fibers (density = 2.7 g/cm^3) and silicon-carbide whiskers (density = 3.2 g/cm^3), it also appears that the efficiency of deep-lung deposition increases for thinner and for longer structures as the density of the structures increases. Given the observed density effect, longer and thinner

chrysotile fibers would be deposited in the deep lung less efficiently than (denser) amphibole fibers of the same size. However, shorter and thicker chrysotile structures would be deposited somewhat more efficiently than similarly sized amphiboles. This suggests that a greater fraction of the mass of chrysotile that gets deposited in the deep lung will be composed of very short fibers and somewhat longer bundles than the mass fraction of short fibers or longer bundles in the air breathed. Also, to the extent that chrysotile fibers are curved, these would be deposited somewhat less efficiently than straighter (amphibole) fibers of comparable size.

Based on the deposition efficiencies predicted by Yu and coworkers, fibrous structures that reach the deep lung in humans are effectively limited to those thinner than approximately 1 μm. It is also apparent that aspect ratio constraints affect only the shortest fibers (i.e., those shorter than approximately 3 μm). The thickness constraint for all longer structures is best described as a maximum width (rather than an aspect ratio).

Rats versus Humans

Yu and coworkers also modified their models to evaluate the rates that fibrous materials are deposited in rat lungs and compared these with results for humans. Such comparisons have implications for the manner in which results from animal inhalation studies are extrapolated to humans.

Results from Yu et al. (1994) suggest that pulmonary deposition of all fibrous structures with lengths between about 1 and 100 μm and thinner than approximately 1 μm occurs at much higher rates in rats than in humans. Fibers as long as 90 μm are deposited in rat lungs at efficiencies exceeding 20% while fewer than 5% of structures this long are deposited in the pulmonary region of human lungs. In fact, it is only structures between 1 and about 20 μm within a very narrow range of thicknesses (centered around 1 μm) that are deposited more efficiently in the deep lungs of humans than in rats.

Yu et al. (1995a) also indicate that, even when deposition efficiencies are comparable in rats and humans, due to differences in the total lung mass and breathing dynamics across species, the resulting lung burdens (i.e. the mass or number of structures per mass of lung tissue) are five to 10 times higher in the rat than in humans for any given exposure. Lung burden per lung surface area are also higher in the rat than in humans.

To illustrate, assume rats and humans are similarly exposed to a concentration of 0.1 f/cm^3 (100 f/L)of some fibrous material with a length at which both species retain

approximately 10% of the fibers inhaled. The Following Table 7.1 then indicates the calculations required to determine the relative rates at which the lung (volume and surface area) burdens in each species would develop.

Table 7-1:
ESTIMATION OF LUNG VOLUME AND LUNG SURFACE AREA LOADING RATES FOR RATS AND HUMANS

Species	Body Weight (kg)	Lung Volume (L)	Lung Surface Area (m^2)	Rest Breaths per Minute (bpm)	Tidal Lung Volume (L)
Human	70	5	140	15	1.5
Rat	0.15	0.01	0.4	70	0.0019

Species	Breathing Rate (L/min)	No. Fibers Inhaled per Minute (f/min)	No. Fibers Deposited per Minute (f/min)	Lung Volume Loading Rate (f/L-min)	Lung Surface Area Loading Rate (f/m^2-min)
Human	21.7	2170	217	43.4	1.6
Rat	0.13	13.3	1.3	130	3.3

From the above table, it is clear that rats exposed to comparable airborne concentrations as humans will increase their loading of fibers per volume (or mass) of lung at a rate that is approximately three times that of humans (for fibers in sizes that are deposited with 10% efficiency in both species). Similarly, the fiber load per surface area of lung will increase in rats at a rate that is approximately twice that of humans. Moreover, even higher relative mass or surface area loading rates are expected for the rat than shown in the above table, due to the greater efficiency with which most fiber sizes are deposited in rat lungs. Data used to compute the loading rates in the table (which are also presented) are derived from Gehr et al. (1993) and supplemented with information from Stober et al (1993). A more detailed description of this information is provided in Section 4.4.

7.1.3 The Effects of Electrostatic Charge on Particle Respirability

Electrostatic charge has been shown to affect the retention of particles within the lungs (see, for example, Vincent 1985). Since processes that generate airborne particles generally involve some form of abrasion, airborne dust particles frequently exhibit varying degrees of electrostatic charge. Although this potentially leads to variation in the efficiency of particle retention in the lungs as a function of the source of the dust, a detailed relationship between surface charge and retention was not described in this paper. A more detailed and quantitative treatment was developed by Chen and Yu (1993) and the implications of the Chen and Yu model are described below (following discussion of results reported by Davis et al.).

Davis et al (1988) report that animals exposed to dusts containing fibrous chrysotile, whose surface charge is reduced with a beta minus source, retain significantly less chrysotile than animals dosed with dusts containing particles whose surface charge has not been reduced. However, the magnitude of the difference in the mass of fibers retained is less than a factor of two, implying that the absolute variation due to this effect may be small. Further research in this area is needed.

Chen and Yu (1993) report that, based on modeling of lung deposition, overall deposition increases with increasing charge density on the particles inhaled. However, due to the pre-filtering by the naso-pharyngeal and and tracheo-bronchial portions of the respiratory tract, the effects of electrostatic charge on deep lung deposition appear to be only slight to modest.

Given the results of the above studies, the overall effects of electrostatic charge on particle deposition in the deep lung appear to be relatively minor. Therefore, such effects do not need to be considered explicitly when evaluating the health consequences of asbestos.

7.1.4 General Conclusions Concerning Particle Respirability

Based on the information provided in the last several sections, it is apparent that in humans:

- deposition of asbestos fibers in the pulmonary portion of the lung occurs primarily at alveolar duct bifurcations;
- electrostatic effects on pulmonary deposition are likely minor;

- fibers that are deposited in the pulmonary portion of the lung are largely thinner than approximately 0.7 μm and virtually all are thinner than 1 μm (except during mouth breathing, when thicker and more complex structures may be respired);

- the length of a fiber has limited impact on respirability up to a length of approximately 20 μm, but the efficiency of deposition of longer fibers decrease slowly with increasing length for longer fibers;

- as the length of the fibers that are inhaled increases, the thinner fibers are deposited with greater efficiency. Thus, the longer the fibers inhaled, the thinner the fibers retained;

- due to differences in density, shorter and thicker chrysotile structures will be deposited more efficiently in the pulmonary portion of the lung than corresponding amphibole structures and longer and thinner amphibole structures will be deposited more efficiently than corresponding chrysotile structures;

- curly chrysotile structures are less likely to reach the pulmonary portion of the lung than straight amphibole (or chrysotile) structures;

- except for a very narrow range of fiber sizes (centered around 6 μm in length and 1 μm in diameter), virtually all size fibers are deposited with greater efficiency in rat lungs than human lungs;

- due to body morphology and the dynamics of breathing, rats exposed to similar air concentrations will accumulate fiber burdens both per mass (volume) of lung tissue and per lung surface area at a rate that is several times the rate such burdens accumulate in humans; and

- the dynamics of fiber lung deposition can now be accurately predicted in great detail using currently available models.

7.2 FACTORS AFFECTING DEGRADATION, TRANSLOCATION, AND CLEARANCE

Degradation and clearance mechanisms compete with deposition to determine the fraction of asbestos that is retained in the lungs. Other (translocation) mechanisms mediate the movement of asbestos from sites of initial deposition to various target tissues within the lung and mesothelium. These factors affect all of the toxic end points of interest. Studies indicating the dependence of the various contributing mechanisms

on fiber size and mineralogy are highlighted as well as studies indicating differences between mechanisms in humans and laboratory animals.

The three units of the respiratory tract defined in the last section (naso-pharyngeal, tracheo-bronchial, and bronchio-alveolar units) differ primarily by the types of clearance (and translocation) mechanisms operating in each unit (Raabe, 1984). These are summarized in Table 7-2 along with rough estimates of the time frames over which each mechanism may operate.

TABLE 7-2

RELATIVE RATES, HALF-LIVES FOR PARTICLES CLEARED BY THE VAROUS OPERATING MECHANISMS OF A HEALTHY LUNG

(This table needs to be completed)

TISSUE/LUNG REGIME Mechanisms (Component Mechanisms)	SPECIES	FIBER TYPE	PARTICLE HALF-LIFE* (days)	KINETIC ORDER	MINERALOGICAL EFFECTS	SIZE EFFECTS	REFERENCE	COMMENTS
NASAL-PHARYNGEAL								
Expectoration and Swallowing	Human		minimal					
Muco-ciliary Transport	Human	Particles	0.0028	Zero	No Effect	No Effect	Raabe 1984	
TRACHEO-BRONCHIAL								
Muco-ciliary Transport	Human	Particles	0.021-0.21	Zero	No Effect	No Effect	Raabe 1984	
PULMONARY (BRONCHIO-ALVEOLAR)								
AM Phagocytosis, Transport to MC Escalator	Rat	Particles	49	Ps - First	No Effect	Inhibited by Length/Conc	Stober et al. (1990) in Stober et al. (1993)	
	Rat	Short Chr	14			Fibers < 4 um	Yu et al. (1990)	
Dissolution in Extracellular Fluid	In-vitro	Chr	180	Zero	Affects Rate	Diameter determines lifetime	Hume and Rimstidt 1992	
	In-vitro	Crc	11000				Zoltus et al. 1997	
Transport to the Interstitium	Rat	Particles	2.3	???	???	???	Stober et al. (1990) in Stober et al. (1993)	
(Phagocytosis and expulsion by epithelial cells)								
(AM phagocytosis, transport through epithelium)								
(Diffusive transport through the epithelium)								
(Forced mechanical transport through the epithelium)								
Sequestration								
(Phagocytosis and internalization by epithelial cells)								
(AM phagocytosis, immobilization due to overload)								
PULMONARY (INTERSTITIAL)								
IM Phatogyctosis, Transport to Lymphatics	Rat	Particles	2300		Unspecified Negative Effect	Inhibited by Length/Conc	Stober et al. (1990) in Stober et al. (1993)	
CHECK THIS	Dog	Ams	2200				Oberdorster et al. (1988)	
Diffusive Fluid Transport to Lymph ???			2200		check - should be none	check	Churg 1994	
Dissolution in Extracellular Fluid		(Same as Above)						
Transport to Endothelium, Pleura								
(IM phagocytosis, transport through interstitium)								
(Diffusive transport through the interstitium)								
(Forced mechanical transport through the interstitium)								
Sequestration								
(Encapsulation in granulomatous tissue)								
(Internalization by interstitial/endothelial cells)								
THE PLEURA								
PM Phatogyctosis, Transport to Lymphatic Stomata								
Dissolution in extracellular fluid								
Sequestration								
(Encapsulation by granulomatous tissue)								
(Phagocytosis by mesothelial cells)								

Notes:

* For zero order mechanisms, half-lives reported are half of the time required for complete clearance for the process that is constant with time
For first order mechanisms, the ture half-lives (i.e. the time required for half of the initial population to disappear) is reported.

TABLE 7-2

Briefly, the structures of the nose and throat are bathed in a continual flow of mucous, which is ultimately swallowed or expectorated. The mucous traps deposited particles and carries them out of the respiratory tract. The air channels of the tracheo-bronchial section of the respiratory tract are lined with cilia and mucous secreting cells. As in the nose and throat, the mucous traps particles deposited in these air pathways and the ciliary escalator transports the mucous up to the throat where it may be swallowed or expectorated.

Neither the alveolar ducts nor the alveoli of the pulmonary compartment of the lung are ciliated (inferred from St. George et al. 1993). Therefore, particles deposited in this section of the respiratory tract can only be cleared by the following mechanisms:

- if the deposited particles are soluble, they may dissolve and be transported away from the lungs in blood or lymph; or

- if they are sufficiently compact, they may be taken up by alveolar macrophages and transported outward to the muco-ciliary escalator of the tracheo-bronchial portion of the respiratory tract.

Due to a combination of chemical and physical stresses in the environment of the lung, deposited asbestos structures may degrade by splitting. Longitudinal splitting, primarily of bundles, produces thinner structures and transverse splitting produces shorter structures. In both cases, the number of structures produced may be larger than the number of structures initially deposited.

By changing the size and number of structures that were initially deposited in the lungs, splitting may affect the rates and efficiency with which the various other degradation and clearance mechanisms operate.

Particles and fibers that are deposited in the pulmonary portion of the lung may also be transported by a variety of mechanisms into and through the epithelium lining the alveolar ducts and alveoli to the underlying interstitium and endothelium that are located within the interalveolar septa (See Section 4.4). In those portions of the lung parenchyma that lie proximal to the pleura, such mechanisms may also facilitate transport to the mesothelium. Putative mechanisms by which such transport may occur include:

- if particles are sufficiently compact to be phagocytized by alveolar macrophages, they may be transported within macrophage "hosts" through the epithelium to the interstitium;

TABLE 7-7:
SUMMARY DATA FOR ANIMAL INHALATION EXPERIMENTS CONDUCTED BY DAVIS AND COWORKERS[1,2]

Fiber Type	Description	Abbreviations	Mass Concentration (mg/m³)	PCM f/ml	Number of Animals	Number of Benign Pulmonary Tumors	Number of Malignant Pulmonary Tumors	Total Number of Pulmonary Tumors	Mesotheliomas	Reference
Chrysotile	UICC-A	UC	2	390	42	6	2	8	1	Davis et al. 1978
Chrysotile	UICC-A	UC	10	1,950	40	7	8	15	0	Davis et al. 1978
Chrysotile	Long	LC	10	5,510	40	8	12	20	3	Davis et al. 1988a
Chrysotile	Short	SC	10	1,170	40	1	6	7	1	Davis et al. 1988a
Chrysotile	UICC-A	UC	9.9	2,560	36	6	8	14	0	Davis et al. 1988b
Chrysotile	UICC-A (Discharged)[3]	DC	9.9	2,670	39	4	6	10	1	Davis et al. 1988b
Chrysotile	WDC Yarn[4]	WC	3.6	679	41	5	13	18	0	Davis et al. 1988b
Amosite	UICC	UA	10	550	43	2	0	2	0	Davis et al. 1978
Amosite	Long	LA	10	2,060	40	3	8	11	3	Davis et al. 1988a
Amosite	Short	SA	10	70	42	0	0	0	1	Davis et al. 1988a
Crocidolite	UICC	UR	4.9	430	43	2	0	2	1	Davis et al. 1978
Crocidolite	UICC	UR	10	860	40	1	0	1	0	Davis et al. 1978
Tremolite	Korean	KT	10	1,600	39	2	16	18	2	Davis et al. 1985
None	Control	C	0		20	0	0	0	0	Davis et al. 1978
None	Control	C	0		36	0	0	0	0	Davis et al. 1985
None	Control	C	0		61	1	1	2	0	Davis et al. 1988a
None	Control	C	0		64	1	1	2	0	Davis et al. 1988b
None	Control	C	0		47	1	1	2	0	Davis et al. 1988a

1. Source: Berman et al. 1995

2. Exposure occurred for 7 hours per day, 5 days per week for 1 year.

3. UICC-A chrysotile in this experiment was treated with mixed polarity air (produced with a source of beta radiation) following generation to reduce the surface charge on individual particles within the dust.

4. Chrysotile samples used for dust generation in this experiment were obtained from material treated by a commercial wet dispersion source.

- if particles are sufficiently compact to be phagocytized by the epithelial cells lining the air passageways of the deep lung, they may be transported into cell interiors or transported through to the basement membrane, the interstitium, the endothelium, and (eventually) the pleura;

- particularly when associated biological effects cause changes in the morphology of epithelial cells (Section 7.3.6), particles may diffuse between the cells of the epithelium to underlying tissues; and/or

- particles may be transported through respiratory epithelium mechanically due to physical stresses associated with respiration within the lung.

Although the transport of fibers and particles from airway lumena to the interstitium is apparent in many studies (see below), the precise mechanisms by which such transport actually occurs has yet to be delineated with certainty.

Particles deposited in the interstitium can also be cleared and the processes by which these particles are ultimately cleared are similar to, but may be substantially slower than, the mechanisms by which particles deposited in airway spaces can be cleared. Such mechanisms include:

- if the deposited particles are soluble, they may dissolve and be transported away from the lungs in blood or lymph; or

- if the particles of the interstitium are sufficiently compact to be phagocytized by interstitial macrophages, they may be taken up and transported to the lymphatic system for removal.

The mechanisms by which particles that reach the pleura and mesothelium may be cleared are also similar to those operating in the interstitium:

- if the deposited particles are soluble, they may dissolve and be transported away from the lungs in blood or lymph; or

- if the particles that reach the pleura are sufficiently compact to be phagocytized by pleural macrophages, they may be taken up and transported to the lymphatic system for removal.

Note, particles cleared from the pleura by macrophages appear subsequently to be deposited at sites of lymphatic drainage along the pleura (i.e. at lymphatic ducts) from where they are ultimately cleared in lymph (Kane and McDonald 1993).

The various degradation, clearance, and transport mechanisms that affect the retention of asbestos in the lung and other target tissues (identified above) exhibit disparate kinetics that may be further altered by the size, shape, mineralogy, and concentration of the particles affected. Therefore, the kinetics of these mechanisms are considered below. The mechanisms evaluated include:

- dissolution;
- muco-ciliary transport;
- macrophage phagocytosis and transport; and
- diffusional transport.

Evidence for the existence of these mechanisms and inferences concerning their kinetics derive primarily from retention studies, which may include both studies of retained structures in animals following either short-term or chronic exposure or human pathology studies in which the lung burdens of deceased individuals are correlated with their exposure history. Other information also comes from in-vitro studies. Various, increasingly sophisticated models have also been developed to predict the individual and combined effects of these mechanisms.

7.2.1 Animal Retention Studies

Retention studies track the time-dependence of the lung burden of asbestos or other particulate matter (i.e. the concentration of particles in the lung) during or following exposure. Thus, such studies are designed to indicate the degree to which inhaled structures are retained. Depending on the time frame evaluated, however, effects due to deposition and those due to clearance may not easily be distinguished in such studies. Moreover, due to the near impossibility of isolating the various compartments of the lung when preparing for quantitative anlaysis of tissue burden (e.g. the pure respiratory components vs. the larger airways or the tissues directly associated with airway lumena vs. the underlying interstitium or endothelium), it is nearly impossible to separate the effects of the various clearance mechanisms, which typically operate over vastly different time scales (Table 7-2). This is why modeling has proven so important to distinguishing effects attributable to individual mechanisms.

Results from retention studies must be evaluated carefully. In addition to the limitations highlighted above, the lung burden estimates from such studies may be affected by the

manner in which asbestos is isolated from lung tissue for measurement and the manner in which the concentration of asbestos is quantified (Chapter 5). For example, lung burden estimates may vary substantially depending on what portions of lung parenchyma are sampled or whether whole lungs are homogenized. Results may also vary depending on whether lung tissue is ashed or dissolved in bleach during sample preparation. More importantly, because several clearance mechanisms are affected by the size and even the mineralogy of the structures being cleared, studies (particularly older studies) that track lung burden by mass or by total fiber number may not adequately capture such distinctions.

7.2.1.1 Studies involving short-term exposures

The latest retention studies tend to focus on the fate of long fibers (typically those longer than 20 µm) in support of the generally emerging recognition that these are the fibers that cannot be readily cleared from the pulmonary compartment of the lung and that, not coincidentally, contribute most to disease (Section 7.4).

Hesterberg et al. (1998a), for example, tracked the time-dependent retention in rats of two fiber categories: (1) WHO fibers[1] and (2) WHO fibers longer than 20 µm for a range of manmade vitreous fibers (MMVF's), a refractory ceramic fiber (RCF1a), and amosite following a 5-day (6 hr/day), nose-only exposure. Rats were sacrificed at intervals up to a year following exposure. The amosite was size selected to contain a high proportion of fibers longer than 20 µm. Aerosol concentrations were also adjusted to maintain target concentrations of 150 f/cm^3 for long fibers for each sample tested. Airborne mass concentrations varied between 17 mg/m^3 for amosite to as much as 60 mg/m^3 for the other fiber types. Lungs (without trachea or main bronchi) were weighed and stored frozen. For analysis, each lung was dried to constant weight, minced and a portion was ashed. The ashed portion was further washed with filtered, household bleach, then filtered and applied to an SEM stub. Fiber numbers and dimensions (in both aerosols and tissue) were determined by SEM with a minimum of 200 fibers counted. In addition, analysis continued until a minimum of 30 fibers longer than 20 µm were counted.

Hesterberg et al. tracked the ratios of retained fiber concentrations with time to the concentration retained 1-day following cessation of exposure. The observed time-dependent decay in these ratios were then fit to one-pool (single first order decay) or two-pool (weighted sum of two first order decays) models. With zero time assumed to

---

[1] WHO fibers are those longer than 5 µm, thinner than 3 µm with an aspect (length to width) ratio greater than 3 (WHO 1985).

be the time immediately following cessation of exposure. The authors recognize that at least some clearance likely takes place during the five days of exposure so they expected the assumption that retained concentrations at the end of exposure on day 5 to be equal to deposited concentrations would cause their analysis to slightly underestimate clearance rates. They also recognized that waiting 24-hours after cessation of exposure to measure retention allows some short-term clearance of upper airways, so that they expected their analysis would better focus on slower clearance from deeper in the lung.

Results reported by Hesterberg et al. indicate that the dimensions and concentrations of fibers in aerosols from the five synthetic fibrous materials were all similar but that the amosite aerosol contained a substantially greater number of fibers (including the longest fibers) but that the fibers, on average, were somewhat shorter and substantially thinner than the other aerosols. Of the fibers initially deposited in the lung (based on measurements made 1-day following cessation of exposure, comparable fiber numbers of long (> 20 μm) fibers were retained across all six fiber types. Deposited concentrations of fibers 5-20 μm in length were more variable, but values within one standard deviation still overlapped. About 6 times as many short amosite fibers (< 5 μm) were initially deposited than for any of the other fiber types. The authors also indicate that the dimensions of retained fibers were generally shorter and thinner than the original aerosol and were much more similar across retained fiber types than the original aerosols.

Clearance of long fibers (>20 μm) for all six fiber types could best be described using a two-pool model. The first pool cleared relatively rapidly (within the first 90 days) and represented a minimum of 65% of the lung burden observed 1-day following exposure. The second pool cleared much more slowly. For amosite fibers in the second pool, during the approximately 275 days of clearance, retention was only reduced to 80% of the 90-day value. In contrast, all five of the synthetic fibers were reduced to less than 30% of their 90-day value during this period. For amosite, the first pool decayed with a half-life of 20 days (90%CL: 13-27) and all of the other fibers with half-lives of 5-7 days (with varying confidence bounds). For the slower pool, amosite fibers exhibited a half-life of 1160 days (90% CL: 420-∞) with the other fibers showing half lives varying between 24 and 179 days. The combined, weighted half-life for amosite was 418 days (90%CL: 0-1060). The authors also note that data reanalyzed from an earlier study (Hesterberg et al. 1996) indicate a corresponding weighted half life for crocidolite of 817 days (246-∞) and indicate that this was best fit using a single exponential (a one-pool model).

Hesterberg et al. indicate that in this and previous studies approximately 20 to 60% of long fibers typically clear from the lung within 2-weeks post exposure. They further

suggest that this rapid clearance may be attributable to muco-ciliary clearance from the upper respiratory tract. They further report from the present study that short amosite fibers cleared much more rapidly than long fibers. Fibers < 5 µm in length were reduced by 90% in the first 90 days (in comparison to 65% for long fibers). However, from 90 to 365 days, little or no clearance was observed for amosite fibers of any length.

For four of the synthetic fibers, long fibers cleared at the same rate as short fibers (all more rapidly than amosite) and the authors report that the data suggest transverse breakage for these fibers. Moreover, they attribute the more rapid clearance of long fibers among the MMVF's to dissolution, since these fibers exhibit in-vitro dissolution rates that are rapid relative to the time scale of macrophage clearance. One synthetic fiber MMVF34, which is a stonewool) disappeared much more rapidly than any other fiber and the long fibers disappeared more rapidly than the short fibers. MMVF34 shows the greatest in-vitro dissolution rate at neutral pH for any of the fibers tested in ths study and dissolves particularly rapidly at pH 4.5 (the pH found in the phagosomes of macrophages). The authors postulate that clearance of all of the synthetic fibers are enhanced over amosite by dissolution and breakage.

In summary, Hesterberg et al. observed that:

- multiple clearance mechanisms (operating over multiple time scales) contribute to clearance;
- for sufficiently soluble fibers, long fibers clear more rapidly than short fibers;
- for insoluble fibers, a subset of long fibers clears rapidly within the first few months following exposure and the remaining long fibers clear only extremely slowly, if at all;
- short fibers of all types are cleared at approximately the same rate (much more rapidly than long, insoluble fibers);
- a small, residual concentration of short fibers may not always clear and may remain in the lungs (sequestered in alveolar macrophages) for extended periods; and
- in this study, there is some suggestion that short amosite fibers clear somewhat more slowly than short fibers of the other, non-asbestos mineral types studied.

Regarding the last observation, whether this is attributable to differences in fiber thicknesses among the various mineral types, due to partial contributions (even among short structures) to dissolution, or due to a unique, toxic effect of amosite is unclear. However, the likeliest of these candidate hypotheses is that the effect is due to partial dissolution.

This general pattern of observations are consistent with the findings of most, recent retention studies following short-term exposure.

In an earlier study of similar design, Bernstein et al. (1996) evaluated the deposition and clearance of a series of 9 glass and rock wools. These authors similarly found that clearance could be modeled using a double exponential for all length fibers (in similar length categories of < 5, 5-20, and > 20 μm) and that for soluble fibers, long fibers clear more rapidly than short fibers (with the intermediate length fibers in between).

For the Bernstein et al. study, if one assumes that the pool of longer-lived fibers is representative of macrophage clearance, this suggests that the efficiency of clearance by macrophages decreases with increasing fiber length and that the longest structures are not phagocytized at all, so that they remain exposed to the extracellular medium where dissolution occurs. Lending further support to this interpretation, the authors also report that the clearance rate for long fibers correlate with measured in-vitro dissolution rates at neutral pH while the clearance rates for short fibers neither correlate with in-vitro dissolution rates at neutral pH or at pH 4.5. Although the latter pH corresponds to the pH found in the phagosomes of macrophages, there is likely too little fluid available in such organelles to support efficient dissolution. The authors also indicate that a sufficient number of fibers were counted during the study to suggest that breakage is not playing a role in clearance (except at very early times) and that the clearance rate for short fibers appears to be the same or slower than that observed for nuisance dusts.

In another, earlier study of similar design Eastes and Hadley (1995) evaluated four types of manmade mineral fibers (MMMF's) and crocidolite. All of the samples (including crocidolite) had been size-selected to assure a large fraction of fibers longer than 5 μm. Unfortunately, due to differences in reporting, it is not possible to compare the initial loading of crocidolite fibers to those reported for amosite in the Hesterberg et al. (1998a) study. However, results from this study further support the physical interpretation of clearance suggested in the studies discussed above. In fact, the authors report that the time-dependent size distribution of retained fibers observed in this study agree well with a computer simulation of fiber clearance. The simulation assumes that long fibers dissolve at the rate measured for such fibers in vitro and that

short fibers of every type are removed at the same rate as short fiber crocidolite (which is practically insoluble). This is strong evidence that short fibers are cleared by macrophage phagocytosis and that long fibers cannot be cleared by macrophages, but may dissolve in extracellular fluid provided that they are sufficiently soluble.

Regarding crocidolite, the data from the Eastes and Hadley study suggest that short crocidolite fibers appear to clear at a rate that is somewhat slower than observed for any of the short MMVF fibers. Importantly, however, the interpretation of short fiber clearance in this paper is somewhat confounded because, unlike the studies discussed above, short fibers in this paper are defined as all fibers < 20 μm so there may be some confounding with MMVF fibers that are dissolving. As previously indicated, the Hesterberg et al. (1998) work also suggests that short asbestos (amosite) fibers may clear more slowly than short fibers of differing mineralogy and Hesterberg et al. only includes fibers < 5 μm in their definition. Nevertheless, it is still possible that some effects due to dissolution may still be affecting the clearance of these shorter fibers.

Surprisingly, a visual inspection of the data presented in their table suggests a lack of any long-term clearance for long fiber crocidolite (> 20 μm). Yet, the authors model long fiber crocidolite clearance using a single exponential (suggesting no rapidly clearing compartment). The long-term half-life reported for crocidolite in this study is approximately 220 days (with estimated confidence limits of 165 to 566 days). This overlaps with the long term clearance half-life reported by Hesterberg et al. (1996) for crocidolite of approximately 820 days (246-∞).

Equally surprising, Hesterberg et al. also modeled crocidolite clearance as a single exponential, which might suggest better penetration to the deep lung by crocidolite, less clearance by muco-ciliary transport or alveolar macrophage transport, or better penetration to the interstitium than other fibers. More likely, however, it may simply indicate that the two-pool model does not represent a statistically significant improvement in model fit over the one pool model. However, relative size distributions would need to be evaluated carefully before drawing any such conclusions. Eastes and Hadley also report clearance of short fiber crocidolite is modeled as a double exponential with short and long half-lives of: 25 and 112 days, respectively. Since this fiber category contains fibers up to 20 μm in length (in this study only), this does suggest at least some contribution from muco-ciliary and alveolar macrophage mediated clearance for crocidolite.

In two studies, Coin et al. (1992 and 1994) evaluated the fate of chrysotile fibers in rats exposed for 3 hrs to 10 mg/m^3 (reportedly containing > 5000 fibers longer than 5 μm/cm^3). For lung analysis, the left lung was separated into peripheral and central

regions under a dissecting microscope. Slices of peripheral and central portions were separately weighed and minced. Tissue was digested in sodium hypochlorite and then filtered. A quality control test indicated that the digestion process caused a slight (~10%) decrease in fiber number and slight decreases in fiber diameter and fiber length. Fiber size distributions were evaluated by SEM. A stratified counting procedure was employed to assure equal precision for each length category of interest. Measurements for each category were then converted to mass equivalents.

Results from the Coin et al. studies indicates no difference between deposition in central or peripheral regions of the lung. They also confirm that chrysotile splits longitudinally in the lungs with a half life that is competitive with the clearance rates measured in this study. Clearance was found to be very length dependent so that rates decrease from a half life of about 10 days for fibers about 4 μm in length through 30 days for fibers 8 μm to 112 days (which is no different from zero) for fibers longer than 16 μm (all after adjusting for longitudinal splitting). Importantly, the brief followup period (30 days) is too short to provide an adequate evaluation of the longer term clearance pools observed in other studies and certainly too short to evaluate any effects potentially associated with chrysotile dissolution. Also, that the decay curves for clearance were limited to four points, makes evaluation of the slopes for these curves highly uncertain.

Coin et al. also report that the mass of chrysotile deposited during these short exposures (i.e. no more than 20 μg) is very small compared to levels at which overload has been reported to occur (approximately 1 mg, see, for example, Yu and Yoon 1991) and that the volume of the 16 μm fibers, which have an average diameter of 0.2 μm and therefore a mean volume of 0.5 μm^3, is small relative to the volume at which macrophage clearance of non-fibrous particles is reported to be hindered (Morrow 1988). Thus, the authors conclude that fiber length presents an additional constraint on macrophage clearance, independent of any other overload. They also indicate that inhibition of clearance due to fiber length is independent of fibrosis.

Coin et al. also discuss the effect of fibrosis on clearance. They indicate that, although increased concentrations of short fibers are observed in focal areas of fibrosis, it is more likely that such fibers accumulate because clearance is hindered by fibrosis in these areas than the hypothesis that the short fibers are causing fibrosis. This is because, as they point out, there are too many studies demonstrating the lack of ability of short fibers to induce fibrosis.

Evidence in the Coin et al. studies suggests that no translocation from central to peripheral regions of the lung were detected. An upper bound rate that is about 20% of

clearance is reported. However, the short followup time in this study would have precluded slower processes from being detected. Despite the lack of evidence of translocation, the authors report that duct bifurcations in peripheral regions of the lung where fibers are deposited are no more than 1-2 mm from the visceral pleura. In fact, in the 1994 study, the authors show that 50% of the primary duct bifurcations in the peripheral portion of the rat lung occur within 1 mm of the visceral pleura and some occur as close as 220 µm. Deposited fibers may also affect the pleura by inducing generation of diffusable, inflammatory agents.

A short term inhalation study by Warheit et al. (1997) evaluated retention of chrysotile and aramid fibers. In this study, rats (and hamsters) were exposed nose-only for 6 hrs/day, 5 days/wk for 2 weeks by inhalation to UICC chrysotile and p-aramid fibers (each at two doses of 460 or 780 fibers/ml, although the size range of these fibers is not stated nor is the manner in which they were analyzed). Fixed lungs were digested in chlorox during preparation for asbestos analysis. Animals were followed for up to a year post exposure.

As in studies described above, results from the Warheit et al. study indicate rapid clearance of short chrysotile fibers but slow to non-existent clearance of fibers longer than 20 µm. In contrast, aramid fibers apparently degrade and are subsequently cleared fairly rapidly in vivo. Based on the data provided in figures, although the reported concentrations of chrysotile and aramid fibers to which animals were exposed were equivalent, at both the lower and higher concentrations, it appears that rats initially retain three to five times as many aramid fibers as chrysotile fibers (at least for the size range counted, which was not reported). For both fiber types, clearance appears rapid for an initial period of approximately 90 days post exposure. During this time, the mean length of chrysotile fibers also appears to increase steadily, which suggests rapid, preferential clearance of short structures. After the initial period, it appears that (as the authors suggest), a residual concentration of longer fibers are cleared only very slowly, if at all.

Oberdorster et al. (1988) instilled a 3 ml suspension of irradiated amosite into the bronchio-alveolar space of the right diaphragmatic lobe of the lungs of dogs to evaluate clearance and transport. The amosite used was modified by sedimentation from UICC amosite to contain only fibers shorter than 20 µm. One dog also had unmodified UICC amosite instilled directly into a lymph node in the thigh. The dogs had been cannulated to allow collection of lymph from the right lymph duct-RLD and the thoracic duct- TD (both in the neck).

Results from Orberdorster et al. indicate that within 4 hours following instillation in the lung, low activity was noted in postnodal lung lymph but not in either the RLD or TD. Within 24 hours, however, activity and fibers (determined by SEM) were observed in both the RLD and the TD. The median length of fibers observed in the lymph were significantly longer than the instilled material, although there appeared to be a cutoff length of 16 µm in fibers observed at nodes and 9 µm in fibers observed directly in lymph. Fibers recovered from lymph were also significantly thinner and appeared to exhibit an absolute cutoff at a maximum width of 0.5 µm. Fibers recovered from the TD and RLD in the dog that had unmodified UICC amosite instilled directly into leg lymph were all short (with a maximum length of 6 µm). Since collection times were all short, the authors indicate that it is unknown whether longer fibers would have been observed at later times. The authors also note the almost total absence of fibers shorter than 1 µm in lymph, which they assume are cleared rapidly and efficiently by alveolar macrophages.

Oberdosrster et al. also report that a rough calculation, based on the fraction of the material originally instilled that was recovered in the first 24 hours, it would take approximately 6 years to clear all of the instilled asbestos (assuming no other clearance mechanisms were active).

Everitt et al. (1997) performed a short-term inhalation study that is interesting particularly because it focused on pleural (as opposed to lung) fiber burden. The authors exposed rats and hamsters to one type of refractory ceramic fiber (RCF-1) by nose-only inhalation for periods of 0, 4 and 12 weeks and animals were held for observation for up to an additional 12 weeks post exposure. Exposures were conducted for 4 hrs/day, 5 days/wk, at 45.6 +/- 10 mg/m^3 Groups of 6 animals were held for 0,4, 12, and 24 weeks to determine pleural fiber burden. An agarose casting method was reportedly used to recover fibers from the pleura. Analysis was by electron microscopy. Fibers were observed in the pleura at each time point examined (including samples from rats sacrificed immediately following the last day of a five-day exposure). Fibers were all reported to be short and thin (geometric mean length: 1.6 µm with GSD: 1.8, geometric mean diameter: 0.1 µm with GSD: 1.5). Concentrations averaged approximately 40,000 fibers (per whole pleura??? - units not reported). The authors indicate that such fibers would not typically be visible by optical microscopy. They also indicate that use of casts may be a more efficient method of recovering fibers from the pleura.

Everitt et al. indicate that observation of rapid translocation of short, thin fibers to the pleura has also been observed in studies of chrysotile so these results are not unique. Although it is stated that the mechanisms facilitating translocation are currently

unknown, the authors indicate that their finding of site-specific mesothelial proliferation supports observations by Boutin et al. (1996) that asbestos fibers accumulate in the parietal pleura of humans at sites associated with lymphatic drainage. Kane and McDonald (1993) have suggested that fibers are transported to these locations by pleural macrophages. However, the mechanisms by which fibers are transported from the lung to the pleura are still unconfirmed.

Older Retention Studies

Although the older retention studies generally support the results of newer studies (such as those cited above), older studies are sometimes limited by such things as the tracking of lung burden in terms of fiber mass or use of analytical techniques such as infrared spectroscopy for detection of asbestos, which are neither capable of distinguishing individual fibers nor provide any information on their sizes. Tracking of lung burdens in terms of mass may not reflect the fate of long, thin fibers, which (by increasing concurrence) appear to be the legitimate focus of studies evaluating biological hazards attributable to asbestos.

In two studies (Roggli and Brody 1984 and Roggli et al. 1987), Roggli and coworkers tracked the behavior of chrysotile (not UICC) and UICC crocidolite in rats following 1 hr exposure by inhalation to 3.5-4.5 mg/m^3 dusts. The authors indicate that this results in deposition of approximately 21 µg of dust. Portions of the lower lung lobes of selected rats were collected and digested for asbestos analysis using a scheme that was shown to be representative. To evaluate size distributions, more than 400 fibers from each sample were characterized by SEM. Fiber dimensions were then used to estimate total fiber mass.

Based on their study, Roggli and coworkers indicate that similar fractions of inhaled chrysotile and crocidolite dust are deposited in the lung during inhalation (23% and 19%, respectively). The authors therefore concluded that respirability and deposition do not depend on fiber type. Importantly, however, the manner in which this study was conducted does not facilitate distinguishing deposition in the deep lung from deposition in the upper respiratory tract.

Roggli and coworkers further indicate that clearance rates for the two fiber types appear comparable. Of the chrysotile initially deposited, they report that 81% of this material is cleared after four weeks. Similarly, 75% of the crocidolite is cleared. Importantly, because this is based on total mass (estimated by summing volume contributions from observed fibers), it may not reflect the specific behavior of long, thin structures. Therefore, it is difficult to compare such results with those of more recent studies.

However, the authors do report that short structures are cleared more readily than long structures and that chrysotile is observed to split longitudinally in vivo (based on observation that the total number of chrysotile structures initially increases and the mean length increases). The authors further conclude that clearance rates appear to be independent of fiber type.

In another short-term study, Kauffer et al. (1987) report that the average length of retained chrysotile structures increases in rat lungs following 5-hrs inhalation of chrysotile dust. Based on their results, the authors report that fibers shorter than approximately 8 μm are preferentially cleared. Kauffer and coworkers also confirm that chrysotile fibrs split longitudinally in the lung. In fact, several other studies (Le Bouffant et al. 1978, Kimizuka et al. 1987) also provide supporting observations that chrysotile fibers (or bundles) split longitudinally in the lung.

In two studies (Morgan et al. 1978 and 1980), Morgan and coworkers report on the fate of fibers following short term inhalation of radio-labeled fibers by rats. In the first study (Morgan et al. 1978), rats inhaled UICC anthophyllite at 35 mg/m^3 for a total of 8.4 hrs spread over three days. The authors report that the rats retained approximately 190 μg of dust at the end of exposure, mostly in the alveolar region; the authors assumed that conducting airway clearance is sufficiently rapid to clear this portion of the lung within a few days. Beginning about 7 days following exposure, the rats were then sacrificed serially for a period up to 205 days following exposure. Because anthophyllite fibers are relatively thick, fibers were analyzed by optical microscopy. Fibers were determined both in free cells (mostly macrophages) recovered in bronchopulmonary lavage and in lung tissue. Tissue samples and cells were digested in KOH and peroxide in preparation for fiber analysis.

Based on this first study, Morgan et al. report that anthophyllite lung content declined steadily by a process that could be described as a simple first order decay with a half life of approximately 76 days. Free macrophages recovered by lavage, initially contained about 8 pg and this too declined steadily with a half life of about 49 days. The authors further indicate that, if the number of macrophages remains constant with time (i.e. they are replaced at the same rate they are cleared), then the decay of the load in the macrophages should match what is observed in the rest of the lung. They suggest that the discrepancy may be due either to an influx of an increasing number of macrophages in response to injury with time and/or to transfer of some fibers through the alveolar wall. They also cite unpublished work indicating that uptake of fibers by alveolar macrophages is essentially complete within hours after cessation of exposure.

The authors also report that, initially, the lengths of fibers recovered in lung lavage was greater than in the original aerosol but that the prevalence of the longest fibers decreased after the first seven days. In lung tissue, however, the fraction of longer fibers (among total fibers) steadily increased with time. This suggests rapid clearance of naked fibers by muco-ciliary transport (which is a length independent process) with later times dominated by slower clearance in the deep lung by alveolar macrophages, which is a length-dependent process.

Morgan and coworkers also radiometrically determined the fraction of fibers in rat faeces (prior to sacrifice). They assumed that after 14 days, this would represent the fraction of asbestos cleared primarily from the alveolar region of the lung. Initially 1.4% of lung anthophyllite content was excreted daily but this fell to 0.5% after 120 days. The authors indicate that this suggests that the elimination from asbestos in lung tissue cannot be described by a single exponential because multiple processes are involved and that, over longer periods of time, the slower processes become increasingly important.

In the second study, Morgan et al. track the fate of several size-selected radiolabeled glasses in rats, again following short term inhalation. From an analysis of the size dependence of deposited fibers in this study, the authors suggest that alveolar deposition in the rat is limited to structures with aerodynamic equivalent diameters less than about 6 μm and that deposition in this region of the lung falls precipitously for fibers with thicknesses between about 2 and 3 μm (aerodynamic equivalent diameter). For fibers that are the density of asbestos, this represents an upper bound limit to alveolar deposition for the absolute thickness of a fiber of approximately 1.5 μm with fibers deposition of fibers thicker than approximately 0.7 μm being drastically reduced. This is in concordance with conclusions concerning deposition provided in Section 7.1.4. Alveolar deposition efficiency is also shown to decrease with increasing fiber length, at least for fibers longer than approximately 8 μm, also in concordance with findings presented in Section 7.1.4.

Intratracheal Instillation

The fate of fibers following intratracheal instillation into the lungs has also proven informative in some studies. For example, Wright and Kushner (1975) intratracheally instilled paired samples each of several types of glass fibers, fluoramphibole, and crocidolite into guinea pigs. For each mineral tested, a sample with predominantly short structures (25 mg total dose for crocidolite, reportedly 99% < 5 μm) and another with predominantly long structures (4 mg total dose for crocidolite, reportedly 80% > 10 μm) were evaluated. Unfortunately, the authors do not report how fibrous structures were

characterized. Results in the cited paper report observations only after 2-years following the last injection.

Wright and Kuschner report that long structures uniformly caused fibrosis (primarily involving the respiratory bronchioles and alveoli and abutting the terminal bronchioles) while the short structures were uniformly phagocytized and generally removed to thoracic lymph nodes. Among other things, clearance to lymph suggests that fibers reached the interstitium (Section 7.2.5). It is interesting that, even after 2 years of recovery, the authors observe elevated levels of macrophages in the alveoli of animals dosed with short structures. Based on the relative size distributions of the samples analyzed, the authors report that structures up to 10 μm in length appear to be efficiently scavenged by macrophages. Based on the observation of larger numbers of short structures than expected in comparison with their fractions in the original samples, the authors further conclude that glass structures underwent biodegradation so that longer structures broke down into shorter structures that could be phagocytized.

Wright and Kuschner also report that long fibers are occasionally visible within the fibrotic interstitium of dosed animals. The long-fiber dosed animals also show macrophages in hilar lymph nodes containing fibers that are too small to resolve and all of them are short. In short-fiber dosed animals, some fibers are seen to remain in the lung within aggregates of macrophages, both in alveoli and the interstitium. Short-fiber dosed animals also show many more macrophages within the hilar lymph nodes than long-fiber dosed animals.

In two reports of the same study (Bellmann et al. 1986 and 1987), Bellmann and coworkers followed the fate of UICC chrysotile, UICC crocidolite, several fibrous glasses, and other manmade mineral fibers following a single intratracheal instillation of 0.3 ml of fibrous material in rats. Groups of rats were then sacrificed at 1, 6, 12, 18, and 24 months following instillation. Lungs were low temperature ashed and the resulting, filtered suspension analyzed by transmission electron microscopy. Some of the fiber types were also acid treated with 0.1 M oxalic acid for 24 hrs prior to instillation.

Bellmann and coworkers report that short fibers (< 5 μm) from all of the fiber types were shown to be cleared from the lungs with half-lives of approximately 100 days, with the asbestos varieties tending to exhibit slightly longer half lives than the other fibers. Short crocidolite fibers exhibited a half life of 160 days The half-life for clearance of short chrysotile was reported to be 196 days (the longest of all). However, this was attributed to positive contributions from breakage of longer fibers.

Bellmann and coworkers report that the behavior of the different long fibers (> 5 μm) for the different fiber types was radically different. The authors report no observed net decline in long crocidolite fibers over the 2 yrs of followup. The also report no observable changes in width of these fibers with time. In contrast, long chrysotile fibers increased in number with time throughout the 18 month followup period and this was attributed to longitudinal splitting. The width of these fibers reportedly decreased with time.

Bellmann et al. also report that a more detailed examination of the time dependence of the width of chrystoile fibers indicates a rapid increase in the number of thin fibrils (< 0.05 μm in width) and thin bundles (< 0.1 μm in width) within 100 days (at the expense of thicker bundles). The authors suggest that this would result in rapid decrease in the number of chrysotile structures visible by optical microscopy and, possibly, increased clearance of the thinnest fibrils by dissolution, but this study shows no increased rate of clearance for thinner chrysotile structures compared to thicker structures (when viewed by electron microscopy). In contrast, long chrysotile fibers that were acid-leached prior to instillation reportedly disappeared with a half life of 2 days.

Generally, the rate of clearance of the long fractions of the other fibers reported in the Bellmann et al. papers varies as a function of solubility and overall thickness. Importantly, all half lives are reported to have high standard errors in this study, due to the small number of animals included for examination.

In summation, virtually all short-term retention studies indicate that:

- fibers retained in the lung tend to be shorter and thinner than the aerosols from which they derive and the size distributions of retained structures tend to be more similar overall than the size distributions observed in the original aerosols;

- chrysotile asbestos undergoes rapid, longitudinal splitting in the lung while amphiboles do not;

- by mass, chrysotile and amphibole asbestos are deposited in the lung with comparable efficiencies, although it is not clear whether chrysotile dusts tend to contain sufficient numbers of curly fibers to limit deposition in the deep lung;

- multiple clearance processes operate over different time frames and some of these processes are strongly length-dependent. Fibers shorter than

approximately 10 µm appear to be cleared rapidly relative to longer fibers and those longer than approximately 20 µm are not cleared efficiently at all (if the fibers are insoluble). The Bellmann et al. studies appear to contrast with other studies in this regard in that they suggest fibers longer than 5 µm do not readily clear;

- the quickest clearance process (presumably muco-ciliary clearance) is not dependent on length; and

- the effects of fiber diameter on clearance have not been well delineated overall, although fibers that reach the deep lung appear to be largely limited to those thinner than approximately 0.7 µm.

These findings are in addition to those mentioned previously from the newer studies:

- multiple clearance mechanisms (operating over multiple time scales) contribute to clearance;

- for sufficiently soluble fibers, long fibers clear more rapidly than short fibers;

- for insoluble fibers, a subset of long fibers clears rapidly while the remaining long fibers clear only extremely slowly, if at all;

- short fibers of all types are cleared at approximately the same rate (much more rapidly than long, insoluble fibers);

- a small fraction of short fibers may be retained for long periods under certain circumstances (sequestered in alveolar macrophages) despite overall rapid clearance of these structures; and

- there is some suggestion that short asbestos fibers clear somewhat more slowly than short fibers of the other, non-asbestos mineral types studied.

Regarding specifically the clearance of long fibers, it appears that a component of all such fibers clears rapidly within the first two weeks and this likely represents muco-ciliary clearance. A second component (representing as much as 60% of the fibers) clears within 90 days and this likely represents clearance by alveolar macrophages. The remaining long fibers are cleared only very slowly, if at all, and this likely represents fibers that are sequestered in granulomas or that escape into the interstitium.

7.2.1.2 Studies involving chronic or sub-chronic exposures

Although the results of older retention studies following longer term (sub-chronic or chronic) exposure were difficult to reconcile with the results following shorter-term exposures, newer studies suggest greater consistency and a clearer picture of the fate of fibers in the lung. Moreover, although there are further suggestions of mineralogy-(fiber type) dependent effects with some clearance mechanisms, it is important that size effects be considered simultaneously, if the dynamics of these processes are to be understood.

In some of the latest studies, for example, Heterberg et al. (1993, 1995, and 1998b) exposed rats (nose-only) by inhalation to a series of manmade vitreous fibers (including a variety of fibrous glasses, rock wools, and refractory ceramic fibers) and two kinds of asbestos: chrysotile (intermediate length NIEHS fiber) and crocidolite (size selected). Animals were dosed for 6 hrs/day, 5 days/wk for up to two years at target concentrations of 10 - 60 mg/m^3. The target concentration for chrysotile and crocidolite was 10 mg/m^3. Animals were periodically sacrificed during the exposure regimen to determine the character of the retained fibers. Vitreous fiber aerosols were characterized by PCM, SEM or, for chrysotile, by TEM. The right accessory lung lobe of sacrificed animals was tied off, frozen, and stored for lung burden analysis.

For analysis, lung lobes were dried to constant weight, ashed, the residue suspended in distilled water, and then filtered on Millipore filters (for examination by optical microscopy) or Nuclepore filters (for analysis by SEM or TEM for chrysotile). Approximately 100 fibers were reportedly characterized to establish fiber size distributions. However, this is problematic for this study because chrysotile asbestos concentrations in the aerosols to which the animals were exposed contained approximately 100 times as many fibers as the other aerosols. Thus, although no fibers longer than 20 μm were observed during characterization of the chrysotile, the concentration of such long fibers could still have been larger in this aerosol than the other aerosols and it would not necessarily have been observed. This is also true of lung burden analyses especially because indirect preparation tends to magnify the number of short chrysotile structures observed in a sample.

A comparison of the retention patterns of chrysotile and RCF-1 from the Hesterberg et al. studies is particularly instructive. First, it should be noted that, in contrast to the values reported by the authors of this study, chrysotile and RCF-1 in fact appear to exhibit comparable in-vitro dissolution rates (12.7 vs. 8 ng/cm^2-hr, respectively) when rates are measured using comparable techniques (see discussion in Section 7.2.4).

The dissolution rates quoted in the Hesterberg study are not derived in comparable studies.

Although a full set of time-dependent analyses are not apparently available for chrysotile, it is reported that approximately 14% of those chrysotile WHO fibers observed to be retained after 104 days of exposure continue to be retained after 23 days of recovery. Under the same conditions, it is reported that 43% of RCF-1 fibers are retained, which suggests more rapid clearance for chrysotile. Even adjusted for the fraction of RCF-1 structures that are longer than 20 μm (and that are presumably cleared even more slowly), approximately 37% of the RCF-1 WHO fibers (< 20 μm) are apparently retained over this period, which is still more than twice the rate reported for chrysotile. Still, more detailed characterization of the size distributions of these two fiber types would need to be evaluated before it could be concluded with confidence that chrysotile is cleared more rapidly than RCF-1 or that dissolution plays a role. In fact, dissolution would tend to cause more rapid clearance only of the longest fibers (i..e. the ones that cannot be cleared by macrophages – see Section 7.2.1.1), which would further reduce the apparent retention rate of the shorter RCF fibers, making it even more comparable to the chrysotile number.

Based on these studies, Hesterberg et al. report that fibers deposited and retained in the lung tend to be shorter and thinner on average than the sizes found in the original aerosol. It is also apparent from their data that long RCF-1 fibers clear more rapidly than short RCF-1 fibers (although a small fraction of long structures are retained at all time points following a recovery period after cessation of exposure), which is consistent with observations in other studies for fibers that dissolve at reasonable rates. In the short term study performed by the same laboratory, Hesterberg et al. 1998a, long fiber (> 20 μm) RCF-1a appears to clear at approximately the same rate as the shorter structures (< 5 μm), although the scatter in the data (and an unexplained initial rise in long-fiber RCF) prevent a more careful comparison. Similar results are also apparent in the data presented for MMVF21. It should be noted that the dissolution rates for RCF-1 and MMVF21 bracket the estimated dissolution rate for chrysotile asbestos (when the three are derived from comparable studies, see Section 7.2.4).

The data presented in Table 3 of Hesterberg et al. (1998b), which are reproduced in the following Table 7-3, can also be used to evaluate the time-trend of retention during chronic exposure.

Table 7-3:
Fraction of Fibers Retained Following Chronic Exposure[1]

Exposure Period (wks)	Chrysotile WHO Fibers f/lung x 10^6	Chrysotile Lung/Aerosol Ratio	RCF-1 WHO Fibers f/lung x 10^6	RCF-1 Lung/Aerosol Ratio	RCF-1 Long WHO fibers f/lung x 10^6	RCF-1 Lung/Aerosol Ratio
0.0357			0.009	4.81E-05	0.002	1.98E-05
13	250	0.024	39	0.209	3	0.030
26	180	0.017	56	0.299	6	0.059
52	1020	0.096	119	0.636	20	0.198
78	853	0.080	173	0.925	21	0.208
104	1600	0.151	143	0.765	25	0.248
Aerosol Concentration:						
(f/ml)	10600		187		101	

1. Source: Hesterberg et al. (1998b)

The values presented in Columns 2, 4, and 6 of the above Table present, respectively, measurements of the lung burden for chrysotile WHO fibers, RCF-1 WHO fibers, and RCF-1 long WHO fibers (> 20 μm) in animals sacrificed immediately following cessation of exposure for the time period indicated in Column 1. Unlike results reported in some earlier chronic studies based on mass (see below), there is no evidence from this table (based on fiber number) that chrysotile lung burdens reach a plateau. Rather chrysotile lung burdens (as well as RCF-1 lung burdens) continue to increase with increasing exposure.

The data presented in Table 7-3 can also be used to gauge the relative efficiency with which the chrysotile and RCF fibers are retained. Considering that the number of fibers inhaled (N_{inh}) over the period of exposure would be equal to the product of the aerosol concentration (C_{air} in f/cm^3) , the breathing rate of the exposed animal (R_B in cm^3/wk), and time (in weeks):

$$N_{inh} = C_{air}*R_B*t \qquad 7.1$$

and the efficiency of retention is simply equal to the quotient of the number of fibers retained (N_{lung}) and the total number inhaled: N_{lung}/N_{inh}, then the efficiency of retention is estimated by the following simple relationship:

$$\text{Efficiency of retention} = N_{lung}/(C_{air}*R_B*t) \qquad (7.2)$$

By rearranaging Equation 7.2, one obtains:

$$\text{Efficiency of retention*t} = (N_{lung}/(C_{air})*(1/R_B) \qquad (7.3)$$

Because the breathing rate for the rats in the Hesterberg et al. study can be considered a constant for all experiments, Equation 7.3 indicates that the slope of a plot of N_{lung}/C_{air} versus time should yield estimates of the relative efficiency of retention for each of the fiber types evaluated. The plot for chrysotile is presented in Figure 7-3. Results from this plot and similar plots for RCF-1 WHO fibers and long WHO fibers (data not shown), result in the following estimates of the relative efficiencies of retention (along with the corresponding R^2 value for the fit of the linear trend line):

chrysotile WHO fibers: 0.0014, $R^2 = 0.856$

RCF-1 WHO fibers: 0.0095, $R^2 = 0.694$

RCF-1 long, WHO fibers 0.0026, $R^2 = 0.880$

Thus, it appears that chrysotile WHO fibers are retained somewhat less efficiently than either RCF-1 WHO fibers or RCF-1 long WHO fibers. However, whether this is due to less efficient deposition or more efficient clearance cannot be determined from this analysis. It is also not possible to determine whether such differences are due to the effects of differences in size distributions among the various fiber types. Interestingly, based on the data presented by Hesterberg et al., which indicates that long RCF-1 WHO fibers clear more rapidly than regular RCF-1 WHO fibers, the differences in the relative retention of these two length categories of fibers is due primarily to relative efficiency of clearance.

Figure 7.3:
[Chrysotile Lung Burden/Aerosol Concentration] vs. Time of Exposure

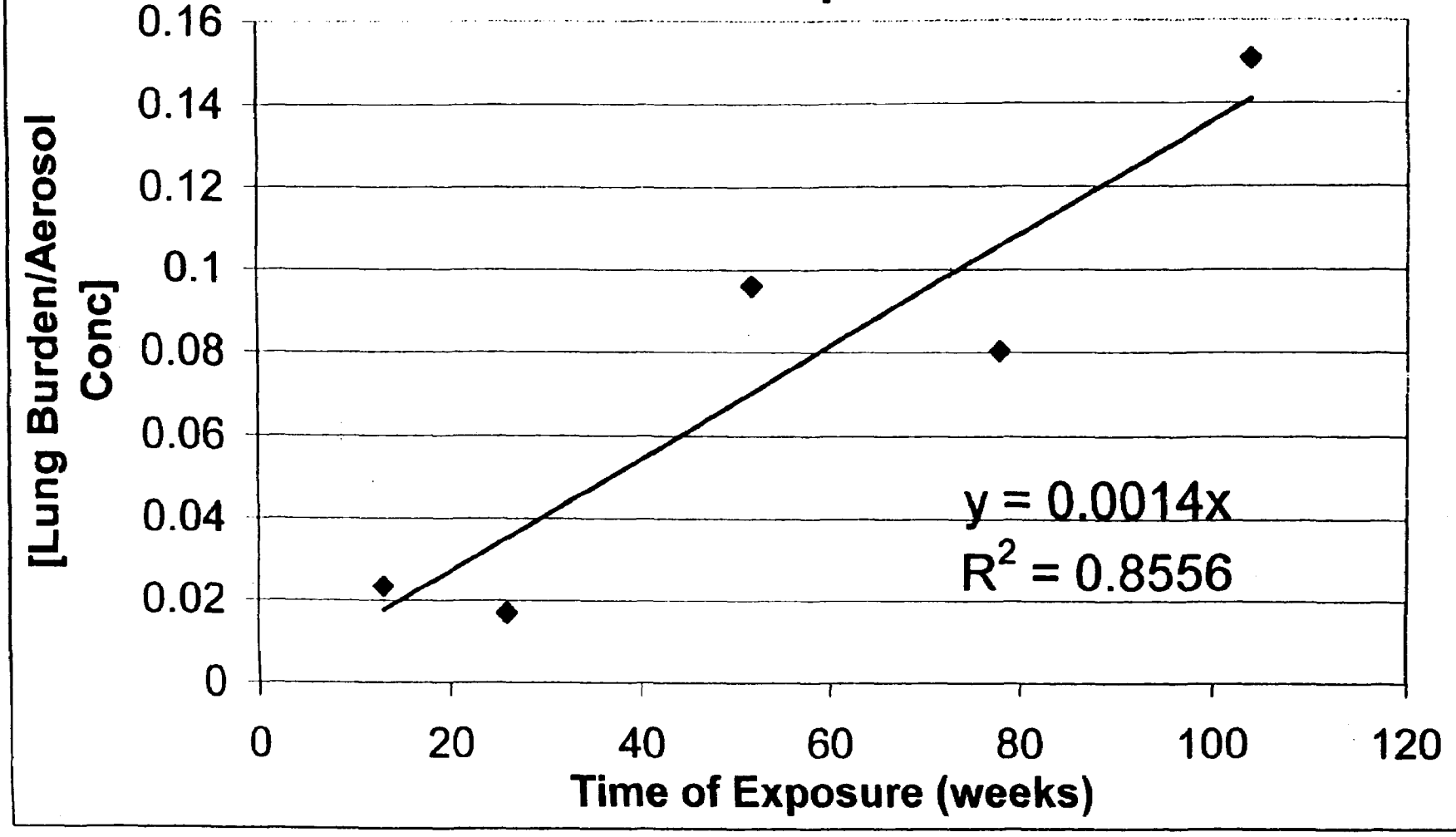

Figure 7-3

In a similar study involving chronic exposure to syrian golden hamsters (Hesterberg et al. 1997), fiber retention and biological effects associated with exposure to amosite and a series of MMVFs were evaluated. The amosite was size selected and hamsters were exposed to one of three levels (0.8+/-0.2, 3.7+/-0.6, and 7.3+/-1.0 mg/m^3). Amosite lung burdens were shown to increase regularly with dose and time of exposure. The time dependence for accumulation of some of the MMVF's was more complicated. None of the animals were apparently followed for any recovery periods following cessation of exposure. The authors also indicate that the severity of the effects observed (inflammation, cellular proliferation, fibrosis, and eventually several mesotheliomas), appear to correlate well with the concentration of fibers longer than 20 μm.

Earlier Studies

Earlier studies, in which asbestos concentrations tend to be monitored as total mass tend commonly to show that chrysotile asbestos is neither deposited as efficiently as various amphibole asbestos types nor is it retained as long (i.e. it is cleared much more rapidly from the lungs). In fact, several such studies tend to show that chrysotile asbestos concentrations eventually reach a plateau despite continuing exposure, which suggests that clearance and deposition come into balance and a steady state is reached. In contrast, amphibole asbestos concentrations continue to rise with increasing exposure, even at the lowest exposure levels at which experimental animals have been dosed.

Such observations do not appear to be entirely consistent with those reported in newer studies (see above) that track fiber number concentrations (in specific size categories). In these newer studies, chrysotile retention is not observed to level off, but continues to increase in a manner paralleling amosite or other fibers. As indicated below, however, the limitations associated with these older studies suggest that, although it may not be easy to reconcile them quantitatively with the newer studies, results from these studies are not necessarily inconsistent with those of the newer studies. Moreover, the trends observed in the newer studies are likely more directly relevant to issues associated with the induction of asbestos related disease.

The problems with the older studies are that:

- the trends seen in the older studies (based on mass) may mask the more important trends associated with deposition and retention of long, thin fibers. Thus, results from such studies may not be directly relevant to considerations of risk; and

- the observed differences between chrysotile and the amphiboles may be attributed to differences in size distribution (among other possibilities). Thus, lacking detailed information on size distributions, it is difficult to reconcile the results from the older studies with results from the newer studies, which explicitly track specific size ranges of fibers.

Given these limitations, the earlier studies are only mentioned briefly.

Middleton et al. (1979) tracked the fate of asbestos (as mass measured by infrared spectroscopy) in rats following inhalation of several asbestos aerosols (UICC chrysotile A, UICC amosite, and UICC crocidolite) at multiple concentrations (reported at 1, 5 or 10 mg/m^3). To account for possible differences in the nocturnal (vs. daytime) activity level of rats, several groups of rats were also exposed in a "reversed daylight" regimen (in which cages were darkened during the real day and bathed in light during the real night). Acclimatized rats in these groups were thus dosed at times corresponding to their night. Exposure continued for 7 hrs per day, 5 days per week, for six weeks.

Results from the Middleton et al. study were fit to a three compartment model (originally proposed by Morgan et al. 1977) and the authors concluded that clearance was independent of fiber type, but that the initial deposition of fibers was very dependent on fiber type. This was indicated by a "K-factor" representing the efficiency of initial deposition. Chrysotile showed K factors that range between 0.17 and 0.36 and vary inversely with the initial exposure concentration. In contrast, amosite exhibits a K factor of 0.69 and crocidolite a K factor of 1.0 and both are independent of exposure level. Although the design of this experiment precluded fitting of the shortest two compartments of the model (with half lives of 0.33 and 8 days, from Morgan et al. 1977), they did optimize the half life of the longest compartment. Fibers in this compartment were cleared with a half life of 170 days.

In a series of studies, Davis and coworkers (1978, 1980, 1988a, and 1988b) report that retention of asbestos (measured in terms of mass) appears to be a function of fiber type and surface charge in addition to fiber size. With regard to fiber type, for example, Davis et al (1978) report that substantially more amphibole (amosite) asbestos appears to be deposited and retained in the lungs of exposed rats than chrysotile. Chrysotile is also apparently cleared more readily than amosite. However, mineralogical effects should only be judged after adjusting for fiber size.

Rats in the Davis et al. studies were dosed at 6hrs/day, 5 days/wk for up to one year at dust concentrations of 2, 5 or 10 mg/m^3 (depending on the specific experiment). Right

lungs (used for determining lung burden) were ashed and the residue was washed in distilled water and filtered. The residue was formed into a potassium bromide disc and asbestos (mass) content was determined by infrared spectroscopy.

Jones et al. (1988) report that the lung-tissue concentration of amosite increases continually with exposure (at 7 hrs/day, 5 days/wk for up to 18 months) and the rate of increase is proportional to the level of exposure. A leveling off of amphibole concentrations in lung-tissue was not observed in this study as long as exposure continued, even for the lowest level of exposure (0.1 mg/m^3) studied. The lowest exposure concentration evaluated in this study is only 1% of the concentration at which chrysotile lung burdens were shown to reach equilibrium in other retention studies (see below). Importantly, however, these are only the older studies in which fiber burden is tracked by mass. The newer studies don't show this effect.

The authors also report lack of any apparent change in size distribution with time among the fibers recovered from the animal's lungs, which suggests lack of substantial clearance even of short fibers. However, the longest recovery period following the cessation of exposure evaluated in this study is only 38 days, which may be too short to allow evidence for differential clearance as a function of size to become apparent (at least in a chronic study; the time dependence in chronic studies such as this are more complicated than for short-term studies). Moreover, the apparent inclusion of lymph nodes as part of the lung homogenate may have caused short fibers initially cleared from the lung to be added back in. In this study, lungs were recovered intact including the associated mediastinal and hilar lymph nodes, which were ashed in toto. Ash residue was washed in acid and water, ultrasonicated and filtered for electron microscope analysis. Note that such a procedure would include any fibers cleared to local lymph nodes.

In a widely cited study, Wagner et al. (1974), report that amphibole lung burdens increase continually as long as exposure to amphiboles continues and that amphibole concentrations in lung tissue decrease only slowly following cessation of exposure. In contrast, chrysotile lung burdens reach a plateau despite continued exposure Importantly, asbestos content was estimated by determining total lung silica content and adjusting for similar analysis on filtered samples of the original aerosols. Thus, in addition to suffering from the limitations associated with tracking fiber burden by mass, there are questions concerning the validity of using total silica to represent asbestos content. Therefore, for these reasons and the additional reason of the lack of controlling for fiber size, the ability to interpret this study and reconcile its conclusions with those of newer studies is severely limited.

Chronic Inhalation of Non-fibrous Particulate Matter

A recent study involving chronic inhalation of non-fibrous materials is helpful at elucidating the relative localization of particles in rats and primates. Nikula et al. (1997) studied lung tissue from a two-year bioassay originally conducted by Lewis et al. (1989), in which cyanomolgus monkeys and F344 rats were exposed to filtered, ambient air or air containing one of three particulate materials: diesel exhaust (2 mg/m3), coal dust (2 mg/m3, particles < 7 um in diameter), or a 50-50 mix of diesel exhaust and coal dust (combined concentration: 2 mg/m3).

Results from Nikula et al. (1997) indicate that responses to all three particulate materials were similar. The particles tended to localize in different compartments of the lung in a species-specific manner:

- 73% of particles remain in the alveolar lumen of rats but only 43% in monkeys. The remainder can be found in the interstitium;
- in both the alveolar lumen and in the interstitium, virtually all of the particles are observed to be isolated within macrophages; and
- the particles in the interstitium reside in macrophages within the alveolar septa, the interstitium of respiratory bronchioles, the adventitia and lymphatic capillaries surrounding arterioles and veins of pulmonary parenchyma, or in the pleura.

It is not known whether free particles penetrate the epithelial lining of the airway lumena and escape into the interstitium or whether such particles are first engulfed by macrophages and then transported in their macrophage "hosts" into the interstitium.

Importantly, even after two years of exposure, the particles in the interstitium do not appear to have elicited a tissue response. Also, the aggregates of particle-laden macrophages observed in alveolar lumena elicited significantly less of a tissue response im monkeys than in rats. Such responses included: alveolar epithelial hyperplasia, inflammation, and focal septal fibrosis.

The authors further indicate that "epithelial hyperplasia concomitant with aggregation of particle-laden macrophages in alveolar lumen is a characteristic response to many poorly soluble particles in the rat lung, both at exposure concentrations that result in lung tumors and at concentrations below those resulting in tumors. Such a response, however, was not characteristic of what was observed in monkeys. Among other things, these differences in responses suggest that rats may not represent a good

model for human responses to inhalation of poorly soluble particulate matter. It would also have been interesting had they tested a "benign" dust such as TiO_2.

In summation:

- results of (newer) sub-chronic and chronic retention studies are generally consistent with those of retention studies that track lung burden following short-term exposure (Section 7.2.1.1);

- there is some indication in these sub-chronic and chronic studies that chrysotile asbestos may not be retained as efficiently as amphibole asbestos. It is likely, however, that such distinctions are due more to fiber size than fiber type so that definitive conclusions concerning such effects cannot be reached until better studies that properly account for both size and type are conducted;

- although earlier studies that track mass instead of fiber number suggest otherwise, chrysotile and amphibole asbestos concentrations (when measured by fiber number) continue to increase with time as long as exposure continues. Due to a lack in the ability to distinguish among size-dependent effects when lung burdens are tracked by mass, the results of the earlier studies are not necessarily inconsistent with the results of the later studies;

7.2.2 Animal Histopathological Studies

Studies in which the lungs of dosed animals are examined to determine the fate and effects of inhaled asbestos are helpful for understanding the movement and distribution of retained particles within the lung and surrounding tissue. Both the newest retention studies and the older retention studies tend to include at least some of this type of information. They also tend to indicate a consistent picture of the fate and effects of asbestos. While such studies tend to confirm that translocation in fact occurs, they are less helpful for elucidating the specific mechanisms by which translocation occurs.

Newer Studies

Ilgren and Chatfield (1998) studied the biopersistence of three types of chrysotile ("short chrysotile" from Coalinga in California, "long' Jeffrey fiber from the Jeffrey mine in Asbestos, Quebec, and UICC - B (??) Canadian Chrysotile, a blend from several mines in Quebec). Both the Coalinga fiber and the Jeffrey fiber were subjected to

further milling prior to use. In this study, rats were exposed via inhalation for 7 hrs/day, 5 days/wk for up to two years. Concentrations were: 7.78 +/- 1.46 mg/m3 for Coalinga fiber, 11.36 +/- 2.18 mg/m3 for Jeffrey fiber, and 10.99 +/- 2.11 mg/m3 for the UICC-B fiber. An additional group of rats was also dosed for a single 24-hour period with Jeffrey fiber at a concentration of 5,000 f/ml > 5 um. Estimates of lung content of chrysotile were based on measurements of total silica content. The character of the three chrysotile types evaluated in this study was previously reported (Campbell et al. 1980, Pinkerton et al. 1983). The animal studies were conducted previously with the overall approach reported by McConnell et al. (1983a and b) and Pinkerton et al. (1984). Based on the characterization presented in these papers, Coalinga fiber is short, but not as extremely short as suggested by the authors:

Ratio of fibers longer than: 5 µm: 10 µm: 20 µm

Coalinga fiber:	200: 78: 0.98
Jeffrey fiber:	591: 220: 78

Such calculations also suggest that the single, "high" dose in this experiment was equivalent only to a concentration that is approximately 10 times the other concentrations studied, so that it is equivalent only to a 10-day exposure and small relative to the longer term (up to 2 yrs) exposures considered in this study.

Results reported by Ilgren and Chatfield indicate that the lung burden for short fiber chrysotile initially increases with exposure, reaches a steady state, and then decreases steadily following cessation of exposure. Approximately 95% of this material is cleared within 2 years. Thus, short fibers appear to exhibit the trend suggested by the older chronic retention studies that tracked burden by mass and is consistent with the newer studies indicating rapid clearance of short structures (Section 7.2.1.2).

In the studies reported by Ilgren and Chatfield, most short fibers are found initially within alveolar macrophages and, while concentrations in Type I epithelium, interstitial cells, and interstitial matrix increase with time, little appears to be taken up by Type II epithelium. Small amounts of short fiber chrysotile are also observed to be taken up by endothelial cells. There is also little sign of inflammation or fibrosis following exposure to the Calidria chrysotile.

Jeffrey chrysotile also initially appears to be taken up primarily by alveolar macrophages but later becomes most prevalent in the interstitial matrix and, to a lesser extent, in interstitial cells. Substantial numbers of fibers are also taken up by Type I epithelium and small amounts by endothelial cells. Similar, but slightly delayed effects

were seen for UICC-B chrysotile (which has a smaller fraction of long fibers and therefore, the authors suggest, takes longer to accumulate). Note that, by 12 months, the majority of long fibers from both these types were found in interstitial matrix while the majority of Calidria material was still found in alveolar macrophages This is consistent with observations concerning behavior between short and long fibers reported by Wright and Kushner (1975), Section 7.2.1.1. At this point, the Jeffrey material also caused substantial thickening of the basement membrane and most fibers in the interstitium were trapped within the collagenous matrix. The authors note that some of the most severe interstitial changes occurred adjacent to areas of bronchiolar metaplasia. Such effects were not seen with Calidria exposure.

Thickened basement membranes, calcium deposits, metaplastic changes, and structural abnormalities were all observed with long fiber exposure but not with calidria exposure. Interstitial macrophages also showed morphological changes following phagocytosis of fibers. While calidria material was about evenly distributed between interstitial matrix and cells, the vast majority of long fiber material was found in the matrix. Movement into the matrix was also observed to increase even after exposure ceased. With time, the number of long fibers in interstitial cells declined modestly but declined precipitously for Calidria material

Jeffrey fibers accumulated in Type I epithelial cells during exposure and then levels decreased slowly after exposure ceased. UICC-B fibers accumulated more slowly, never reaching the same levels as for Jeffrey and decreased more rapidly. Concentrations of Calidria fibers in Type I epithelial cells was low at all time points.

Type II epithelial cells accumulated very few fibers of any type (although they took up slightly more Jeffrey fiber than the others). All three fiber types caused substantial increases in interstitial cells (mostly macrophages) at three months and this increase persisted for the Jeffrey fiber but decreased to background after 24 months for the other two fiber types. Fibroblast numbers also increased with the long fiber types but not Calidria chrysotile.

Type II epithelial cells showed decreases in volume and number that persisted until exposure to long fiber ceased and these cells displayed dramatic structural aberrations despite absence of a fiber load. One possible explanation for the observed changes in Type II cells, especially the reduction in their number, is that they were undergoing terminal differentiation to Type I cells (see Section 4.4) In fact, the apparent absence of fibers observed within Type II cells might be explained by such cells taking up fibers but being induced to terminally differentiate, once fibers are accumulated. Overall, Type II cells displayed greater cellular response than Type I cells (which might also suggests a

role for cytokines). All effects were observed to be fiber length dependent and all were exaggerated following exposure to long fiber material.

Rats exposed to long fiber had numerous accumulations of dust-laden interstitial macrophages and/or small focal accumulations of dust within the interstitium at the end of the lifetime study, but such changes were not observed for Calidria exposed animals

The lung burden for rats exposed to the single, "high" Jeffrey fiber exposure (based on total silica) at 12 months (i.e. 12 months post exposure) was not different from controls. Therefore, the authors conclude that short-term, "high" exposures are rapidly cleared (even exposures containing substantial quantities of long fibers). Other changes induced by the single, short-term high exposure of Jeffrey fiber that was followed for 24 months also showed reversion to close to background status. Importantly, these observations are not based on quantitation of fiber burden in lung tissue. Rather they are inferred by observing the effects caused by the presence of fibers. This may suggest, for example, that more than 10 day's worth of exposure would be required at this level of exposure before irreversible lesions develop.

In the study by Hesterberg et al. (1997), which was previously discussed (Section 7.2.1.2), the authors note (among dosed hamsters) that the magnitude of cellular effects appeared to differ among the fibrous glasses as a function of their relative biodurability. For animals dosed with the least biopersistent glass, only transient effects (influx of macrophages, development of microgranulomas) were observed and these did not progress further. For the more persistent glasses, injury progressed through more intense inflammation, interstitial fibrosis, pleural collagen deposition, mesothelial hypertrophy and hyperplasia and eventually, mesothelioma. The authors also suggest that amosite appears to be more potent than chrysotile, even when aerosols contain comparable numbers of fibers longer than 20 μm.

Choe et al. (1997) exposed rats to chrysotile and crocidolite (both NIEHS samples) by inhalation for 6 h/d, 5 d/wk, for 2 weeks. The rats were then sacrificed and their pleural cavities lavaged. Results indicate that significantly more pleural macrophages were recovered in plueral lavage fluid at one and six weeks following exposure than sham exposed rats. The centrifuged pellet from pleural lavage fluid from one of four rats also exhibited long (> 8 μm), thin (< 0.5 μm) crocidolite fibers (one week following exposure). The concentration of fibers in this pellet suggested approximately 1 f per 4000 cells in the pleura. Note that chrysotile rats were not examined for fiber content.

Older Studies

In the series of studies by Davis et al. (1978, 1980, 1985, and 1986a), the authors generally report similar histopathological observations that emphasizes a marked distinction between effects from long and short fibers. From the 1986 study, for example, Davis et al. report that at the end of 12 months of exposure, rats exposed to long fibers (amosite in this case) exhibited deposits of granulation tissue around terminal and respiratory bronchioles. They further indicate that the granulation tissue consists primarily of macrophages and fibroblasts with occasional foreign body giant cells.

As the animals aged, there was increased evidence of collagen deposits in these lesions and the oldest lesions consist mainly of acellular, fibrous tissue. The alveolar septa in these older animals showed progressive thickening. Initially, this was apparently due primarily to hyperplasia of Type II epithelial cells but with time was increasingly due, first, to reticulin and, later, to collagenous deposits in the septal walls. Asbestos dust was frequently visible in these deposits. Epithelial cells lining alveoli adjacent to the oldest lesions also tended to become cuboidal in shape. As the animals aged, these areas of interstitial fibrosis became more extensive.

In contrast, animals exposed to short fibers (also amosite in this case) showed no such lesions (peribronchial fibrosis) at any point in time. At the end of exposure, the lungs of these animals contained large numbers of pulmonary macrophages packed with fibers, but these cells remained free in the avleolar spaces. The authors report that large numbers of laden macrophages sometimes aggregated in alveoli close to respiratory bronchioles, but that there would be no formation of graunulation tissue or thickening of alveolar septa at these locations. Thus, with the exception of the presence of dust-laden macrophages, the structure of the lung of these rats was not altered.

In the Davis et al. 1987 study of chrysotile, a slight variation of the above scenario is worth noting. In this study, the development of peribronchial fibrosis was reported for animals dosed both with the long fiber material and with the short fiber material. However, the authors also report that the short fiber chrysotile in this study in fact contains a sizable fraction of longer structures and this finding was corroborated by more formal size characterization (Berman et al. unpublished) later conducted in support of a study to evaluate the effects of size (Berman et al. 1995).

In this study, Davis et al. also reported observations on the morphological changes observed in the mesothelium during these studies. The authors indicate that the older animals in these studies exhibit "areas of vesicular pleural metaplasia consisting of loose, fibrous tissue containing large vesicular spaces lined with flattened cells." The

authors also report that examination in previous studies indicates that these cells are of a mesothelial type.

Davis et al. report that, "...occasionally the walls between vesicular spaces were so thin that they consisted of two closely opposed layers of extended and flattened cells with no basement membrane in between them. Where cells were supported by areas of fibrous tissue, a basement membrane was present. While no method for the direct quantification of this pleural metaplasia has been developed, its occurrence is closely related to the presence of advanced interstitial fibrosis or adenomatosis in the lung tissue and it is particularly common where patches of this type of parenchymal lesion have reached the surface. It is not known whether such lesions are precursors to mesothelioma." Davis et al. also note that neither of the two mesotheliomas observed in this study showed histological patterns consistent with the observed vesicular hyperplasia.

Brody et al (1981) tracked the distribution of chrysotile following inhalation by rats. Asbestos was initially deposited almost exclusively at alveolar duct bifurcations. In agreement with Pinkerton et al (1986), the degree of deposition appeared to be an inverse function of the pathlength and bifurcation number for each alveolar duct. Uptake by macrophages and type 1 epithelial cells were observed following deposition. Asbestos was observed both in lipid vesicles and free in the cytoplasm of type 1 cells. After 8 days, alveolar duct bifurcations became thickened with an influx of macrophages. Asbestos was also observed in basement membrane below the epithelium. Apparently, structures had been transported through type 1 cells to the basement membrane. Once in the basement membrane, asbestos may enter the interstitium. Predominantly short structures were monitored in this study. Long structures were not readily observed (but this is likely a counting problem; under such circumstances, short structures may serve as surrogates for the presence of other structures).

Intratracheal Instillation

Bignon et al (1979) studied the rate of translocation of various materials in rats. Chrysotile, crocidolite, and glass fibers were intrapleurally injected into rats and their concentration was monitored as a function of time in lung parenchyma and other tissues removed from the pleura. Within one day following injection, asbestos was detectable in lung parenchyma. After 90 days, asbestos was found in all of the tissues analyzed. Based on the rate of translocation to the lung, crocidolite migrates about 10 times more rapidly than chrysotile (on a mass basis). The rate of migration of glass is in between the two asbestos types. Structures initially found in the lung were

significantly shorter than the average size of structures injected. After seven months, however, the average lengths of structures in all tissues monitored were longer than the average length of structures originally injected. Thus, short structures migrate more rapidly than longer structures (possibly by a different mechanism) but long structures eventually translocate as well. Within a target tissue, preferential clearance of short structures also contributes to observed increases in the average length of the structures with time.

Studies of Non-Fibrous Particulate Matter

Studies of the fate and effects of respirable, non-fibrous particulate matter provide evidence for at least one mechanism by which particles (and fibers) may be transported to the interstitium.

Li et al. (1997) evaluated the effect of urban PM 10, carbon black, and ultrafine carbon black on rats following intratracheal instillation (0.2 ml volume instilled containing between 50 and 125 µg of particles). After 6 hrs, there was a noted influx of neutrophils (up to 15% of total cells observed in bronchioalveolar lavage – BAL fluid) and increases in epithelial permeability was surmised based on increased total protein (including increases in levels of lactate dehydrogenase, which is a marker for cell membrane damage) in BAL fluid.

Conclusions

Overall, observations among both the newer and the older studies (including the study by Wright and Kuschner 1975, see Section 7.2.1.2) tend to be highly consistent, particularly with regard to the distinction between the effects of short and of long fibers. Typically, long fibers initially produce substantial inflammation characterized by an influx of macrophages and other inflammatory cells. Ultimately, exposure to such fibers cause thickening of alveolar septa (particularly near avleolar duct bifurcations) due to a combination of epithelial hyperplasia and deposition of reticulin and, later, collagen resulting in interstitial fibrosis. In contrast, short fibers cause an initial influx of macrophages and, long term, show persistent accumulations of fiber-laden macrophages both in alveolar lumena and in pulmonary lymph nodes, but otherwise no structural changes are observed in the lung tissue of these animals.

These studies also provide ready evidence of the effects of fiber translocation, but generally offer only limited evidence for elucidating the mechanisms by which such translocation occurs. There is evidence that Type I (and possibly Type II) epithelium phagocytize particles and fibers and it is possible that such fibers may be passed

through to the basement membrane and the interstitium. For Type I cells, the distance between the alveolar lumen and the basement membrane averages less than 1 μm in any case (Section 4.4). Certainly fibers are also observed in the interstitium. Particulate studies also indicate that oxidative stress induced by particulate matter and fibers may cause morphological changes in Type II cells with consequent loss of integrity of the epithelium, which increases it's permeability overall and may also allow diffusional passage of particules and fibers.

7.2.3 Human Pathology Studies

Human pathology studies provide additional information concerning the nature of asbestos deposition, clearance, and retention. These are the studies in which lung burdens are measured in samples of lung tissue and correlated with the exposures received by the individuals from which the lung samples derive.

Among the advantages of human pathology studies is that they provide direct insight into the behavior of asbestos in humans. They are also limited, however, by the lack of ability to obtain time-dependent estimates of lung burden (because samples are derived from deceased individuals), by the manner in which lung tissue is stored (several of the fixatives employed to store tissue samples have been shown to enhance dissolution of asbestos, Law et al. 1990 and 1991), by the manner in which samples are prepared for asbestos analysis, by the manner in which asbestos is analyzed, and by the limited ability to re-construct the uncontrolled exposures experienced by study subjects (Section 5.2).

Perhaps most importantly, the ability to construct anything but the coarsest quantitative comparisons across subjects is also typically limited by use of "opportunistic" tissue samples (i.e. use of samples that happened to have been collected and stored during autopsy or necropsy) because such samples are not controlled for location on the respiratory tree (i.e. the linear distance and branch number from the trachea) that is represented by the sample. Because it has previously been shown that deposition is a strong function of such location (see, for example, Yu et al. 1991), comparisons across lung samples not controlled for these variables are problematic. In fact, it has also been shown that samples collected from adjacent locations in lung parenchyma can in fact exhibit strikingly different fiber concentrations due specifically to the differences in the location of the respiratory tree represented by the alveoli and respiratory bronchioles in the spatially adjacent samples (Pinkerton et al. 1986, Brody et al. 1981, Section 5.2).

Despite the above indicated cautions, when interpreted carefully, human pathology studies can provide useful evidence regarding fiber deposition, clearance, and retention in the human lung.

Newer Studies

Among the most recent studies, Finkelstein and Dufresne (1999) evaluated trends in the relationship between lung burdens for different fiber types and different size ranges as a function of historical exposure, the duration of such exposure, the time since last exposure, and other variables. The analyses were performed among 72 cases from which tissue samples could be obtained (including 36 asbestosis cases, 25 lung cancer with asbestosis cases, and 11 mesothelioma cases).

Due to the excessive scatter in the data, most of the analyses presented depend on "Lowess Scatterplot Smoothers." **NEED TO COMMENT ON THIS** Moreover, although not stated, it is likely that the tissue samples obtained were "opportunistic" in that they were not matched or controlled for relative position in the respiratory tree.

The authors employed the multi-compartment model developed by Vincent et al. (1985) to evaluate trends in their data. The features of this model include:

- a compartment representing conducting airways that are cleared within minutes to hours by muco-ciliary transport;
- a compartment representing the subset of fibers reaching the pulmonary portion of the lung that are cleared by alveolar macrophages and transported to the muco-ciliary escalator. This type of clearance is also considered relatively rapid with half lives of no more than several days to several weeks. Macrophage clearance is also considered size-dependent and long fibers are cleared less efficiently than short fibers;
- when sufficient dust is inhaled (or dust is sufficiently cytotoxic) to impair the motility of macrophages (either by volumetric overload or by toxicity), a sequestration compartment forms that consists of laden but immobile macrophages. Although this compartment may ultimately be cleared to lymphatic drainage, such clearance is assumed to be slow and size dependent (with half lives of 2 or 3 years for short fibers and 8 years for fibers longer than 10 μm); and

- once the macrophage system is overloaded, fibers may cross the alveolar epithelium and reach the interstitium and this compartment must be cleared by transport to lymphatic drainage, which is assumed to be an extremely slow process.

Finkelstein and Dufresne indicate that chrysotile splits both longitudinally and transversely in the lung and that chrysotile lung burdens decrease significantly with time since last exposure (with short fibers clearing even faster than long fibers) while tremolite burdens do not appear to decrease with time since last exposure. They also suggest that smoking does not appear to affect clearance rates.

Finkelstein and Dufresne indicate that these type of studies are not useful for examining the behavior in rapidly clearing compartments of the lung but they may provide insight concerning the more slowly clearing compartments. Based on their modeling, they suggest that tremolite is transferred to the sequestration compartment at rates that are 6 to 20 times that of chrysotile (which they indicate is comparable to what was found for crocidolite by DeKlerk). The authors suggest that retained chrysotile concentrations tend to plateau after accumulation of about 35 years of exposure while tremolite concentrations continue to increase. They also, suggest, however, that chrysotile concentrations may begin to increase again after 40 years (suggesting the overload is eventually reached for chrysotile as well). Reported half-lives from the long-term compartment are:

chrysotile	
fibers shorter than 5 µm	3.8 yrs
fibers 5-10 µm in length	5.7 yrs
fibers longer than 10 µm	7.9 yrs
tremolite	
fibers shorter than 5 µm	14.3 yrs (not different from ∞)
fibers 5-10 µm in length	15.8 yrs (not different from ∞)
fibers longer than 10 µm	150 yrs (not different from ∞)

In a case-control study, Albin et al. (1994) examined the lung burdens of deceased workers from the asbestos-cement plant previously studied for mortality (Albin et al. 1990). In this study, details of the procedures used to prepare lung tissue for analysis were not provided. It is also assumed that available tissue samples were "opportunistic" in that they were not matched or controlled for relative position in the respiratory tree.

Results from Albin et al. (1994) are consistent with, but do not necessarily demonstrate that, chrysotile is cleared more readily from a long-term sequestration compartment than amphiboles. The authors also report that chrysotile fibers observed in this study are much shorter than the amphibole fibers observed, so that differences in clearance rates might be attributable to size differences. The authors also suggest that clearance is impaired by fibrosis.

Studies of Quebec Miners

Several authors also studied the lung content of various groups of deceased chrysotile miners in Quebec and found, despite overwhelming exposure to chrysotile from the ore (which contains only trace quantities of tremolite, see Section 6.2.3 and Sebastien et al. 1986), a substantial number of fibers (in some cases the majority of fibers) observed in the lungs of deceased miners from this area are tremolite. Thus, for example:

- in a study of lung burdens in 6 mesothelioma victims, Churg et al (1984) showed that amphiboles structures were 5 to 15 times as plentiful as chrysotile despite the predominantly chrysotile exposure;

- in a study of lung tissue from 20 asbestosis cases, Pooley (1976) found substantial concentrations of tremolite in the lungs of deceased Quebec chrysotile workers; and

- in a much larger study comparing lung burdens of Quebec workers with those from the South Carolina textile mill, which has also been extensively studied for asbestos-related mortality (Section 6.2.3), Sebastien et al. (1989) examined 161 lung tissue samples (89 from the Quebec mines). Results from this study indicate that geometric mean tremolite fiber concentrations were more than three times mean chrysotile fiber concentrations (18.4 vs. 5.3 f/µg dry lung tissue) among the deceased Quebec miners evaluated. It was also found that, despite these differences, the overall size distributions of tremolite and chrysotile fibers observed in lung tissue were approximately the same. A more detailed discussion of the results of this study is provided in Section 6.2.3.

- McDonald, Gibbs and Rowlands (1985) suggest that lung burden data from quebec indicate little evidence of decreasing chrysotile concentration with time since last exposure. Rather they suggest simply that tremolite is initially deposited in the deep lung more efficiently. These authors also

indicate that tremolite fibers are mostly optical while chrysotlie are mostly "Stanton" or thinner.

These authors report good correlation of both tremolite and chrysotile with estimated past exposures. Reported geometric mean measurements for the various fibers in lung are: tremolite: $1x\ 10^6$ - 18.2×10^6, chrysotile : 1.5×10^6 -15.7×10^6, respectively, when exposure varied from < 30 mpcf to >300 mpcf. Note that, if these are PCM measurements, this may not be telling the whole story. The authors also report that 66% of those who died 10 yrs since first exposure and half of those who died 30 yrs since first exposure showed high chrysotile concentrations in their lungs.

These observations provide evidence that either amphibole (tremolite) asbestos is deposited more efficiently in the compartments of the lung where clearance is slow or chrysotile asbestos is cleared more rapidly and efficiently from even the slowest clearing compartments of the lung (or both). Moreover, this conclusion appears to apply similarly to both short and long fibers.

Some of the pathology studies that have been published suggest that at least some clearance mechanisms show a dependence on fiber size, which is consistent with what is observed in animal studies (Section 7.2.1). Notably, for example, Timbrell (1982) studied deceased workers and relatives from the Paakkila anthophyllite mine in Finland. He found that structures shorter than 4 µm and less than 0.6 µm in diameter are completely cleared from healthy lungs. The efficiency of clearance decreases slowly with increasing size. Structures longer than 17 µm and thicker than 0.8 µm in diameter are not significantly cleared. The study is based on a comparison of structure size distributions in lungs compared to the structure size of the material in the original dust exposure. Timbrell also noted that asbestosis suppresses the removal process.

When considering the dependence of clearance on size (particularly via mechanisms involving phagocytosis), it is necessary to address differences in human and animal physiology. Due to differences in the morphology, for example, human macrophages have been shown capable of phagocytizing larger particles and longer fibers than macrophages found in mice and rats (Krombach et al. 1996, for details, see Section 4.4). Thus, the range of fibrous structures that are efficiently cleared from human lungs is expected to include longer fibers than the range efficiently cleared in mice or rats. Unfortunately, given the limited precision of the available data, the size ranges that are reported to be cleared efficiently in rats and humans, respectively, cannot be easily distinguished.

Several human pathology studies also support observations from animal studies indicating that clearance may be inhibited by the development of fibrosis (Albin et al. 1994, Churg et al. 1990, Morgan and Holmes 1980) or by heavy smoking. However, other studies do not indicate such hindered clearance either with smoking (Finkelstein and Dufresne 1998) or with fibrosis.

Older Studies

Morgan and Holmes (1980) examined tissue samples from 21 patients in England (10 who died of mesothelioma, 3 who died of lung cancer, and 8 who died of other causes). In this study, formalin-fixed tissue samples were digested with hypochlorite. The residue was then rinsed, diluted, and an aliquot filtered. The filter was mounted on a microscope slide and clarified for analysis by phase contrast optical microscopy. Importantly, the authors note that chrysotile fibers were ignored in this study because they would not generally have been detected by this technique. Portions of the filters were also carbon coated and prepared for TEM analysis. Based on the observation that only 19% of the fibers observed in this study were between 2.5 and 5 μm, when the authors expect airborne distributions to contain closer to 90% of the fibers within this size range, the authors conclude that short fibers are preferentially cleared from the lung. They also conclude, based on one subject with asbestosis whose lung tissue exhibited 72% short fibers, that asbestosis hinders clearance. The authors also note that fewer than 1% of ferrugenous bodies (iron-coated asbestos bodies) are less than 10 μm in length, which indicates (in agreement with previously published work) that such bodies seldom form on short fibers. They also suggest that virtually all fibers longer than 20 μm tend to be coated in the distributions they observe.

Le Bouffant (1980) studied the concentrations, mineralogy, and size distributions of asbestos fibers found in the lungs and pleura of deceased asbestos workers. Based on the analysis, he found that the average ratio of chrysotile fiber concentrations found in the lung versus the pleura is 1.8 while for amosite the ratio is 34. This indicates that chrysotile migrates from the lung to the pleura more rapidly than amphiboles resulting in a higher fraction of total fibers in the pleura being composed of chrysotile (3% in the lungs versus 30% in the pleura). With regard to size, the researchers found the size distribution of amosite is virtually identical in the lung and pleura while chrysotile fibers found in the pleura are much shorter than chrysotile fibers found in lung tissue. This suggests that the movement of chrysotile is a result of a combination of translocation and degradation to shorter fibers (or that tissue samples have been contaminated with environmentally ubiquitous short, chrysotile structures). The authors indicate that chrysotile fibers apparently degrade to shorter fibers more rapidly than amosite and translocate to the pleura more rapidly than amosite. Thus, a greater fraction of

chrysotile fibers (albeit short fibers) reach the pleura than amosite fibers over fixed time intervals. However, the results of this study also confirm that the longer amosite fibers do eventually translocate, although on a much more extended time scale than the translocation of chrysotile.

Importantly, the results of this study need to be evaluated carefully. Boutin et al. (1996) showed that the majority of asbestos fibers in the pleura (particularly the long fibers) are aggregated in localized "black spots" (which surround the sites of lymphatic drainage). Thus, if the tissue samples analyzed by Le Bouffant do not contain representative sets of such spots, the conclusions drawn by Le Bouffant may be subject to question.

In summation, human pathology studies tend generally to support the findings of other studies regarding the size effects of asbestos (i.e. short fibers tend to clear more rapidly than long fibers, which can be retained in pulmonary tissues for extended periods). They also appear to highlight drastically different behavior between chrysotile and the amphibole asbestos types (particularly tremolite) regarding the heavily favored retention of the latter, which has also been indicated in animal studies. Unfortunately, the ability to draw quantitative conclusions from human pathology studies is hampered by the severe limitations of these studies (Section 5.2).

7.2.4 Studies of Dissolution/BioDurability

Although asbestos minerals are relatively insoluble in vivo in comparison, for example, to various fibrous glasses or other manmade mineral fibers (see, for example, Hesterberg et al. 1998a or Estes and Hadley 1996), they do eventually dissolve in the body. Therefore, this pathway may contribute importantly to the overall biological clearance of asbestos. Moreover, it has been suggested by several researchers (see, for example, McDonald 1998 and other references cited below) that differences in biodurability between chrysotile and the amphiboles may at least partially explain the disparate potencies observed for these fiber types toward the induction of mesothelioma and, potentially, lung cancer (see Sections 6.2.4.2 and 6.3.3.2).

> Note that the term "biodurability" is used here to indicate the persistence of a particle or fiber attributable specifically to solubility (in the absence of other clearance or degradation mechanisms). In contrast, the term "biopersistence" is used to indicate the overall persistence of a particle or fiber in the body attributable to the combined effect of all mechanisms by which it might be removed. Thus, for example, while biopersistence can be evaluated in vivo, biodurability can best be inferred from in vitro dissolution studies so that effects from other clearance mechanisms can be eliminated.

Several studies further indicate that both the in-vivo biopersistence and the bio-activity (including carcinogenicity) of various fiber types may be linked to their observed, in-vitro dissolution rates (Eastes and Hadley 1995, 1996, Bernstein et al. 1996, Hesterberg et al. 1998a, 1998b). Such studies, however, typically involve fiber types with dissolution rates that are rapid relative to the rates of clearance by other mechanisms (Sections 7.2.1.1 and 7.2.1.2). In such studies, moreover, the various types of asbestos are typically employed as negative (insoluble) controls. In fact, most of these studies are based on experiments with rats and the 2-yr lifetime of a rat is comparable to the anticipated lifetime of chrysotile asbestos in the body and short compared to the anticipated lifetimes for the amphiboles (see below). Therefore, such studies are not particularly sensitive to differences in the relative biodurability of the different asbestos types. In fact, in the majority of these studies, the dissolution rates reported for asbestos were derived indirectly by analogy with other minerals or are quoted from other studies that derive rates similarly and may therefore be somewhat unreliable. Nevertheless, a review of a subset of these studies is instructive.

- Eastes and Hadley (1995 and 1996) report a simple model that reasonably predicts the relative fibrogenicity and tumorigenicity for a range of synthetic fibers based on the dissolution rates of the fibers measured in vitro. The authors found that they could explain observations by assuming that the effects of the various fibers are a function of an adjusted dose that accounts for biodurability. Thus,

  $$F = f(ax)$$

  where "F" is the observed incidence of the end point, "f" is the dose-response function proposed for the effect, "x" is the measured dose, and "a" is an adjustment factor that accounts for durability.

  In the model, "a" is determined simply as "t_d/t_L" where t_d is the time that a fiber of diameter, "D" remains in the lung and t_L is the lifetime of the exposed animal (e.g. 2 years for rats). This simple model reasonably reconciles the results observed in animal inhalation and injection studies of manmade mineral fibers (MMVF's), refractory ceramic fibers (RCF's), and asbestos for end points including lung tumors, degree of fibrosis, and (for intrapleural injection studies) mesothelioma. Based on a chi-square test, the simple model is shown to adequately fit the data to a number of databases reviewed. In contrast, the unadjusted doses do not. Importantly, the dissolution rates used for the various asbestos minerals in

this study were estimated by analogy with similar minerals and therefore may be unreliable.

- In studies comparing in-vivo biopersistence with dissolution rates measured in-vitro, Bernstein et al. (1996) and Hesterberg et al. (1998a), indicate that it is necessary to consider only long fibers (typically longer than 20 μm), because shorter structures are typically cleared by other mechanisms. They also indicate, at least for this type of study in which whole lungs were homogenized and dissolved prior to preparation for asbestos analysis, that clearance is initially rapid. This reflects muco-ciliary clearance from the upper respiratory tract. Therefore, it is clearance of long fibers from a longer term pool that tracts in-vitro dissolution rates.

  These authors also report that long, soluble fibers (longer than 20 μm) are actually cleared more rapidly than short fibers in these studies. They indicate that this is likely due to long fibers being too long to be effectively phagocytized by macrophages so that they are left to dissolve in the extracellular fluid at neutral pH. Shorter fibers are effectively taken up by macrophages so that dissolution is hindered by the more acidic environment of the phagosomes (pH 4.5) and by the limited volume of fluid within which to dissolve.

- Law et al. (1991) studied the dissolution of a range of fibers in solutions used as common fixatives for biological samples. The authors report that chrysotile and crocidolite, as well as many other fibers, dissolve at measureable rates in the fixatives studied (Karnovsky's fixative and formalin fixative). They therefore recommend that fiber concentrations and size distributions obtained from tissue samples stored in such fixatives should be evaluated carefully to account for the possible effects of the fixatives.

- Although Coin et al. (1994) reported seeing no effective reduction in long fiber (> 16 μm) chrysotile (nor other evidence of dissolution) in their study of fiber biopersistence, the limited time frame of this study (30-days) may have been too short to allow detectable changes to accumulate.

The most consistent data for the comparative biodurability of chrysotile and the amphiboles (specifically crocidolite) is found in two in-vitro studies of the dissolution rates of fibers that were conducted under comparable conditions. In the first of these

studies, Hume and Rimstidt (1992) measured the dissolution rate for chrysotile asbestos at neutral pH under conditions analogous to biological systems. The dissolution rate that they report for chrysotile converts to: K_{diss} = 12.7 ng/cm^2-hr and this is reportedly independent of pH. In a comparable study Zoitus et al. (1997) report the following dissolution rate for crocidolite: K_{diss} = 0.3 ng/cm^2-hr, which is 40 times slower than for chrysotile. Dissolution rates for several MMVF's and RCF-1 are also reported in the latter paper, which are listed from fastest dissolving to slowest in Table 7-4.

Table 7-4:
Measured In-Vitro Dissolution Rates for Various Fibers[1]

Fiber Type	K_{diss} (ng/cm^2-hr)
MMVF 10	259
MMVF 11	142
MMVF 22	119
MMVF 21	23
Chrysotile	12.7[2]
RCF 1	8
Crocidolite	0.3

[1] Source: Zoitus et al. (1997)
[2] Source: Hume and Rimstidt (1992)

Note that dissolution rates for other amphiboles, such as amosite are probably no more than a factor of two or three different than that reported above for crocidolite (see, for example, Hesterberg et al. 1998a,b).

To compare the effect of biodurability on the in-vivo biopersistence of asbestos and other fiber types, both the detailed kinetics of dissolution and the distribution of fiber sizes must be considered.

As reported by Zoitus et al. (1997), at a sufficiently high rate of fluid flow, the rate of mass loss from a fiber is proportional to its surface area, A. Thus:

$$-dM/dt = -kA. \qquad (7.4)$$

This means that for a uniform mass fiber dissolving congruently:

$$1-(M/M_o)^{0.5} = 2kt/D_o\rho \qquad (7.5)$$

where:

M is the mass at time t;
M_o is the initial mass at time t = 0;
D_o is the initial diameter of the fiber; and
ρ is the density of the fiber.

Substituting the equation relating the mass and the diameter of a fiber ($M = \rho\pi d^2 h/4$) into the above equation, cancelling terms, and rearranging indicates that (during dissolution) the diameter of a fiber decreases linearly with time:

$$D = D_o - 2kt/\rho \qquad (7.6)$$

where:

D is the diameter at time t; and
all other terms have been previously defined.

Furthermore, the rate of reduction in radius is given by: k/ρ. Based on the dissolution rates given above for chrysotile and crocidolite, the radius reduction rates (v_{rad}) for these fiber types are determined to be: 1.26×10^{-6} µm/sec and 2.6×10^{-10} µm/sec, respectively. Thus, the dissolution of each fiber is a zero order process (i.e. the rate is constant with time and independent of concentration). Given these rates, a chrysotile fiber 1 µm in diameter will disappear in approximately a year (3.9×10^7 sec) and a crocidolite fiber of the same diameter in approximately 60 years (1.9×10^9 sec).

The number rate of disappearance of a population of fibers due to dissolution is a function of the rate of radial reduction for the fiber type and the distribution of fiber diameters in the population. The time at which the entire population finally dissolves can be estimated simply by dividing the radius of the largest fiber by the radius reduction rate, v_{rad}, that is appropriate for the fiber type. The number of fibers remaining from the population at time t will be equal to the number of fibers in the original distribution with radii larger than $v_{rad}t$ for the reduction rate that is appropriate for the fiber type.

Note that dissolution will not cause an immediate reduction in fiber concentration. The number of fibers will not begin to decrease until sufficient time has elapsed for the thinnest fibers to completely dissolve. Eastes and Hadley (1994) therefore recommend tracking the time dependence of the mode of the distribution of fiber diameters to best gauge the effects of dissolution in vivo.

Importantly, fibers in vivo will only dissolve at the rates predicted by the above equations if the fluid in which they are dissolving flows past the fibers sufficiently rapidly to prevent saturation from limiting the rate (Mattson 1992). Especially for slow dissolving materials like asbestos, however, it is expected that the observed dissolution rate in vivo will generally be slower than the rates predicted based on in vitro measurements. Even for more rapidly dissolving fibers like most fibrous glasses and manmade mineral fibers, dissolution is hindered in compartments of the body in which the volume of available solute is limited.

In summary, dissolution is a zero-order (i.e. constant with time, independent of concentration) clearance mechanism that is dependent on fiber mineralogy, that the effect it has on fiber populations (concentrations) is a function of the distribution of fiber diameters within the population, and that the theoretical rate of dissolution may not be achieved in all tissues in all compartments of the lung or mesothelium due to limits in the rate of in-vivo solute flow.

7.2.5 Dynamic Models

Unlike particle deposition in the lungs, which is an entirely mechanical process, clearance, transport, and degradation mechanisms tend to be complex biochemical processes. Due to the incomplete understanding of such processes, state-of-the-art of degradation and clearance modeling is not as advanced as that for deposition. Even the most sophisticated of these models remain semi-empirical. Although, current models in this area show general agreement with the sparse, available data, there are clearly areas of weakness that require additional research. Nevertheless, the models provide a good indication of the kinds of processes that are important in the body and their overall constraints. It is also noted that models for degradation and clearance in humans tend to be better developed than those for animals primarily due to confounding uncertainties associated with animal ventilation rates. An overview of the state of the art, which was current as of the date of publication, can be found in Stober et al. (1993).

According to Stober et al. (1993), the general conclusions that can be drawn from the current models are that:

- clearance from ciliated airways is rapid, independent of particle/fiber type, apparently independent of particle size, and can be described as the sum of two, weighted exponentials (i.e. an assumed combination of two first-order decay processes), although the process may in fact be zero order (i.e. the reduction in concentration with time is constant and independent of concentration) with rates

that differ primarily by the distance that a particle must traverse to return to the trachea.

Based on studies of particle clearance reported by Raabe (1984), muco-ciliary transport in the nose and throat generally exhibits a half life for clearance of 4 minutes. Clearance of the tracheo-bronchial section of the respiratory tract is a function of the distance from the trachea and generally varies from a half life of 30 minutes for the largest bronchi to approximately 5 hours for the smallest and most remote bronchi. In healthy humans, material deposited in this region is generally cleared within 24 hours. In contrast, the clearance mechanisms operating in the deep lung, beyond the muco-ciliary escalator, operate over time frames of many days to years (see Table 7-2);

- clearance of insoluble particles from the pulmonary portion of the lung occurs primarily by macrophage transport and such transport has several components. One component represents the population of "free" macrophages located within the alveoli that engulf particles and transports them to the muco-ciliary escalator. Macrophages are also renewed at some rate of recruitment that may be dependent on particle concentrations. In fact, numerous studies have demonstrated that macrophage recruitment is induced by the deposition of asbestos and other particles in the lung (Section 7.3.5). Particles also migrate into the interstitium where another population of macrophages clears these particles to lymph. This second component (interstitial clearance) is much slower than the first (see Table 7-2);

- each macrophage can carry a maximum load and the mobility of each macrophage decreases with increasing load. At sufficient loading, macrophages become immobile and aggregates of overloaded macrophages in the alveoli may then sequester particles for some period of time as this clearance mechanism is shut down. In the interstitium, masses of immobile macrophages may trigger development of granulomas that sequester particles for extended periods of time by effectively preventing clearance of the particles within such tissue, at least until or unless the granulomas resolve. Thus, these models incorporate overload mechanisms and the incorporation of such overload mechanisms are required to explain observed trends in experimental results; and

- in various published studies, overload (immobilization of laden macrophages) has been modeled as dependent on the total volume or mass of phagocytized material (for compact particles) and (additionally) on the length of phagocytized material (for fibers). It is also possible that the motility of macrophages and the

consequent overall rate of this clearance process is additionally a function of fiber diameter and/or particle toxicity (the latter for special cases).

Interestingly, while it is reported that large particles are not readily cleared by this mechanism, the range of sizes over which clearance becomes hindered corresponds reasonably well to the limits of overall respirability. In contrast, fibers that are clearly too long to be cleared by macrophages, if they are sufficiently thin, are quite respirable. Thus fibrous materials present a unique challenge to the respiratory tract based solely on the dimensions of these materials.

Stober et al. (1993) also notes that many models incorporate the assumption that most clearance processes are first order (i.e. that the rate of reduction of mass or fiber number is proportional to the remaining mass or fiber number, respectively, and independent of other factors) and that the combined effects of multiple clearance processes can therefore be expressed as a weighted sum of exponentials, has been fairly successful. This means, however, that the half-lives "$t_{1/2}$'s" attributed to the various first order decays are empirical and do not necessarily correspond to any specific physiological or biochemical features of the processes being modeled. Depending on the specific process, clearance rates may be zero order or may be a more complicated function of multiple variables than can be described by a first order decay. Nevertheless, models incorporating these simplifying assumptions have shown good success at adequately describing observed effects.

Note that half lives for first order decay processes represent the time required for half of the initial mass to decay (or be transported or whatever) and can be estimated as: $t_{1/2} = (\ln 2)/k$ with k being the first order rate coefficient or proportionality constant between rate and mass. This is why so many of the retention studies cited above provide estimates of a series of decay constants or half-lives that are assumed to correspond approximately to the major clearance processes contributing to the observed, overall reduction in concentration.

Due to the complexity of the processes involved, only a small number of dynamic models for fiber retention have been developed. Interpretation of the results of these models requires that the meaning of the term "retention" first be reconciled across studies.

- Dement and Harris (1979) report that, based on a mathematical model, the fraction of structures retained in the deep lung is unlikely to vary by more than a factor of 2 for different asbestos mineral types. In this study,

however, the term retention appears to refer primarily to a very short time period that primarily includes consideration of deposition but not clearance processes;

- Using a definition for retention that reflects long-term residence in the lung, Yu et al. (1990a) developed a model of chrysotile retention that explicitly incorporates longitudinal splitting, dissolution, and size-dependent clearance. Time-dependent lung burden estimates derived using the model were shown to compare reasonably well with published data (Abraham et al. 1988, as cited by Yu et al.) both in terms of fiber concentrations and fiber size-distributions.

- In a later modification of their retention model for chrysotile, Yu et al. (1991) also considered the effect of airway asymmetry on fiber retention. In this version of the model, Yu and coworkers incorporated information concerning the geometry of the bronchio-alveolar tree (including mean distance and the mean number of airway bifurcations between the trachea and the alveoli in each section of the lung) and studied the effects of such considerations. The modified model predicts a non-uniform distribution of the asbestos that is retained in the lung and the predictions reasonably reproduce the distributions observed by various researchers and measured formally by Pinkerton et al. (as cited by Yu et al.).

- Yu et al. (1990b) also modeled the long term retention of amosite in rat lungs. In contrast to the models employed for chrysotile, the model presented for amosite incorporates a term for the clearance rate that is not a constant but, rather, is a function of the lung concentration of asbestos, which was adapted from an earlier model for diesel soot. This modification was incorporated to adequately mimic the suppression of clearance with increasing lung burden that has been observed by several research groups (e.g. Wagner et al. 1974 or Davis et al. 1978) for amphiboles. Conditions under which elevated asbestos (or dust) concentrations are observed to reduce clearance are referred to as "overload" conditions. Model predictions were shown to reasonably reproduce the time-dependence of amosite lung burdens (in terms of mass) in several studies.

Importantly, the overload conditions addressed in the Yu et al. (1990b) model were primarily observed among older retention studies where lung burden was tracked as total asbestos mass (Section 7.2.1). Such studies

tend to suggest a difference in the behavior of chrysotile and the amphiboles. As indicated in Section 7.2.1, however, later retention studies, which track lung burden as a function of fibers number (in specific size categories) tend to show this effect is a function of fiber length more than fiber type and newer models may need to incorporate such factors that indicate reduced macrophage motility as a function of fiber length.

Moreover, it is important to consider the major, confounding effects, if the goal is to develop a model that not only reproduces the time-dependence of clearance but also captures relevant physical phenomena. Thus, for example, Yu et al. (1994) were able to reproduce the time-dependence of the retention in rats of inhaled RCF-1 (as a function of fiber size) using a model in which macrophage motility was limited only be total lung burden and not dependent on fiber size. However, these authors also failed to consider that long RCF-1 fibers in fact dissolve at rates competitive with the clearance of short fibers (see Section 7.2.1), which is probably why they did not find a dependence on length; the two effects cancelled out.

7.2.6 General Conclusions Regarding Deposition, Translocation, and Clearance

The current literature on deposition, translocation, and clearance paint a consistent picture of the fate of fibrous structures in the lung. The ultimate fate of biodurable fibers depend overwhelmingly on their size. Although there may be additional effects due to mineralogy (addressed further in Section 7.3) and for rare, special cases this may be important: generally such effects appear to be minor.

The primary effect attributable to mineralogy that is important to consider in relation to clearance is that associated with biodurability. Fibers that dissolve in the lung at rates that are competitive with the other clearance mechanisms described below may be cleared sufficiently rapidly to preclude adverse effects, even when such fibers are too long to be cleared efficiently by macrophages (see Section 7.2.1).

A schematic representation of the complex set of mechanisms that contribute to the translocation and clearance of fibrous structures that have been deposited in the deep lung is presented in Figure 7-4. This description was developed based on the complete spectrum of observations reported in each of the previous sections of this Chapter including, primarily, the descriptions of the most sophisticated of the models reviewed by Stober et al. (1993).

As shown in Figure 7-4, briefly, the first reaction to the introduction of fibers (or other particulate matter) into the alveolar lumen is scavenging by alveolar macrophages. It has been reported that the initial uptake by macrophages is a rapid process that is essentially complete within hours after initial deposition. Rates for several of the mechanisms depicted in Figure 7-4 have been estimated in the literature and are summarized in Table 7-2.

FIGURE 7-4

FIGURE 7-4, PAGE 2

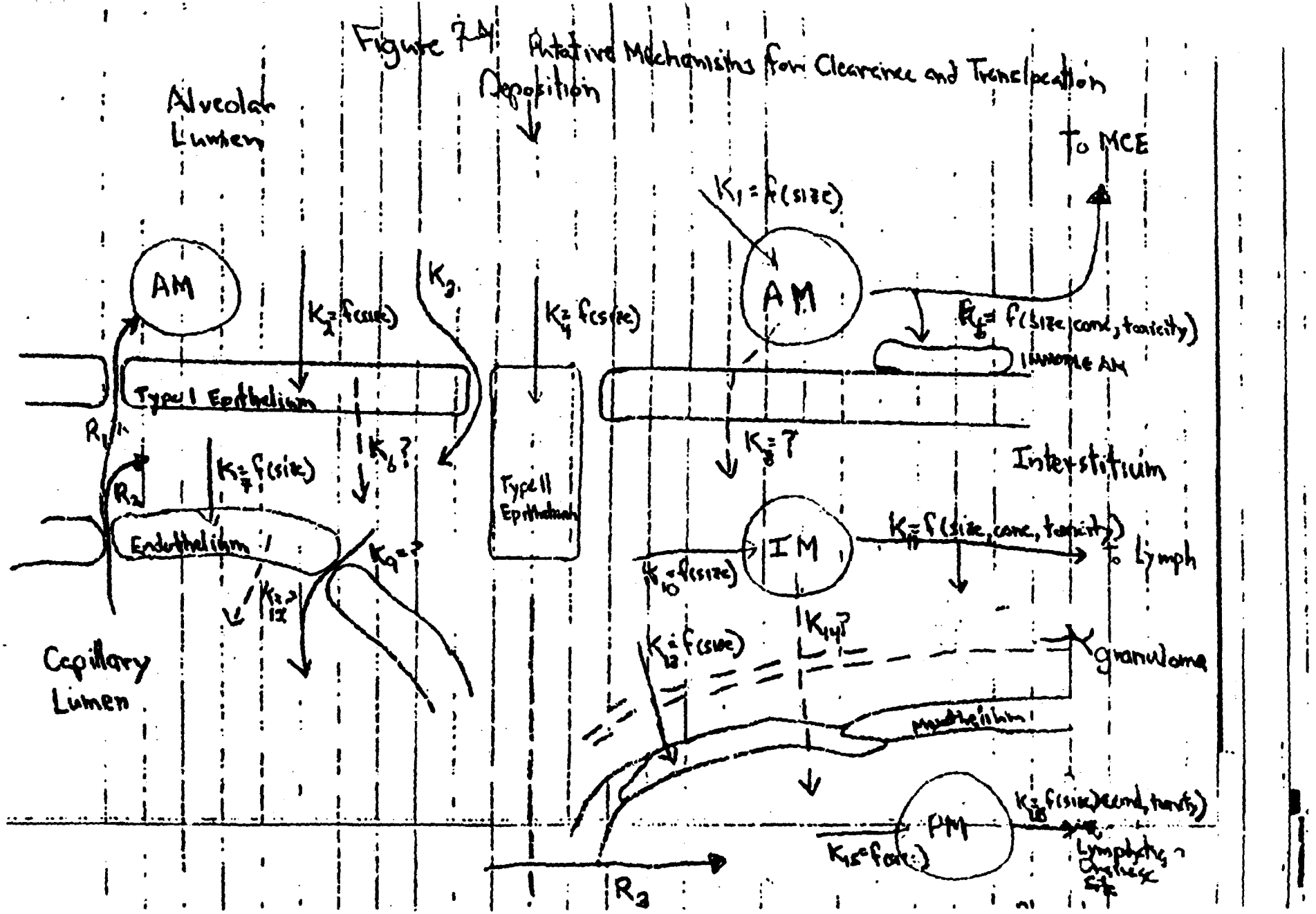
Figure 7-4: Putative Mechanisms for Clearance and Translocation
Alveolar Lumen
Deposition
To MCE
AM
AM
Type I Epithelium
Type II Epithelium
Endothelium
Interstitium
IM
PM
Capillary Lumen
granuloma
to Lymph
Lymphatics
R1
R2
R3

Figure 7-4 (cont., page 2 of 4)
Key for Putative Mechanisms for Clearance and Translocation of Fibers in the Lung

K_1 = rate constant for phagocytosis of fibers by alveolar macrophages. This mechanism is an inverse function of fiber length and, likely, diameter. This mechanism is likely pseudo first order (assuming sufficient numbers of macrophages, the rate will be proportional to the number of fibers);

K_2 = rate constant for phagocytosis of fibers by Type I epithelial cells. This mechanism is an inverse function of fiber length and, likely, diameter. This mechanism is likely pseudo first order;

K_3 = rate constant for diffusion of fibers from the alveolar air space (lumen) through the epithelial lining to the underlying interstitium. This mechanism is diffusion limited and likely independent fiber size or type. This mechanism likely parallels the behavior of diffusion in through a finite, column of fixed diameter **CHECK THIS**;

K_4 = rate constant for phagocytosis of fibers by Type II epithelial cells. This mechanism is an inverse function of fiber length and, likely, diameter. This mechanism is likely pseudo first order;

K_5 = rate constant for transport by macrophage to the muco-ciliary escalator. This mechanism is likely an inverse function of fiber length and the volume (or mass) of the fibers phagocytized. Macrophages that become immobilized tend to aggregate in alveolar lumena. For macrophages with fixed loads, this mechanism may be first order or zero order **CHECK THIS**;

K_6 = rate constant for putative discharge to interstitium of phagocytized fibers by Type I epithelial cells. There has been no direct verification of this mechanism;

K_7 = rate constant for phagocytosis of fibers by endothelium. This mechanism is an inverse function of fiber length and, likely, diameter. This mechanism is likely pseudo first order;

K_8 = rate constant for putative mechanism in which fibers internalized by macrophages are transported through the epithelial lining of the alveolar space to the underlying interstitium. There has been no direct verification of this mechanism;

K_9 = rate constant for diffusion of fibers from the interstitium through the endothelial lining to the enclosed, capillary lumen. This mechanism is diffusion limited and

Figure 7-4 (cont., page 3 of 4)
Key for Putative Mechanisms for Clearance and Translocation of Fibers in the Lung

likely independent fiber size or type. There has been no independent verification of this mechanism;

K_{10} = rate constant for phagocytosis of fibers by interstitial macrophages. This mechanism is an inverse function of fiber length and, likely, diameter. This mechanism is likely pseudo first order (assuming sufficient numbers of macrophages, the rate will be proportional to the number of fibers);

K_{11} = rate constant for transport by macrophage from the interstitium to the lymphatic system. This mechanism is likely an inverse function of fiber length and the volume (or mass) of the fibers phagocytized. Macrophages that become immobilized tend to induce formation of interstitial granuloma. For macrophages with fixed loads, this mechanism may be first order or zero order **CHECK THIS**;

K_{12} = rate constant for putative discharge to capillary lumena of phagocytized fibers by endothelial cells. There has been no direct verification of this mechanism;

K_{13} = rate constant for phagocytosis of fibers by mesothelial cells of fibers transported to the mesothelium. This mechanism is an inverse function of fiber length and, likely, diameter. This mechanism is likely pseudo first order;

K_{14} = rate constant for putative mechanism in which fibers internalized by macrophages are transported from the interstitium through intervening tissue and the mesothelium to the pleural space. There has been no direct verification of this mechanism;

K_{15} = rate constant for phagocytosis of fibers by pleural macrophages. This mechanism is an inverse function of fiber length and, likely, diameter. This mechanism is likely pseudo first order (assuming sufficient numbers of macrophages, the rate will be proportional to the number of fibers);

K_{16} = rate constant for transport by macrophage to sites of lymphatic drainage (lymphatic ducts) along the pleura. This mechanism is likely an inverse function of fiber length and the volume (or mass) of the fibers phagocytized.For macrophages with fixed loads, this mechanism may be first order or zero order **CHECK THIS**;

Not shown: apparently fibers that are too large to pass through lymphatic ducts attract accumulation of macrophages at sites of lymphatic drainage (Kane and McDonald (1993).

Figure 7-4 (cont., page 4 of 4)
Key for Putative Mechanisms for Clearance and Translocation of Fibers in the Lung

R_1 = rate constant for the renewal of the alveolar macrophage population. While the there is likely a steady state rate for background renewal, given that the average life of an alveolar macrophage is reported to be on the order of seven days (REF), this rate is also stimulated in response to insult by foreign substances in the lung;

R_2 = rate constant for the renewal of the interstitial macrophage population. While the there is likely a steady state rate for background renewal, this rate is also expected to be stimulated in response to insult by foreign substances in the lung;

R_2 = rate constant for the renewal of the interstitial macrophage population. While the there is likely a steady state rate for background renewal, this rate is also expected to be stimulated in response to insult by foreign substances in the lung;

R_3 = rate constant for the renewal of the interstitial macrophage population. While the there is likely a steady state rate for background renewal, this rate is also expected to be stimulated in response to insult by foreign substances in the lung;

The rate of removal (to the muco-ciliary escalator) by alveolar macrophages is then determined by a variety of effects. Macrophage motility is a size dependent-process so that only fibers that are sufficiently compact (< ~20 μm) can be removed from the lung. The rate of removal by this process may also be suppressed both for fibers of intermediate lengths (10 - 20 μm, which are short enough to be phagocytized but long enough to suppress macrophage motility) and by the overall mass/volume of particles deposited (and, proportionally, taken up by each macrophage). Note that the dimensions provided are the ones that are apparently appropriate for humans. For rats, the corresponding dimensions may be somewhat smaller.

Likely competing with scavenging by macrophages are (1) phagocytosis by the epithelial cells lining the alveolus and (2) diffusive transport to the intersititium. Both Type I and Type II epithelial cells appear to phagocytize fibers. Although relatively few fibers are observed to be taken up by Type II cells, as previously discussed (Section 7.2.2), one possible explanation for the limited observation of fibers in Type II cells is that uptake of fibers induces terminal differentiation to Type I cells. It is expected that phagyctosis by epithelial cells is a size-dependent process.

Especially when the presence of fibers (or other particulate matter) induces morphological changes in Type II cells that increase the overall permeability of the epithelial lining (Section 7.3.7), fibers can apparently diffuse into the interstitium. This process, potentially supplemented with expulsion of phagocytized fibers by epithelial cells and/or transport of fiber laden macrophages through the epithelial lining, represents the set of putative mechanisms by which fibers may reach the interstitium. It is expected that these processes are somewhat slower than uptake by alveolar macrophages (see Table 7-2). Therefore, if this latter mechanism is operating at peak efficiency, relatively few fibers may reach the interstitium. Note that diffusive transport is likely independent of fiber length, but may be dependent on fiber width with thinner fibers more rapidly diffusing to the interstitium.

Fibers reaching the interstitium are likely cleared primarily by interstitial macrophages, which phagocytize the fibers and transport them to the lymphatic system. Both the efficiency of phagocytosis and motility of macrophage transport in the interstitium likely depend on fiber size and the total volume/mass of fibers in the same way described above for transport by alveolar macrophages. However, all such mechanisms are substantially slower in the interstitium than in the alveolar lumen (see Table 7-2).

Macrophages that have been immobilized (due to fiber size or volume/mass) in the interstitium tend to aggregate and induce formation of granulomas, which may sequester the fibers in these cells. Although there is less evidence for this, fibers free

in the interstitial matrix might also trigger such a process. Such fibers would typically be too large to have been effectively phagocytized by any of the cells of the interstitium.

Fibers may also reach the endothelium and be taken up by endothelial cells lining the capillaries of the deep lung. Because fibers have also been observed in capillary lumena, mechanisms similar to those described for transport through the alveolar epithelium to the interstitium may be operating to transport fibers into capillary lumena. While it is expected that such mechanisms will also show size dependence similar to that previously described, little is known about the details or the rates of such processes.

Also by mechanisms similar to some or all of the putative mechanisms described for translocation of fibers from the alveolar lumen to the interstitium, fibers may reach the pleura. Whether fibers can also reach the pleura via transport in blood or lymph has not been definitively determined. Fibers reaching the pleura may be phagocytized by mesothelial cells or may pass through such cells to the pleural cavity. Fibers reaching the pleural cavity are apparently phagocytized by pleural macrophages (probably showing a similar size or volume/mass effect as described above for similar mechanisms) and are apparently transported to (and deposited at) sites of lymphatic drainage along the pleura. If such fibers are then too large to pass through the lymphatic ducts, they may trigger accumulation of additional macrophages and other inflammatory cells.

Overall, the effects of size appear to be:

- few fibers thicker than approximately 0.7 μm and virtually none thicker than approximately 1.5 μm appear to reach the deep lung. Of these, the longer the fiber, the thinner the fiber. Importantly, the distribution of sizes of structures deposited in the deep lung tend to be much more similar across studies than the distributions in the aerosols originally inhaled. Thus, deposition is a very effective filtering process; and

- short fibers (or compact particles) that are shorter than somewhere between 10 and 20 μm tend to be taken up almost entirely by macrophages and are either cleared via the muco-ciliary escalator, isolated in immobilized macrophages that remain within alveolar lumena, or transported to lymphatics (presumably after first reaching the interstitum). These processes appear to be efficient for the shortest of the fibers in this range (and all shorter fibers) so that no further effects are manifest. In contrast, longer fibers, which are not efficiently cleared or

isolated by macrophages either in the alveolar lumen or the interstitium appear to trigger a range of additional responses, some of which appear to lead to disease.

Therefore, based on deposition, translocation, and clearance, it is fibers thinner than approximately 0.7 μm and longer than a minimum of approximately 10 μm (with relative contributions increasing with increasing length up to at least 20 μm) that likely contribute to disease. Modifications to this range of structure sizes due to effects attributable to direct biological responses are addressed further in Section 7.3.

Regarding putative differences in behavior between chrysotile asbestos and amphibole asbestos, such effects are adequately addressed by the unifying discussion provided above. To make sense of such differences, the effects of fiber size must first be explicitly considered. Thus, chrysotile fibers may not be as efficiently deposited in the deep lung to the extent that they are curlier or occur in thicker bundles than amphibole fibers. The overall load of chrysotile deposited in the deep lung may also be cleared more rapidly than amphiboles to the extent that (1) short, thin fibrils ultimately represent a greater fraction of the total load of chrysotile than the amphiboles and (2) a subset of long chrysotile fibers, not sequestered in an environment with limited fluid flow, may be cleared more rapidly than similarly long amphibole fibers due to contributions from dissolution.

Importantly, the concentrations of asbestos to which humans are exposed are much lower than the concentrations to which animals were exposed in the various literature studies cited. Moreover, as indicated in Section 7.1.2, for virtually any exposure of interest, the resulting (volumetric or surface area) lung burden will be substantially higher in rats than in humans. Therefore, overload conditions or other processes that might impede or alter the clearance mechanisms described above, will never occur in humans without first having affected the results of the animal studies reported. Thus, conclusions concerning size-dependence and related effects (except to the extent that they need to be adjusted for cross-species differences) should remain valid when extrapolated between animals and humans.

7.3 FACTORS GOVERNING CELLULAR AND TISSUE RESPONSE

For inhaled structures that survive degradation and clearance, a series of complex reactions between the structures retained in the lung and surrounding tissue may induce a biological response. Asbestosis (fibrosis), pulmonary carcinomas, or mesotheliomas may result. Mesotheliomas are likely associated with structures that are translocated from the lung to the mesenchyme, although diffusable growth promoters

and other chemical signals produced by asbestos exposed cells in lung tissue immediately proximal to the mesothelium may also play a role (see Adamson 1997, as described in Section 7.3.4.1).

That the specific biochemical triggers for asbestos-related diseases have not been definitively delineated as of yet is not surprising. Despite great progress in elucidating candidate mechanisms, the number of candidate mechanisms is large and confounded by "cross-talk" between mechanisms. Moreover, similar toxic end points may result from entirely independent mechanisms that exhibit disparate dose-response characteristics but, nevertheless, may be triggered by the same or similar toxins. In such cases, however, the relative contributions from each mechanism to a particular end point may vary substantially. Unfortunately, the ability to compare results across studies of different mechanisms is currently limited due to the inability to reconcile the quantitative effects of dose and response across dissimilar studies.

Table 7-5 illustrates the range and complexity of the biological responses triggered by asbestos in lung tissue. The table was developed based on the information gleaned from the studies described in this Section. Importantly, not all of the mechanisms listed contribute equally to the toxic end points that are attributable to asbestos, but their relative importance has yet to be entirely delineated. The toxic end points of potential interest to which each of the listed mechanisms potentially contribute are indicated in bold italics.

As indicated previously (Section 7.0), although much has been learned about specific components of the underlying mechanisms by which asbestos causes the above-listed diseases, substantial knowledge gaps remain. Moreover, because of these gaps, multiple candidate effects have been explored as potential contributors to carcinogenicity (or fibrogenicity) and one of the goals of this document is to distinguish among those effects that are likely to contribute to the induction of cancer from those that are less likely or unlikely to contribute (given the current state of knowledge). Accordingly, an overview of recent studies is presented below following a brief description of the current model of the general mechanism for cancer. Note that, due to the availability of several recent reviews (including, for example, Floyd 1990, Kamp et al. 1992, Kane and McDonald 1993, Economou et al. 1994, Oberdorster 1994, Mossman et al. 1996, Mossman and Churg 1998 and Robledo and Mossman 1999), only the most recent primary articles are included in the following review.

Also, as indicated below, many of the biological responses provoked by retained asbestos are in fact dependent on fiber size and type. Therefore, studies that distinguish among effects induced by different size fibers (or fibers and non-fibrous

particles) of the same mineralogy and studies that distinguish among effects induced by comparably sized fibers (or non-fibrous particles) but differing mineralogy are highlighted. However, due to the limits with which fibrous materials have tended to be characterized in many of these studies, the database from which to distinguish among the effects of size and mineralogy are limited and conclusions from differing studies must be compared with caution.

Table 7-5, Page 1

Table 7-5:
Putative Mechanisms by Which Asbestos May Interact with Lung Tissue to Induce Disease Following Inhalation

Asbestos (in vivo):

- generates reactive oxygen species (ROS)
  - may affect neighboring cells and tissues
- interacts with macrophages
- interacts with lung epithelium

Asbestos interacts with macrophages:

- induces generation and release of reactive oxygen species/reactive nitrogen species (ROS/RNS)
  - may affect neighboring cells and tissues
  - may induce inflammatory response ***(which may promote cancer)***
  - may induce fibrogenesis ***(which may promote cancer)***
  - induces signaling cascades in macrophages and neighboring tissues
    - mediates apoptosis ***(which may regulate cancer)***
    - mediates proliferation ***(which may promote cancer)***
  - causes genotoxic effects in neighboring tissues
    - ***may cause cancer initiation***
    - may induce arrest of cell cycle
    - induces signaling cascades
      - mediates apoptosis ***(which may regulate cancer)***
      - mediates proliferation ***(which may promote cancer)***
  - depletes reserves of antioxidants in macrophages and neighboring tissues
    - may induce cytotoxicity ***(which may promote cancer, by inducing proliferation)***
    - may increase susceptibility to insult by other toxic agents ***(which may promote cancer)***
- induces release of various cytokines
  - affects neighboring cells and tissues
  - mediates inflammatory response ***(which may promote cancer)***
  - mediates fibrogenesis ***(which may promote cancer)***
  - induces signaling cascades in macrophages and neighboring tissues
    - mediates apoptosis ***(which may regulate cancer)***
    - mediates proliferation ***(which may promote cancer)***
  - mediates proliferation in neighboring tissues ***(which may promote cancer)***
- induces signaling cascades and mediates apoptosis in macrophages ***(which may regulate cancer)***
- at high enough concentrations, promotes cytotoxic cell death ***(which may promote cancer by inducing proliferation)***

Asbestos Interacts with Lung Epithelium:

- induces release of reactive oxygen species/rreactive nitrogen species (ROS/RNS)
  - may affect neighboring cells and tissues
  - may induce inflammatory response ***(which may promote cancer)***
  - may induce fibrogenesis ***(which may promote cancer)***
  - induces signaling cascades in epithelium and neighboring tissues
    - mediates apoptosis ***(which may regulate cancer)***
    - mediates proliferation ***(which may promote cancer)***
  - causes genotoxic effects in epithelium and neighboring tissues
    - ***may cause cancer initiation***
    - may induce arrest of cell cycle
    - induces signaling cascades
      - mediates apoptosis ***(which may regulate cancer)***
      - mediates proliferation ***(which may promote cancer)***
  - depletes reserves of antioxidants in epithelium and neighboring tissues
    - may induce cytotoxicity ***(which may promote cancer by inducing proliferation)***
    - may increase susceptibility to insult by other toxic agents ***(which may promote cancer)***
- induces release of various cytokines
  - affects neighboring cells and tissues
  - mediates inflammatory response ***(which may promote cancer)***
  - mediates fibrogenesis ***(which may promote cancer)***
  - induces signaling cascades in epithelium and neighboring tissues
    - mediates apoptosis ***(which may regulate cancer)***
    - mediates proliferation ***(which may promote cancer)***
  - mediates proliferation in epithelium and neighboring tissues ***(which may promote cancer)***
- causes genotoxic effects
  - ***may cause cancer initiation***
  - may induce arrest of cell cycle
  - induces signaling cascades
    - mediates apoptosis ***(which may regulate cancer)***
    - mediates proliferation ***(which may promote cancer)***
- induces signaling cascades
  - mediates apoptosis ***(which may regulate cancer)***
  - mediates proliferation ***(which may promote cancer)***
- increases epithelial permeability
  - encourages fibrosis ***(which may promote cancer)***
  - facilitates translocation
- at high enough concentrations, promotes cytotoxic cell death ***(which may promote cancer by inducing proliferation)***

Table 7-5, Page 2

A large body of evidence supports the conclusion that it is primarily (if not exclusively) long fibers (those longer than a minimum of 5 to 10 μm) that contribute to disease (see Sections...7.2.1, 7.2.2 and 7.4). Much evidence also indicates that the potency of long fibers increases with length at least up to a length of approximately 20 μm. Therefore, because short and long fibers are both respirable (for fibers that are sufficiently thin, less than approximately 0.7 μm in diameter), differences in the ultimate response to short and long fibers must be attributable to differences in tissue and cellular responses to the retained fibers in each size range.

At least at a histopathological level, clear differences have been observed in the responses evoked by short and long structures (see Sections 7.2.1. and 7.2.2). It is a goal of this section to determine whether the biochemical triggers that mediate the disparate responses to short and long fibers can also be identified. Unfortunately, while a large body of knowledge has been amassed, definitive conclusions are not yet possible. This is because the specific mechanisms by which asbestos acts have still not been definitively determined, although many candidate mechanisms have been elucidated (see above). However, important inferences can still be gleaned from the available studies.

Evidence for the relationship between fiber diameter and disease is somewhat less clear. Although there appears to be a fairly sharp cutoff in the diameter of fibers that are respirable (see Section 7.1.4), several studies suggest that the most potent fibers are substantially thinner than the sharp cutoff in respirability (see Section 7.4). If these latter observations are valid then, as with length, differences in the ultimate response to thick and thin fibers must be attributable to differences in the tissue and cellular responses elicited by retained fibers of each width. As indicated with length, however, definitive conclusions regarding biochemical triggers and the effect of size on such triggers are not yet possible because the specific triggers that lead to specific asbestos-related diseases have not been definitively identified. Still, useful inferences can be developed.

7.3.1 The Current Cancer Model

The following description of the current model for cancer is derived from the ideas presented in Moolgavkar et al. 1988, Mossman 1993, and Economou et al. 1994.

In the current model of cancer, normal cells must accumulate specific, multiple mutations before a tumorigenic cell is created that can lead to the development of cancer. Each successive mutation produces an initiated cell (a cell that is transformed from normal cells because it incorporates one or more of the requisite mutations, but

that has not yet acquired all of the changes needed to produce cancer). Each initiated cell may then proliferate to generate a population of similarly initiated cells, which increases the probability that other events will lead to further mutation in at least one of these cells. Individual mutations may occur spontaneously or may be induced by exposure to mutagens.

Generally, the minimum, heritable changes required before a normal cell is transformed into a metastatic tumor cell include, but may not be limited to (see, for example, Hei et al. 1997 or Kravchenko et al. 1998):

- escape from terminal differentiation or programmed cell death (especially in response to DNA damage);
- escape from anchorage/neighbor dependent growth inhibition;
- development of self-promoting growth and proliferation; and
- active expression of cytokines needed to promote angiogenesis and allow tissue invasion.

It is not clear whether the mutations associated with these changes need to occur in a particular order, although the first of the above-listed changes would facilitate accumulation of all later changes. It is also unclear which of the above changes contribute to the time dependence of tumor development and this may vary among tumor types. It is likely that only a subset of the required mutations determine the ultimate time development of the associated cancer. For example, once a cell begins self-promoting growth, later mutations (even relatively rare ones) may become incorporated rather quickly. Also, some mutations may be rare or may require intervention by a toxic agent, while other mutations may occur spontaneously and may thus occur frequently, once a sufficient number of initiated precursor cells are generated. This is one of the reasons that models with as few as one or two stages have proven successful at predicting the time course of many types of cancer (see, for example, Moolgavkar et al. 1988).

To produce cancer, the mutations that occur must also be "heritable" meaning that they must be preserved and passed on to daughter cells during mitosis. Thus, it is not only necessary to cause alteration in the DNA of a cell (genetic damage), but the mechanisms by which the cell subsequently repairs such changes or prevents cell division (e.g. arrest of the cell cycle, programmed cell death, terminal differentiation) in the presence of such changes must also be defeated. Generally, if a cell proceeds

through DNA synthesis (in preparation for mitosis) before accumulated alterations to DNA are repaired, the sites of such alterations can lead to errors in replication during synthesis, which in turn result in permanent, heritable mutations in one or both of the daughter cells that are created from mitosis.

Toxic agents that (directly or indirectly) cause DNA alterations may contribute to the development of cancer by inducing one or more of the set of requisite mutations required for cancer to develop. In traditional parlance, such agents are termed "initiators". In addition, any toxic agent that enhances proliferation also facilitates the development of cancer both by increasing the probability of creating spontaneous mutations (due to errors that infrequently but unavoidably occur whenever DNA is synthesized in support of mitosis) and by increasing the numbers of any initiated cells that may be present, which may then serve as additional targets for initiators or may incorporate additional spontaneous mutations. Agents that facilitate the development of cancer by inducing proliferation are traditionally termed "promoters."

Multiple mechanisms have been identified by which both initiators and promoters may act. Initiators, for example, may react directly with DNA to cause genetic damage, or may induce generation of other reactive species (such as reactive oxygen species or reactive nitrogen species) that, in turn, react with DNA to cause genetic damage. In addition, fibrous materials may uniquely damage chromosomes by interfering with mitosis causing aneuploidy (incorporation of an incorrect number of chromosome copies in cells) and/or various clastogenic changes (alterations in the organization and structure of specific chromosomes).

Promoters may also induce proliferation via a variety of mechanisms. Cytotoxic agents, for example, may induce proliferation in a tissue by damaging or killing cells and thereby induce stem cells to proliferate to replace the damaged cells. Promoters may also induce release of various growth factors that, in turn, induce proliferation in targeted tissues. This may occur, for example, as part of the inflammatory response to tissue insult.

Promoters that are biopersistent (such as long asbestos fibers) or promoters that are continually reintroduced (through chronic, external exposure) may also chronically up regulate (or down regulate) certain cell signaling cascades that may contribute to cancer development in a variety of ways including: (1) activation of genes that mediate proliferation or production of various growth factors (including any of various oncogenes) or (2) suppression of genes that inhibit proliferation or growth (including any of various tumor-suppressor genes).

There is growing evidence that all varieties of asbestos fibers (and certain other fibrous materials) can act both as cancer initiators and promoters. However, the biological responses to these materials appear to vary in different tissues so that it may be important to separately evaluate the behavior of asbestos in specific tissues. Biological responses to varying fiber types also appear to vary, particularly in relation to a fiber's biopersistence (Sections 7.2.1 and 7.2.4). Accordingly, an overview of the generic evidence that specific types of asbestos may act as an initiator and, separately, as a promoter is reviewed below, followed by consideration of the more limited data suggesting tissue-specific variation in biological responses.

7.3.2 Evidence for Transformation

Several recent studies provide evidence that specific types of asbestos can induce transformation of cells in specific tissues (both lung epithelium and mesothelium) to create tumor cells. This provides further, confirmatory support for the whole animal studies in which cancer is induced by exposure to asbestos (see Sections 7.4).

- An immortalized but non-tumorigenic cell line of human bronchial epithelial cells (BEP2D cells) was transformed by a single exposure to 4 ug/cm^2 UICC chrysotile B (Rhodesian). Surviving cells (the treatment caused 18% cell death) went through several transformations including: altered growth kinetics, resistence to serum induced terminal differentiation, and loss of anchorage dependent growth, before becoming tumorigenic (Hei et al. 1997). Tumorigenicity developed in the various exposed cell lines over a period of several to 11 weeks following exposure. When injected into nude mice, secondary tumors developed with a latency of 8 to 10 weeks.

  The authors indicate that there were no mutations in these cells at either codon 12 or 13 or the ras gene (mutations that have sometimes been observed in asbestos-induced lung cancers. Also, because this cell line already contains alterations in genes for p53 (a protein that plays a role in cell-cycle control, among other things, see Table 7-6) and Rb (Table 7-6), the authors speculate that such changes are not rate controlling for transformation to cancer.

  It should also be noted that cultures of Type II cells have been particularly difficult to maintain due to the tendency of these cells to undergo terminal differentiation (to Type I cells) once they are removed from their natural environment in the epithelial lining of lung alveoli (see Leikoff and Driscoll 1993, as described in Section 4.4).

- Kravchenko et al. (1998) indicates that, unlike cultures of lung epithelial cells, in-vitro cultures of rat mesothelial cells tend to transform spontaneously to tumorigenic cells. The major changes that occur with time include: altered response to epithelial growth factor (from growth-proliferation inhibition by this factor to growth-proliferation stimulation), morphological changes (from polygonal epithelial-like cells to elongated fibroblast-like cells and, eventually, polynucleated cells exhibiting broad polymorphism), and multi-layered growth and an ability to grow as colonies and masses in semi-solid agar. Eventually, these cells become immortal and induce cancer when harvested and injected into other rats. The authors indicate that asbestos-induced transformations in such cultures proceed through identical stages but that they occur much more rapidly. For example, incorporation of the stimulating response to EGF occurs spontaneously at passages 9 or 10 but at passages 6 or 7 when induced by asbestos. Asbestos was applied at 5 ug/cm^2, which was noted to be sub-lethal (95% cell survival was noted at this rate of application).

- In a study in which p53 deficient mice were intrapleurally injected with UICC crocidolite (200 µg/week), Marsella et al. (1997) showed that p53 deficient mice exhibited substantially increased susceptibility to development of mesothelioma. In this study, 12.5% of homozygous mice (p53 deficient) developed mesothelioma and the rest died of lymphomas or hemangiosarcomas that develop spontaneously in these mice; 76% of heterozygous mice died of mesothelioma, and only 32% of wild-type mice (p53 competent) died of mesothelioma. The authors suggest that p53 deficient mice are susceptible to excess proliferation induced by crocidolite due to loss of control at the G1/S check point that is normally mediated by p53.

  In further confirmation of this hypothesis, Marsella et al. report in the same study that 7.5 µg/cm^2 of crocidolite applied to wild murine mesothelial cells in culture induced substantial apoptosis while p53-deficient cells were resistant to apoptosis. The authors also note that most of the p53-deficient cells are tetraploid (suggesting a loss of a spindle check point) while the wild type cells are all diploid.

Note that, although these studies suggest that asbestos alone can induce complete transformation of both lung epithelial cells and mesothelial cells, such studies must be evaluated with caution. In the case of the Hei et al. study, for example, the effects of the (asbestos-independent) mutations required to initially establish the immortal line of lung epithelial cells are not entirely known. Therefore, the response to asbestos of epithelial cells in vivo may be substantially different.

In the case of the Kravchenko et al. study, it is clear that mesothelial cells in vitro do not behave in the same manner as those in vivo; in vitro, they spontaneously transform to tumorigenic cells. This suggests that one or more growth inhibitory signals exist in vivo (which are absent in vitro) that are critical to maintaining the health of the mesothelium.

7.3.3 Evidence that Asbestos Acts As a Cancer Initiator

As indicated in a review by Jaurand (1997), historically, the status of asbestos as a mutagen was questioned, due primarily to the failure to produce detectable gene mutations in short-term assays. However, more recent studies provide clear evidence that asbestos (and other fibrous materials) can produce mutations. Moreover, fibrous materials may induce mutations by multiple mechanisms including, for example:

- direct interference with mitosis;
- production and release of reactive oxygen species (ROS); or
- production and release of reactive nitrogen species (RNS).

Of these, the most consistent, positive evidence that asbestos can act as a cancer initiator (that is, a genotoxin or mutagen) has been from assays designed to detect the kinds of genetic damage that result from interference with mitosis (Jaurand 1997). Although generation of ROS and RNS plays a clear role in mediating asbestos-induced disease, the direct link to a role of asbestos as an initiator is somewhat more tenuous (see Sections 7.3.3.2 and 7.3.3.3).

7.3.3.1 Interference with mitosis. Apparently, the physical presence of asbestos fibers can interfere with proper spindle formation and the function of other structural units required for mitosis (Jaurand 1997). This typically leads to aneuploidy (an incorrect number of copies of the chromosomes contained within a cell), development of micronuclei (fragments of chromosomes enclosed in a membrane that are isolated from the main nucleus of the cell), and has also been shown to lead to clastogenic effects (changes in the organization and structure of the chromosomes). Assays for these kinds of genetic alterations have consistently shown asbestos capable of inducing these effects.

Jaurand (1997) also indicates that:

- fibers must be phagocytized by the target cells before they can interfere with mitosis;

- once phagocytized, all asbestos types are observed to interfere with mitotic activity; and

- samples enriched in long, thin fibers enhance these effects. In contrast, short fibers do not appear to contribute to these effects.

Jaurand notes, however, that results related to fiber size have not been entirely consistent, primarily because not all studies have rigorously controlled for or even adequately characterized the sizes of the fibrous structures in test materials. Jaurand also notes that this mechanism is not dependent on the formation of reactive oxygen species or any other reactive free radicals.

Among studies that suggest that surface chemistry (or presumably fiber type) may not be an important factor in determining the degree to which asbestos (or other fibrous materials) interfere with mitosis, Keane et al. (1999), exposed cultured V79 cells (hamster lung fibroblasts) to untreated and HCl-treated chrysotile asbestos. The acid treatment substantially reduces the magnesium content on the surface of the chrysotile. The authors also noted a "small" effect on fiber size due to treatment (treated fibers showed a 20% excess of short fibers). Cells were exposed to doses ranging between 0.4 and 12.7 $\mu g/cm^2$ (each dose left in place for 24 hrs and then rinsed off). Cells were harvested after an additional 24 hrs and evaluated for cytotoxicity and the presence of micronuclei.

Results from the Keane et al. study indicate that untreated fibers were shown to be slightly more cytotoxic than treated fibers but both treated and untreated fibers were observed to increase the abundance of micronuclei in a similar, dose-dependent fashion. The induction of micronuclei appeared to saturate at approximately 35/1000 cells observed at an applied asbestos concentration of 40 $\mu g/cm^2$. In contrast, substantial cytotoxicity was only observed at the highest doses employed. The authors thus concluded that surface chemistry (at least in terms of magnesium content) does not appear to have a major affect on induction of micronuclei and that the observed genetic damage and cytotoxicity appear to occur through entirely independent mechanisms.

In other studies, cultured cells were assayed for a variety of genotoxic effects following exposure to a range of fibrous materials.

- For example, Dopp and Shiffmann (1998) dosed human amniotic fluid (HAF) cells or Syrian Hamster Embryo (SHE) cells with UICC amosite, Rhodesian

chrysotile, crocidolite, or ceramic fibers at concentrations of 0.5, 1.0, 5.0, and 10.0 μg/cm^2 and assayed the cultures for formation of micronuclei and a variety of clastogenic effects.

Based on their study, Dopp and Shiffmann report that all asbestos types induced formation of micronuclei in SHE cells in a dose-dependent fashion at rates that were significantly elevated over control animals. The effect appeared to saturate at doses between 1 and 5 μg/cm^2 and rates appeared to peak at between 48 and 66 hrs post exposure. Ceramic fibers, which were noted to be longer but thicker than the asbestos fibers tested, also showed significantly increased induction of micronuclei, but at rates less pronounced than for asbestos. However, it is difficult to judge whether this is due to differences in fiber type because the data in the paper are not adequate to distinguish effects of fiber size and number from effects of fiber type. Similar results were obtained with HAF cells, but overall rates were about one third those observed in SHE cells.

The authors also note observing various disturbance of chromatin structure during interphase. They report observing formation of chromatin bridges and chromosome displacements in meta and anaphases and impaired chromatin separation in mitosis. They also report that cytokinesis was frequently blocked.

In addition to the effects that they observed that are attributable to fiber interference with mitosis, Dopp and Shiffmann report observing a variety of clastogenic effects. In all cases where authors labeled specific regions of specific chromosomes, fiber-exposed cells showed significantly greater frequencies of DNA breaks over controls or gypsum-exposed animals. Different regions of various chromosomes also showed significantly different frequencies of breakage with patterns that were specific to the different fiber types. The authors hypothesize that the observed clastogenic effects may be due to production of reactive oxygen species, to formation of some type of clastogenic factor, or to the direct interactions between fibers and chromosomes during mitosis that are the apparent cause of the disturbances discussed in the previous paragraphs. However, It was not possible to distinguish among hypothetical causes of the observed clastogenic effects in this study.

- Kodama et al. (1993) exposed cultures of human bronchiolar epithelial (HBE) cells to asbestos (chrysotile at 0 to 4 μg/cm^2 and crocidolite at 0 to 300 μg/cm^2). They then examined cells at 24, 48, 72, and 96 hrs following exposure for cytotoxic effects and cytogenetic effects. Results indicate that both fiber types

induced concentration-dependent inhibition of cell proliferation and colony-forming ability but chrysotile was 100 to 300 times more toxic. The authors report this translates to a 40 fold increase in toxicity on a fiber for fiber basis (although the range of sizes included in this count is not indicated).

Kodama et al. also report that, at 72 hrs, chrysotile (4 $\mu g/cm^2$) caused a 2.7 fold increase in binuclei and a 1.6 fold increase in micronuclei. Over the same time interval, at 300 $\mu g/cm^2$, crocidolite caused a 1.9 fold increase in binuclei but did not cause micronuclei. They also report that chrysotile failed to produce significant numerical chromosome changes in HBE cells and increased structural aberrations only at the 24 hr time point. The frequency of neither aneuploidy or polyploidy was increased at any time point following exposure to asbestos in this study. The authors indicate that this contrasts with observations of relatively high incidences of asbestos-induced chromosome changes observed in some rodent cell cultures and clastogenic effects observed in human mesothelial cell lines. They further speculate that phagocytic cells with high mitogenetic activity are likely most susceptible to the effects of asbestos, which primarily interferes with mitosis. However, they suggest that epithelial cells that are exposed to fibers may undergo terminal differentiation (from Type II to Type I cells) and thus cease mitosis. This would effectively prevent adverse genetic effects from asbestos exposure. Such pathways are not available to mesothelial cells.

- Hart et al. (1994) studied the effects of a range of fiber types (with varying size distributions) on chinese hamster ovary (CHO) cells. The authors indicate that such cells are very different from cells in pulmonary tissues in that they are immortalized, aneuploid, undifferentiated, and preneoplasic. They also note that the responses observed in these cells differs from responses observed in cells from pulmonary tissues. Nevertheless, the implications concerning fiber size are instructive. Fibers evaluated included long, medium, short, and UICC crocidolite and chrysotile along with a range of manmade vitreous fibers (MMVF's), refractory ceramic fibers (RCF's), and fibrous glasses. Exposure concentrations ranged between 10 and 225 $\mu g/cm^2$.

  Results from the Hart et al. study indicate that all of the fibers caused qualitatively similar toxic effects: concentration-dependent reduction in cell numbers and an increase in the incidence of abnormal nuclei with little or no loss in viability. Fiber-induced cell death in CHO cells appears to be minor, even at relatively high exposure concentrations. Based on mean dimensions (which is problematic), the diameter dependence on the observed toxic effects, particularly on the formation of aberrant nuclei, was slight or absent. However, the effect

with length was striking. For lengths up to at least 20 μm, potency toward both cytotoxicity and the induction of aberrant nuclei increased dramatically with increasing length. The authors also note that the lack of an observed fiber composition associated effect on the toxicity of CHO cells does not correlate with findings from recent rodent inhalation studies using the same test fibers. The authors therefore speculate that CHO cells may not represent an appropriate in-vitro model for fiber effects. However, it may also be that effects in vitro occur over time scales that are rapid relative to those that occur in vivo so that biodurability is not important in vitro.

- In a study by Takeuchi et al. (1999) cultured human mesothelioma cells (MSTO211H) and, separately, cultured human promyelocytic leukemia cells (HL60), which are not phagocytic, were dosed with crocidolite between 0.6 and 6.6 μg/cm^2 (no size range indicated). Studies with latex beads confirmed that the mesothelioma cells are actively phagocytic but that the leukemia cells are not. The authors indicate that dosed mesothelioma cells showed significantly increased numbers of polynucleated cells, tetraploid cells, and cells with variable DNA content at the G0/G1 transition in the cell cycle and that the extent of effects was dose-dependent. Leukemia cells showed no such effects.

  The authors further indicate that, when the mesothelioma cells were sorted by fiber content, those with the highest fiber content showed the greatest effects. The authors also indicate that cells are stimulated neither to release superoxide nor NO at the concentrations of crocidolite studied. However, they hypothesize that intracellular ROS may have been generated because they report finding increased levels of 8-OH-dGua (and oxidized form of one of the DNA bases) following crocidolite exposure. Nevertheless, the authors conclude that the mechanisms by which crocidolite induce cytotoxicity and, potentially, carcinogenicity is related to phagocytosis. Importantly, the effects described in the Takeuchi et al. study are entirely consistent with effects attributable to interference with mitosis, despite any speculation by the authors.

7.3.3.2 Generation of reactive oxygen species (ROS). ROS have been implicated as mediators in a variety of toxic effects (including cancer initiation) associated with a broad range of toxins (see, for example, Floyd 1990). Moreover, substantial evidence indicates that asbestos can induce generation of ROS by several mechanisms and that asbestos-induced ROS plays a role in several of the toxic effects attributable to asbestos (see below). However, whether ROS plays an important role in asbestos-associated cancer initiation is less clear and needs to be evaluated carefully. Therefore, evidence that asbestos induces the production of ROS and that ROS

contributes to the adverse health affects attributable to asbestos are reviewed below with particular attention to effects that may contribute to the initiation of cancer. Contributions by ROS to other asbestos-related toxic effects are also evaluated in later sections of this chapter.

Note, that generation of certain reactive nitrogen species (specifically the peroxinitrite ion) is closely associated with ROS generation so that evidence for the generation of certain reactive nitrogen species (Section 7.3.3.3) constitutes additional evidence for the generation of ROS.

Asbestos-Induced Generation of ROS

Asbestos has been shown capable of generating a variety of reactive oxygen species (ROS) including hydrogen peroxide (H_2O_2), superoxide ($O2^-$), and hydroxyl radical ($OH\bullet$) via several mechanisms (see, for example, Kamp et al. 1992, Jaurand 1997, Fubini 1997) including:

- catalytic production of superoxide from oxygen in aqueous solution;
- catalytic production hydrogen peroxide from oxygen in aqueous solution;
- catalytic production of hydroxyl radical by the Fenton reaction (degradation of hydrogen peroxide catalyzed by iron on the surface of fibers or mobilized from the surface of fibers);
- catalytic production of several ROS by redox cycling of iron on the surface of fibers or mobilized from the surface of fibers (Haber-Weiss type reactions);
- catalytic production of ROS by release of heme and heme protein from various cellular components;
- by inducing release of various ROS species from phagocytes during "frustrated" phagocytosis; and
- by binding to cell receptors, integrins for such receptors, or other features of surface membranes that trigger signaling cascades mediating the production and release of various ROS (and RNS).

For a general review of the chemistry involved in these processes, see Floyd (1990).

Fenton, Haber-Weiss, and related reactions. Most of the evidence for Fenton and Haber-Weiss reactions (and related free radical generating reactions) that take place on the surface of asbestos fibers comes from experiments in cell-free systems (see below) Therefore, their relevance to the conditions found in vivo may be limited. Moreover, the size of the fibers (especially in terms of their cumulative surface area) and the history of their surfaces (in terms of metal contaminants or coatings that might be present) may substantially alter the effects of such experiments (Fubini 1997). Unfortunately, however, few of the available studies report characterization of fiber sizes or surface conditions in sufficient detail to judge the importance of these effects.

For fibers:

- Zalma et al. (1987) evaluated a range of fibers (UICC crocidolite, UICC amosite, UICC Canadian and Zimbobwean chrysotile, industrial chrysotile, and magnetite) for their ability to produce free radicals by the direct reduction of oxygen in aqueous solution. In some cases, hydrogen peroxide was also added to the solution. Results indicate that all of the fibers tested were able to generate hydroxyl radicals (even in the absence of hydrogen peroxide) but that the efficiency of production was a strong function of the activation (by grinding) or pacification (by coating with benzene or other agents) of the fiber surface. Chrysotile was reported to be the most efficient at generating radicals and the authors assumed that this is due to iron contamination on the surface (since iron is not a component of the "ideal" chrysotile fiber). However, such conclusions are difficult to evaluate in the absence of simultaneous consideration of fiber size.

- Governa et al. (1998) evaluated the ability of wollastonite fibers to generate ROS in both a cell free system and a suspension of polymorphonucleocytes (PMN's). The fibers were observed to produce ROS in both systems and that ground wollastonite produced substantially more ROS than unground. The efficiency of ROS generation in PMN suspension is also reported to be greater for wollastonite than for either chrysotile or crocidolite (tested in previous studies). However, no size information is given. Based on additional work with various inhibitors added to the system, the authors also indicate that only a fraction of the ROS generated was composed of hydroxyl radicals.

- Brown et al. 1998 subjected several different fiber types (amosite, silicon carbide whiskers, RCF-1, and various fibrous glasses) to two standard chemical assays for free-radical production (in cell-free systems). The authors indicate that, of the fiber types tested, only amosite showed free radical activity significantly above

controls in both assays and only RCF-1 additionally showed significantly elevated free radical activity in one assay. However, there is not enough information provided in this study to determine whether the observed differences are due to differences in fiber sizes, sample preparation (i.e. surface condition), or fiber type. In apparent contrast, for example, Gold et al. (1997) report that amosite and crocidolite produce few free radicals in cell free systems, unless they are ground.

- Weitzman and Graceffa (1984) indicate that chrysotile, crocidolite, and amosite are all capable of catalyzing the generation of hydroxyl radicals and superoxide from hydrogen peroxide in vitro and that, based on experiments with various iron chelators, these reactions are iron dependent. The authors further indicate that hydrogen peroxide is produced in large quantities as a normal bi-product of tissue metabolism, but that it is effectively scavenged by various enzymes. The authors speculate that, by physically damaging cell membranes, asbestos may allow release of the precursor hydrogen peroxide before it can be scavenged.

For particles:

- Silica, residual fly ash, and ambient air dusts also can create ROS in vitro and the efficiency of production correlates with ionizable concentrations of various transition metals complexed on the dust (Martin et al. 1997). In vivo, such metal containing particles also cause release of ROS from macrophages (Martin et al. 1997). Additionally, binding of silica to plasma membranes of airway lung cells and phagosomes provokes generation of ROS.

- Castronova et al. (1997) further indicate that it is the concentration of contaminating iron on the surface of freshly fractured quartz that enhances free radical production in aqueous solution (in cell free systems). These authors also showed that high iron-containing (430 ppm) quartz dust inhaled by rats (at 20 mg/m^3 for 5 hrs/day for 10 days) induced five times more leukocyte recruitment, two times more lavageable red blood cells, 30 to 90% increase in macrophage production of ROS, 71% increase in nitric oxide production by macrophages, and 38% increase in lipid peroxidation of lung tissue than observed in rats exposed to low iron-containing (56 ppm) quartz.

Although iron is required for the reactions considered here, studies indicate that the iron content of the fiber itself is not a good indicator of reactivity (Gold et al. 1997). Studies also indicate that the iron that participates in these reactions need not originate with the fiber (Jaurand 1997, Fubini 1997) and biological systems contain abundant sources of

iron. Therefore, both iron-containing fibers and iron-free fibers have been shown to participate in these reactions in vivo.

Release of heme and heme protein. At least one research group (Rahman et al. 1997) indicates that heme and heme protein cause extensive DNA damage in the presence of asbestos in vitro and, based on previous studies, that this may involve heme catalyzed production of ROS following asbestos-induced release of heme from cytochrome P-450, from prostaglandin H synthetase (or perhaps from other heme containing proteins). Importantly, the authors indicate that such observations relate to a nuclear pool of heme, which suggests that ROS generation via this mechanism may occur in the immediate vicinity of DNA. The work by this group suggests at least one additional pathway by which asbestos may induce the production of ROS and by which ROS-mediated damage to DNA might occur.

Frustrated phagocytosis. Numerous studies indicate that long asbestos fibers (longer than somewhere between 10 and 20 μm) cannot be efficiently phagoycitized by macrophages (see, for example, Sections 4.4 and 7.2) and that macrophages that are damaged by such "frustrated" phagocytosis release ROS (see, for example, Mossman and Marsh 1991 or Kamp et al. 1992). Due to the differences in the size of macrophages across species (see discussion of Krombach et al. 1997 in Section 4.4) The minimum length beyond which phagocytosis may become frustrated may differ in different animals. However, it is clearly longer fibers that contribute to this mechanism for generating ROS. Shorter fibers (< 10 μm) are unlikely to cause frustrated phagocytosis in any of the mammalian species of potential interest.

- Lim et al. (1997) showed that alveolar macorphages in culture (after stimulation with lippopolysaccharide) generated free radicals (ROS) when subsequently exposed to chrysotile, crocidolite, or amosite (all UICC). They found chrysotile to be the most potent inducer of free radical activity (which is not surprising given that UICC chrysotile contains the highest fraction of long fibers of the UICC samples tested (Berman unpublished). Based on tests with various inhibitors, the authors indicated that the free radicals generated by the alveolar macrophages occurred through a pathway mediated by protein tyrosine kinase, phospholipase C, and protein kinase C and that the effects are dose-related.

- Kostyuk et al. (1998) cultured peritoneal macrophages and showed that treatment with chrysotile asbestos (1 μg, no size data given) resulted in production of frustrated phagocytosis and cell injury (the latter as evidenced by release of lipid dehydrogenase - LDH, a marker for membrane damage). By working with various chelators and flavonoids (natural plant products, some of

which quench superoxide and some of which chelate iron), the authors indicate that cell injury was likely induced by superoxide and that the superoxide was likely produced by an iron-dependent mechanism. Note that this contrasts with the above studies that suggests production of radicals by frustrated phagocytosis in culture is an iron-independent mechanism.

- At least for one kind of phagocyte: polymorphonucleocytes (PMN's), a study by Ishizaki et al. (1997) suggests that crocidolite and erionite may induce production of ROS from PMN's by each of two mechanisms. The first requires phagocytosis and may represent the traditional, "frustrated" phagocytosis pathway indicated above. The second pathway is triggered by an interaction between the fiber and the cell surface and is mediated by NADPH. The authors also cite evidence that chrysotile may similarly act through both of these pathways.

- Afaq et al. (1998) cultured alveolar macrophages and peripheral red blood cells (RBC's) that were harvested from rats 30-days following a single 5 mg intratracheal instillation of UICC crocidolite, UICC chrysotile, or ultrafine titanium dioxide. The authors indicate that populations of alveolar macrophages were significantly increased (over sham-exposed rats) for all three particle types and that acid phosphatase and lipid dehydrogenase (LDH), which are markers of cell membrane damage, were observed in cell-free lung lavage from animals exposed to all three particle types. Both alveolar macrophages taken from asbestos-exposed animals (both types) showed significantly elevated lipid peroxidation and hydrogen peroxide production over titanium dioxide exposed animals. However, the latter also showed elevated peroxidation and peroxide production that were significantly elevated over sham-exposed animals. Similar results were observed among RBC's from asbestos-exposed animals but not from titanium dioxide-exposed animals. Note, it is possible that ROS production induced by TiO_2 occurs by a different mechanism (or set of mechanisms) than that for asbestos (see, for example, Palekar et al. 1979, Section 7.3.4.4)

In-vivo evidence for asbestos-generated ROS. Several studies involving whole animals also indicate that asbestos exposure induces the generation of ROS. Importantly, in such studies, evidence for generation of ROS is generally determined based on observation of the putative effects of ROS, rather than ROS directly.

- Ghio et al. (1998) intratracheally instilled 500 µg of crocidolite (NIEHS) into rats. This was observed to induce a neutrophilic inflammatory response within 24 hours (in contrast to saline-exposed rats). The authors collected chloroform extracts from exposed lungs and subjected them to electron spin residence

(ESR) spectrometry. Results indicate the presence of a carbon-centered radical adduct that has a structure consistent with products of lipid-peroxidation. The radical signal was only observed in asbestos-exposed animals and persisted even after one-month following exposure. The authors also report that depletion of neutrophils did not affect the signal and that dextrin-induced inflammation did not produce the signal.

- Yamaguchi et al. (1999) studied effects in rat lung tissue at 1, 3, 5, 7, and 9 days following a single intratracheal instillation of 2mg of either glass fiber or UICC crocidolite. The authors indicate significantly increased levels of 8-OH-Guanine (an oxidized form of the DNA base Guanine) one day after crocidolite instillation and increasing repair activity for this oxidized form of guanine with time that became significant at days 7 and 9 following instillation. Glass fibers (noted to be non-fibrogenic and non-tumorigenic) did not produce either increases in 8-OH-Gua or its repair activity. The effects associated with crocidolite were all noted to be dose related.

Several of these studies also suggest distinctions in ROS generation (either the absolute generation of ROS or generation of specific ROS species by specific tissues) due to differences in fiber (or particle) size or type :

- Nehls et al. (1997) intratracheally instillled rats either with quartz (2.5 mg) or corundum (2.5 mg). The latter mineral is reportedly non-tumorigenic. Results indicate that lung epithelial cells in quartz exposed rats exhibited increased 8-oxo-Guanine levels (a DNA adduct generated by reaction with ROS, see above) that persisted for up to 90 days post exposure. Elevated levels of the DNA adduct appeared in all cell types in all areas of the lung. The authors suggest that the observed persistence of the elevated levels of 8-oxo-Guanine suggests that it was produced at a rate in excess of the lung's capacity for repair. The authors also report enhanced and persistent inflammation, cell proliferation, and an increase in neutrophil population in bronchio-alveolar lavage (BAL) fluid and an increase in in tumor necrosis factor alpha (TNF-α) in BAL fluid in the quartz exposed animals. TNF-α is a cytokine linked to a variety of effects including the recruitment of inflammatory cells (see Table 7-6) In contrast, exposure to corundum produced none of the effects observed with quartz.

- Timblin et al. (1998b) report that ROS induced responses by rat lung epithelial cells vary depending on whether exposure is to crocidolite, hydrogen peroxide, or cadmium chloride ($CdCl_2$). In response to ROS generation induced by the first two agents increase levels of cJun protein (a protooncogene, Table 7-6) and

crocidolite, but not hydrogen peroxide, causes elevation in the levels of manganese-containing superoxide (MnSOD) dismutase (an enzyme that catalyzes dismutation of superoxide, Table 7-6). Neither of these agents affect levels of either of two common stress proteins (Table 7-6): GRP78 or HSP72/73, nor do they affect cellular glutathione levels. In contrast, cadmium chloride does not alter MnSOD levels but increases levels of GRP78 and HSP72/73 in addition to cJun protein. Therefore, ROS-related mechanisms may be complex and may be toxicant-specific. Thus, it may not be correct to assume that all fibers and particles act through common ROS-related pathways.

- In contrast to the results of the above study (which showed no affect on glutathione levels), Golladay et al. (1997) showed that human lung epithelial cells (cultured A549 cells) exposed to crocidolite (NIEHS sample) showed substantial reduction in intracellular levels of glutathione (without increases in the oxidized forms of glutathione). Rather, an associated increase in extracellular, reduced glutathione was observed, suggesting that crocidolite induces release of glutathione from the interior of these cells to the environment. The authors also indicate that, given that the half-life for reduced glutathione outside of cells is on the order of an hour, while extracellular reduced glutathione levels remained elevated for more than 24 hrs following exposure, cells must have be releasing reduced glutathione continuously. Because no concomitant release of lipid dehygrogenase (LDH) or labeled adenine was observed (despite loading of cells with labeled adenine prior to the experiment), the authors conclude that release of glutathione is not associated with membrane disruption or apoptosis (which is induced to some degree by exposure to crocidolite). Also, all of the effects described above were similarly associated with exposure to de-ironized crocidolite. Thus, the iron content of the fibers does not play a role in this process.

- Kaiglova et al. (1999) intrapleurally injected rats with 10 mg of long amosite and collected bronchio-alveolar lavage (BAL) fluid 24 hours following exposure and at later time intervals. They indicate that total protein and alkaline phophatase (AP) were both elevated in BAL 24 hrs after exposure and that AP remained elevated for at least 3 mo following exposure. They also noted increased levels of lipid peroxides in BAL at 24 hrs but not 3 mo following exposure. The authors indicate that antioxidants were significantly decreased following exposure: glutathione was significantly decreased in lung tissue at both 24 hrs and 3 mo following exposure but was normal in BAL fluid at all time points; α-tokopherol and retinol were significantly decreased at 3 mo in lung tissue; and ascorbic acid was significantly decreased in both lung tissue and BAL at 24 hrs and remained

low at 3 mo. The authors indicate that decreases in antioxidants implies a role for ROS (or RNS) in lung tissue injury. It is also possible that the varied responses of specific antioxidants may suggest a role for toxin- and injury-specific ROS/RNS.

Note that the apparent difference in the reported effect of crocidolite exposure on intracellular glutathione levels in the above two studies might be due (individually or in combination) to differences in the cell-types studied, differences in the size distribution of the crocidolite employed, differences in study design, or other factors. Insufficient information is available to distinguish among these possibilities.

Conclusions concerning generation of ROS. Except for frustrated phagocytosis (which is unique to long fibers), ROS generation by the mechanisms discussed above are generally considered a common response to respiration of particles in general (see, for example, Martin et al. 1997 who suggest that ROS "...may be a global signaling mechanism mediating response to particulate insult mostly by activation of kinases and transcription factors common to many response genes." They further indicate that if the load of ROS generated is to great, or the airway in which it is generated has been previously impaired, "...these same mechanisms can result in deleterious respiratory lesions and outright pathology"). However, not all non-fibrous particles are similarly capable of inducing production of ROS. As indicated above, for example, while crystalline silica is a potent inducer of ROS production, carundum is not (Nehls et al. 1997). Moreover, the spectrum of ROS species that are induced by particular toxicants are generally specific to the offending toxicant (Timblin et al. 1998b). Therefore, the generic grouping of ROS mediated pathways by particles and, especially, by particles and fibers, does not appear justified. These mechanisms are more complex and individualized than such generic grouping suggests.

ROS can be generated by multiple pathways that are variously dependent on particle size, whether a particle is a fiber, fiber size, and particle or fiber type (i.e. chemical composition). The primary mechanism(s) through which is ROS generated in response to one type of particle or fiber may be very different than that through which ROS generation is induced by another and the resulting suite of ROS may also differ. Importantly, the relationship between dose and response for each mechanism may also differ (see, for example, Palekar et al. 1979, Section 7.3.4.4).

Given the above, comparing among the ability of fibrous materials and non-fibrous analogs to induce generation of ROS requires that such analogs be properly matched before valid conclusions can be drawn. Thus, for example, the appropriate non-fibrous analog for crocidolite is the massive habit of reibeckite and the appropriate analog for

chrysotile is the massive habit of antigorite or lizardite. Due to differences in both chemistry and crystal structure, crystalline silica is not an appropriate non-fibrous analog for any of the asbestos types. Moreover, because ROS can be generated by different mechanisms, critical comparison across analogs requires more than the simple confirmation that ROS is generated or even whether the relative efficiency with which ROS is generated is comparable. It is also necessary to contrast the specific complexion of ROS generated and the specific tissue/cellular environments (i.e. locations within a cell) in which they are generated in response to each analog.

It is also clear that ROS is generated by both iron-dependent and iron-independent pathways. Even for the iron-dependent pathways, however, the source of iron need not derive from the fibers or particles themselves. Therefore, since iron is abundant in vivo (and the environment), both iron-containing and iron-free fibers (or particles) can potentially participate in both the iron-independent and the iron-dependent pathways.

Effects Mediated by ROS

ROS have been implicated as mediators in a variety of toxic effects (including cancer initiation) associated with a broad range of toxins (see, for example, Floyd 1990, Martin et al. 1997). Cellular and tissue effects that have been associated with the effects of ROS include:

- enhancement of overall uptake of particles by epithelium;
- stimulation of inflammatory responses;
- stimulation of various signaling cascades and production of cytokines;
- inducement of apoptosis;
- cytotoxicity;
- mediation of cell proliferation;
- formation of oxidized macromolecule (including DNA) adducts; and
- induction of DNA strand breaks.

However, only the last two of the above list of ROS effects are potentially relevant to the initiation of cancer (the topic of this section). The other effects in the above list likely contribute to the induction of other asbestos-related diseases and may even promote (but not initiate) asbestos-related cancer. Thus, they are addressed further in later sections of this chapter (see below).

Although, ROS generation is associated with exposure to various particles and fibers (including all forms of asbestos), generation of ROS does not necessarily imply carcinogenesis. For example, Zhu et al. (1998) indicate that ROS generation is

induced in response to exposure to asbestos, crystalline silica, and coal mine dust. However, based on an extensive record of human exposure, the latter (coal mine dust) is not carcinogenic in humans. Therefore, evidence related to the last two of ROS-associated effects listed above, are examined in more detail below.

Several studies indicate that, once generated by exposure to asbestos, ROS can interact with DNA in vitro and in vivo to produce oxygenated adducts, primarily 8-oxo-Guanine. Of the studies reviewed above, for example, Yamaguchi et al. (1999) observed that crocidolite but not (non-tumorigenic) glass produced dose-dependent increases in 8-oxo-Guanine in rat lung tissue following intratracheal instillation. Also, Leanderson et al. (1988), Park and Aust (1998), Keane et al. (1999) indicate that asbestos induces formation of oxidized DNA adducts in in-vitro assays. Brown et al. (1998) indicate that asbestos induces ROS-mediated DNA strand breaks.

However, not all DNA strand breaks attributable to asbestos occur through pathways involving ROS. Ollikainen et al. (1999) exposed cultures of human mesothelial cells (MeT-5A, transfected with SV-40 but nontumorigenic) to hyrdrogen peroxide (100 μM) or crocidolite (2 - 4 $\mu g/cm^2$), either alone or in combination with TNF-α and performed assays for DNA strand breaks. The authors note that the concentrations of asbestos evaluated are well below those that have been associated with cytotoxic effects. Crocidolite alone was shown to produce DNA strand breaks at the concentrations tested. The authors also note that, at lower concentrations, only reversible effects were observed (presumably indicating DNA repair). Co-exposure to crocidolite and TNF-α increased the observed incidence of DNA damage, but the effect was less than additive. The authors indicate that additional studies with antioxidants indicate that the DNA damage induced by crocidolite in this study occurs through a mechanism that does not involve ROS. In fact, a potentially much more substantial mechanism by which asbestos may induce DNA breaks and various clastogenic alterations involves its ability to interfere with mitosis (Section 7.3.3.1).

There is also evidence that different tissues may respond to asbestos-induced ROS generation differently. For example, Zhu et al. (1998) indicate that MnSOD is found in the mitochondria of Type II epithelial cells of rats exposed to crocidolite. The authors further indicate that, because fibroblasts, alveolar macrphages, or endothelial cells do not display this protein when stimulated by exposure, this suggests a difference in the susceptibility of epithelial cells to certain types of asbestos-induced injury.

Importantly, although these studies provide evidence that indicates asbestos is capable of producing oxidized DNA adducts (or strand breaks) through ROS mediated processes, they do not address the question of whether such adducts can lead to

heritable mutations in DNA in vivo nor do they indicate whether such adducts lead to tumor production. Therefore, such studies should only be construed to suggest a potential that asbestos can act as a cancer initiator through ROS-mediated pathways.

As previously indicated, not all mechanisms involving the generation or effects of ROS are similarly fiber-size fiber-type dependent and those that are do not necessarily depend on these variables in the same way. At this time, it is not possible to distinguish among the relative importance of the different mechanisms so that it is difficult to judge the importance of the relative effects. However, the overall general implication (with the few exceptions noted) is that ROS more likely contributes to other asbestos-related diseases and cancer promotion than cancer initiation.

One final note concerning the effects of ROS that specifically involves the behavior of the hydroxyl radical is also warranted. The hydroxyl radical, is an extremely reactive species. Whether in vitro or in vivo, this species will react with virtually 100% efficiency with every organic molecule it encounters. Therefore the effects attributable to the hydroxyl radical are limited to those involving reactions in the immediate vicinity of the location at which it is generated. Thus, unless asbestos-induced generation of this radical occurs within the nucleus and in the immediate vicinity of susceptible strands of DNA, it is unlikely that these radicals are the direct cause of DNA damage.

Rather, hydroxyl radicals tend to react with cell membranes and other cellular components to produce further intermediate radicals (primarily lipid peroxides), which are much more stable than the hydroxyl radical and may migrate substantial distances before having an effect. It is likely that these intermediate radicals are ultimately responsible for any ROS-mediated DNA damage that may be attributed to asbestos.

7.3.3.3 Generation of reactive nitorgen species (RNS). Nitric oxide (NO) is produced ubiquitously in biological systems and serves many functions (**REF**). It is highly reactive and, therefore, generally a short-lived in vivo. However, nitric oxide has been shown to react with superoxide (O_2^-) to form the peroxynitrite ion ($ONOO^-$) at near diffusion-limited rates (see, for example, Zhu et al. 1998). This RNS may represent the primary species responsible for the effects attributed to RNS.

Asbestos-induced Generation of RNS

Alveolar macrophages, lung endothelial and epithelial cells, and alveolar epithelium (in both rats and humans), when stimulated by inflammatory agents generate both superoxide and over-produce nitric oxide that then combine to produce the perxoynitrite ion (Zhu et al. 1998, Martin et al. 1997). These cells up-regulate production of NO

when stimulated by various cytokines, lipopolysaccharide, and interferon γ. Because the peroxynitrite ion is a strong oxidant and nitrating agent and is extremely reactive, evidence for its production is generally indicated in most studies by the presence of nitrotyrosine, the stable product of tyrosine nitration, (Zhu et al. 1998). Evidence for production of NO is frequently indicated by observation of nitrite. Numerous studies also provide evidence of nitric oxide and peroxynitrite ion production specifically in response to exposure to asbestos in various tissues.

- Both chrysotile and crocidolite up-regulate the production of nitric oxide by alveolar macrophages in the presence of interferon-γ and the interaction between asbestos and interferon is synergistic. Non-fbrogenic carbonyl iron did not induce nitric oxide formation (Zhu et al. 1998). These authors also cite a study in which intratracheal instillation of silica and coal mine dust caused more inflammation and nitric oxide formation than TiO2 or carbonyl iron (on an equal particle basis) This suggests both the geometry and chemical composition of particles determine their ability to up-regulate nitric oxide.

- Inhalation of chrysotile or crocdolite induce secretion of both TNF-α and nitric oxide by pleural macrophages (Tanaka et al. 1998) Tanaka et al. (1998) studied the effects of RNS in rats exposed by inhalation to 6 to 8 mg/m^3 crocidolite or chrysotile (both NIEHS samples) for 6 hrs/day, 5 days/wk for 2 wks. Rats were sacrificed at 1 and 6 weeks following exposure. The authors indicate that asbestos induces formation of stable products of nitric oxide in cells obtained by lung lavage 1 wk after asbestos exposure. Nitrotyrosine (a marker for $ONOO^-$ formation) was also observed. Also, a greater number of alveolar macrophages and pleural macrophages were shown to express iNOS protein (the inducible form of nitric oxide synthase, Table 7-6) than sham exposed animals. Exposed rats showed significantly elevated immuno-staining for nitrotyrosine in the region of thickened duct bifurcations as well as within bronchiolar epithelium, alveolar macrophages, and mesothelial cells of both the visceral and parietal pleura. Nitrotyrosine staining was persistent, being observed at both 1 and 6 wks following exposure.

- Quinlin et al. (1998) studied the production of nitric oxide in rats exposed to crocidolite or chrysotile asbestos (both NIESH reference samples). Rats were exposed by inhalation at 6 hrs/day, 5 days/wk and lavaged at 3, 9, and 20 days. Lavaged macrophages showed significantly increased nitrite/nitrate (indicating production of nitric oxide) and this was suppressed with inhibitors to iNOS. Thus, nitric oxide is produced via an iNOS pathway. The authors also note that nitric oxide production correlated temporally with neutrophil influx in the lavage

fluid. They also indicate that asbestos exposed animals showed a 3 to 4 fold increase in iNOS positive macrophages in their lungs.

Quinlin et al. also exposed cultured murine alveolar macrophages (RAW 264.7 cells) to crocidolite, riebeckite, and crstobalite silica in vitro. These cells showed increased iNOS mRNA following exposure to asbestos and even greater increases if the cells were also stimulated with lipopolysaccharide (LPS). Both crocidolite and riebeckite (but not cristobalite silica) stimulated increased iNOS promoter activity when applied in combination with LPS. Thus, in this case, their appears to be a mechanism that is sensitive to particle composition but not size.

- Park and Aust (1998) treated cultures of human lung epithelial (A549) cells with crocidolite and observed induction of iNOS and reduction of intracellular glutathione (GSH) levels. Based on studies with inhibitors, the authors further indicate that iron mobilized from crocidolite was required both for formation of nitric oxide and to generate 2'-deoxy-7-hydro-8-oxoguanosine but not for the observed decrease in intracellular glutathione. The authors note that approximately five times as much chrysotile (containing approximately 3% iron) as crocidolite was required to produce the same level of nitric oxide formation. Importantly, these experiments were conducted in vitro in serum-free medium, so that no extra-biological source of iron was present.

- Choe et al. (1998) dosed cultured rat pleural mesothelial cells with either chrysotile or crocidolite (both NIEHS samples) at concentrations between 1.05 and 8.4 $\mu g/cm^2$ with or without co-stimulation with 50 ng/ml of interleukin-1β (IL-1β). The authors report that mRNA for iNOS in asbestos and IL-1β dosed cells increased progressively from 2 to 12 hours following exposure. Both types of asbestos also stimulated production of nitric oxide (measured as nitrite) in IL-1β stimulated cells in a dose- and time- dependent fashion. Both types of asbestos also induced expression of iNOS protein and formation of nitrotyrosine (based on nitrate detection) in IL stimulated cells. In contrast, carbonyl iron particles did not induce any of the effects observed for asbestos in IL stimulated cells. Thus, formation of RNS appears to be either fiber size dependent (not induced by particles) or mineralogy-dependent (or both).

As with the production of ROS, RNS production is apparently a function of multiple, complex mechanisms. Also, as with production of ROS, the dose-response characteristics of the various mechanisms differ. Several of the mechanisms show a strong dependence on fiber size and some dependence on fiber type. However, there are other mechanisms that are dependent primarily on fiber (or particle) type, but may

not be dependent on size (or at least not dependent on fiber size). At this point in time, it is not possible to gauge the relative importance of the various mechanisms by which RNS may be generated, except that it is likely that the importance of the various mechanisms likely differ in different cells and tissues and likely differ as a function of the specific toxin whose presence is inducing RNS production.

There are also indications that production of RNS may be species specific. For example, Jesch et al. (1997) report that alveolar macrophages harvested from rats expressed iNOS when stimulated with either LPS (lippopolysaccharide) or interferon-γ. In contrast, iNOS expression could not be induced in hamster, monkey or human macrophages.

Effects Mediated by RNS

Based on Zhu et al. (1998), over-production of nitric oxide can:

- inactivate critical enzymes;
- cause DNA strand breaks that result in activation of poly-ADP-ribosyl transferase (PARS);
- inhibit both DNA and protein synthesis; and
- form peroxynitrite by reaction with superoxide.

In turn, peroxynitrite ion may:

- initiate iron-dependent lipid peroxidation;
- oxidize thiols;
- damage the mitochondrial electron transport chain; and
- nitrate phenolics (including tyrosine).

Also, some of the damage to alveolar epithelium and pulmonary surfactant system previously attributed to reactive oxygen species may actually be caused through ROS generation of peroxynitrite. For example, Chao et al. (1996) report that crocidolite treatment of human lung epithelial cells (A549 cells) results in formation of 8-hydroxy-2'-deoxyguanosine (8-OHdG) in DNA and synthesis of mRNA for iNOS. An iNOS inhibitor reduces intracellular nitrite and eliminates production of 8-OHdG. Addition of independent NO donor, recovers production of 8-OhdG. Thus, production of the oxygenated DNA adduct in this case appears to be generated by reaction with RNS.

As with ROS, it is primarily the potential for RNS to contribute to DNA damage (e.g. strand breaks or generation of oxygenated adducts) that represent the primary pathways by which RNS might participate in cancer initiation (as opposed to cancer promotion or other asbestos-related diseases). It appears that RNS-mediated DNA

damage is closely associated with ROS generation and mediation of DNA damage (see Section 7.3.3.2). Thus, there is little to add here.

7.3.3.4 Conclusions concerning asbestos as a cancer initiator.

The strongest, most consistent evidence that asbestos can act as a cancer initiator relates to the tendency of asbestos to interfere with mitosis. Although there is evidence that asbestos may induce production of DNA adducts and DNA strand breaks (through ROS and RNS mediated pathways), whether such adducts or breaks ultimately lead to permanent, heritable changes to DNA remain to be demonstrated. The relative importance of the ROS/RNS mediated pathways compared to the pathway involving interference with mitosis also remains to be determined. As indicated in later sections, however, ROS/RNS mediated pathways may play substantial roles in cancer promotion and induction of other asbestos-related diseases.

Regarding the primary mechanism by which asbestos may initiate cancer (interference with mitosis), the pathway is length dependent (short fibers do not appear to contribute to the effect). Further, although there may also be a dependence on fiber type (chemical composition), it is apparent that all types of asbestos can act through this pathway. The dependence of this pathway on fiber diameter is less clear. Thus, other than to suggest that fibers must be respirable (and therefore thinner than approximately 0.7 μm to have an opportunity to act, Section 7.1), whether further diameter constraints are associated specifically with the mechanism of cancer initiation is not known.

Importantly, although crystalline silica may also act to produce some of the same effects as asbestos (including potentially carcinogenicity), there is substantial evidence that this material does not act through the same pathways and that the characteristics of its respective dose/response relationships may differ. Thus, for example, while asbestos likely initiates cancer through a mechanism that favors long (and potentially thin) fibers, silica more likely acts through a mechanism that is dependent on total surface area, with freshly and finely ground material likely being the most potent. In contrast, grinding asbestos fibers tends to lesson its carcinogenicity overall. Due to differences in chemistry and crystallinity (reinforced by studies indicating a lack of correspondence in behavior) crystalline silica does not appear to be an appropriate analog for any of the asbestos types. Rather, for example, the appropriate non-fibrous analog for crocidolite is riebeckite and the appropriate non-fibrous analog for chrysotile is antigorite or lizardite.

There is also some evidence that the relative importance of asbestos as a cancer initiator may differ in differing tissues. Thus, the results of Zhu et al. (1998) suggests

that Type II epithelial cells (but not alveolar macrophages, fibroblasts, or endothelial cells) express MnSOD (manganese-dependent superoxide dismutase) in mitochondria in response to exposure to asbestos, which may serve to mitigate effects associated with ROS mediated mechanisms.

More importantly, the results reported by Kodama et al. (1993) indicate that human bronchiolar epithelial cells are relatively resistant to the overall ability of asbestos to induce genotoxic effects (including those associated with interference with mitosis) in comparison, for example, to human meosthelial cells or various animal cells lines that have been studied by others.

Further, Sanden et al. (1992) indicates from a prospective cohort study of shipyard workers that the risk of lung cancer decreases with time since last exposure and the authors argue that the time-dependence of disease is more consistent with asbestos as a promoter than an initiator.

Taken as a whole, the above studies suggest that asbestos may serve primarily as a promoter of lung cancer, rather than an initiator. In contrast, it appears that asbestos may serve as both an initiator and a promoter of mesothelioma. Among other things, this may suggest a reason for the observed difference in the time-development of these two diseases among asbestos exposed individuals.

7.3.4 Evidence that Asbestos Acts As a Cancer Promoter

Primarily, asbestos may promote cancer by facilitating tissue proliferation. However, additional mechanisms associated with the observed synergism between asbestos exposure and smoking (see, for example, Hammond et al. 1979) also need to be considered.

Substantial evidence exists indicating that asbestos induces proliferation in target tissues associated with lung cancer and mesothelioma and this is summarized below followed by an overview of studies that suggest the various mechanisms by which asbestos may facilitate such proliferation. Evidence suggesting the various mechanisms related to the synergism between smoking and asbestos exposure are also briefly reviewed.

There are numerous mechanisms by which asbestos may facilitate proliferation including:

- direct cell signaling to induce proliferation. This may occur by:

  - direct interactions between fibers and receptors on the cell surface;
  - interaction with integrins for such receptors;
  - interactions between phagocytized fibers and intracellular components of signaling cascades;
  - or interactions between cells and intermediate species (e.g. ROS or RNS) whose generation and release has been induced by asbestos; or

- response to induced cell death in target tissues, which then stimulates stem cells to proliferate to replace killed cells. Cell death may be induced either through:
  - inducing apoptosis (programmed cell death); or
  - direct cytotoxic effects, which leads to necrosis.

These pathways are summarized in Table 7-5, which provides a perspective on the complexity of the interactions between asbestos and the cells and tissues of the body.

Regarding asbestos-induced cell death, asbestos-induced apoptosis (and all of the other effects described above) typically occurs at exposure concentrations that are much lower than required to induce frank cytotoxic effects (Sections 7.3.4.3 and 7.3.4.4). Therefore, it is primarily the former that is of potential interest in terms of implications for asbestos-induced diseases in humans. Due to the high exposure concentrations typically required, the importance of contributions from frank cytotoxicity to human disease is unclear (Section 7.3.4.4).

7.3.4.1 Asbestos-induced proliferation. Numerous in-vivo studies indicate that all types of asbestos induce proliferation in target tissues relevant to lung cancer and mesothelioma. Such proliferation is also suggested by the animal histopathological observations previously described (Section 7.2.2). Moreover, many of these studies suggest that the underlying mechanisms may be fiber size- and fiber-type specific. Responses may also be species-specific.

Importantly, there are some studies (primarily in-vitro studies) that suggest asbestos acts to inhibit (rather than induce) proliferation. Although it is likely that the contrasting observations found in such studies are due to differences in conditions, timing, dose, or the type of asbestos employed, the underlying reason for the contrasting observations is not always apparent.

The evidence for proliferation is summarized by tissue below.

In lung epithelium:

- Brody et al. (1997) showed that rats and mice exposed for a brief (5 hr) period to chrysotile asbestos at 1000 fibers/cm^3 (no size indicated) exhibited focal scarring at bronchio-alveolar duct junctions that are identical to those seen in asbestos-exposed humans. After 3-consecutive exposures, the lesions persisted for 6 months. In regions where fibers are deposited, macrophages are observed to accumulate, epithelium is injured, and proliferation is observed to occur. In this study, the authors also showed by immunohybridization staining that the four genes required to express three peptide growth factors (TGF-α, TGF-β, and the A and B chains of PDGF) and the proteins themselves are expressed in bronchio-alveolar tissue within 24 hrs of exposure. PDGF is expressed almost immediately and expression remains elevated for 2-weeks post exposure, but only in regions where fibers are deposited.

  The authors report that PDGF is a potent growth factor for mesenchymal cells, TGF-α is a potent mitogen for epithelial cells, and TGF-β inhibits fibroblast proliferation but stimulates synthesis of extra-cellular matrix (Table 7-6). The authors also report additional experiments with knockout mice indicate that TNF-α is required to induce the early stages of proliferation. The authors also indicate that Type II cells produce TGF-β1 and TGF-β2 (two of three isoforms of this protein) and that they are stimulated to do so when co-cultured with macrophages.

- Adamson (1997) intratracheally instilled size-separated (by sedimentation) long and short crocidolite fibers into rats (0.1 mg in a single dose) and noted that the long fibers damaged the bronchiolar epithelium and that fibers were incorporated into the resulting connective tissue; granulomas formed with giant cells containing fibers). The long fibers also appeared to escape into the interstitium. Labeled thymidine uptake (which indicates DNA synthesis and suggests proliferation) following long fiber exposure was seen in lung epithelial cells, fibroblasts, and pleural mesothelial cells. Such labeling peaked at 2% in mesothelial cells and 3% in epithelial cells within one week following exposure. Proliferation appeared to end shortly beyond one week. Short fibers were observed to have been efficiently phagocytized by alveolar macrophages and a small increase in macrophage population appeared to have been induced. Otherwise, none of the other effects attributable to long fibers (described above) were observed with short fibers. Note that such observations are entirely consistent with those reported for the range of studies described in Section 7.2.2.

- McGavran et al. (1989) exposed both normal (C5+) mice and compliment deficient (C5-) mice to asbestos (at 4 mg/m^3) by inhalation and observed proliferation of bronchio-alveolar epithelium and interstitial cells at alveolar duct bifurcations (based on incorporation of tritiated thymidine) between 19 and 72 hrs after a single, 5-hr exposure. Sham exposed rats showed fewer than 1% of epithelial and interstitial cells at alveolar duct bifurcations incorporate labeled thymidine. In contrast, thymidine uptake in asbestos exposed animals is significantly elevated for the first few days, begins to decrease at 8 days, and returns to normal by one month following exposure. Both C5+ and C5- mice show similar increases in volume density of epithelial and interstitial cells at 48 hrs post exposure. However, one month following exposure C5+ mice developed fibrotic lesions while C5- mice were no different than controls. The authors conclude that the depressed macrophage response in C5- mice does not appear to change the early mitogenic (and proliferative) response to asbestos but apparently attenuates later fibrogenesis.

- Chang et al. (1989) describes the morphometric changes observed in rats following 1 hr inhalation exposure to chrysotile (at 13 mg/m^3). Within 48 hrs following exposure: the volume of the epithelium increased by 78% and the interstitium by 28% at alveolar duct bifurcations relative to sham-exposed animals. Alveolar macrophages increased 10 fold and interstital macrophages 3 fold. Numbers of Type I and Type II epithelial cells increased by 82% and 29%, respectively. At one month following exposure, the numbers of Type I and Type II pneumocytes were still elevated, but not significantly. However, the volume of the interstitium had increased by 67% accompanied by persistently high numbers of interstitial macrophages, accumulation of myofibroblasts, smooth muscle cells, and an increased volume of interstitial matrix.

In lung endothelium:

In addition to the general evidence for proliferation of endothelial cells provided by Adamson (1997), McGavran et al. (1989), and Chang et al. (1989), as cited above, a more detailed description of the nature of asbestos-induced proliferation of endothelial cells is also available.

- Proliferation of endothelial cells and smooth muscle cells of arterioles and venules near alveolar duct bifurcations is induced in rats inhaling chrysotile (no size information given) for 5 hrs at 4 mg/m^3 (McGavran et al. 1990). This is based on the observed uptake of labeled thymidine (which indicates DNA

synthesis and suggests proliferation) that is significantly increased over controls between 19 and 72 hrs following exposure. 28% of vessels near bifurcations exhibited labeled cells 31 hrs after exposure. One month following exposure, the thickness of the smooth muscle layers around these blood vessels is significantly increased (doubled). In contrast, labeling of these same endothelial and smooth muscle cells in sham exposed rats is zero. The authors indicate that endothelial cells and smooth muscles associated with pulmonary blood vessels are normally quiescent with turnover rates on the order of years.

In mesothelium:

- In the second part of the study addressing epithelial proliferation, Adamson (1997) reports that rats instilled with 0.5 mg of unmodified, UICC crocidolite were sacrificed at one week and six weeks following exposure and subjected to bronchiolar lavage and pleural cavity lavage. Lavaged alveolar macrophages were observed to contain fibers but pleural macrophages did not. At one week, collected pleural macrophages were shown to induce proliferation of fresh mesothelial cells in culture and pleural lavage fluid showed an even greater effect. No effects were observed at six weeks. Further work with anti-bodies to various cytokines indicated that early, transient proliferation of mesothelial cells was dependent on kertinocyte growth factor (KGF) but not on PDGF, FGF, or TNF-α (Table 7-6). This suggests that early, transient proliferation is induced by diffusing cytokines rather than direct fiber exposure. Adamson further reports that KGF is a fibroblast-derived cytokine that acts on epithelial cells so that it's up-regulation likely results from epithelial injury with penetration of asbestos to the interstitium (where fibroblasts are found, Section 4.4). A similar transient proliferative response in mesothelial cells was also observed following exposure to chrysotile and in response to crystalline silica exposure. Thus, it appears that the mesenchymal proliferative response may be mineralogy specific for particles and is size-specific for fibers.

- Everitt et al. (1997) exposed rats and hamsters by inhalation to RCF-1 (45 mg/m^3 - 650 f/cm^3) for 12 weeks and then let them recover for up to an additional 12 weeks prior to sacrifice. The authors indicate that both rats and hamsters showed qualitatively similar levels of inflammation at time examined (4 wks and 12 wks). They also indicate the mesothelial cell proliferation was observed in both animal types but was more pronounced in hamsters at all time points examined. The greatest proliferation in both species was in the parietal pleura lining the diaphragm. The authors also report that fibers (primarily short and thin) were also observed in the pleural cavities of both species at all time points.

Several in vitro studies provide evidence that asbestos either induces or inhibits proliferation in lung tissues of interest and that at least some of the mechanisms involved are fiber size and mineralogy dependent. As previously indicated, the specific reasons for the apparent contrast between results observed in vivo (where asbestos consistently promotes proliferation) and the inhibition sometimes observed in in-vitro studies is not always apparent. However, it must be due to the special conditions that must be created to conduct in-vitro studies, which may not support certain mechanisms that are important in vivo.

- Timblin et al. (1998a) completed a study in which rat pleural mesothelioma (RPM) cells in culture were dosed with crocidolite or various cation-substituted erionites. The expression of several gene and gene products were then tracked. Cultures in this study were exposed to 1, 5 or 10 ug/cm^2 of the various fibrous materials. Analysis of the fibrous materials indicated that crocidolite contained many more fibers per gram of material (probably because they are thinner) and that the preparation contains somewhat longer fibers than the erionites evaluated. In crocidolite, for example, 88% of the fibers are longer than 5 um, 68% longer than 10 um, and 37.5% longer than 20 um. All of the cation substituted erionites showed approximately the same size distribution: 50% longer than 5 um, 10-20% longer than 10 um, and 1-5% longer than 20 um.

  Results indicate that the various cation substituted erionites behave differently and that the Na substituted erionite shows the largest overall potency, at least for some end points but not others. Fe, Na, and Ca substituted erionite all appear to induce c-fos expression in a dose-dependent fashion (increasing regularly among the 1, 5, and 10 ug applications). K-erionite may also show the same pattern, but the changes were not indicated as significant over controls (apparently due to greater variability). Only Na-erionite showed significantly increased expression of c-jun (at 1 and 5 ug applications but not significantly at 10 µg, apparently due to greater variability. However, the mean result for 10 ug shows a consistent trend with the lower concentration application results).

  Na-erionite induces c-fos at the same or greater rates as crocidolite asbestos for the same mass application (but not the same fiber number). Crocidolite also appears to show a dose-response trend for c-jun expression, but only the result for the highest application (10 ug) is significantly different from controls. In contrast, Na-erionite appears to show greater induction of c-jun expression at lower dose than crocidolite, but the increase with increasing dose is much lower for Na-erionite. Crocidolite also appears to induce substantial apoptosis (even at

the low dose of 5 ug) and that the induction is dose-dependent. In contrast, non-fibrous riebeckite does not appear to induce apoptosis. Comparison between crocidolite dosed cultures and Na-erionite dosed cultures indicate that crocidolite induces substantial apoptosis at all time periods following application but that Na-erionite induces little apoptosis even at higher mass dose and longer time periods than crocidolite. The authors also indicate that crocidolite and Na-erionite appear to stimulate DNA-synthesis, which appears to be a compensating mechanism to fiber cell toxicity. The authors indicate that chemistry is important in fiber toxicity as Na-erionite was a strong inducer of c-jun, even at relatively low concentrations, but several of the other cation substituted erionites (including Fe-erionite) were not. They further suggest that, given the difference in the fiber lengths of the crocidolite samples and Na-erionite samples, that fiber length may be a less important consideration than fiber surface chemistry. However, despite the author's assertion, considering that non-fibrous riebeckite does not induce any of the effects observed for crocidolite, there appears to be a clear size effect. It may simply require that a defined, minimum length is necessary to induce the effect.

The authors also indicate that balance between proliferation and apoptosis is required to maintain homeostatis in healthy tissue. They further indicate that other studies suggest that c-Jun expression is linked to proliferation and induction of cancer, while c-fos expression is linked to apoptosis. Thus, suppression of c-fos may be linked to carcinogenesis by allowing establishment or maintenance of a transformed cellular phenotype. This is in fact an early step in carcinogensis. Many environmental agents stimulate both apoptosis and proliferation and, depending on the degree, may cause imbalances that lead to disease. Relative stimulation of c-fos and c-jun may reflect some of these pathways. Since crocidolite induces both c-fos and c-jun in this study, the implication is that it mediates both apoptosis and proliferation.

- Wylie et al. (1997) dosed hamster tracheal epithelial (HTE) cells and rat pleural mesothelial (RPM) cells with various asbestos and talc samples and evaluated proliferation based on a colony-forming efficiency (CFE) assay. The samples were NIEHS crocidolite and chrysotile and three different talcs. Samples were characterized in the paper by mineralogical composition, surface area, and size distributions.

The authors indicate that both asbestos samples increased colony formation of HTE cells (suggesting induction of proliferation) but talc samples did not. RPM cells, in contrast, showed only dose-dependent decreases in colony forming

efficiency for all samples, which the authors indicate is a sign of cytotoxicity. The authors report that all samples show corresponding effects when concentrations are expressed as fibers longer than 5 µm or by total surface area. They also suggest that the "unique" proliferative response by HTE cells could not be explained by either fiber dimension or surface area and suggests a mineralogical effect. **NOTE: MY OBSERVATIONS FROM RESULTS OF THIS STUDY ARE THAT ABESTOS AFFECTS BOTH HTE AND RPM CELLS, BUT THAT TALC ONLY APPEARS TO AFFECT RPM CELLS. EXPRESSING EXPOSURE AS LONG FIBER NUMBER CONC OR SURFACE AREA TENDS TO PARTIALLY BUT NOT COMPLETELY NORMALIZE DOSE-RESPONSE ACROSS SAMPLE TYPES FOR RPM CELLS, BUT NOT FOR HTE CELLS. THE TWO ASBESTOS SAMPLE TYPES BEHAVE SIMILARLY TWARD BOTH CELL TYPES WHEN EXPOSURE IS EXPRESSED EITHER AS LONG FIBERS OR SURFACE AREA (NEED TO GO BACK AND DEMONSTRATE THIS WITH TABLES FROM THE PAPER.)**

- Barchowsky et al. (1997) dosed cultured (low passage) endothelial cells to NIEHS chrysotile, crocidolite, or RCF-1. After 1 to 3 hrs exposure to 5 µg/cm^2 (non-lethal concentrations), asbestos (but not RCF-1) causes changes in cell morphology (cells elongate), increases in cell motility, and increases in gene expression. Further work by the authors indicate that these effects are mediated by interaction between asbestos and the receptor for urokinase-type pasminogen activator (uPAR). The authors also suggest that attachment of asbestos to cell membranes, internalization of asbestos fibers by the cells, and the morphological changes induced by asbestos are each mediated by different proteins.

Examples of in vitro studies that indicate asbestos (and other fibrous materials) may inhibit proliferation in culture include the following.

- In contrast to the above, Levresse et al. (1997) found that chrysotile and crocidolite act to inhibit proliferation in cultured rat pleural mesothelioma (RPM) cells. In this study, RPM cells (diploid, no more than 25 passages) were dosed with either UICC crocidolite or NIEHS Zimbabwean Chrysotile at concentrations varying between 0.5 and 20 µg/cm^2. The authors also note that the chrysotile sample contains approximately four times the number of fibers as the crocidolite samples. Cells were then examined at 4, 24 and 48 hrs following treatment. In untreated cultures, the number of cells in replicative phase decrease with time, which indicates that such cells are headed for confluence (completion of a monolayer on the culture medium). At 48 hrs, for example, 10% of untreated

control cells were observed to be in replicative stage. Chrysotile (but not crocidolite) decreased the fraction of cells in replicative phase in a time- and dose-dependent manner. At 48 hrs, for example, cells treated with 10 $\mu g/cm^2$ chrysotile showed only 1.5% in replicative phase. Further tests confirmed that this was due to blockage of cells at the G1/S boundary of the cell cycle. Both chrysotile and crocidolite appears to induce a time-dependent increase in the number of cells at G2/M in the cell cycle, although this effect was not observed to be dose-dependent for chrysotile. Even on a fiber-number basis, chrysotile appears to be elicit a greater response (arrest a greater percentage of cells) than crocidolite.

The authors also indicate that chrysotile caused nuclear-localized, time-dependent increases in p53 concentrations. Crocidolite produced much lower levels that were not detectable in the nucleus. Chrysotile was also observed to produce blockage at the G0/G1 transition of the cell cycle, but crocidolite did not. They also note that p53 is known to mediate arrest at this stage in the cycle so observing that chrysotile induces arrest at this transition in the cell cycle may be consistent with the observed increased expression of p53. The authors also note that chrysotile triggers apoptosis in this study and that crocidolite shows a smaller, but detectable effect. Spontaneous apoptosis in untreated cultures ran between 0.5 and 1% at 24 to 48 hours whereas chrysotile induced 4% apoptosis, peaking at 72 hrs following exposure to 10 $\mu g/cm^2$. The authors indicate that the lower level of effects observed with crocidolite could be due to the substantially smaller number of long fibers in UICC crocidolite compared to NIEHS chrysotile.

- The previously reviewed (Section 7.3.3.1) study by Hart et al. (1994) also suggests that long, medium, short, and UICC crocidolite and chrysotile along with a range of MMVF's show a dose-dependent inhibition on proliferation of cultured CHO cells and that potency toward the effect is a direct function of fiber length.

Several of the above-described studies, in addition to providing evidence that asbestos induces proliferation in various lung tissues, also suggests certain mechanisms. Asbestos may induce proliferation, for example, by inducing production of specific cytokine growth factors (Brody et al. 1997, Adamson 1997), or by inducing certain signaling cascades (Barchowsky et al. 1997, Timblin et al. 1998b). It is also possible that the two effects may be related (i.e. that stimulation of a particular signaling cascade may result in production of certain growth-stimulating cytokines). Other mechanisms may also be important (Table 7-5).

7.3.4.2 Asbestos induced cell signaling. Asbestos has been shown to induce a variety of cell signaling cascades in a variety of target cell and tissue types. Such signaling may then trigger effects in the stimulated cells that may include:

- proliferation;
- morphological changes;
- generation and release of various cytokines, enzymes, or extracellular matrix; or
- programmed cell death.

Note, due to the large number of chemical species that need to be considered in this discussion, Table 7-6 provides a summary of the sources of such species (Table 7-6A) and the effects attributable to such species (Table 7-6B).

In specific cases, asbestos may initiate cell signaling by interacting directly with receptors on the cell surface, by interacting with integrins for such receptors, by causing generation and release of intermediate species (e.g. ROS or RNS) that trigger cell signaling, or (for phagocytized fibers) by interacting with intracellular components of a particular signaling cascade. The specific responses to cell signaling induced by asbestos are frequently cell- or tissue- type specific. Moreover, depending on the specific mechanism, cell signaling by asbestos may be dependent on fiber size and/or type.

- Barchowsky et al. (1998) showed in a set of studies that long chrysotile and long crocidolite but not RCF-1 fibers (at concentrations between 1 and 10 $\mu g/cm^2$), which is reportedly below levels that typically induce cytotoxic effects) induced up-regulation of urokinase-type plasminogen activator (uPA) and its receptor (uPAR) in both lung endothelial cells (vascular cells) and lung epithelial cells. They also showed that the increased pericellular protolytic activity (requiring cleavage of plasminogen to plasmin) that is induced by asbestos in these cells is mediated by uPA.

In prior studies, chrysotile has been shown to cause endothelial cells to elongate and increase expression of adhesion molecules for phagocytes. They also show enhanced proteolytic activity and matrix interactions. Chrysotile has also been shown to stimulate fibrinolytic activity in lung epithelial cells and extravasating macrophages. All such stimulation appears to result from up-regulation of uPA. Thus, this mechanism may explain the observed asbestos-induced changes in lung endothelial and epithelial cells including vascular remodeling, development of vascularized granular tissue, increased matrix turnover, and leukocyte extravasation (which in turn may be caused by cell

activation and elaboration of proteases and adhesion molecules). The authors suggest that asbestos-induced up-regulation of uPA and uPAR expression may represent a global mechanism for pulmonary toxicity and fibrosis induced by crystalline fibers. Importantly, chrysotile was shown to induce uPA and uPAR expression in the absence of serum, so the effect is apparently due either to direct binding of fibers to cell-surface receptors or integrins for such receptors.

- Mossman et al. (1997) observed that concentrations of 1.25 to 5 $\mu g/cm^2$ of crodidolite (sample from TIMA) caused expression of c-jun and AP-1 in both cultured hamster tracheal epithelial (HTE) cells and cultured rat pleural mesothelial (RPM) cells. Crocidolite was also observed to trigger the EGFR-regulated kinase (ERK) and mitogen activated protein kinase (MAPK) pathways in RPM cells. The authors indicate that these pathways are also stimulated by hydrogen peroxide and that NF-$\kappa\beta$ induction stimulated by crocidolite is also stimulated by crystalline silica (although silica stimulation of the MAPK pathway was not investigated). They also note that the non-fibrous analog to crocidolite, riebeckite does not elicit these activities.

Table 7-6A, page 1

Table 7-6A:
Sources of Various Cytokines and Other Chemical Transmiffers

Chemical Species	Abbreviati	Sources	Reference
Signal Transmitters			
Activator Protein-1	AP-1		
	BAX	induced by high concs of p53	Lechner et a. 1997
	Bcl-2		
Fifth Component of Compliment	C5		
Cyclin Dependent Kinases	CDK's		
Cyclin Dependent Kinase Inhibitors	CDI's		
Cytokine-induced Neutrophil Chemoattractant	CINC		
Epithelial Growth Factor	EGF		
Epithelial Growth Factor Receptor	EGFR		
EGFR regulated kinase	ERK		
Granulocyte-macrophage colony Stimulating Factor	GM-CSF		
	GRP78		
human neutrophil elastase	HNE	released from asbestos activated PMN	Kamp et al. 1993
	HSP72/73		
Intercellular adhesion molecule-1	ICAM-1	released by lung epithelial and endothelial cells following exposure to silica but not TiO2 enhanced expression by RPM cells exposed to chrys or crc	Nario and Hubbard 1997 Choe et al. 1997
Interleukin-1	IL-1		
Interleukin-6	IL-6	induced by ROS in Type II epithelial cells	Luster and Simeonova 1998
Interleukin-8	IL-8		
Inducible Nitric Oxid Synthase	iNOS	expressed by activated macrophages, but not in primates	Jesch et al. 1997
Keritonizing Growth Factor	KGF	derived from fibroblasts???	Adamson 1997
Mitogen Activated Protein Kinase	MAPK		

Macrophage Inflammatory Protein-1alpha	MIP-1alpha		
Macrophage Inflammatory Protein-2	MIP-2		
Matrix Metalloproteinases	MMP's	relative expression affected by cigaret smoke and fiber exposure	Morimoto et al. 1997
	Neu		
Nuclear Factor-KB	NF-KB		
Nitric Oxide Synthase	NOS		
Ornithine Decarboxylase	odc		
Platelet-Derived Growth Factor	PDGF	Activated macrophages	Bauman et al. 1990
		Elevated expression in mesothelioma cells	Lechner et al. 1997
		asbestos and iron treated AM and interstitial macrophages release PDGF	Osornio-Vargas et al. 1993
	p53	Induced by DNA damage	Lechner et al. 1997
poly(ADP-ribosyl)polymerase		Inhibited by 3aminobenzamide	Broaddus et al. 1997
????	Rb		
Tissue Inhibitors of MMP's	TIMP's	relative expression affecte	Morimoto et al. 1997
Tumor Necrosis Factor Alpha	TNF-alpha	some particles induce activated macrophages to release this (shown both in vitro and in viv	Driscoll et al. 1997
		regulated by oxidant-sensitive transcription of NF-KB	Driscoll et al. 1997
		macrophages in BAL from asbestosis and idiopathic interstitial fibrosis patients release TNI	Zhang et al. 1993
Transforming Growth Factor Alpha	TGF-alpha	expressed in BA epithelium exposed to asbestos	Brody et al. 1997
Transforming Growth Factor Beta	TGF-Beta	expressed in BA epithelium exposed to asbestos	Brody et al. 1997
		macrphage stimulated Type II epi cells produce both TGF-beta1 and TGF-beta2	Brody et al. 1997
		all three isoforms expressed in the fibrotic lesions (by hyperplatic type II cells) of asbestosis	Jagirdir et al. 1997
		mesothelial tumor cells expressed only TGF-beta1 and 2	Jagirdir et al. 1997
		also type II cells of silicosis patients express all three forms	Jagirdir et al. 1997
		asbestos and iron treated AM and interstitial macrophages release TGF-beta	Osornio-Vargas et al. 1993
Urokinase-type Plasminogen Activator	uPA		

Vascular Cell Adhesion Molecule	VCAM-1	enhanced expression by RPM cells exposed to chrys or crc	Choe et al. 1997
	WT1		
Enzymes			
Mn-dependent SuperOxide Dismutase	Mn-SOD		
Gene Products			
	c-fos		
	c-jun		
	mdm2		
	c-myc		
	H-RAS		
	K-RAS		

Table 7-6B:
Effects of Various Cytokines and Other Chemical Transmiffers

Chemical Species	Abbreviat	Effects	Reference
Signal Transmitters			
Activator Protein-1	AP-1	a transcription factor: binds the DNA promoter region of genes governing inflammation, proliferatin, and apoptosis	Mossman and Churg 1998 (Citing:
	BAX	induces apoptosis	Lechner et al. 1997
	Bcl-2	inhibits apoptosis	Lechner et al. 1997
Fifth Component of Compliment	C5	mediates asbestos-induced fibrosis	McGavran et al. 1989
Cyclin Dependent Kinases	CDK's	mediates cell cycle	Lechner et al. 1997
Cyclin Dependent Kinase Inhibitors	CDI's	inhibits advance of cell cycle	Lechner et al. 1997
Cytokine-Induced Neutrophil Chemoattractant	CINC		
Epithelial Growth Factor	EGF	inhibits proliferation of mesothelial cells stimulates proliferation of mesothelioma tumor cells	Kravchenko et al. 1998 Goodglick et al. 1997
Epithelial Growth Factor Receptor	EGFR	mediates MAPK signaling	Mossman et al. 1997
EGFR regulated kinase	ERK	mediates apoptosis	Mossman et al. 1997
Granulocyte-macrophage colony Stimulating Factor	GM-CSF		
	GRP78		
human neutrophil elastase	HNE	By itself, increases pulmonary epithelial cell detachment in culture with asbestos, increases pulmonary epithelial cell lysis	Kamp et al. 1993 Kamp et al. 1993
	HSP72/73		
Intercellular adhesion molecule-1	ICAM-1	facilitates migration of leukocytes out of blood to sites of injury	Narlo and Hubbard 1997
Interleukin-1	IL-1		
Interleukin-6	IL-6	is a pleiotropic cytokine	Luster and Simeonova 1998
Interleukin-8	IL-8	is a neutrophil chemoattractant	Luster and Simeonova 1998
Inducible Nitric Oxid Synthase	iNOS		
Keritonizing Growth Factor	KGF	induces transient proliferation of mesothelial cells	Adamson 1997
Mitogen Activated Protein Kinase	MAPK	mediates transcription of AP-1 mediates ERK signaling	Mossman et al. 1997 Mossman et al. 1997
Macrophage Inflammatory Protein-1alpha	MIP-1alpha		
Macrophage Inflammatory Protein-2	MIP-2	a chemoattractant for PMN's, but may not be involved with inflammatory response	Osler et al. 1997

Matrix Metalloproteinases	MMP's		
	Neu		
Nuclear Factor-KB	NF-KB	a transcription factor that regulates genes involved with the inflammatory response, cell adhesion, and growth c	Barchowsky et al. 1998
Nitric Oxide Synthase	NOS		
Ornithine Decarboxylase	odc	promoted by AP-1	Mossman and Churg 1998
		encodes a key enzyme for the biosynthesis of polyamines	Mossman and Churg 1998
Platelet-Derived Growth Factor	PDGF	induces proliferation of lung fibroblasts	Bauman et al. 1990
		induce proliferation of mesothelial cells	Brody et al. 1997
		is a chemotactic attractant for rat lung fibroblasts	Osornio-Vargas et al. 1993
	p53	at low conc, arrests cell cycle at G1/S	Unfried et al. 1997
		at higher conc, induces BAX protein, which induces apoptosis	
poly(ADP-ribosyl)polymerase			
????	Rb	????	????
Tissue Inhibitors of MMP's	TIMP's		
Tumor Necrosis Factor Alpha	TNF-alpha	induces JNK arm of MAPK cascade	Mossman et al. 1997
		is involved in the recruitment of inflammatory cells	Driscoll et al. 1997
		stimulates macrphages, epithelial cells,endothelial cells, fibroblasts to secrete chemokines and adhesion molec	Driscoll et al. 1997
		can induce apoptosis among neutrophils	Leigh et al. 1997
		can induce ROS production in leukocytes	Kalglova et al. 1997
		intradermal inj stimulates focal accumulation of fibroblasts and collagen	Zhang et al. 1993
		in vitro, stimulates fibroblast DNA synthesis and proliferation	Zhang et al. 1993
Transforming Growth Factor Alpha	TGF-alpha	is a mitogen for epithelial cells	Brody et al. 1997
Transforming Growth Factor Beta	TGF-Beta	inhibits fibroblast proliferation but stimulates formation of extracellular matrix	Brody et al. 1997
		can induce apoptosis in different types of cells	Leigh et al. 1997
		does not appear to induce chemotaxis of rat lung fibroblasts	Osornio-Vargas et al. 1993
		induces chemotaxis of rat mononuclear leukocytes	Osornio-Vargas et al. 1993
Urokinase-type Plasminogen Activator	uPA	associated with increased pericellular protyolytic activity in endothelial tissue	Barchowsky et al. 1998
Vascular Cell Adhesion Molecule	VCAM-1		
	WT1	forms a heterodimer w p53 and alters behavior	Unfried et al. 1997

Enzymes

Mn-dependent SuperOxide Dismutase	Mn-SOD	

Gene Products

c-fos	linked to apoptosis	Timblin et al. 1998
	transcription factor that activates the TGF-beta1 promotor	Jagirdar et al. 1997
	proteins of c-fos dimerize with c-jun to create activator protein-1 (AP-1)	Mossman and Churg 1998
c-jun	linked to proliferation	Timblin et al. 1998
	transcription factor that activates the TGF-beta1 promotor	Jagirdar et al. 1997
	transcription factor that activates the TGF-beta1 promotor	Mossman and Churg 1998
mdm2	a protococoncogene that inhibits p53	Lechner et al. 1997
c-myc		
H-RAS		
K-RAS		

Table 7-6B, Page 3

The authors indicate that induction of the NF-κβ cascade was inhibited by excess glutathione, which is stimulated by N-acetylcysteine (NAC), suggesting that this pathway is induced by asbestos-caused oxidative stress (perhaps through ROS or RNS intermediates). Application of NAC also diminished crocidolite induced c-fos and c-jun RNA levels and inhibited activation of the ERK-MAPK cascade. Further work suggests that asbestos triggers the MAPK pathway by interaction with the Epithelial Growth Factor Receptor (EGFR), either directly or by phosphorylation of this receptor by ROS. At the concentrations examined, crocidolite induces substantial apoptosis (apparently through activation of the ERK-MAPK cascade). In contrast, the authors note that TNF-α induces the JNK arm of the ERK-MAPK cascade, which leads to proliferation. Asbestos does not elevate JNK over the time-period of the study. The authors note that it has been shown in some studies that inhibition of ERK in some cells, also inhibits asbestos-induced apoptosis. Importantly, given that these processes are induced by crocidolite but not by its non-fibrous analog, riebeckite, induction of the ERK-MAPK cascade appears to be a fiber-size dependent process.

- In a related study to that conducted by Mossman et al. (1997), Zanella et al. (1999) report that the (TIMA) crocidolite (at concentrations of 2.5 to 10 ug/cm^2, but not its non-fibrous analog, riebeckite, eliminated binding of EGF to its receptor EGFR. Because EGF does not bind to crocidolite in the absence of membrane, this is not simply a case of crocidolite tying up ligand. Crocidolite also induces a greater than twofold increase in steady-state message and protetin levels of EGFR.

The authors also note that the tyrphostin, AG-1478 (which specifically inhibits the tyrosine kinase activity of EGFR), significantly mitigated asbstos-induced increases in mRNA levels of c-fos but not c-jun and that the asbestos action was not blocked by a non-specific tyrphostin, AG-10. Moreover, pretreatment of RPM cells with AG1478 significantly reduced asbestos-induced apoptosis. Therefore, the authors concluded that asbestos -induced binding to EGFR initiates signaling pathways responsible for increased expression of the protooncogene c-fos and the development of apoptosis. This apparently occurs through the EGFR-extracellular signaling regulated kinase (ERK). It is hypothesized that asbestos may induce dimerization and activation (phosphorylation) of EGFR, which also prevents binding of EGF. Asbestos apparently serves the same role as EGF in that it promotes aggregation of EGFR, which in turn promotes binding to the extracellular domain of tyrosine kinase receptors and the activation of their intracellular kinases. The authors also indicate that other work suggests that

crocidolite fiber exposure leads to aggregation and accumulation of EGFR at sites of fiber contact and that asbestos also stimulates biosynthesis of the EGFR and activates ERK in an EGFR-dependent manner.

The authors speculate that asbestos binding may not be ligand-site specific but may be charge related or may induce EGFR phophorylation by local production of ROS, which has previously been demonstrated to cause EGFR activation. As previously indicated, that this effect is driven by crocidolite exposure but not by exposure to riebeckite indicates that this mechanism is fiber-size specific.

- Johnson et al. (1997) showed that UICC crocidolite, but not JM-100 glass, applied to a culture of immortalized human Type II epithelial (A549) cells at non-cytotoxic concentrations (for 20 hours) results in increased expression of p53, Cip1, and GADD153 in a dose- and time-dependent fashion. Expression was observed to be maximum at 18 hours. The crocidolite treatment was also shown to cause an increase in the number of cells arrested in Stage G2 of the cell cycle (with a persistent decrease in the number of cells in G1). This was considered surprising because both p53 and Cip1 are known to mediate arrest in Stage G1. The authors suggest that these findings indicate a strong dependence on both fiber type and fiber size (JM-100 glass contains substantially more long fibers than crocidolite). However, it is not possible to separate the effects of fiber type versus fiber size in this study.

- Luster and Simeonova (1998) indicate that at high concentrations, ROS may induce frank cytotoxicity. At low or moderate levels, ROS is more likely to induce cell signaling cascades that may, in turn, contribute to asbestos-related disease. The authors dosed cultures of immortalized human Type II epithelial (A549) cells, originally derived from a lung carcinoma, and normal human bronchioepithelial (NHBE) cells with long (Certain-Teed supplied) crocidolite (reported mean length: 19 μm) at concentrations ranging between 0 and 24 μg/ml. Results indicate that secretion of both Interluken-8 (IL-8) and IL-6 was stimulated by crocidolite exposure in a dose-dependent manner. In contrast, increases in LDH levels (which indicate cell damage) was only detected at the highest exposure concentrations tested. Further work indicates that stimulation of IL-6 and IL-8 secretion occurs through ROS that is generated in an iron-dependent process (that may also include NF-κβ induction). Note that the trend of cell signal induction at low and moderate levels of asbestos exposure with evidence for cytotoxicity observed only at the highest exposure concentrations is common to many of these kinds of studies.

- Choe et al. (1999) conducted a combined in-vivo/in-vitro study of the effects of low level exposure to chrysotile or crocidolite at inducing leukocyte attachment to rat pleural mesothelial cells. The authors note that similar populations of rat pleural leukocytes (74% macrophages, 2% neutrophils, 10% mast cells, and 10% eosinohils) were observed in both asbestos-exposed and unexposed rats.

  In the second part of the study, cultured RPM cells were exposed to either crocidolite or chrysotile (both NIEHS samples) at concentrations ranging between 1.25 and 10 $\mu g/cm^2$, which was noted to be below levels at which substantial cytotoxicity is observed. Attachment of rat pleural leukocytes to RPM cells was then observed to increase with increasing dose of asbestos to the RPM cells. In contrast, carbonyl iron (a non-fibrous particle) also induced enhanced attachment but at much lower levels and the effect was not dose-dependent. Further analysis indicated that asbestos-induced adhesion is mediated by up-regulation of IL-1β (but not dependent on TNF-α or nitric oxide production, although it is noted that TNF-α independently increases attachment). Asbestos also induces increased expression of vacular cell adhesion molecule (VCAM-1). The authors also note that rat pleural leukocytes harvested from asbestos-exposed rats also showed increased adhesion to in-vitro RPM cells over leukocytes harvested from sham exposed rats. Thus, asbestos appears to trigger alterations in these cells as well.

- In a recent paper, Driscoll et al. (1997) reviewed the role of tumor necrosis factor alpha (TNF-α) in mediating the inflammatory response to lung insult by particulate matter. The authors indicate that quartz, coal dust, crocidolite, and chrysotile are all potent inducers of TNF-α production. Titanium dioxide (TiO_2), corundum (aluminum oxide: Al_2O_3), and latex beads are not. Pulmonary macrophages have been shown to secrete TNF-α in vivo in response to exposure to some of the dusts listed above (including asbestos). This is also observed among macrophages from asbestosis patients.

  The authors indicate that rats immunized against TNF-α show reduced recruitment of neutrophils, which demonstrates that TNF-α is involved in the recruitment of inflammatory cells. TNF-α stimulates macrophages, epithelial cells, endothelial cells, and fibroblasts to release chemokines that include adhesion molecules (Eselectin, ICAM, VCAM). Inflammatory cells then interact with such molecules and migrate along gradients from vascular structures in the lung to the lung interstitium and even the lung air spaces. It has also been shown that release of TNF-α by macrophages is apparently dependent on oxygen stress (i.e. exposure to ROS/RNS) that is induced in pathways that

require iron. Production of TNF-α and other compounds that mediate the inflammatory response are regulated by the oxidant-sensitive transcription factor NF-κβ. This factor exists as a heterodimer in the cytoplasm in an inactive form because it is bound to the inhibitory 1-kappaBalpha (1-κBα), which masks a nuclear translocation signal. Appropriate stimulation of a cell induces phosphorylation of 1-κBα, which then marks it for proteolytic degradation. Then, NF-κβ translocates to the nucleus and induces transcription. The process is stimulated by oxidants and inhibited by antioxidants.

- In another review, Finkelstein et al. (1997) indicated that Type II epithelial cells and Clara cells (non-ciliated bronchiolar epithelial cells) respond to and produce specific cytokines during the inflammatory process. Early responses to particle challenge include increases in mRNA and protein for IL-1β, IL-6, and TNF-α. These are also accompanied by changes in specific epithelial genes including those for surfactant protein C and Clara cell secretory protein. The authors further indicate that these responses are due to direct interaction with particles rather than a result of macrophage-derived mediators and they suggest a more significant role for epithelial secretions in the overall pulmonary response than previously suspected. Results also suggest that Type II pneumocyte-derived growth factors may play a significant role in the pathogenesis of pulmonary fibrosis.

  Also in this paper, Finkelstein et al. report that intratracheal instillation of lipopolysaccharide (a potent inflammatory agent) caused increases in both lavage fluid and plasma levels of TNF-α and IL-6. Intrapleural injection induced primarily increases in plasma levels. The authors indicate that this suggests that the observed cytokines are produced primarily at the site of injury. The authors further indicate that IL-6 is elevated in lavage fluids following exposure to Ni_2S_3, a suspected human carcinogen, but not following exposure to TiO_2 or NiO. In vitro studies indicate that release of IL-1β and TNF-α by Type II cells occurred only following exposure to crocidolite or ultrafine TiO_2, but not pigment grade TiO_2. The authors also indicate that protein C and Clara cell secretory protein were both expressed in their respective source cells following exposure only to the fibrogenic of the above particles. They also report that crystalline silica has been shown to promote cytokine release and hypertrophy in Type II cells.

- Jagirdar et al. (1997) used immunohistochemistry in a study to show that all three isoforms of TGF-β (1,2, and 3) are expressed in the fibrotic lesions of asbestosis and pleural fibrosis patients from the Quebec mines, primarily by Type II pneumocytes. The cases examined averaged 38 years of exposure to

the Quebec chrysotile. The authors also indicate that the hyperplastic epithelium of silicosis patients also show elevated expression of all three isoforms. They further indicate from previous studies that mesothelioma tumor cells frequently express TGF-β2 while the cells in the stroma of such tumors frequently express TGF-β1. It is also noted in this study that jun and fos are both transcription factors that activate the TGF-β1 promoter.

- Zhang et al. (1993) indicate that macrophages obtained in BAL fluid from idiopathic pulmonary fibrosis (IPF) patients and asbestosis patients show significantly increased secretion of TNF-α and asbestosis patients also showed significantly increased secretion of IL-1β. Macrophages and monocytes obtained from both kinds of patients also show elevated expression of mRNA for these cytokines. In an in-vitro part of this study, Zhang and coworkers, showed that chrysotile, crocidolite, amosite, and crystalline silica all stimulated IL-1β and TNF-α release and up-regulated their respective mRNA in both macrophages and monocytes. The authors also report that these two cytokines have been shown to up-regulate collagen Types I and III and fibronectin gene expression in human diploid lung fibroblasts after short term, serum free exposure in vitro.

- Holian et al. (1997) exposed cultures of normal human alveolar macrophages (AM) (obtained by lavage) to varying concentrations (up to 25 μg/ml) of short chrysotile, UICC crocidolite, ground silica, wollastonite, and titanium dioxide to determine whether these materials cause a phenotypic shift in macrophage populations by inducing selective apoptosis. The authors indicate that normal lungs contain: 40-50% RFD1+7+ suppressor AM, and 5-10% RFD1+ immune activator. In this study, the fibrogenic subset of the particles tested (not wollastonite or titanium dioxide) increased the ratio of activator/suppressor AM by a factor of 4 within a few hours and the effect was seen to increase with time. The authors also note that fibrogenic particles decrease the abundance of RFD7+ AM (phagocytic), but the consequences of this phenotypic shift are unclear.

The authors indicate that AM taken from fibrotic patients release a variety of proinflammatory mediators capable of stimulating fibroblast proliferation and collagen synthesis. Even in the absence of evidence of fibrosis, workers who have been heavily exposed to asbestos yield similarly activated AM. In contrast, they also note that, in vitro studies in which AM are stimulated with fibrogenic particles, while such AM are activated to release inflammatory cytokines, such releases are orders of magnitude less than that seen from AM derived from

fibrotic patients. The authors indicate that the apoptosis-driven phenotypic shift in AM that is indicated by this study may explain the apparent discrepancy.

- In a previously described study, Timblin et al. (1998a), see Section 7.3.4.1, showed that crocidolite asbestos and several cation substituted erionites all stimulate c-jun and c-fos in rat pleural mesothelial cells, but to varying degrees depending on fiber chemistry. The effect also appears to be size dependent as crocidolite but not its non-fibrous analog riebeckite induces the effect.

In general, the kinds of signaling cascades that are potentially stimulated by exposure to asbestos are important due to their potential to contribute to the promotion of cancer. Such pathways, for example, may mediate proliferation or may suppress apoptosis. Alternately, they may mediate an inflammatory response that in turn may lead to proliferation or to production and release of other, mutagenic agents (e.g. ROS or RNS). Pathways that facilitate development of fibrosis may also contribute to cancer promotion, given the apparent link between fibrosis and the development of lung cancer, which may relate (among other possibilities) to inhibition of fiber clearance (Section 7.3.4.5).

The ERK-MAPK signaling pathway evaluated in multiple studies by Mossman and coworkers (Mossman et al. 1997, Timblin et al. 1998a and b, Zanella et al. 1999) in rat pleural mesothelial (RPM) cells is a case in point (see above). These studies suggest that crocidolite stimulates the ERK-MAPK cascade through interaction with the EGF receptor. This ultimately leads to transcription of mRNA for c-fos. Crocidolite has also been shown to induce c-jun (apparently through a separate mechanism) and the balance between c-jun and c-fos has been implicated in guiding a cell toward either proliferation or apoptosis. Although the direct connection between c-jun/c-fos and apoptosis has not been established, it is observed that crocidolite induces substantial apoptosis in RPM cells at the same concentrations at which it induces substantial expression of c-fos and c-jun. The link is also implied because inhibition of the ERK pathway has been shown in some studies to inhibit asbestos-induced apoptosis. Na-erionite has also been shown to induce c-fos at levels comparable or higher than crocidolite for comparable exposures (at least on a mass basis) and induce c-jun at higher levels. However, it is not known whether Na-erionite and crocidolite act via the same pathways. Potentially due to the increased, relative expression of c-jun induced by Na-erioinite, increased apoptosis is not observed in association with exposure to Na-erionite. However, the link between increased c-jun expression and inhibition of apoptosis has not been demonstrated explicitly.

Both crocidolite and Na-erionite were also shown by Mossman and coworkers to induce uptake of bromodeoxyuridine (BrdU) by RPM cells in these same experiments. Uptake of BrdU is an indicator of DNA synthesis. Since it has also been shown that crocidolite is capable of damaging DNA via ROS and other pathways (Sections 7.3.3) and both crocidolite and erionite are known to induce mesotheliomas in any case, the balance between proliferation and apoptosis in this cell population that is struck by exposure to these toxins may very well determine whether development of cancers are promoted or prevented. Of course, both proliferation and apoptosis may also be mediated by other pathways independent of the ones described here.

The problem is that the range of responses that are induced by asbestos in the lung are varied and complex (see Table 7-5) so that it has not yet been possible to definitively identify the biochemical triggers that lead to lung cancer or mesothelioma. It is even likely, for example, that different mechanisms (or combinations of mechanisms) predominate under different exposure conditions or in association with differing fiber types or particle sizes. Still, examination of the dependence of candidate mechanisms on fiber type and particle size can be instructive, especially to the degree that such indications are consistent with observations in whole animal studies (see, for example, Section 7.2.2). For the signaling cascade described above by Mossman and coworkers, for example, the effects attributable to crocidolite are clearly dependent on fiber size because the non-fibrous analog to crocidolite, riebeckite does not induce any of the effects. It also appears that the chemistry of the fibers is important, given the observed differences in responses among the various, substituted erionites.

7.3.4.3 Asbestos-induced apoptosis. Apoptosis (programmed cell death) is generally triggered when a cell accumulates certain types of genetic damage, when cell signaling cascades are triggered by external stimuli that may occur, for example, as part of the need to maintain tissue homeostasis or to cause a phenotypic shift in response to toxic challenge (see, for example, Holian et al. 1993, Section 7.3.4.2), or when a cell has completed a pre-programmed number of divisions. Asbestos can induce apoptosis in a variety of cells by several mechanisms including primarily:

- by causing sufficient genetic damage to trigger apoptosis; or
- by triggering a signal cascade that leads to apoptosis.

As previously indicated, asbestos may trigger signaling cascades by interacting directly with receptors on the cell surface, by reacting with integrins for such receptors, or by inducing production of intermediate species (such as ROS or RNS) that may in turn induce cell signaling.

Some of the mechanisms by which asbestos may act to induce apoptosis may be fiber size- or type-dependent. Also, responses may vary in different target tissues.

Fibers:

- As indicated in Section 7.4.3.2, crocidolite (but not the non-fibrous analog riebeckite) induces apoptosis in hamster tracheal epithelial cells and rat pleural mesothelial cells when applied at non-cytotoxic concentrations (Mossman et al. 1997). Results from the study also indicate that apoptosis is triggered in this case by inducing an ERK-MAPK signaling cascade as a consequence of interaction with EGF receptors on the cell surface. The interaction may be direct or may be caused by asbestos-induced ROS. In a related study (also previously summarized, Section 7.3.4.1), Timblin et al. (1998a) indicate that the asbestos-induced apoptosis reported in the Mossman et al. work is fiber-type specific and the pathway involved appears to stimulate expression of c-fos.

- In a study previously reported in greater detail (Section 7.3.4.1), Levresse et al. (1997) indicate that chrysotile induces apoptosis in cultured rat pleural mesothelioma cells with the effect peaking at 4% at 72 hours following exposure to 10 $\mu g/cm^2$. Although the authors observed a much smaller effect with crocidolite, they indicate that the difference is likely due to the much smaller number of long fibers in the particular crocidolite sample evaluated.

- Broaddus et al. (1997) indicates that crocidolite (not UICC) but not wollastonite, glass beads, or non-fibrous riebeckite cause substantial apoptosis in rabbit pleural mesothelioma cells in culture in a dose-dependent fashion. The extent of apoptosis induced was inhibited by treatment with catalase and by 3-minobenzamide (an inhibitor of poly(ADP-ribosyl) polymerase. The former indicates a role for ROS mediation and the latter indicates that this enzyme, which mediates DNA repair, also mediates asbestos-induced apoptosis (perhaps triggered by asbestos-induced DNA damage). Asbestos induced apoptosis was also inhibited by treatment with desfeoxamine, but effects were restored by adding iron to the medium. The authors note that in other studies, crocidolite has been shown to induce DNA strand breaks within 2 hrs after exposure and induces unscheduled DNA synthesis within 24 hrs following exposure. Asbestos also induces production of poly(ADP-ribosyl) polymerase

Non-fibrous particles:

- Leigh et al. (1997) intratracheally instilled rats with silica (a non-fibrous particle) at doses varying between 2 and 22 mg. They then collected cells by bronchio-alveolar lavage (BAL) 10 days after instillation. The authors observed large numbers of apoptotic cells in BAL fluid and that the number of such cells was dose-dependent. The dead cells were primarily neutrophils (so that this might represent some type of mechanism to restore homeostasis). Engulfment of apoptotic cells by macrophages was also observed. The authors report that, 56 days after instillation, apoptotic cells were observed in granulomatous tissue within the lungs of rats exposed to silica. This suggests that apoptosis may also occur in response to chronic inflammation. The authors conclude that silica induces apoptosis among granulomatous cells and alveolar cells and that such apoptosis and the subsequent engulfment of apoptotic cells by macrophages may play a role in the evolution of silica-related disease. The authors also note that granuloma formation is a hyperplasia-related event.

At least some of the mechanisms suggested above for asbestos-induced apoptosis are dependent on fiber size (the non-fibrous analog of crocidolite does not induce the effect) and dependent on the chemistry of the fibers involved (various, cation-substituted analogs of erionite exhibit disparate ability to induce the effect). Although non-fibrous particles (such as crystalline silica) may also induce apoptosis, as previously suggested, this may be through separate mechanisms from those responsible for asbestos-related effects, even if the same end point results.

7.3.4.4 Asbestos-induced cytotoxicity. While there is ample evidence from various in-vitro studies that asbestos is cytotoxic, such effects are observed almost exclusively at the highest concentrations evaluated in an experiment (for example, Luster and Simeonova 1998, Section 7.3.4.2 and Choe et al. 1999, Section 7.3.4.2). Many experiments are conducted at concentrations below those for which cytotoxicity is important because the other toxic effects attributable to asbestos occur at substantially lower exposure levels and researchers prefer to study such effects in the absence of potentially confounding cytotoxicity. For in-vitro studies, for example, non-cyotoxic effects are typically studied at concentrations less than approximately 10 $\mu g/cm^2$ (or 20 $\mu g/ml$) while substantial cytotoxicity is not typically observed until exposure concentrations are several times higher.

Because most of the other effects attributable to asbestos occur at concentrations that are substantially lower, this begs the question as to whether frank cytotoxicity is an effect that is relevant to human exposures. There is also substantial evidence that the mechanisms associated with asbestos-induced cytotoxicity are separate from the mechanisms that mediate most of the other asbestos-related effects of interest.

- Kamp et al. (1993) dosed cultured pulmonary epithelial (PE) cells with UICC amosite asbestos. In some studies, polymorphonuclear leukocytes (PMN) were also added to the culture. Typical doses in this experiment were on the order of 250 μg/cm^2, which is quite high for these types of studies. For example, compare this level with the levels reported for studies of ROS/RNS generation (Section 7.3.3), cell signaling (Section 7.3.4.2), proliferation (Section 7.3.4.1) or apoptosis (Section 7.3.4.3).

  Kamp and coworkers indicate that the effect of amosite exposure on cultured PE cells (at the concentrations studied) was to induce substantial cell lysis (cytotoxicity) and little cell detachment (from the culture medium), which would indicate increased cell motility. Addition of PMN to the culture resulted in both increased cell lysis and cell detachment for comparable exposures to amosite. The observed cell detachment was mitigated in a dose-dependent fashion by adding protease inhibitors. Further work indicated that asbestos induces release of human neutrophil elastase (HNE), which may mediate the combined effects with PMN. PE cell exposure to HNE alone causes increases in cell detachment in a dose-dependent fashion. However, when combined with asbestos exposure, cell lysis increases at the expense of cell detachment. The authors suggest that HNE becomes bound to asbestos, which also becomes bound to PE cells and this facilitates augmented cytotoxicity by proteases that are secreted by PMN's.

- Blake et al. (1998) studied the effect of fiber size on the cytotoxicity of alveolar macrophages in vitro. Cultured cells were dosed with concentrations varying between 0 and 500 μg/ml of each of 5 different length preparations of JM 100 glass fiber. Cytotoxicity was monitored by assays for extracellular LDH and by chemiluminescence following zymosan addition. The latter assy is intended to show macrophage stimulation. Results indicate that all samples showed dose-dependent increases in toxicity (i.e. increasing LDH and decreasing chemiluminescence). Comparing across samples, relatively long fibers (mean = 17 μm) showed the greatest toxicity. The authors further indicate that microscopic examination suggests that frustrated phagocytosis plays a role in cytotoxicity.

- Goodglick and Kane (1990) studied the effect of three different length preparations of crocidolite (long, short, and UICC) on elicited macrophages (stimulated initially with thioglycolate) in vitro and in vivo. The long and short samples were reportedly prepared from the UICC sample by repeated centrification. Goodglick and Kane report that all three types of crocidolite

stimulated release of ROS from macrophages. At sufficiently high concentrations, all three also caused substantial cytotoxicity, although apparently due to the longer time required to settle in culture, the full effects from short fibers take longer to develop. They suggest that, on a total fiber number or surface area basis, long and short crocidolite appear to exhibit approximately equal potency toward the cytotoxicity of macrophages. Further work with various inhibitors indicates that cytotoxicity is mediated by production of ROS and that ROS is produced via an iron-dependent pathway. They also indicate that, among the effects of crocidolite exposure is that macrophage mitochondrial membranes are depolarized

Goodglick and Kane also evaluated the effects of long and short crocidolite in vivo. This was done by evaluating the effects of intraperitoneal injection of the various samples (long, short, or mixed crocidolite or titanium dioxide particles) in C57B1/6 mice. Results indicate that a single injection of long crocidolite (480 µg) induced an intense inflammatory response, leakage of albumin, and fibers observed scattered across the diaphragm. In contrast, a single injection of short crocidolite (600 µg) induced only a relatively mild inflammatory response and only limited clusters of fibers observed on the surface of the diaphragm.

To test whether short fibers would show a greater response, if they were not cleared more readily than long fibers, Goodglick and Kane also subjected mice to 5 consecutive, daily injections of 120 µg of short crocidolite and noted more substantial aggregations of fiber clusters along the diaphragm as well as a more pronounced inflammatory response. Cell injury was also assessed by Trypan blue staining (which indicates cell death). All mice singly or multiply injected with mixed or long crocidolite showed marked Trypan blue staining. Single injections of short structures showed only limited Trypan blue staining. However, following 5 daily injections of short fibers, multiple Trypan blue stained cells were observed on the diaphragm in the vicinity of the locations were clusters of fibers were also observed. The authors also indicate (in contrast) that neither single injections of 160 or 800 µg nor 5 consecutive (160 µg) injections of titanium dioxide produced any Trypan blue staining.

The authors conclude from this study that both short and long crocidolite fibers appear to be cytotoxic to macrophages while titanium dioxide particles are not (suggesting that not only fiber length, but fiber type is important to cytotoxicity). They further suggest that, while short fibers tend to be cleared rapidly in vivo, when such clearance mechanisms are overwhelmed (such as by repeated insult through repeated, daily injections in this study), then the toxic effects of short

structures becomes apparent. As indicated in other studies, however, there may be multiple mechanisms working to produce similar responses, that such mechanisms may exhibit varying dose-response characteristics, and that cytotoxicity may not generally be directly related to mechanisms that contribute to carcinogenesis. Moreover, there almost certainly are at least some longer fibers in the short fiber preparation and extended analysis to determine their relative concentration with adequate precision would be helpful to see if the relative magnitude of the observed effects correlate.

- Palekar et al. (1979) studied the ability of four different samples of commingtonite-grunerite, each also subjected to varying degrees of grinding, to induce hemolysis of mammalian erythrocytes and cytotoxicity to Chinese hamster ovary (CHO) cells. The samples studied include: UICC amosite (4.13 m^2/g surface area/mass), which is denoted as "asbestiform grunerite; "semi-asbestiform" commingtonite (3.88 m^2/g); acicular commingtonite (ground to three particle sizes: 3.76, 2.45, and 0.82 m^2/g), and acicular grunerite (2.82 m^2/g).

  Results from this study indicate that amosite induced the greatest hemolysis of erythrocytes by far (approximately 50%) while acicular, unground grunerite caused no hemolysis. However, grinding the acicular grunerite to increasingly smaller particle sizes and greater surface area ultimately results in some hemolysis. Both semi-asbestiform and acicular, unground commingtonite show hemolytic activity between amosite and unground, acicular grunerite and grinding acicular commingtonite also increased its hemolytic activity.

  Similar results were also observed for cytotoxicity. Amosite was by far the most cytotoxic and the effect was dose-dependent. A dose of 0.05 mg/ml caused approximately 75% cell death for CHO cells. At 0.2 mg/ml, only 1% of cells survived. Acicular grunerite was nontoxic even at 0.5 mg/ml. With grinding, acicular grunerite cytotoxicity increased, albeit only slowly. The most heavily ground sample killed fewer than 25% of cells at 0.2 mg/ml and killed only 65% at 0.5 mg/ml. The cytotoxicity of semi-asbestiform commingtonite was substantially less than amosite but greater even than ground, acicular grunerite. For this material, 0.2 mg/ml killed approximately 65% of cells and 0.5 mg/ml killed approximately 90%. Interestingly, approximately the same dose-response curve for cytotoxicity was observed for the 3.88 and 1.61 specific surface area samples of this material. The 1.21 samples was somewhat less cytotoxic. Acicular commingtonite was somewhat less cytotoxic (for corresponding doses) than semiasbestiform commingtonite at the highest specific surface area (3.76) and its toxicity decreased with decreasing surface area.

> The authors also indicate that neither surface charges on crystal particles nor Magnesium ion content appear to correlate with biological activity. The authors conclude that the degree of "asbestiform" character of a mineral has a dominant effect on biological activity. Moreover, although non-fibrous particles may also be biologically active (and their activity increases with increasing specific surface area), the effects of particles and fibers lie along entirely separate dose-response curves. The biological activity of fibrous materials does not appear to depend directly on specific surface area.

Importantly, the results of the Palekar et al. (1979) study are also consistent with the possibility that fibrous structures within a specific range of sizes and shapes contribute strongly to biological activity while largely non-fibrous particles act through a separate mechanism that depends primarily on total surface area but that, particle-for-particle, elicits a substantially lower overall response than the mechanism by which fibers act. Such a scenario is supported by several studies. Jaurand (1997), for example, indicate that ROS is implicated in the cytotoxicity of long but not short fibers on tracheal epithelial cells. Although the evidence for distinct mechanisms for fibers and particles discussed here is specific to cytotoxic and hemolytic effects, evidence in other studies suggest similar scenarios for other toxic end points (potentially including end points that contribute to carcinogenicity).

Comparisons of the rate and extent of effects observed in epidemiology studies, whole animal dose-response studies, and in vitro studies suggests that cytotoxicity may not be important to human exposures. Unfortunately, however, there is currently insufficient information to compare doses and exposures across these studies in a more quantitative fashion. Therefore, the importance of cytotoxicity to human asbestos exposure cannot be definitively determined at this time.

7.3.4.5 Association between fibrosis and carcinogenicity. The hypothesis that lung tumor induction is associated with the fibrosis has been examined by several authors. There appears to be a debate as to whether fibrosis is a necessary precursor for development of lung cancer (associated with exposure to fibers), whether the presence of fibrosis is an additional factor contributing to increased risk for lung cancer, or whether the two diseases are largely unrelated. This is an important consideration because the characteristics of the dose-response relationship between asbestos and lung cancer or asbestosis (fibrosis) apparently differ (see Chapter 6 and Sections 7.3.6 and 7.4).

Based on animal studies, Davis and Cowie (1990) found that rats that developed pulmonary tumors during inhalation experiments exhibited a significantly greater clinical

degree of fibrosis than rats that did not develop tumors. Furthermore, Davis and Cowie reported suggestive evidence that the pulmonary tumors that did develop in the dosed rats tended to develop within portions of the rat's lungs that were already scarred by fibrosis.

As part of a review, Mossman and Churg (1998) indicate that fibrosis of any cause (including diffuse idiopathic fibrosis) appears to be associated with an increased risk of lung cancer and that this is observed in both human and animal studies. They also indicate that only those strains of mice and hamsters that develop fibrotic lesions following exposure to crystalline silica show an increased risk of developing cancer. They also report that, in parallel to what is reported for asbestos by Davis and Cowie (1990), lung tumors that develop following exposure to crystalline silica tend to occur primarily (if not exclusively) in those portions of the lung where fibrotic lesions predominate.

In contrast, Case and Dufresne (1997) from their study of lung burdens among Quebec miners and millers indicate that there is high overlap in the range of concentrations that lead to both lung cancer and asbestosis and those that lead to lung cancer alone, which the authors suggest show a lack of relationship between the two diseases (one is not predictive of the other). The authors indicate that, based on regression of the 111 cases they examined, the only indicator that reasonably tracks lung cancer is severity of smoking and they indicate that this is true despite the level of fiber content in the lung.

Although a definitive determination concerning the relationship between fibrosis (asbestosis) and lung cancer cannot be developed at this time, it does appear that there is some association between the two diseases. Most likely, fibrosis is an additional risk factor for lung cancer and thus represents an additional set of mechanisms that may contribute to the overall risk of developing lung cancer in association with exposure to asbestos. However, based on the evidence as a whole, including the evidence that the character of the dose-response relationship for lung cancer and asbestosis differ, it is not clear that development of fibrosis is an absolute precursor that is required before asbestos-related lung tumors can develop. Interestingly, based on the studies reviewed by Mossman and Churg (1998), the relationship between fibrosis and lung cancer induced by silica may be substantially stronger than that between fibrosis and lung cancer induced by asbestos.

7.3.4.6 Synergism between asbestos and smoking. Numerous studies have confirmed the synergistic relationship between smoking and asbestos exposure toward the induction of lung cancer (see, for example, Hammond et al. 1979, Kamp et al. 1992,

Kamp et al. 1998, Mossman et al. 1996). Smoking is also suspected to facilitate development of asbestos-induced fibrosis (Kamp et al. 1992).

Putative mechanisms that may contribute to synergism between asbestos exposure and smoking include:

- facilitated transport of carcinogenic components of smoke that may be adsorbed on the surface of asbestos fibers, which may then serve as vehicles to transport these materials through cell membranes to cell interiors and even to locations adjacent to or within the nucleus (see, for example, Fubini 1997, Mossman et al. 1996);

- asbestos-catalyzed production of more highly mutagenic metabolites of the various components of smoke, including benzo(a)pyrene (see, for example, Mossman et al. 1996);

- smoke-product induced inhibition of clearance of asbestos fibers and/or asbestos induced inhibition of clearance of smoke products (see, for example, Mossman et al. 1996); and

- smoke-product induced facilitation of uptake of asbestos by lung epithelium (see, for example, Mossman et al. 1996).

Although much progress has been made at elucidating the nature of these mechanisms and other candidate mechanisms, at this point in time it is possible to indicate definitively neither what mechanisms are important to the observed synergism between smoking and asbestos exposure nor to indicate the relative magnitude of the contributions from such mechanisms. Moreover, a detailed review of such mechanisms is beyond the scope of this document.

7.3.4.7 Conclusions concerning asbestos as a promoter. There is strong evidence that asbestos acts as a promoter for cancer. While this may primarily involve mechanisms the contribute to the induction of proliferation, mechanisms associated with the well-established synergism between smoking and exposure to asbestos (for the induction of lung cancer; smoking does not appear to affect mesothelioma) are also important. There also appears to be an association between the development of fibrosis and an increased risk for lung cancer.

Evidence indicates that multiple mechanisms may be involved with asbestos-induced cancer promotion and that such mechanisms may be complex and interacting. The

different mechanisms also appear to exhibit dose-response relationships with differing characteristics. While there are indications that the most important among these mechanisms may be strong functions of fiber size (with long fibers contributing most to the induction of disease), mechanisms that depend primarily on surface area or total fiber (particle) number (for any size range) may also contribute to overall cancer promotion. Importantly, these latter mechanisms also appear to be strongly associated with the composition of fibers (particles) and may therefore contribute more substantially to the disease induction of agents that have been shown to be particularly toxic (such as crystalline silica), as opposed to particles, fibers, or asbestos in general.

At this point in time, the available data may not be sufficient to distinguish among the relative contributions from the various mechanisms to the overall promotion of cancer, at least in terms of the mechanistic data itself. Importantly, however, the mechanistic data should not be considered to be inconsistent with the results from whole animal studies, where there are clearer indications that fiber size plays a major role in carcinogenicity and fiber (particle) type is also important (see Sections 7.2 and 7.4). Such studies indicate, for asbestos (and other biodurable fibers) that:

- short fibers (less than somewhere between 5 and 10 μm) do not appear to contribute to disease;
- potency likely increases regularly for fibers between 10 μm and a minimum of 20 μm (and, perhaps, continues to increase up to lengths of at least 40 μm); and
- fiber type may be important primarily in determining biodurability.

They further indicate that particularly (or uniquely) toxic particles (such as crystalline silica) may act through a different set of mechanisms that are not dependent on fiber length but that induce toxic end points paralleling those observed for asbestos.

Importantly, the mechanisms by which asbestos may act as a promoter appear to occur in cell lines that may contribute both to the induction of lung cancer and mesothelioma.

7.3.5 Evidence that Asbestos Induces an Inflammatory Response

There is ample evidence that asbestos induces an inflammatory response in pulmonary tissues and the pleura (see, for example, Sections 7.2.2 and 7.3). Moreover, there appears to be multiple biochemical triggers that mediate this response and various mechanisms may be fiber size- and/or fiber type-specific (Table 7-5). Because the role

that inflammation plays in the induction of cancer has been addressed elsewhere (Sections 7.3.3 and 7.3.4), it is beyond the scope of this document to provide a detailed review of the mechanisms that lead specifically to inflammation.

7.3.6 Evidence that Asbestos Induces Fibrosis

There is ample evidence that asbestos induces fibrosis in pulmonary tissues (see, for example, Sections 7.2.2 and 7.3). Moreover, there appears to be multiple biochemical triggers that mediate this response and various mechanisms may be fiber size- and/or fiber type-specific (Table 7-5). Because the role that fibrosis plays in the induction of cancer has been addressed elsewhere (Sections 7.3.3 and 7.3.4), it is beyond the scope of this document to provide a detailed review of the mechanisms that lead specifically to fibrosis. Such mechanisms have also been the subject of recent reviews (see, for example, Mossman and Churg 1998 and Robledo and Mossman 1999).

7.3.7 Evidence that Asbestos Mediates Changes in Epithelial Permeability

As previously indicated (Section 4.4), maintaining the overall integrity of the epithelial surface of the lung is among the various functions of Type II epithelial cells (Leikauf and Driscoll 1993). It has been shown that asbestos induces changes in the morphology of Type II epithelial cells (see, for example, Ilgren and Chatfield 1998), which has the effect (among others) of increasing the overall permeability of lung epithelial tissue to various macromolecules and, potentially to asbestos fibers themselves. The former plays a role in asbestos-induced fibrosis (by allowing cytokines that stimulate fibroblast proliferation or stimulate fibroblasts to generate extracellular matrix to pass through the epithelium and reach the underlying fibroblasts, Section 7.3.6). The latter may be important to facilitating transport of asbestos from the alveolar lumen to the interstitium (see, for example, Lippmann 1994).

Changes in epithelial permeability may be triggered by cytokines released from other cells or by the action of asbestos fibers on epithelial cells directly. Moreover, some of the mechanisms that mediate this response may be sensitive to fiber size and/or fiber type. For example, Gross et al. (1994) showed that monolayers of human bronchial epithelial cells cultured over a porous medium and exposed to cryogenically ground chrysotile (average length: 1 μm, average aspect ratio:14 at 15 μg/culture plate) became permeable to fibrin breakdown products (FBP's). The cultures were grown over human serum with labeled fibrinogen. This was based on observed increased concentrations of FBP's (double in 24 hrs) in the ablumenal chambers of exposed cells compared to cells in control cultures. Because the epithelium showed greater permeability to all concentrations, the increased concentrations were not due to

increased breakdown. The observed FDP flux was not vectoral, not saturable, and required neither proteolytic processing nor active transport. Thus, asbestos increases the paracellular flux of intact FDP across airway epithelium.

7.3.8 Conclusions Regarding the Biochemical Mechanisms of Asbestos-Related Diseases

That the specific biochemical triggers for asbestos-related diseases (particularly, the asbestos-related cancers) have not been definitively delineated as of yet is not surprising. The detailed interactions between fibers (and particles) and the cells and tissues of the lung are complex and there are complex, multiple, interacting mechanisms by which such interactions may contribute to disease. Despite great progress in elucidating candidate mechanisms, the number of candidate mechanisms is large and distinguishing among their relative contributions has been difficult. This is because, among other things, the ability to compare results across studies of different mechanisms is currently limited due to the inability to reconcile the quantitative effects of dose and response across dissimilar studies.

Nevertheless, a number of important implications can be gleaned from the available literature. First, it appears that asbestos can function both as a cancer initiator and a promoter. It also appears that both the initiation and promotion of cancer may occur through more than one mechanism.

Regarding cancer initiation, asbestos likely acts primarily through a mechanism involving interference with mitosis. By this mechanism, asbestos fibers are phagocytized by target cells, migrate to perinuclear locations, and interact with the spindle apparatus and other cell assemblages required to complete mitosis. This tends to result in aneuploidy and may cause various clastogenic effects. This mechanism is driven by long fibers; short fibers do not appear to contribute to the effect. It also appears that all asbestos fiber types (and potentially other durable fibers with sufficient dimensions) cause genetic damage via this mechanisms. If there are effects due to fiber type, they appear only to play a secondary role.

Although there is also evidence that asbestos may induce production of DNA adducts and DNA strand breaks (through ROS and RNS mediated pathways), whether such adducts or breaks ultimately lead to permanent, heritable changes to DNA remain to be demonstrated. The relative importance of ROS/RNS mediated pathways for initiating cancer, compared to the pathway involving interference with mitosis, also remains to be determined.

There is also some evidence that the relative importance of asbestos as a cancer initiator may differ in different tissues. Lung epithelial cells, for example, appear to be relatively resistant to the mechanisms by which asbestos may initiate cancer. Mesothelial cells are not. Among several possibilities, this may be due to the ability of proliferation-competent lung epithelial cells (Type II cells) to undergo terminal differentiation when challenged with certain toxins and this is a pathway not available to mesothelial cells.

The mechanisms by which asbestos may promote cancer primarily involve mechanisms that contribute to the induction of proliferation, although mechanisms associated with the well-established synergism between smoking and exposure to asbestos to induce lung cancer are also important. There also appears to be an association between the development of fibrosis (including asbestosis) and an increased risk of lung cancer.

Evidence indicates that multiple mechanisms may be involved with asbestos-induced cancer promotion and that such mechanisms may be complex and interacting. The different mechanisms also appear to exhibit dose-response relationships with differing characteristics. While there are indications that the most important of these may be strong functions of fiber size (with long fibers contributing the most to carcinogenicity), mechanisms that depend primarily on surface area or total fiber number (for any size range) may also contribute to overall cancer promotion. These latter mechanisms also appear to be strongly associated with the composition of fibers and may therefore contribute more substantially to the disease induction of agents that have been shown to be particularly toxic, as opposed to particles, fibers, or asbestos in general.

Although crystalline silica may act to produce some of the same effects as asbestos (including carcinogenicity), there is substantial evidence that this family of materials do not act through the same pathways and that the characteristics of their respective dose-response relationships may differ. Thus, for example, while asbestos likely induces cancer through mechanisms that favor long (and potentially thin) fibers, silica more likely acts through a mechanism that is dependent on total surface area, with freshly and finely ground material likely being the most potent. In contrast, grinding asbestos fibers tends to lesson its carcinogenicity overall. Due to differences in chemistry and crystallinity (reinforced by studies indicating a lack of correspondence in behavior), crystalline silica does not appear to be an appropriate analog for any of the asbestos fiber types. Rather, for example, the appropriate non-fibrous analog for crocidolite is riebeckite and the appropriate non-fibrous analog for chrysotile is antigorite or lizardite.

7.4 ANIMAL DOSE RESPONSE STUDIES

Ideally, human epidemiology studies (reviewed in Chapter 6) provide the best data from which to judge the effects of asbestos in humans and they certainly provide the only reliable information from which to derive dose-response factors for humans. However, animal dose-response studies have proven useful for elucidating certain features of the relationship between asbestos dose and response that cannot be adequately explored in the human studies, primarily due to limitations in the manner that exposures were characterized in the human studies (see Chapter 5).

Unlike human epidemiology studies, exposures in animal studies are controlled and better quantified. Frequently, the characteristics (in terms of fiber size, shape, and type) of such exposures have also been better quantified and this has allowed exploration of the effects that such characteristics (fiber size, shape, type) have on disease response. Accordingly, an overview of animal dose-response studies is provided in this section. Both injection-implantation studies and inhalation studies are reviewed. Particular attention is also focused on a "supplemental" animal inhalation study that we conducted with the specific aim of identifying the characteristics of asbestos that best relate to risk. The strengths and limitations of these kinds of studies are described in Chapter 5.

7.4.1 Injection-Implantation Studies

Because the fibrous materials in injection and implantation studies are placed immediately against the target tissue, the effects of processes associated with inhalation, retention, and translocation are avoided. The only active mechanisms that need to be considered in these studies are those that occur directly in the target tissue (including degradation, clearance, and biological responses of the types described in the previous sections of this chapter) Fibrous materials placed against the tissue surface are subject to dissolution, phagocytosis by macrophages, and phagocytosis by the cells of the target tissue. These mechanisms are described in greater detail in Section 7.2. A range of biologic responses have also been observed (described in Section 7.3).

Numerous researchers have performed these types of studies.

The work of Stanton et al. In a series of studies, Stanton et al. (1972, 1977, and 1981) implanted fibrous materials and induced mesotheliomas in rats. In the studies, a pledgette composed of coarse glass is loaded with hardened gelatin containing sample material and is surgically implanted immediately against the left pleura of the rats. Control studies demonstrate that the coarse glass of the pledgette does not induce significant tumors in the absence of other tumorigenic agents in the gelatin.

Although the mass dose of material implanted was the same for all experiments (40 mg), the observed incidence of mesothelioma varied among samples. By characterizing the dimensions of fibrous structures in the samples using a microscope, the researchers were able to explore the relationship between fiber size and the incidence of mesothelioma. By studying a wide range of fibrous materials, Stanton and his coworkers concluded that the induction of mesothelioma is determined primarily by the physical dimensions of fibers and that mineral composition is secondary. Further, potency appears to increase with the length and decrease with the diameter of fibrous structures. The researchers also concluded that the incidence of malignant tumors correlates with the degree of fibrosis induced by the presence of the fibrous materials. This does not necessarily imply, however, that fibrosis is a necessary step in the induction of asbestos-induced tumors (see Section 7.3.4.5).

Conclusions from the Stanton et al. studies indicating that mineralogy is not a factor in biological response conflicts with evidence provided in Chapter 6 and implications gleaned from mechanism studies presented in Section 7.3. However, the Stanton et al. studies have been shown to suffer from certain methodological limitations (Berman et al. 1995) so that results from these studies should be considered more qualitative than quantitative.

Due to limitations in the ability to produce samples composed of uniform fibers, quantitative relationships between size and potency were explored by Stanton et al. (1972, 1977, and 1981) using a regression analysis. Structures longer than 8 μm with diameters less than 0.25 μm or longer structures with diameters less than 1.5 μm were found to represent the range of sizes that best correlate with carcinogenicity. It was further stated that such correlations did not eliminate the possibility that other size ranges also contribute to potency, only that the two size ranges identified appear to correlate best. Samples that varied significantly from the reported correlations were attributed to errors in the characterization of structure size distributions in those samples. However, other methodological limitations might also have contributed to the observed deviations or such "outliers" may also suggest evidence for a mineralogical effect that is similar to what is reported in other studies (see Section 7.3 and Berman et al. 1995).

The precision of estimates for the ranges of sizes that contribute to biological activity that are derived from the Stanton et al. studies is limited so that such estimates should also be considered qualitative. Size distributions were determined by characterizing 200 to 1,000 structures using TEM and there is no indication that statistically balanced counting rules were employed (Section 4.3). Under such conditions, counts of structures longer than 8 μm are likely small and subject to large uncertainties for most

of the samples characterized. Confidence intervals are not provided for any of the counts presented in these studies.

Potentially larger errors in the Stanton et al. studies could have been introduced by the method employed to relate fiber counts to sample mass. As indicated in Chapter 5, estimating contributions to mass by sizing total particles and assuming that this is proportional to total sample mass is subject to error from the limit to the precision of characterizing structure dimensions (particularly diameter) and by not accounting for nonasbestos (and possibly nonfibrous) material in the samples.

Thus, for example, there is no discussion of the precision with which the cut point of 8 μm was determined in these studies. Based on the manner in which size distribution data are presented, it is unlikely that cut points that vary by up to a factor of 2 would lead to substantial difference in the quality of the correlation. For example, a cut point of 5 μm may not be distinguishable from 8 μm within the database examined.

Re-analysis and extension of the Stanton studies. Several researchers have re-evaluated data from the implantation studies to test additional hypotheses. Using the Stanton data, Bertrand and Pezerat (1980) examined the relationship between mesothelioma incidence and several characteristics not evaluated by Stanton et al. including: average fiber length, average fiber diameter, average fiber aspect ratio, total fiber surface area and total fiber volume. Results from the regression analysis indicate that potency varies directly with average length and inversely with average diameter but that neither parameter is a good indicator alone. Combining the effects of length and diameter, average aspect ratio is highly correlated with potency. Biological activity does not correlate highly with structure count, surface area or volume except when fiber sizes are restricted to the long, thin structures that Stanton defined. Results of this study are not inconsistent with those originally presented by Stanton except that they emphasize a set of characteristics that relate parametrically to biological activity rather than expressing exposure as a single restricted size range of structures.

It is important to note that Bertrand and Pezerat were able to find good correlations between response and specific "average" characteristics of the samples that are not proportional to the quantity of the material present in the sample ("intensive" characteristics). Such intensive characteristics as average aspect ratio, average length, or average diameter are properties that are independent of the mass of material in a sample. Since response must be a function of the quantity of sample present, intensive characteristics should have to be multiplied by characteristics that are proportional to the mass of a sample (e.g. fiber number, sample mass, or sample volume) in order to

relate them to response. Properties that vary with the mass of a sample are termed "extensive" properties.

The correlations between intensive properties and response reported by Bertrand and Pezerat likely succeed within the Stanton database because a constant sample mass (40 mg) was employed for all of the implantation experiments. However, to apply dose/response relationships that are dependent only on intensive characteristics beyond the Stanton data (where mass dose will not be constant), it is necessary to pair intensive characteristics with extensive characteristics (such as mass or number of fibers per sample). Therefore, it is unclear how the conclusions from this paper may be generalized to other data sets.

In a similar study, Bonneau, et al. (1986) also examined parametric relationships between structure characteristics and mesothelioma induction. The paper examined specifically correlations between carcinogenicity and dose in terms of two specific relationships: dose expressed as fibers longer than 8 μm that are thinner than 0.25 μm ("Stanton" fibers) and dose expressed as mean aspect ratio. The researchers conclude that mean aspect ratio provides an excellent indication of carcinogenicity for individual fiber types but that each fiber type must be treated separately. Poorer correlations are found for the relationship between the concentration of "Stanton" fibers and mesothelioma, even when fiber types are considered independently. Although these results appear to be consistent with findings reported from mechanistic studies (Chapter 6, Sections 7.2 and 7.3) in that they posit a role for fiber mineralogy, the relationships evaluated by Bonneau et al. also suffer from the limitation of expressing dose only in terms of intensive quantities, as discussed above. Direct comparison with other studies is therefore difficult.

Following up on the reported problems characterizing crocidolite in Stanton's work, Wylie et al (1987) reanalyzed seven crocidolite samples originally studied by Stanton. She and coworkers then used the new size distributions to reevaluate the "Stanton hypothesis" (that the concentration of Stanton fibers in a sample correlates with carcinogenicity). Wylie and coworkers note that substantial deviations from the Stanton hypothesis occur for specific samples. They conclude that a specific structure size range alone is not sufficient to characterize biological activity and that a parametric relationship with other structure characteristics (potentially including mineral type) may be necessary to sufficiently describe biological activity.

Conclusions from the Wylie et al. paper must be interpreted carefully because the researchers evaluated only the relationship between carcinogenicity and the single specific size range indicated ("Stanton" fibers). Thus, the possibility that improved

correlations exist between biological activity and different size ranges or a combination of size ranges cannot be ruled out. Qualitatively, conclusions presented in this paper are not inconsistent with the conclusions reported by Stanton et al. regarding the general relationship between response and fiber dimensions.

The Wylie et al. study appears to suffer from several methodological problems. These relate to the manner in which the sample reanalysis was performed. The drop method for preparing electron microscopy grids (used in this study) is not satisfactory for preparing grids. In fact, as reported in the study itself, grids prepared as duplicates by this method were shown to be non-uniform at the 95% confidence interval using a chi squared test. In addition, only 100 to 300 fibers were counted for each sample. Since there is no indication that statistically balanced counting was performed, the uncertainty associated with counts of Stanton fibers may be substantial. Such errors would be further multiplied by uncertainty introduced during the sizing of total particles to determine the number of fibers per unit mass.

In a later study, Wylie et al. (1993) examined the effect of width on fiber potency. In this latter study, results from animal injection and implantation studies were pooled and subjected to regression analyses to identify correlations between exposure and tumor incidence. The animal studies selected for inclusion in this analysis were performed on a variety of tremolite samples exhibiting a range of morphological and dimensional characteristics.

In their regression analyses, Wylie et al. evaluated a range of exposure indices that emphasize different morphological or size characteristics to help elucidate the characteristics of asbestos that induce a biological response. Because all of the animal studies included in their analyses involved tremolite, mineralogy was not an issue.

Results from the Wylie et al. study suggest that fibers longer than 5 μm and thinner than 1 μm best correlate with tumor incidence among the animal injection and implantation studies examined. Further, they suggest that a width limit, rather than a limit on aspect ratio, better reflects the bounds of the asbestos characteristics that determine biological activity. They also suggest that complex structures (bundles and clusters) need to be evaluated as part of the determination of exposure because such structures can breakdown and contribute to the population of thinner fibers.

Although the results of the Wylie et al. study are interesting and tend to support the general conclusions in this document related to width, if not to length (see Section 7.5 and Appendix B), as the authors themselves indicate, such results should be

considered qualitative due to the limitations imposed on their study by the methodology employed. Their study was conducted by:

- combining results from multiple studies without careful consideration of variation introduced by methodological differences across the studies;
- employing asbestos concentrations determined by SEM and without careful consideration of differences in the counting methodologies employed by differing research groups across studies; and
- considering injection and implantation studies, which (as opposed to inhalation studies) do not account for all of the mechanisms that affect the dose-response relationship in humans.

The limitations imposed by the above constraints are highlighted in Chapters 4 and 5 of this report.

Other injection studies. A series of injection studies were conducted by several research groups. In these studies, fibrous materials were suspended in saline and injected into rats immediately adjacent either to the pleura or peritoneum. A large number of fibrous materials have now been studied by this process, as reported by Pott et al. (1974, 1976, 1978, 1982, and 1987), Muhle et al. (1987), Bolton et al. (1982, 1984, and 1986), Davis et al. (1985, 1986a, 1986d, 1987, and 1988a), and Wagner et al. (1976, 1980, 1982, 1984, and 1985). Newer studies are also discussed in Section 7.2. Results confirm that it is the fibrous nature of the materials that is the primary factor leading to the induction of tumors and that potency appears to depend directly on length and inversely on diameter.

The authors of these studies tend to indicate that, except where fibers are not persistent in vivo due to solubility or other degradation processes, the mineralogy of the fibers appears to play only a secondary role in determining disease incidence. Researchers conducting injection experiments also tended to report a correlation between tumor incidence and the degree of fibrosis induced by the sample. These observations are consistent with the ideas originally articulated by Stanton.

Pott developed Stanton's ideas further by suggesting that carcinogenicity is a continuous function of fiber dimensions, which decreases rapidly for lengths less than 10 μm and also decreases with increasing diameter. The possibility was also raised that the apparent inverse dependence on diameter may be an artifact due to the limited number of thick fibers that can be injected in a sample of fixed mass.

Although the published injection studies indicate that potency decreases with decreasing length, researchers in these earlier studies were reluctant to identify a length below which contributions to carcinogenicity can be considered inconsequential. This may be due in part to the skewed distribution of fiber sizes typical of asbestos dusts. Thus, for example, even if structures less than 5 μm are only 1% as potent as structures longer than 5 μm, they may be as much as 100 times as plentiful in some asbestos dusts, so that the total contribution to potency would be equal for both size fractions.

Reasonable dose/response curves have been generated using various sample masses of a single material in some of these studies. This has been demonstrated for UICC crocidolite and UICC chrysotile "A" (Bolton 1984). Results indicate that the relationship between tumor incidence and the log of the dose may be linear and there is no effective threshold. A consistent difference between the two dusts is apparent; the points lie along separate curves and chrysotile appears to be more potent per unit sample mass.

In general, details of the analytical techniques used for quantifying size distributions in these studies are not fully documented. To the extent that they are, it appears that similar approaches were adopted to those described for the implantation studies above. Consequently, similar limitations apply to the interpretation of results. Briefly, large uncertainties are likely associated with counts of long fibers and estimates of the number of fibers per unit sample mass. Counts in several of the studies also suffer from limitations in the ability of SEM or PCM to detect thin fibers (Section 4.3); whenever SEM or PCM was employed, the thinner fibers were likely under-represented in reported fiber size distributions.

Because samples are placed against mesenchyme in the published implantation and injection studies, results of these studies most directly represent processes associated with the induction of mesothelioma. Assuming, however, that clearance and degradation processes are similar in the deep lung, once a fiber reaches a target tissue, results from the implantation and injection studies may also provide a model of biological response in lung tissue and the factors that lead to the induction of pulmonary tumors. Such a model must be considered qualitative at best, however, because it has been shown that the mechanisms of tissue response to the presence of asbestos in lung parenchyma and in the mesenchyme differ in detail (Section 7.3). The time periods over which the various clearance mechanisms operate in the deep lung and the mesenchyme also differ (Section 7.2), although, it is apparent that the general nature of the clearance and degradation processes in the two tissue types are generally similar.

7.4.2 Animal Inhalation Studies

Animal inhalation studies measure response to exposure in controlled systems that model all of the relevant variables associated with asbestos disease mechanisms in humans (including respirability, retention, degradation, clearance, translocation, and tissue-specific response). Thus, the available inhalation studies are the best database from which to evaluate the integrated effects that lead to the development of asbestos-related disease. Such studies can be used both to identify the characteristics of asbestos that determine biological activity and to qualitatively elucidate the nature of the corresponding relationship between exposure (via inhalation) and the induction of disease.

In this section, the nature and results of the existing animal inhalation studies are described. In the following section, a project undertaken to overcome the limitations of the existing animal inhalation studies is described (the supplemental inhalation study). Because this latter project was specifically designed to support the risk protocol presented in this document, the nature and results of this latter project are described in detail.

The existing animal inhalation database consists of approximately 30 studies of which approximately 20 contain dose/response information based on lifetime monitoring of exposed animals, including the work of Davis et al. (1978, 1980, 1985, 1986a, 1986d, 1988a, and 1988b), Wagner et al. (1974, 1982, 1985, and 1987), Bellman et al. (1987, 1995), Bolton et al. (1982), Le Bouffant et al. (1987), Lee et al. (1981), McConnel et al. (1982), Muhle et al. (1987), Platek et al. (1985), Smith et al. (1987), and Goldstein et al. (1983). The studies are similar in overall design, although detailed differences potentially affect the comparability of results from separate studies.

In the inhalation studies, plugs are formed from bulk samples of fibrous asbestos and related materials, which are placed in a dust generator to be aerosolized. The generators (Beckett 1975), usually a modified version of the apparatus originally designed by Timbrell (Timbrell et al. 1968), consist of a rotating brush that sweeps over an advancing plug of bulk material liberating fibers that are entrained in the controlled air flow passing through the device. The airborne dust is then passed either into a delivery system for nose-only exposure or into an exposure chamber where animals are kept for fixed periods of time (usually 7 hours per day) on a weekly routine (typically 5 days per week). The exposure routine is continued for as long as 2 years in some of the studies. In some, but not all of the studies, fiber-containing air is passed through a cyclone or elutriator prior to the exposure chamber so that exposure consists primarily of particles sized within the respirable range.

Asbestos concentrations in the animal inhalation experiments are monitored by a combination of techniques. The concentration of total dust in the chamber is generally monitored gravimetrically. Simultaneously, membrane filter samples are collected and fibers counted by PCM. The quotient of these two measurements yields the number of (PCM) fibers per unit mass of dust (Section 4.3). The distribution of fiber sizes within the dusts introduced into the animal exposure chambers may also be determined in these studies by any of a variety of methods. As indicated previously (Section 4.3), however, the utility of such measurements depends on the precise manner in which they are derived.

To derive fiber size distributions, dust samples from these studies have generally been collected on polycarbonate filters for analysis by SEM. However, such distributions suffer both from the limitations of SEM (Section 4.3) and from the manner in which they are tied to the inhalation experiments (see Chapter 5).

Theoretically, the dose of any fiber size fraction can be estimated in a two-step process. The procedure incorporates consideration of a size fraction termed the PCM-equivalent fraction (PCME), which is the fraction of structures measured by SEM (or TEM) that correspond to the size range of structures known to be visible and therefore countable by PCM. First, the concentration of the PCM-equivalent fraction of the fiber size distribution (measured by SEM) is normalized by dividing its value by the PCM-measured concentration per unit dust mass observed in the inhalation experiment. This ratio is then multiplied by the fractional concentration of any specified size range of interest within the distribution (measured by SEM) to determine the exposure level for that size fraction. However, because bivariate (length by diameter) size distributions have not typically been developed in the available studies and because the number of total fibers longer than 5 μm observed by SEM (without adjustment for width) does not correspond to the number of total fibers longer than 5 μm observed by PCM, it is not possible to derive a true PCME fraction from the SEM data. Therefore, the theoretical approach described above for estimating exposure to specific size fractions cannot generally be applied in the existing studies.

As indicated above, the data within the published animal inhalation studies are further constrained by the limitations of the analytical methods employed to generate the data (Section 4.3). Comparison of data between studies is also hindered by the lack of sufficient documentation to indicate the specific methods and procedures employed in each study. Frequently, for example, it is unclear whether respirable dusts or total dusts have been monitored. Also, several studies fail to report one or both of two critical pieces of information: fiber-number-to-mass conversion factors and fiber size

distributions. In addition, few studies indicate the precise counting rules employed for generating size distributions.

When structure-number-to-mass conversion factors are provided, unless the conversion factor is derived by counting fibers in a specific size range in a known mass of sample and fiber concentrations in other size ranges are normalized to this count, several types of error may be introduced. For example, if total sample mass is assumed proportional to calculated mass derived from volume characterizations of the particles counted, unless isometric particles are sized along with fibers and both asbestos and nonasbestos particles are included in the count, a bias will be introduced in the conversion factor because total sample mass will have been under represented to the extent that such particles are ignored in the estimation of fiber mass. Even if such particles are included, significant uncertainty may result from estimating the volumes of irregular particles and the limited precision associated with the count of the largest particles (due to their limited number). The uncertainty in the measurement of a fiber's diameter is squared in contributing to the uncertainty associated with a mass estimate.

Among reported variations in study design, differences in the detailed design and operation of the aerosolization chamber and the frequency and duration of exposure also potentially contribute to variation in results between studies. Also, use of differing animal strains and species across the various studies suggest the possibility that physiological differences may contribute to the observed variation in study results. Such differences are discussed further in Chapter 5.

A small subset of the asbestos dusts evaluated in the animal inhalation studies have been analyzed by TEM. However, even the published fiber size distributions from these TEM studies are subject to variation from differences in procedures used for sample preparation, from differences in counting rules, and from precision limitations due to the limited number of fibers actually characterized (Section 4.3). This latter limitation particularly affects the precision with which longer fibers are counted.

Although fiber size distributions are primarily based on SEM analyses rather than TEM analyses in the existing animal inhalation studies, results generally echo the results of the injection and implantation studies. Thus, longer fibrous structures are observed to contribute most to asbestos biological activity, at least qualitatively. For example, dusts containing predominantly long amosite or long chrysotile fibers induce far more pulmonary tumors than samples containing predominantly short structures (Davis et al 1986a and 1988b). However, dusts evaluated in the existing inhalation experiments have not been characterized sufficiently to distinguish the dependence of biological activity on fiber diameter. Neither are the existing studies sufficient to evaluate the

importance of mineralogy (or other potentially important asbestos characteristics) in determining risk.

7.4.3 Supplemental Inhalation Study

Given the problems with the existing animal inhalation studies, a project was undertaken to overcome some of the attendant limitations. To control for effects from variation in study design and execution (including choice of animal strain, animal handling procedures, equipment design, sample handling procedures, dosing regimen, and pathology protocols), the project focused on a set of studies generated from a single laboratory (i.e., the studies published by Davis et al.). Ultimately, the results from six studies covering nine different asbestos samples (including four types of asbestos with samples exhibiting multiple size distributions for two asbestos types) and a total of 13 separate experiments (some samples were studied at multiple exposure levels or in duplicate runs) were pooled for analysis. The database of experiments employed in the project is described in Table 7-7.

To overcome the limitations in the Davis et al. studies associated with the characterization of asbestos itself, the dusts studied in the thirteen experiments listed in Table 7-7 were regenerated by the same group who performed the original studies, from the same starting materials, using the same equipment, and reproducing the same conditions under which the original studies were conducted. Samples of the regenerated dusts were then collected and analyzed by TEM using a modified version of the Superfund air method (Chatfield and Berman 1990) to generate bi-variate size distributions that also include detailed characterization of the shapes and complexity of fibrous structures observed.

The total mass concentration of the regenerated dusts and fiber measurements by PCM were also collected to provide the data required to link size distributions in the regenerated dusts to absolute structure concentrations in the original inhalation experiments. The manner in which such calculations are performed has been published (Berman et al. 1995).

The concentration estimates (for asbestos structures exhibiting a range of characteristics of interest) that were derived from the TEM analyses of the regenerated dusts were then combined with the tumor response data from the set of inhalation experiments listed in Table 7-7 and a statistical analysis was completed to determine if a measure of asbestos exposure could be identified that satisfactorily predicts the lung tumor incidence observed. A more limited analysis was also performed to address mesothelioma; the small number of mesotheliomas observed in the Davis et al. data

constrained the types of analyses that could be completed for this disease. The detailed procedures employed in this analysis and the results from the first part of the study have been published (Berman et al. 1995). These are summarized below along with results from the parts of the study that remain to be published.

Table 7-7

In the statistical analysis performed in this study, the individual dose/response profiles from each of the two data sets were fit to a linear dose/response model:

$$P_i = 1 - EXP(- Q_o - \sum_j b_i a_j x_j) \qquad (7.7)$$

where:

"P_i" is the probability of inducing pulmonary tumors observed in the "ith" study. A probability of one is equivalent to 100% incidence among the animals dosed in study i;

"Q_o" is the correction factor for background derived from the background incidence of pulmonary tumors observed among the control populations (pooled from all studies);

"x_j" is the concentration of the "jth" size fraction of fibers in the "ith" study;

"a_j" is the coefficient of potency for the "jth" size fraction of fibers in the "ith" study; and

"b_i" is a coefficient representing a normalization factor accounting for differences between the dose/response factors found for the summed contributions of the "j" exposure indices in the "ith" study.

The "a_j"s in this analysis are constrained to be positive because it is assumed that no fiber prevents cancer. The "a_j"s are also constrained to sum to one so that contributions to overall potency from individual size fractions are normalized to the overall concentration of asbestos. Correspondingly, size fractions evaluated represent disjoint (mutually exclusive) sets.

The dose/response model was set up as indicated in Equation 7.7 to provide flexibility. The model allows separate potency coefficients to be assigned to individual size fractions in a dose/response relationship that depends on multiple size fractions. Simultaneously, the "b" coefficients allows separate potency coefficients to be assigned to different fiber types or to results from different studies performed under different experimental conditions.

Several investigators (Stanton et al. 1977; Bertrand and Pezerat 1980; Bonneau et al. 1986; and Wylie, et al. 1987) have used a logit curve to investigate the dose/response relating various measures of asbestos exposure to tumor response. The logit formula specifies that the tumor probabilities satisfy the relation:

$$\log[P/(1-P)] = a + b \cdot \log x \qquad (7.8)$$

where log x is some measure of asbestos exposure, such as log of concentration of fibers in some size range. In some instances, the logit model was expanded by replacing b·log x with a term representing a linear combination of exposure indices so that multiple exposure indices could be explored simultaneously. The models were fit using standard linear regression based on normal theory.

An equivalent form for the logit model is:

$$P = e^{a}x^{b}/(1 + e^{a}x^{b}) \qquad (7.9)$$

Written in this form, it is clear that this model does not permit a background response (i.e. P = 0, whenever x = 0). This is not a serious limitation when there are no tumors in control animals, such as was the case in Stanton et al. (1977). However, the model will not adequately fit data in which tumors are found in control animals. This was one reason for adopting the linear model (Equation 7.7) used in the investigation of the animal data reported in the study described here.

There is no evidence from this study that the linear model is inadequate. For cases in this study in which the fit between exposure and response is shown to be inadequate, the lack of fit is typically observed to be due to an inconsistent (non-monotonic) dose/response curve so that there is no indication that a non-linear model, such as the logit, would provide a better fit.

The linear model (Equation 7.7) used in this study was fit using a maximum likelihood (Cox and Lindley 1974) approach that utilizes the actual underlying binomial probabilities. This is a more efficient estimation method model than use of regression methods based on normal theory, which was the fitting method used in the earlier studies (described above). The regression procedure indicates only whether the exposure measures that were studied are significantly correlated with tumor response.

In contrast, the statistical analyses performed in this study indicate whether exposures that are described by a particular characteristic (or combination of characteristics)

satisfactorily *predict* the observed tumor incidence. To illustrate, it is apparent from Text Figure 2 of Stanton et al. (1981) that the exposure measure they identify as being most highly correlated with tumor incidence (fibers longer than 8 μm and thinner than 0.25 μm) does not provide an acceptable fit to the observed tumor incidence. Similarly, although all of the univariate exposure measures listed in Table 2 of Berman et al. (1995) are highly correlated with tumor incidence, none of them adequately describe (fit) lung tumor incidence.

To test for the goodness of fit in this study, each relationship was subjected to the standard "P" test where the model was rejected if P was significant at the 5% level indicating that the true model would provide a worse fit only 5% of the time. Among models that were not rejected based on a P test, several hypotheses concerning the relative merit of the various models were also examined according to the method of *maximum likelihoods* (Cox and Lindley 1974).

An example of an adequate fit to the tumor response data is provided in Figure 7-5 (Figure 3 of Berman et al. 1995). Note that Figures 2 and 3 of the original paper were inadvertently switched during publication; the correct Figure 3 is reproduced here. The exposure index plotted in Figure 7-5 is the sum:

$$\text{Exposure} = 0.0017C_1 + 0.853C_2 + 0.145C_3 \qquad (7.10)$$

where:

"C_1" is the concentration of structures between 5 and 40 μm in length that are thinner than 0.3 μm;

"C_2" is the concentration of structures longer than 40 μm that are thinner than 0.3 μm; and

"C_3" is the concentration of structures longer than 40 μm that are thicker than 5 μm.

This index of exposure represents one of the optimum indices reported in Berman et al. 1995.

As is clear from the figure, when exposure is expressed in the manner described above, the tumor responses observed in the 13 separate experiments that were evaluated increase monotonically with increasing exposure. It is also apparent that the data points representing each study fall reasonably close to the line representing the

optimized model for this exposure index. Thus, exposure adequately predicts response.

Results obtained from completing more than 200 statistical analyses to determine whether various measures of asbestos exposure adequately predict lung tumor response (Berman et al. 1995) indicate that:

- neither total dust mass nor fiber concentrations determined by PCM adequately predict lung tumor incidence;
- no univariate measure of exposure (i.e. exposure represented by the concentration of a single size category of structures as measured by TEM) was found to adequately predict lung tumor incidence. Of the univariate measures of exposure examined, the concentration of total structures longer than 20 μm provides the best fit (although still inadequate); and
- lung tumor incidence can be adequately predicted with measures of exposure representing a weighted sum of size categories in which longer structures are assigned greater potency than shorter structures.

The set of analyses completed in support of this work are summarized in Appendix C.

One example of an exposure measure that adequately describes lung tumor incidence is presented in Figure 7-5. Another exposure measure shown to provide an adequate fit is:

$$\text{Exposure} = 0.0024C_a + 0.9976C_b \qquad (7.11)$$

where:

"C_a" is the concentration of structures between 5 and 40 μm in length that are thinner than 0.4 μm; and

"C_b" is the concentration of structures longer than 40 μm that are thinner than 0.4 μm.

The fit of this index is depicted in Figure 7-6.

Figure 7-5

Figure 7-5:
Fit of Model.
Tumor Incidence vs. Structure Concentration by TEM
(Length Categories: 5-40 um, > 40 um, Width Categories: < 0.3 um and > 5 um)

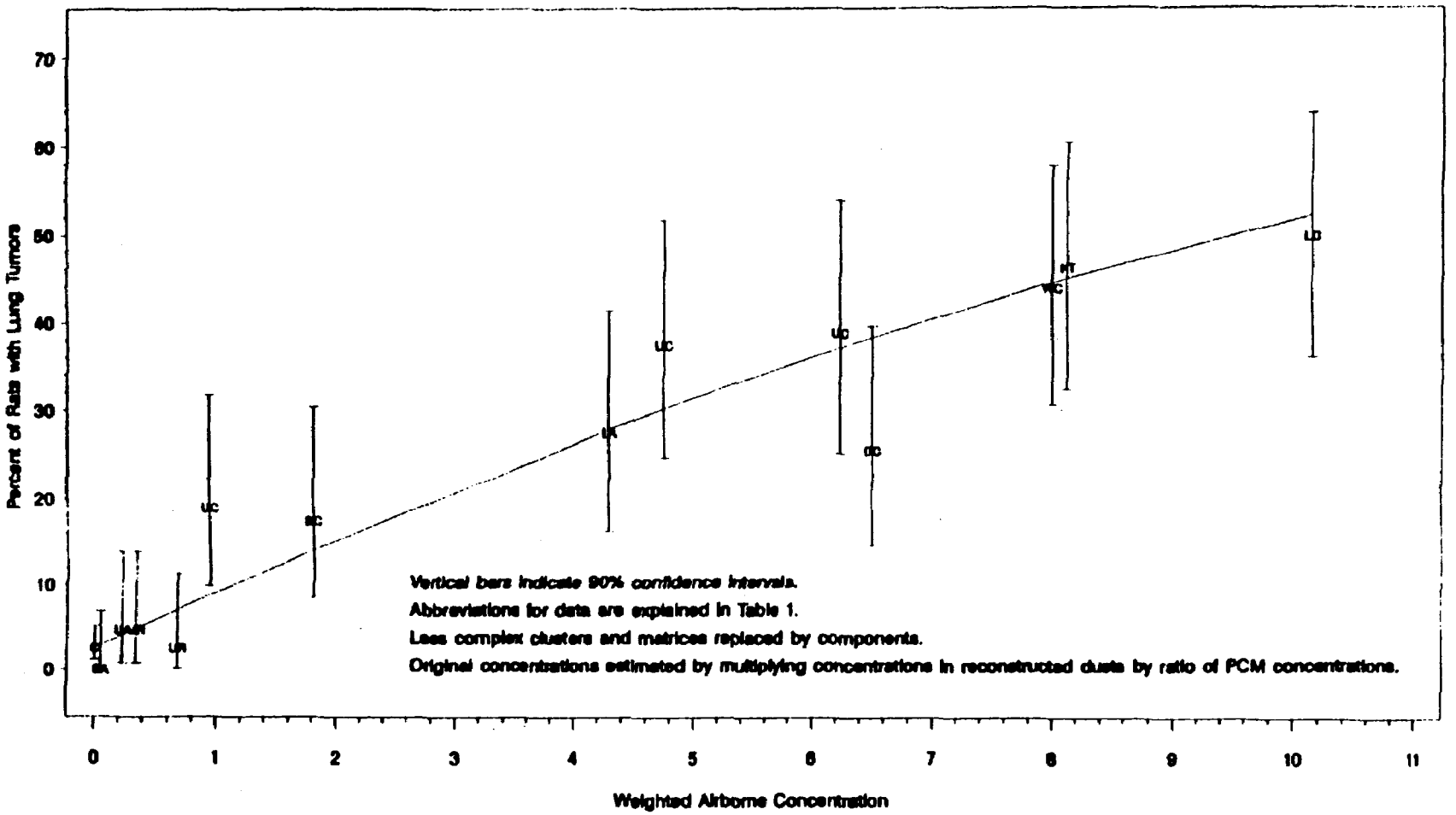

Length Categories: 5μm – 40μm, ≥ 40μm
Width Categories: < 0.3μm and ≥5μm

In addition to the above, a series of hypotheses tests were also conducted to test such questions as: whether fiber type affects potency or whether the component fibers in complex clusters and matrices should be counted individually. Questions concerning whether mesothelioma incidence can be adequately described by the same measure(s) of exposure that describe lung tumor incidence were also addressed. Taken as a whole, the results presented in Berman et al. (1995) support the following, general conclusions:

- structures contributing to lung tumor incidence are thin (< 0.5 μm) and long (> 5 μm) with structures longer than 20 μm being the most potent;
- the best estimate is that short structures (< 5 μm) are non-potent. There is no evidence from this study that these structures contribute anything to risk;
- among long structures, those shorter than 40 μm appear individually to contribute no more than a few percent of the potency of the structures longer than 40 μm;
- lung tumor incidence is best predicted by measurements in which the component fibers and bundles of complex structures are individually counted;
- at least for lung tumor induction in rats, the best estimate is that chrysotile and the amphiboles are equipotent;
- for equivalent size and shape structures, amphiboles are more potent toward the induction of mesothelioma than chrysotile; and
- after adjusting for the relative potencies of fiber type, the size categories that contribute to lung tumor incidence appear also to adequately describe mesothelioma incidence.

A number of supplemental analyses were also conducted, primarily to identify optimal procedures for performing asbestos analysis and for estimating concentrations. These analyses have not yet been published, but they are included in the summaries in Appendix C. The most important results of the supplemental analyses are that:

- tumor incidence can only be adequately fit by data derived from TEM analysis of samples prepared by a direct transfer procedure.

Measurements derived from indirectly prepared samples could not be fit to lung tumor incidence in any coherent fashion; and

Fit of Model:

Tumor Incidence vs. Structure Concentration by TEM
(Length Categories: 5-40 um, > 40 um, Width Categories: < 0.4 um)

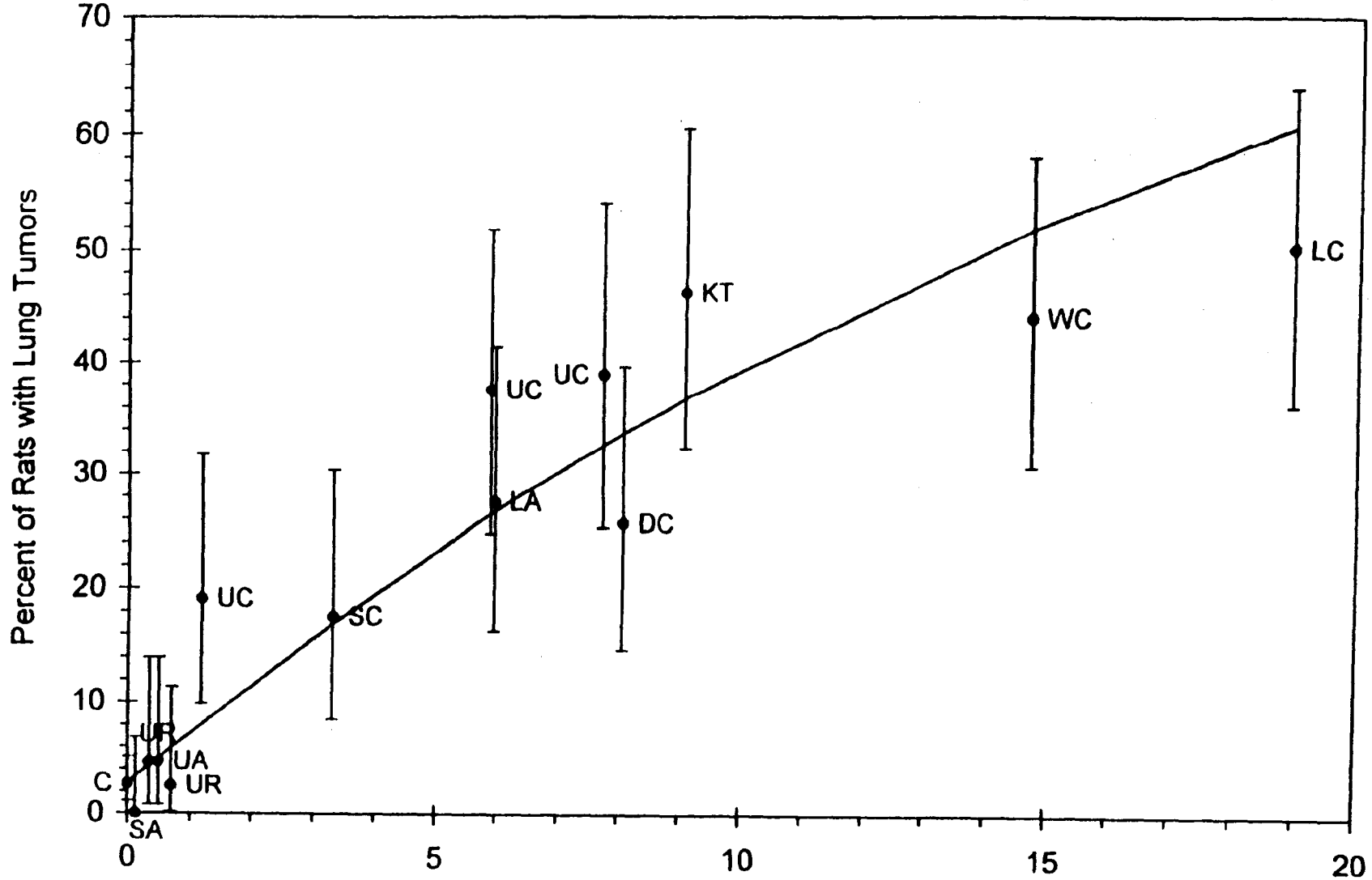

Weighted Airborne Concentration
Length Categories: 5μm-40 μm, ≥ 40 μm
Width Categories: < 0.4 μm

Figure 7-6

- it was not possible to identify an exposure measure in which potency is expressed in terms of a single, continuous function of structure length.

Regarding the last point, although we were not able to identify a continuous function of length that provides an adequate fit to the tumor incidence data, the general results from the above analysis are not inconsistent with the hypothesis that potency is a continuous function of length (i.e. the Pott hypothesis, Pott 1982). The Pott hypothesis suggests that relative potency is low for short fibers, rises rapidly over an intermediate range of length, and approaches a constant for the longest fibers.

7.4.4 Conclusions Concerning Animal Dose-Response Studies

Results from our evaluation of the animal dose-response data for asbestos (including the existing injection/implantation studies, the existing inhalation studies, and our supplemental study) indicate that:

- short structures (less than somewhere between 5 and 10 μm in length) do not appear to contribute to cancer risk;

- beyond a fixed, minimum length, potency increases with increasing length, at least up to a length of 20 μm (and possibly up to a length of as much as 40 μm);

- the majority of structures that contribute to cancer risk are thin with diameters less than 0.5 μm and the most potent structures may be even thinner. In fact, it appears that the structures that are most potent are substantially thinner than the upper limit defined by respirability;

- identifiable components (fibers and bundles) of complex structures (clusters and matrices) that exhibit the requisite size range may contribute to overall cancer risk because such structures likely disaggregate in the lung. Therefore, such structures should be individually enumerated when analyzing to determine the concentration of asbestos;

- for asbestos analyses to adequately represent biological activity, samples need to be prepared by a direct-transfer procedure; and

- based on animal dose-response studies alone, fiber type (i.e. fiber mineralogy) appears to impart only a modest effect on cancer risk (at least among the various asbestos types).

Regarding the last of the above bullets, that only a modest effect of fiber mineralogy was observed in the available animal dose-response studies (when large effects are observed among human studies, Chapter 6), may be due at least in part to the limited lifetime of the rat relative to the biodurability of the asbestos fiber types evaluated in these studies, although it is also possible that different mechanisms drive the effects observed in the animal studies than those that dominate for asbestos-induced cancers in humans and that such mechanisms depend more strongly on mineralogy. Other explanations are also possible. Issues relating to both fiber mineralogy and fiber size are addressed further in Section 7.5 and Chapter 8.

7.5 CONCLUSIONS FROM AN EVALUATION OF SUPPORTING STUDIES

Although gaps in knowledge remain, a review of the literature addressing the health-related effects of asbestos (and related materials) provides a generally consistent picture of the relationship between asbestos exposure and the induction of disease (lung cancer and mesothelioma). Therefore, the general characteristics of asbestos exposure that drive the induction of cancer can be inferred from the existing studies and can be applied to define appropriate procedures for evaluating asbestos-related risk. Furthermore, although it would be helpful to definitively identify the underlying biochemical triggers and associated mechanisms that drive asbestos-induced cancer, this is not an absolute prerequisite for the development of a technically sound protocol for assessing asbestos-related risk.

As previously indicated (Sections 7.3.8), the biochemical mechanisms that potentially contribute to the induction of asbestos-induced cancer are complex and varied. Moreover, different mechanisms appear to exhibit differing dose-response characteristics (i.e. the various mechanisms do not all show the same kind of dependence on fiber size or fiber type). Some mechanisms, for example, suggest that fiber length is important and that only structures that are sufficiently long induce a response. In contrast, other mechanisms suggest that fibers (and even non-fibrous particles) may all contribute to response and that the magnitude of the response is a function of the total surface area of the offending fibers (or particles). Among these mechanisms, additionally, some suggest that fiber type (i.e. mineralogy) is not an important determinant of potency while other mechanisms indicate that fiber type is the predominant determinant of potency.

Unfortunately, the existing studies are not currently adequate to support definitive identification of the specific mechanisms that drive the induction of asbestos-related cancer (versus other mechanisms that may contribute only modestly or not at all).

However, whatever mechanisms in fact contribute to the induction of disease, they must be consistent with the gross characteristics of exposure that are observed to predict response in the available whole-animal dose-response studies and human epidemiology studies. Therefore, the implications from these latter studies regarding the dependence of asbestos-induced cancers on fiber size and type are reviewed here in some detail. Further, in Chapter 8, they are used to support development of a protocol for evaluating asbestos-associated risks.

Fiber Length

Fibers less than a minimum length between 5 and 10 μm do not appear to contribute to risk. This is supported both by the results of our re-analysis of the animal inhalation studies conducted by Davis et al. (Section 7.4.3 and Berman et al. 1995), in which this hypothesis was tested formally, and by inferences from the broader literature. As long as fiber size is adequately characterized, the animal inhalation studies (Section 7.4.2) and injection/implantation (Section 7.4.1) studies consistently indicate lack of ability of short structures to contribute to the induction of cancer. Furthermore, animal retention studies (Section 7.2.1) and histopathology studies (Section 7.2.2) provide strong mechanistic evidence that explains the lack of potency for short structures; they are readily cleared from the respiratory tract. Even when sequestered in large numbers in macrophages within the lung, there is little indication that such structures induce the kinds of tissue damage and related mechanisms that appear to be closely associated with the induction of cancer.

Although there are mechanism studies that may suggest a role for short fibers in the induction of asbestos-related disease (see, for example, Goodglick and Kane 1990, Section 7.3.4.4), such studies do not track cancer as an end point. Therefore, the relationship between the toxic end point observed and the induction of cancer needs to be adequately addressed before it can be concluded definitively that short structures can contribute to cancer.

Beyond the minimum length below which structures may be non-potent, potency appears to increase with increasing length, at least up to a length of 20 μm and potentially up to a length of 40 μm. The latter limit is suggested by our re-analysis of the Davis et al. studies (Section 7.4.3) in which it was also found that structures longer than 40 μm may be as much as 500 times as potent as those between 5 and 40 μm in length. The former limit is suggested by broader inferences from the literature that suggest the cutoff in the length of structures that are at least partially cleared by macrophages from the lung may lie close to 20 μm and that the efficiency of clearance likely decreases rapidly for structures between 10 and 20 μm in length (Section 7.2).

Such inferences are further reinforced by measurements of the overall dimensions of macrophages in various mammals by Krombach et al. (1997), as reported in Section 4.4.

Importantly, the inferences that potency increases for structures longer than 10 µm (up to some limiting length) from these various studies are strongly reinforcing, even though the upper limits to the points at which potency stops increasing do not precisely correspond. Furthermore, that the longest structures are substantially more potent than shorter structures (and that the shortest structures are likely non-potent) dictates that asbestos analyses performed in support of risk assessment need to provide adequate sensitivity and precision for counts of the longest structures.

Fiber Diameter

Because fibers that contribute to the induction of cancer must be respirable, they must also be thin. The studies reviewed in Section 7.1 indicate that respirable fibers are thinner than 1.5 µm and the vast majority of such structures are thinner than 0.7 µm. In fact, the results of injection, implantation, and inhalation studies reviewed in Sections 7.4.1 and 7.4.2 and the results of our supplemental re-analysis of the Davis et al. studies (Section 7.4.3) indicate that the fibers that contribute most to the induction of asbestos-related cancers are substantially thinner than the limit suggested by respirability alone.

Importantly, the results of all of the studies cited above indicate that it is a cutoff in absolute width that defines the bounds of biological activity rather than a cutoff in aspect ratio (the ratio of length to width) that has been used to define fibrous structures heretofore. That is why the exposure index recommended based on our review of the Davis et al. studies incorporates a maximum width as a cutoff, rather than a minimum aspect ratio.

Fiber Complexity

In our supplemental evaluation of the Davis et al. studies, the tumor incidence data from the animal inhalation studies were best fit (predicted) by exposure indices in which the component fibers and bundles of complex structures (clusters and matrices) were separately enumerated and included in the exposure index used to represent concentration (Section 7.4.3). The appropriateness of such an approach is further supported by the observation that loosely bound structures (including, for example, chrysotile bundles) readily disaggregate in vivo (Section 7.2). Therefore, it is recommended in this report that those components of complex structures that

individually exhibit the required dimensional criteria be individually enumerated and included as part of the count during analyses to determine the concentration of asbestos in support of risk assessment.

Fiber Type (Mineralogy)

Two separate but interrelated issues need to be addressed with regard to the effects of fiber mineralogy. The first is that mineralogy appears to be an important determinant of cancer risk. The second is that the magnitude of the mineralogical effect appears to be at best modest in animal dose-response studies but appears to be substantial in human epidemiology studies. It must also be emphasized that, due to confounding, the effects of fiber size and fiber mineralogy need to be addressed simultaneously, if one is interested in drawing useful conclusions concerning fiber mineralogy.

Results from some (but not all) of the animal injection, implantation, and inhalation studies previously reviewed (Sections7.4.1 and 7.4.2) suggest that mineralogy plays an important role in determining biological activity. However, the nature of the effects of mineralogy are not easily separated from size effects, due to the methodological limitations of the studies cited. Therefore, the evidence from these studies can be considered ambiguous. Formal hypothesis testing during our re-analysis of animal inhalation studies (Section 7.4.3) indicates that, when size effects are addressed, chrysotile and the amphiboles exhibit comparable potency toward the induction of lung cancer. In contrast, amphiboles appear to be approximately three times more potent than chrysotile toward the induction of mesothelioma, once fiber size effects are addressed.

Several of the human pathology studies cited previously (Section 7.2.3) suggest that mineralogy is an important factor in determining cancer risk, but these studies similarly suffer from methodological difficulties that introduce ambiguity into the inferences drawn. However, it is clear from the human epidemiology data (Chapter 6) that mineralogy plays a substantial role in the determination of risk for human cancer (primarily, mesothelioma).

The underlying cause(s) for the observed difference in potency between chrysotile and the amphiboles may relate to differences in fiber durability (Section 7.2), to size/shape related differences in fibers that are a function of mineralogy and that cause differences in deposition, retention, or translocation (Sections 7.1 and 7.2), and/or to the dependence on mineralogy of the specific mechanisms underlying the biological

responses of specific tissues (Section 7.3). The relative magnitudes of such effects on animal and human pathology also need to be considered, if the observed differences in potency among animal and human studies, respectively, is to be reconciled. Such considerations are addressed further in Chapter 8.

Importantly, whether the observed differences in the role of mineralogy toward animal and human pathology can be reconciled, the effects of mineralogy can be adequately addressed when assessing asbestos-related cancer risk for humans by incorporating dose-response coefficients explicitly derived from the human epidemiology data. Because this is the approach proposed in this document, effects due to mineralogy are properly addressed.

An Appropriate Exposure Index for Risk Assessment

The optimum exposure index defined based on our re-analysis of the Davis et al. animal inhalation studies is a weighted sum of two fiber size categories:

$$C_{opt} = 0.0024C_a + 0.9976C_b \qquad (7.12)$$

where:

"C_{opt}" is the concentration of asbestos expressed in terms of the optimum exposure index (i.e. as the weighted sum of two size categories);

"C_a" is the concentration of structures between 5 and 40 μm in length that are thinner than 0.4 μm; and

"C_b" is the concentration of structures longer than 40 μm that are thinner than 0.4 μm.

This index was shown to adequately fit (predict) the tumor incidence data across the 13 separate animal inhalation experiments evaluated ($P = 0.09$). Whether the exposure index defined in Equation 7.12 is also optimal for capturing the relevant characteristics of fibers that contribute to the induction of human cancer is an open question. Because it captures the major characteristics (concerning length and diameter) identified above that are indicated to be important for human exposures, it represents a promising candidate. Unfortunately, however, the data required to match this index to a set of human-derived dose response coefficients does not currently exist (Section 6.2.4). Therefore, until such time that the data required to adapt a set of human-derived coefficients to the above index become available, the following interim index (defined

originally in Equation 6.7 and reproduced here), should be used to evaluate asbestos-related cancer risks for humans:

$$C_{asb} = 0.003C_S + 0.997C_L \qquad (7.13)$$

where:

"C_{asb}" is the concentration of asbestos to be used to estimate risk;

"C_S" is the concentration of asbestos structures between 5 and 10 μm in length that are also thinner than 0.5 μm; and

"C_L" is the concentration of asbestos structures longer than 10 μm that are also thinner than 0.5 μm.

Although not optimized (so that, for example, it does not provide an adequate fit to the animal inhalation studies), this index nevertheless captures substantially more of the characteristics (concerning length and diameter) that are indicated to be important for human exposures than the index (traditionally defined for phase contrast microscopy) in current use by EPA (which does not provide an adequate fit to the animal inhalation studies either). The index currently recommended by EPA is defined as "C_{PCM}" and is the concentration of asbestos structures longer than 5 μm, thicker than 0.25 μm, with an aspect ratio greater than 3. A comparison between this index and the "interim" index defined by Equation 7.13 is instructive.

First, we will ignore the limitations in PCM instrumentation (Section 4.3), which among other things has been shown incapable of providing reliable measurements of asbestos concentrations in outdoor settings that are removed from obvious, dominating sources of asbestos (Berman unpublished). Therefore, we will begin this comparison by assuming that measurements for the index currently in use by EPA are actually derived using TEM (so that they can be considered to be "PCM-equivalent concentrations" or C_{PCME}).

Comparing the dimensions of structures incorporated in C_{PCME} and C_{asb}, respectively, it is clear that:

- the interim index, recommended in this document, is weighted toward longer structures (> 10 μm vs. > 5 μm) than the current EPA approach and this better captures the expected trend with length;

- the interim index is focused on the thinnest structures, which also tracks the expected trends in biological activity. In contrast, the current index excludes the thinnest structures (which are likely more potent and more numerous than thicker structures in most environments of interest); and

- even more important, the interim index includes only structures that are respirable while the current index potentially includes counting of a large fraction of structures that are not respirable (which clearly cannot contribute to risk).

As indicated above, the size criteria for the interim index proposed in this document provides substantially better agreement with the characteristics expected of biologically active fibers (described above) relative to the index currently recommended by EPA (which is also the index to which the existing epidemiology studies are currently normalized). It is likely for this reason that human dose-response coefficients adjusted to match the interim index show improved cross-study agreement relative to unadjusted coefficients (Sections 6.2.4.2 and 6.3.3.2). Additional advantages of the interim index are also discussed in Appendix B, where, for example, the interim index is shown to adequately fit (predict) the relative tumorigenicity of six different tremolite samples that vary in the degree of their asbestiform character. In contrast, the index currently recommended by EPA does not adequately fit the tremolite data.

Although the interim index appears to provide substantial improvement in performance for use in risk assessment over the index in current use, conclusions from the literature reviewed in this Chapter indicate that additional, substantial improvement may be gained by adopting an index that more heavily weights structures even longer than10 μm. Although the ideal may be to incorporate separate weights for structures as long as 40 μm, even incorporating separate weights for structures longer than 20 μm would likely achieve most of the desired improvement. However, this will require completion of limited additional study to develop the data needed to adjust the existing human dose-response coefficients to match the improved index. Importantly, it is also likely that, additional improvement over the interim index can be achieved by conducting the additional study in a manner that would provide size data appropriate for the specific facilities evaluated in the existing epidemiology studies (rather than generically similar sites, matched by industry). The adjustments used in this document to match the existing dose-response coefficients to the interim index are industry generic (Section 6.2.4). It is therefore interesting that, even given this cruder approach for adjusting coefficients, improved agreement across the adjusted coefficients is still observed (Sections 6.2.4.2 and 6.3.3.2).

Interpreting Exposure Indices

It is instructive to examine the relationship between the true (but unknowable) function that represents biological activity and the functions represented, respectively, by each of the exposure indices considered in this Section. All of the indices considered above (the current index, the interim index, and the proposed, optimum index) all represent step functions with precise dimensional cutoffs. The existing index is a single-parameter function with cutoffs for minimum length, minimum width, and minimum aspect ratio. Both the interim index and the proposed, optimal index are two-parameter indices with cutoffs for minimum lengths, an interim length (at which potency incrementally increases), and maximum width.

In contrast, the true relationship between fiber dimension and biological activity likely represents a continuous function without distinct, hard boundaries (although relatively steep declines in potency for minimum length and maximum width are likely approximated reasonably well by a hard boundary). Unfortunately, due to the limitations of the studies conducted to date, it has not been possible heretofore to define a continuous function that adequately predicts risk. However, as long as the sensitivity of the associated analysis is set sufficiently low so that a minimum of several structures (say four or five) would be counted to estimate concentrations the relate to levels of risk of potential concern, exposure indices that are step functions (incorporating hard, dimensional boundaries) will provide a reasonably good approximation to results that would be obtained, should the true, continuous function be known. Moreover, agreement between results from a step function and the true, continuous function will improve as the number of structures counted increases (i.e. as the estimated concentration and associated risk increases), due to the averaging of potency over the multiple fibers that are observed.

8.0 DISCUSSION, CONCLUSIONS, AND RECOMMENDATIONS

Although gaps in knowledge remain, a review of the literature addressing the health-related effects of asbestos (and related materials) provides a generally consistent picture of the relationship between asbestos exposure and the induction of disease (lung cancer and mesothelioma). Therefore, the general characteristics of asbestos exposure that drive the induction of cancer can be inferred from the existing studies and can be applied to define appropriate procedures for evaluating asbestos-related risk. Moreover, such procedures provide substantial improvement in the confidence that can be placed in predicting risks in exposure environments of interest compare to predictions derived based on procedures in current use.

Following a general discussions of the findings of this study, specific recommendations (including options) for finalizing a protocol for assessing asbestos-related risks using the procedures identified in this document are provided in Section 8.2. Recommendations are described in Section 8.3 for limited, focused, additional studies to:

(1) settle a small number of outstanding issues (concerning whether the current dose-response models adequately track the time-dependence of lung cancer and mesothelioma) and

(2) provide the data required to fully optimize the approach recommended in this document.

8.1 DISCUSSION AND CONCLUSIONS

8.2.1 Addressing Issues

The issues identified in the introduction (Chapter 2) as part of the focus of this study can now be addressed. These are:

- whether the dose-response models currently in use by the EPA for describing the incidence of asbestos-related diseases adequately reflect the time-dependence for the development of these diseases;

- whether the relative in-vivo durability of different asbestos mineral types affect their relative potency;

- whether the set of minerals included in the current definition of asbestos adequately covers the range of minerals that potentially contribute to asbestos-related diseases;

- whether the analytical techniques and methods currently used for determining asbestos concentrations adequately capture the biologically relevant characteristics of asbestos (particularly with regard to the sizes of the structures included in the various analyses) so that they can be used to support risk assessment; and

- whether reasonable confidence can be placed in the cross-study extrapolation of dose-response relationships that are required to assess asbestos-related risks in new environments of interest.

Time dependence

Regarding the first of the above-listed issues, the lung cancer model appears to adequately reflect long-term risk associated with exposure to amphiboles (for which relative risk remains constant beyond 10 yrs after the end of exposure) but may over-predict long-term risk for chrysotile (Section 6.2.1). Relative risk for chrysotile-exposed individuals appears to decrease substantially with time following 10 yrs after the end of exposure, rather than remain constant, as the model predicts. However, these findings are based on evaluation of only a single chrysotile cohort and a single amphibole cohort so that further evaluation of a minimum of two additional cohorts (one each of amphibole and chrysotile), to determine whether these trends are general, may be warranted (Section 8.3).

Although there are hints from our evaluation that the mesothelioma model may somewhat under-predict long term mesothelioma risk following exposure to amphiboles (Section 6.3.1), the effect appears small and may not be important. Still, because this finding is based on evaluation of only a single amphibole study, evaluation of at least one additional cohort may prove prudent. There was no indication that the mesothelioma model under-predicts risk for chrysotile-exposed individuals, although only small numbers of mesotheliomas were observed in the data sets evaluated for chrysotile.

Biodurability

Because the in-vitro dissolution rate for chrysotile in biological fluids is substantially less than for crocidolite and, likely, other amphiboles (Section 7.2.4), effects potentially

attributable to differences in the relative biodurabiliy of these asbestos types are addressed in several sections of this document. Among other things, this difference may explain the reduction in relative risk for lung cancer following cessation of exposure observed for chrysotile-exposed workers that was not apparent for amphibole-exposed workers (Section 6.2.1). Both of these affects may also explain the small difference in potency toward the induction of lung cancer between chrysotile and the amphiboles observed in this study (Section 6.2.4). Importantly, however, the observed difference is based only on best estimates of relative potency; formally, the difference was not found to be significant.

Although the relative biodurability of chrysotile and the amphiboles may potentially underlie the substantial difference in potency observed between these fiber types toward the induction of human mesothelioma, which is significant, (Sections 6.2.4.2 and 6.3.3.2), direct evidence for the specific effects contributing to this difference are not apparent. Thus, for example, the current mesothelioma model appears to adequately describe the time-dependence for mesothelioma following exposure to both chrysotile and amphiboles (Section 6.3.1), although the chrysotile data sets examined were fairly small, which limits the power of this analysis. Moreover, there is evidence suggesting that, even among the chrysotile-exposed cohorts, the observed mesotheliomas may be attributable to the small concentration of tremolite (amphibole) asbestos that was found as a contaminant in the material to which these cohorts were exposed (Section 6.3.3).

That tremolite fibers represent a substantial (sometimes predominant) fraction of the fibers found in the lungs of deceased workers from these cohorts (Sections 6.2.3 and 7.2.3), despite its trace-level presence in the material handled, suggests either that chrysotile is not deposited as efficiently in the deep lung (which would not be affected by biodurability) or that it is cleared much more rapidly (which may imply a role for biodurability, although size effects may also dominate). Animal retention studies addressing these effects are somewhat ambiguous (Section 7.2.1 and 7.2.2), although they too support the general impression that chrysotile (on a mass basis) is either not deposited as efficiently in the deep lung or cleared more readily from the deep lung (or both). Still, the fact that long fibers of chrysotile (which are expected to contribute most to potency) are observed to be retained for extended periods of time, clouds the potential role for biodurability.

Overall, the substantially larger potency toward the induction of mesothelioma observed in humans may have several causes, but direct evidence for such causes is not definitive either among the supporting animals studies or the in-vitro studies. Thus, while this effect can be adequately addressed by the procedures recommended in this

document for risk assessment (because the recommended risk coefficients are based on human data), it cannot be entirely explained.

Minerals of concern

Regarding the range of fibrous minerals that potentially contribute to lung cancer and mesothelioma, available evidence (Sections 7.2 and 7.4) suggests that:

- several minerals and the most biodurable among synthetic fibers (such as erionite or refractory ceramic fibers) in addition to those included strictly within the definition for asbestos have been shown capable of inducing lung cancer and/or mesothelioma (as long as the corresponding fibers fall within the appropriate size range);

- fibrous minerals that differ radically in chemical composition or crystal structure (such as erionite, chrysotile, and the amphibole asbestos types) appear to exhibit substantially different potencies (even after adjusting for size), which may be largely, but not necessarily entirely, explained by relative biodurability; and

- fibrous minerals that exhibit closely related chemical compositions and crystal structures (such as the family of amphibole asbestos types) appear to exhibit relatively similar potencies (once effects are adjusted for size).

Note, to illustrate that biodurability may not entirely describe relative potencies across the different fiber types, the biodurability-based model by Eastes and Hadley (1995 and 1996), which is described in Section 7.2.4, would (properly) predict different potencies for chrysotile and amphiboles for both lung cancer and mesothelioma. However, because the dose-response models for both lung cancer and mesothelioma are linear in fiber concentration, the Eastes and Hadley model would incorrectly predict that the ratio of relative potencies of chrysotile and the amphiboles would be the same in humans for these two diseases, which is definitely not what is observed (Section 6.4).

Given the above-described observations, it is clear that fibrous minerals beyond those included in the definition for asbestos can contribute to lung cancer and mesothelioma.

It is also likely that potencies for minerals that exhibit similar chemistry and crystal structure (and which therefore likely exhibit similar physical-chemical properties) also exhibit corresponding potency (for similarly sized fibers). However, the carcinogenicity of fibers exhibiting radically different chemical compositions and crystal structures than those already identified as carcinogenic, should likely be evaluated on a case-by-case basis. Two additional considerations may be useful for focusing such evaluations. First, the size distribution for fibers composed of the mineral of concern should be shown to include substantial numbers within the range of structures that potentially contribute to biological activity (i.e. that fall within the size range defined by the interim index, Equation 7.13). Second, such fibers should also be shown to be relatively biodurable (i.e. that they exhibit dissolution rates less than approximately 100 ng/cm^2-hr, Lippmann 2000). Note that, as long as the interim index of exposure is used to define fiber sizes, whether a fiber is strictly asbestiform appears to be irrelevant (Appendix B)

Analytical methods

Given the need to detect the thinnest fibers and the need for reliable measurements in outdoor settings, the only analytical technique that appears to be capable of providing quantitative data useful for supporting risk assessment is TEM (Sections 4.3 and 7.5). Further, given the specific size range of structures that need to be evaluated and the specific manner in which they need to be counted (to assure both cross-study comparability and compatibility with the recommended dose-response coefficients), analyses should be performed using the specific analytical methods recommended in this document. These are ISO 10312 (modified to focus on interim index structures) for air and the Modified Elutriator method (Berman and Kolk 2000) for soils or bulk materials. Note that, on a study-specific basis, other methods may be shown to provide comparable results so that they can also be used as part of a properly integrated investigation.

Confidence in risk assessment

Given the degree of reconciliation achieved across the various epidemiology studies (with the adjustments proposed in this document, Section 6.4), it appears that asbestos-related risks estimated using the recommended procedures may be considered good to within one to two orders of magnitude. Further, if proper procedures are employed to derive exposure estimates that are then properly matched with the recommended dose-response coefficients, the chance of severely underestimating risk can be minimized without the need to introduce overly conservative assumptions.

8.1.2 Comparison with Other, Recent Risk Reviews

Although several other reviews have also recently been published that nominally address risk-related issues for asbestos (including questions concerning the identification of an appropriate exposure index and the relative potency of varying fiber types), these studies are either qualitative or involve analysis of data in a manner that does not allow formal evaluation of nature of the specific dose-response relationships for the various diseases. Therefore, they are not well suited to support development of a protocol for conducting formal assessment of asbestos-related risks. Nevertheless, the general conclusions from these reviews are not inconsistent with our findings.

Hodgson and Darnton (2000)

Hodgson and Darnton (2000) conducted a comprehensive quantitative review of potency of asbestos for causing lung cancer and mesothelioma in relation to fiber type. They concluded that amosite and crocidolite were, respectively, on the order of 100 and 500 times more potent for causing mesothelioma than chrysotile. They regarded the evidence for lung cancer to be less clear cut, but concluded nevertheless that amphiboles (amosite and crocidolite) were between 10 and 50 times more potent for causing lung cancer than chrysotile. In reaching this latter conclusion they discounted the high estimate of chrysotile potency obtained from the South Carolina cohort. Hodgson and Darnton concluded that inter-study comparisons for amphibole fibers suggested non-linear dose response relationships for lung cancer and mesothelioma, although a linear relationship was possible for pleural mesothelioma and lung tumors, but not for peritoneal mesothelioma.

The Hodgson and Darnton study was based on 17 cohorts, 14 of which were among the 20 included in the present evaluation. This study had different goals from the present evaluation and used different methods of analysis. Hodgson and Darnton did not use the dose response information within a study. Instead, lung cancer potency was expressed as a cohort-wide excess mortality divided by the cohort mean exposure. Likewise, mesothelioma potency was expressed as the number of mesothelioma deaths divided by the expected total number of deaths, normalized to an age of first exposure of 30, and by the mean exposure for the cohort. These measures have the advantage of being generally calculatable from the summarized data available from a study. However, since they are not model-based, it is not clear how they could be used to assess lifetime risk from a specified exposure pattern, which is an important goal of the current project. Use of average cohort exposure could cause biases in the estimates, if, e.g., a large number of subjects were minimally exposed. Also, the recognized differences between studies in factors, in addition to level of exposure, that

may affect risk will also affect the reliability of conclusions concerning the dose response shape based on comparisons of results across studies.

Lippmann (1994 and 2000?)

In the most recent of these reviews, although based on a qualitative, anecdotal treatment of the literature, Lippmann reinforces our general findings that it is longer fibers (those longer than a minimum of approximately 5 μm) that contribute to lung cancer and mesothelioma. He further indicates that, based primarily on the limits observed for fibers that can be phagocytized, fibers that contribute most to lung cancer are likely longer than a minimum of 10 μm. In his review, based on a series of comparisons of mean and median dimensions reported for the relevant exposures across a broad range of studies, Lippmann draws several fairly specific conclusions on the ranges of fiber sizes that may contribute to various diseases (i.e. that the minimum length fibers that contribute to asbestosis, lung cancer, and mesothelioma are 2, 5, and 10 μm, respectively). He also suggests that fibers that contribute to mesothelioma may need to be thinner than 0.1 μm while those that contribute to lung cancer may need to be thicker than 0.15 μm. While it is not clear that drawing such specific conclusions can be firmly supported by the kinds of qualitative comparisons across reported mean and median dimensions for exposures in various studies that are described in this paper, the author indicates that further, more formal study of the dose-response relationships that he posits is warranted. It is noted that many of the studies reviewed by Lippmann are the same studies also incorporated in our analysis.

In the earlier review, Lippmann plots lung tumor incidence as a function of inhaled animal dose for data from a series of broadly varying studies based, respectively, on fibers longer than 5, 10, and 20 μm (no widths considered) and suggests that the quality of the fits are comparable. The author further suggests, based on this evaluation, that PCM seems to provide a reasonable index of exposure. However, no formal goodness of fit tests were performed in this analysis and, based on visual inspection, none of the plots would likely show an adequate fit. Moreover, the plot of the tumor response vs. dose as a function of fibers longer than 5 μm appears to be substantially worse than the other two plots; if one removes the single highest point in this plot, it appears that any sign of correlation will largely disappear.

Stayner et al. 1996

In the context of evaluating the "amphibole hypothesis", Stayner *et al.* computed the excess relative risk of lung cancer per fiber/ml/yr from 10 studies categorized by the fiber types to which the cohort was exposed. Each of these studies was also included

in the present evaluation. Both the lowest and highest excess relative risks came from cohorts exposed exclusively to chrysotile. Based on their evaluation, they concluded that the epidemiologic evidence did not support the hypothesis that chrysotile asbestos is less potent than amphibole for inducing lung cancer. However, based on a review of the percentage of deaths in various cohorts from mesothelioma, they concluded that amphiboles were likely to be more potent than chrysotile in the induction of mesothelioma. They also noted that comparison of the potency of different forms of asbestos are severely limited by uncontrolled differences in fiber sizes. None of these conclusions are inconsistent with our general findings.

8.2 RECOMMENDATIONS FOR ASSESSING ASBESTOS-RELATED RISKS

Recommended risk coefficients for lung cancer and mesothelioma (the adjusted K_L values and K_M values) are provided in Tables 6-29 and 6-30, which present best-estimate recommendations and conservative recommendations, respectively. Once it is decided which of these sets of risk coefficients to adopt for general use, the selected set can be incorporated into the procedures described below to evaluate asbestos-related risk. Consistent with the evidence presented elsewhere in this report of a different potency for chrysotile and amphibole (Chapter 6), separate risk coefficients are recommended for chrysotile and the amphiboles.

Importantly, the risk coefficients provided in Tables 6-29 and 6-30 are adjusted to be specifically combined with exposure estimates expressed in terms of the interim exposure index defined by Equation 7-13. Such exposure estimates include *only* asbestos structures longer than 5 μm and thinner than 0.5 μm with those longer than 10 μm weighted more heavily (as described in the equation). Combining the risk coefficients with measurements expressed in terms of any other index of exposure (such as the PCME index in current use) will result in invalid estimates of risk. Note, as indicated in Appendix B, all structures satisfying the dimensional criteria for this index (and exhibiting the requisite mineralogy) should be included in analyses for determining asbestos concentrations; it is not necessary (for example) to distinguish between true asbestiform fibers and cleavage fragments when the interim index is employed.

Three options are described below for evaluating asbestos-related lung cancer and mesothelioma risks using the risk coefficients defined in Tables 6-29 or 6-30 with appropriately derived exposure estimates (expressed in terms of the interim exposure index defined by Equation 7-13). Additional considerations for determining asbestos exposure concentrations are also provided.

Option 1: Using the EPA Dose-Response Models

If there is interest in estimating risk for a particular population that involves time-varying exposures (or a cohort that potentially experiences background mortality rates substantially different from the general population), the EPA models for lung cancer (Equation 6.2) and for mesothelioma (Equation 6.11, for constant exposure, or Equation 6.12 for time-varying exposure) may be directly used to assess risk. This requires knowledge of both the age-specific background lung cancer mortality rate for the population of interest and the age-specific total mortality rate for this population, in addition to the data describing the overall pattern of exposure. The mortality rates can then be used in a lifetable analysis, along with the given exposure pattern and the appropriate values of K_L and K_M (either from Table 6-29 or 6-30) to estimate the additional probability of dying of lung cancer or mesothelioma. Such a lifetable analysis is described in Appendix D.

Option 2: Estimating Risk from a Risk Table

Once it is decided which of the two sets of recommended risk coefficients (Table 6-29 or 6-30) to adopt for general use, a risk table can be constructed (using general U.S. mortality rates) that can then be applied broadly to assess risk. To illustrate this approach, Table 8-1 is a risk table (for lifetime, continuous exposure) that was constructed using the risk coefficients from Table 6-30 (i.e. the "conservative" values).

Note that the values in the table have already been adjusted for lifetime, continuous exposure (so conversions from an occupational exposure scenario are not required).

The only data required to assess risks using this risk table are estimates of long-term average exposure *(derived from appropriate measurements, as described below)* for each particular exposure scenario and population of interest.

Table 8-1 presents estimates of the additional risk of death from lung cancer and mesothelioma attributable to lifetime exposure at an asbestos concentration of 0.0005 f/ml *(for fibrous structures longer than 5 μm and thinner than 0.5 μm)* as determined using TEM methods recommended below. In the table, separate risk estimates are provided for males and females and for smokers and non-smokers. Separate estimates are also presented for exposures containing varying fractions (in percent) of fibrous structures longer than 10 μm.

Separate estimates are presented for smokers and nonsmokers because the lifetime asbestos-induced risk of both lung cancer and mesothelioma differ between smokers and non-smokers. The asbestos-induced risk of lung cancer is higher among smokers because the lung cancer model (Equation 6.2) assumes that the increased mortality rate from lung cancer risk due to asbestos exposure is proportional to background lung cancer mortality, which is higher among smokers. This is consistent with the muitplicative effect between smoking and asbestos exposure reported by several researchers (see, for example, Hammond et al. 1979).

The asbestos-induced risk of mesothelioma is smaller among smokers because the mesothelioma model (Equation 6.11) assumes that risk from constant exposure increases with the cube of age, with the result that the predicted mortality rate is highest among the elderly. Thus, since smokers have a shorter life span than non-smokers, their risk of dying from mesothelioma is also predicted to be smaller.

TABLE 8-XXX:
ADDITIONAL RISK PER ONE HUNDRED THOUSAND PERSONS FROM LIFETIME [illegible]
EXPOSURE TO 0.0005 TEM f/cc LONGER THAN 5.0 µm AND THINNER THAN 0.5 µm

	Percent of Fibers Greater Than 10 µm in Length										
	0	0.05	0.10	0.50	1.00	2.00	5.00	10.00	20.00	50.00	100.00
						CHRYSOTILE					
MALE NON-SMOKERS											
Lung Cancer	0.011	0.013	0.015	0.030	0.05	0.09	0.20	0.39	0.77	1.91	3.81
Mesothelioma	0.004	0.005	0.005	0.011	0.02	0.03	0.07	0.14	0.27	0.67	1.3[illegible]
Combined	0.015	0.018	0.021	0.041	0.07	0.12	0.27	0.53	1.04	2.58	5.14
FEMALE NON-SMOKERS											
Lung Cancer	0.008	0.010	0.011	0.022	0.04	0.06	0.14	0.28	0.55	1.37	2.74
Mesothelioma	0.004	0.005	0.006	0.012	0.02	0.03	0.08	0.15	0.30	0.74	1.4[illegible]
Combined	0.013	0.015	0.017	0.034	0.05	0.10	0.22	0.43	0.85	2.11	4.2[illegible]
MALE SMOKERS											
Lung Cancer	0.097	0.112	0.128	0.256	0.42	0.74	1.70	3.29	6.49	16.08	32.0[illegible]
Mesothelioma	0.003	0.003	0.004	0.007	0.01	0.02	0.05	0.09	0.18	0.45	0.9[illegible]
Combined	0.099	0.116	0.132	0.264	0.43	0.76	1.74	3.39	6.67	16.53	32.9[illegible]
FEMALE SMOKERS											
Lung Cancer	0.067	0.078	0.089	0.178	0.29	0.51	1.18	2.29	4.51	11.18	22.2[illegible]
Mesothelioma	0.004	0.005	0.005	0.011	0.02	0.03	0.07	0.14	0.27	0.66	1.3[illegible]
Combined	0.071	0.083	0.095	0.189	0.31	0.54	1.25	2.42	4.78	11.84	23.61
						AMPHIBOLE					
MALE NON-SMOKERS											
Lung Cancer	0.04	0.05	0.05	0.11	0.17	0.31	0.71	1.37	2.70	6.68	13.2[illegible]
Mesothelioma	2.01	2.34	2.67	5.33	8.65	15.30	35.24	68.45	134.83	333.61	663.6[illegible]
Combined	2.047	2.386	2.725	5.437	8.83	15.61	35.94	69.82	137.53	340.28	676.91
FEMALE NON-SMOKERS											
Lung Cancer	0.03	0.03	0.04	0.08	0.13	0.22	0.52	1.00	1.98	4.89	9.71
Mesothelioma	2.23	2.60	2.97	5.92	9.61	16.99	39.12	75.99	149.68	370.33	736.6[illegible]
Combined	2.257	2.631	3.005	5.995	9.73	17.21	39.64	77.00	151.66	375.22	746.3[illegible]
MALE SMOKERS											
Lung Cancer	0.38	0.45	0.51	1.02	1.66	2.93	6.75	13.12	25.84	63.91	127.0[illegible]
Mesothelioma	1.36	1.58	1.81	3.61	5.86	10.35	23.84	46.32	91.23	225.72	449.00
Combined	1.742	2.031	2.319	4.628	7.51	13.29	30.60	59.44	117.08	289.63	576.0[illegible]
FEMALE SMOKERS											
Lung Cancer	0.27	0.32	0.36	0.72	1.17	2.07	4.76	9.25	18.23	45.10	89.70
Mesothelioma	1.98	2.31	2.64	5.27	8.55	15.12	34.83	67.66	133.27	329.68	655.6[illegible]
Combined	2.255	2.628	3.002	5.989	9.72	17.19	39.59	76.92	151.50	374.78	745.3[illegible]

Table 8-1

Separate estimates are provided for different fractions of fibrous structures longer than 10 µm because the model assumes that structures longer than 10 µm are more potent than structures between 5 and 10 µm in length (in a manner consistent with Equation 7.13). The derivation of this model is described in detail in Chapters 6 and 7. Risks from lifetime exposures to asbestos levels other than 0.0005 may be estimated from the appropriate entry in Table 8-1 by multiplying the value in the selected cell from the Table by the airborne asbestos concentration of interest and dividing by 0.0005 (i.e., by assuming that the additional risk is proportional to the asbestos exposure level). Airborne asbestos concentrations to be used in this manner *must* be estimates of lifetime average exposure and *must* be expressed as structures longer than 5 µm and thinner than 0.5 µm derived as described below. Estimates of the fraction of these structures that are also longer than 10 µm must also be determined to select the appropriate cell of the table from which to derive the risk estimate. Note that the two size fractions that are combined to determine C_{asb} (Equation 7.13) are separately enumerated (not combined) when they are to be used in conjunction with Table 8-1.

The procedure described above for estimating risks using Table 8-1 should provide good approximations as long as the projected risk is no greater than 1,000 per 100,000. Risks greater than 1,000 per 100,000 (i.e. 1 in 100) that are derived from the Table are likely to be over-estimated. However, for risks associated with short-duration exposures or exposures that differ radically over time, it may be better to use a lifetable analysis or a modified version of Table 8-1. This is to avoid substantially under- or over-estimating risk (depending on how the table might otherwise be applied).

Table 8-1 was derived using the approach described in Appendix D by incorporating the age-, sex-, and smoking-specific death rates reported for the general U.S. population and assuming that exposure is constant and continuous at the level indicated in the table. The underlying models are provided in Chapter 6 for cases in which exposure is either not constant or not continuous and for which sufficient data exist to characterize the time-dependence of such exposure. If available, there may also be cases in which it is advantageous to employ mortality data from a control population that better matches the exposed population of interest than the U.S. population as a whole.

Option 3: Estimating Risk from a Unit Risk Factor

A third option for estimating risks based on the approach recommended in this document would be to derive a combined, unit risk factor for asbestos cancer risk similar to the unit risk factor currently recommended by EPA. The new unit risk factor would be derived using the selected set of new risk coefficients (either those in Table 6-29 or Table 6-30) and would be appropriate for use with exposure estimates expressed

in terms of the interim exposure index (rather than the PCME index, as currently recommended). As with the unit risk factor currently in use, some estimate of the fraction of smokers in the general population would also need to be provided as an input. This approach, however, may prove to be somewhat less flexible than the second option above and therefore may be prone to greater errors.

Requirements for Asbestos Measurements

One additional advantage of the approach for evaluating asbestos-related risks recommended in this document (in comparison to the current approach) is that the procedure for assessing risks is tied unambiguously to a specific index for measuring and expressing exposure (i.e. the interim index) and this, in turn, is tied unambiguously to requirements for analyzing asbestos samples.

Estimates of airborne asbestos concentrations that are required to support risk assessment can be derived either by extrapolation from airborne measurements or by modeling release and dispersion of asbestos from sources (soils or other bulk materials). In either case, exposure estimates must be representative of actual (time-dependent or time-integrated) exposure and must provide measurements of the specific size fractions of asbestos that are components of the interim exposure index defined by Equation 7.13. Additional considerations that need to be addressed to assure the validity of risk estimates derived using this protocol include:

- the array of samples collected for estimating airborne asbestos concentrations must be representative of the exposure environment;
- the time variation of airborne asbestos concentrations must be properly addressed;
- airborne samples must to be collected on membrane filters that are suitable for preparation for analysis by transmission electron microscopy (TEM). Appropriate procedures for sample collection are described in Chatfield and Berman (1990) or the ISO Method (ISO 10312)[1];

---

[1] Note that the ISO Method (ISO 10312) is a refinement of the method originally published as the Interim Superfund Method (Chatfield and Berman 1990). It incorporates improved rules for evaluating fiber morphology. Both methods derive from a common development effort headed by Eric Chatfield.

- sample filters must be prepared for analysis using a direct transfer procedure (e.g. ISO 10312). Should indirect preparation be required (due, for example, to problems with overloading of sample filters), a sufficient number of paired samples will need to be collected and analyzed to establish a site-specific correlation between directly and indirectly prepared samples;

- samples must be analyzed by TEM;

- samples must be analyzed using the counting and characterization rules defined in ISO 10312 with one modification: only structures longer than 5 μm and thinner than 0.5 μm need to be enumerated. Separate scans for counts of total structures longer than 5 μm and longer than 10 μm are recommended to increase the precision with which the longest structures are enumerated. Importantly, ISO Method rules require separate enumeration and characterization of component fibers and bundles that are observed within more complex clusters and matrices. Such components, if they meet the dimensional criteria defined in Equation 7.13 must be included in the structure count;

- if risks are to be estimated using the risk models (as described in the first option), asbestos concentrations derived from the above-described measurements must be expressed as the weighted sum of structures between 5 and 10 μm in length and structures longer than 10 μm in length, per the exposure index defined in Equation 7.13. Only structures thinner than 0.5 μm are to be included in these counts. Both fibers and bundles that are isolated structures and fibers and bundles that are components of more complex structures are to be included in structure counts (as long as each structure counted satisfies the defined size criteria for the size category in which it is included);

- if risks are to be estimated using the risk models (the first option), the risk coefficient(s) selected either from Table 6-29 or 6-30 must be appropriate for the fiber type (i.e. chrysotile or amphibole) and the disease end point (i.e. lung cancer or mesothelioma) relevant to the situation of interest; and

- if risks are to be estimated using Table 8-1 (The second option), rather than deriving the weighted sum described in Equation 7.13, the concentration of asbestos structures longer than 10 μm and thinner than 0.5 μm must be derived to determine the appropriate column of the Table

from which to estimate risk and the concentration of total asbestos structures longer than 5 µm and thinner than 0.5 µm must be derived, divided by 0.0005, and multiplied by the risk estimate listed in the appropriate cell of the Table to generate the risk estimate of interest.

Considerations that need to be addressed to assure the validity of risk estimates derived from soil or bulk measurements combined with release and transport modeling include:

- the array of samples collected for estimating source concentrations must be representative of the surface area or volume of source material from which asbestos is expected to be released and contribute to exposure;

- samples must to be prepared and analyzed using the Modified Elutriator Method for soils and bulk materials (Berman and Kolk 1997, 2000), which is the only method capable of providing bulk measurements that can be related to risk;

- membrane filters samples prepared using the tumbler and vertical elutriator per the Superfund method must themselves be prepared for TEM analysis using a direct transfer procedure;

- TEM analysis must be conducted using the counting and characterization rules defined in the ISO Method (ISO 10312) in precisely the same manner that is described above for air measurements. Also, the same size categories need to be evaluated in the same manner described above, whether results are to be used to support assessment using risk models or using the risk table; and

- release and dispersion models that are selected for assessing risks must be appropriate to the exposure scenario and environmental conditions of interest. Such models must also be adapted properly so that they accept input estimates expressed in terms of fiber number concentrations. Procedures suggested for adapting such models are illustrated in a recent publication (Berman 2000).

Note, if we design analytical procedures to focus on long structures, we can evaluate risks cost-effectively. Moreover, even to the extent that shorter structures or other structures might contribute to risk should generally be addressed by default. The alternate approach of spending most time and money counting lots of (potentially non-

potent or marginally potent) short structures while not characterizing longer structures with adequate sensitivity or precision (which is embodied in the current EPA approach) leaves the much greater and more probable danger of falsely missing potentially serious hazards because a small population of extremely potent, long fibers were missed in a particular environment.

8.3 RECOMMENDATIONS FOR FURTHER STUDY

A small number of limited and focused studies (described previously) are previously recommended in this document because they are likely to provide very cost-effective improvements to the quality of this document and may support substantial improvement to the recommended procedures for assessing asbestos-related risks. The recommended studies are:

(1) a focused study to expand our evaluation of the ability of the current EPA models to adequately track the time-dependence of disease (Sections 6.2.2 and 6.3.2); and

(2) a focused study to develop the supporting data needed to define adjustments for potency factors that will allow them to be used with an exposure index that even more closely captures asbestos characteristics that determine biological activity than the currently proposed "interim index" (Section 7.5).

Note that, by properly designing the second of the above-listed studies, it may also be possible to further address another outstanding issue that was previously identified: the question of whether dose-response coefficients derived from mining studies are under-estimated relative to studies involving asbestos products because exposures in the mining studies may contain large numbers of non-asbestos particles contributed by the disturbance of host rock (Section 6.2.3).

For the first of the above-recommended studies, we would need to acquire the raw data from at least one additional cohort exposed primarily to chrysotile and one additoinal cohort exposed primarily to amphiboles to determine whether our observation that the current EPA model for lung cancer adequately describes the time dependence of relative risk associated with exposure to amphiboles but not to chrysotile. Should this finding be confirmed, the potential magnitude and importance of the deviation would also be evaluated along with a candidate adjustment to the model that would likely solve the problem. Simultaneous, additional analysis of the mesothelioma model may also be useful.

Candidate cohorts that may be useful for this evaluation, if they can be acquired, include: (for amphibole exposures) the lung cancer data and *newest* mesothelioma data from Libby (best) or, potentially the lung cancer and mesothelioma data from the Paterson, New Jersey insulation manufacturing plant studied by Seidman and (for chrysotile exposures) the lung cancer data from Quebec (best) or, potentially, the lung cancer and mesothelioma data from the New Orleans asbestos-cement pipe plant studied by Hughes et al. The possibility of obtaining some or all of these data sets needs to be further explored.

For the second of the above-listed studies, we would need to obtain suitable bulk samples of raw ore from the Wittenoom, Libby, and Quebec mines and bulk samples of textile grade (and several other grade) products from the Quebec mines. We have already approached individuals who can provide access to these materials and they have all expressed interest in collaborating.

Ideally, a well-designed field sampling plan would be used to collect and composite raw ore samples and multiple samples (from widely dispersed time-periods of production) would be collected and composited for the fiber product samples. The resulting, limited number of well-constructed composite samples would then be prepared using the Modified Elutriator Method (Berman and Kolk 2000) and subjected to a rigorous analysis by TEM (covering counting and characterization of a very broad range of fibrous structures and non-fibrous particles). The data from these analyses would then be used both to evaluate questions concerning the quality of exposure at mining sites and to adjust the dose-response coefficients derived from studies of these mining sites (and several other studies of facilities that used the products from Quebec). The coefficients would be adjusted to a better optimized exposure index (in which fibers at least as long as 20 μm would be separately weighted) and the degree to which use of this new index improves agreement across certain selected studies would be evaluated.

9.0 REFERENCES

Aalto, M; and Heppleston, AG; "Fibrogenesis by Mineral Fibres: An In-Vitro Study of the Roles of the Macrophage and Fibre Length." Br J Exp Path. Vol. 65, pp. 91-99. 1984.newnew

Adamson, IYR; "Early Mesothelial Cell Proliferation After Asbestos Exposure: In Vivo and In Vitro Studies." Environmental Health Perspectives. Vol. 105, Supplement 5, pp. 1205-1208. September, 1997.newnew

Afaq, F; Abidi, P; Matin, R; and Rahman, Q; "Activation of Alveolar Macrophages and Peripheral Red Blood Cells in Rats exposed to Fibers/Particles." *Toxicology Letters*, Vol. 99, pp. 175-182, 1998.newnew

Albin, M; Magnani, C; Krstev, S; Rapiti, E; Shefer, I; "Asbestos and Cancer: An Overview of Current Trends in Europe." Environ Health Perspectives. Vol. 107, No. 2, pp. 289-298. May, 1999.newnew

Albin, M; Pooley, FD; Stromberg, U; Attewell, R; Mitha, R; Johansson, L; and Welinder, H; "Retention Patterns of Asbestos Fibres in Lung Tissue Among Asbestos Cement Workers." Occup and Environ Med. Vol. 51, pp. 205-211. 1994.newnew

Albin, M; Jakobsson, K; Attewell, R; Johansson, L; Welinder, H; "Mortality and Cancer Morbidity in Cohorts of Asbestos Cement Workers and Referents." Br J Ind Med. Vol. 79, No. 9, pp. 602-610. September, 1990.newnew

Amandus, H.E., Wheeler, R., "The Morbidity and Mortality of Vermiculite Miners and Millers Exposed to Tremolite-Actinolite: Part II. Mortality." American Journal of Industrial Medicine 11:15-26, 1987.

Amandus, H.E., Wheeler, R., Jankovic, J., Tucker, J., "The Morbidity and Mortality of Vermiculite Miners and Millers Exposed to Tremolite-Actinolite: Part I. Exposure Estimates." American Journal of Industrial Medicine 11:1-14, 1987

Armstrong, B.K., DeKlerk, N.H., Musk, A.W., Hobbs, M.S.T., "Mortality in Miners and Millers of Crocidolite in Western Australia." British Journal of Industrial Medicine, Vol. 45, pp. 5-13, 1988.

Asgharian, B. and Yu, C.P., *Journal of Aerosol Medicine*. Vol. 1, pp. 37-50, 1988.

Barchowsky, A; Lannon, BM; Elmore, LC; Treadwell, MD; "Increased Focal Adhesion Kinase- and Urokinase-type Plasminogen Activator Receptor-Associated Cell Signaling in Endothelial Cells Exposed to Asbestos." Environmental Health Perspectives. Vol. 105, Supplement 5, pp. 1131-1137. September, 1997.newnew

Barchowsky, A; Roussel, RR; Krieser, RJ; Mossman, BT; and Treadwell, MD; "Expression and Activity of Urokinase and its Receptor in Endothelial and Pulmonary Epithelial Cells Exposed to Asbestos." Toxicology and Applied Pharmacology. Vol. 152, No. 2, pp. 388-396. 1998.

Baris, Y.I., Simonato, L., Artvinli, M., Pooley, F., Saracci, R., Skidmore, J., Wagner, C., "Epidemiological and Environmental Evidence of the Health Effects of Exposure to Erionite Fibres: A Four-Year Study in the Cappadocian Region of Turkey." International Journal of Cancer, Vol. 39, pp. 10-17. 1987.

Bauman, MD; Jetten, AM; Bonner, JC; Kumar, RK; Bennett, RA; and Brody, AR; "Secretion of a Platelet-Derived Growth Factor Homologue by Rat Alveolar Macrophages Exposed to Particulates in Vitro." European Journal of Cell Biology. Vol. 51, pp. 327-334. 1990.newnew

Beckett, S.T., "The Generation and Evaluation of UICC Asbestos Clouds in Animal Exposure Chambers." Annals of Occupational Hygiene, Vol. 18, pp. 187-198, 1975.

Bellman, B., Konig, H., Muhle, H., Pott, F., "Chemical Durability of Asbestos and of Man-Made Mineral Fibres In Vivo," Journal of Aerosol Science, Vol. 17, No, 3, pp. 341-345, 1986.

Bellman, B., Muhle, H., Pott, F., Konig, H., Kloppeel, H., Spurny, K., "Persistence of Man-Made Fibers (MMF) and Asbestos in Rat Lungs." Annals of Occupational Hygiene, Vol. 31, pp. 693-709, 1987.

Berman, DW "Asbestos Measurement in Soils and Bulk Materials: Sensitivity, Precision, and Interpretation – You Can Have It All." In *Advances in Environmental Measurement Methods for Asbestos, ASTM STP 1342,* M.E. Beard, H.L. Rook, Eds. American Society for Testing and Materials. 2000.

Berman, D.W. and Chatfield, E.J.; *Interim Superfund Method for the Determination of Asbestos in Ambient Air. Part 2: Technical Background Document,* Office of Solid Waste and Remedial Response, U.S. EPA, Washington, D.C., EPA/540/2-90/005b, May, 1990.

Berman, DW and Crump KS; "Methodology for Conducting Risk Assessments at Asbestos Superfund Sites. Part 2: Technical Background Document." Prepared for: Kent Kitchingman, U.S. Environmental Protection Agency, Region 9. Work Assignment No. 59-06-D800 under Contract No. 68-W9-0059. 1999.

Berman, D.W. and Kolk, A.J.;. *Superfund Method for the Determination of Asbestos in Soils and Bulk Materials,* Office of Solid Waste and Emergency Response, U.S. EPA, Washington, D.C., EPA 540-R-97-028, 1997.

Berman, D.W. and Kolk, A.J.;. *Draft: Modified Elutriator Method for the Determination of Asbestos in Soils and Bulk Materials,* unpublished. Aeolus, Inc. 751 Taft St., Albany, CA 94706. 2000.

Berman, D.W.; Crump, K.S.; Chatfield, E.J.; Davis, J.M.G.; and Jones, A.D.; "The Sizes, Shapes, and Mineralogy of Asbestos Structures that Induce Lung Tumors or Mesothelioma in AF/HAN Rats Following Inhalation." Risk Analysis, Vol. 15, No. 2, 1995.

Bernstein, DM; Morscheidt, C; Grimm, H-G; Thevenaz, P; Teichert, U; "Evaluation of Soluble Fibers Using the Inhalation Biopersistence, a Nine-Fiber Comparison" Inhalation Toxicology Vol.8, pp.345-385, 1996.newnew

Berry, G., Newhouse, M.L., "Mortality of Workers Manufacturing Friction Materials Using Asbestos." British Journal of Industrial Medicine, Vol. 40, pp. 1-7, 1983.

Bertrand, R., Pezerat, H., "Fibrous Glass: Carcinogenicity and Dimensional Characteristics." *Biological Effects of Mineral Fibres*, Wagner, J.C., ed., IARC Scientific Publications, pp. 901-911, 1980.

Bignon, J., Monchaux, G., Sebastien, P., Hirsch, A., Lafuma, J., "Human and Experimental Data on translocation of Asbestos Fibers Through the Respiratory System." Annals of New York Academy of Sciences, Vol. 330, pp. 745-750, 1979.

Blake, T; Castranova, V; Schwegler-Berry, D; Baron, P; Deye, GL; Li, C; and Jones, W; "Effect of Fiber Length on Glass Microfiber Cytotoxity" Journal of Toxicology and Environmental Health Vol.54, pp.243-259, Part A, 1998.newnew

Bolton, R.E., Davis, J., Donaldson, K., Wright, A., "Variation in the Carcinogenicity of Mineral Fibres." Annals of Occupational Hygiene, Vol. 26, No. 1-4, pp. 569-582, 1982.

Bolton, R.E., Davis, J.M.G., Miller, B., Donaldson, K., Wright, A., "The Effect of Dose of Asbestos on Mesothelioma Production in the Laboratory Rat." Proceedings of the VIth International Pneumonoconiosis Conference, Vol. 2, pp. 1028-1035, 1984.

Bolton, R.E., Addison, J., Davis, J.M.G., Donaldson, K., Jones, A.D., Miller, B.G., Wright, A., "Effects of the Inhalation of Dusts from Calcium Silicate Insulation Materials in Laboratory Rates." Environmental Research, Vol. 39, pp. 26-43, 1986.

Bonneau, L., Malard, C., Pezerat, H., "Studies on Surface Properties of Asbestos," Environmental Research, Vol. 41, pp. 268-275, 1986.

Boutin, C; Dumortier, P; Rey, F; Viallat, JR; De Vuyst, P; "Black Spots Concentrate Oncogenic Asbestos Fibers in the Parietal Pleura: Thoracoscopic and Mineralogic Study." American Journal of Respiratory and Critical Care Medicine. Vol. 153, pp. 444-449. 1996.newnew

Brass, DM; Hoyle, GW; Poovey, HG; Liu, J-Y; Brody, AR; "Reduced Tumor Necrosis Factor-Alpha and Transforming Growth Factor-Beta-1 Expression in the Lungs of Inbred Mice That Fail to Develop Fibroproliferative Lesions Consequent to Asbestos Exposure." American Journal of Pathology. Vol. 154, No. 3, pp. 853-862. 1999.newnew

Broaddus, VC; Yang, L; Scabo, LM; Ernst, JD; Boylan, AM; "Crocidolite Asbestos Induces Apoptosis of Pleural Mesothelial Cells: Role of Reactive Oxygen Species and Poly(ADP-ribosyl) Polymerase." Environmental Health Perspectives. Vol. 105, Supplement 5, pp. 1147-1152. September, 1997.newnew

Brody, A.R., Hill, L.H., Adkins, B., O'Connor, R.W., "Chrysotile Asbestos Inhalation in Rats: Deposition Pattern and Reaction of Alveolar Epithelium and Pulmonary Macrophages." American Review of Respiratory Diseases, Vol. 123, pp. 670-679, 1981.

Brody, AR; Liu, J-Y; Brass, D; Corti, M; "Analyzing the Genes and Peptide Growth Factors Expressed in Lung Cells In Vivo Consequent to Asbestos Exposure." Environmental Health Perpsectives. Vol. 105, Supplement 5, pp. 1165-1171. September, 1997.newnew

Brown, DM; Fisher, C; and Donaldson, K; "Free Radical Activity of Synthetic Vitreous Fibers: Iron Chelation Inhibits hydroxyl Radical Generation by Refractory Ceramic Fiber." Journal of Toxicology and Environmental Health Part A. Vol. 53, No. 7, pp. 545-561. 1998.newnew

Campbell, W.J., Huggins, C.W., Wylie, A.G., "Chemical and Physical Characterization of Amosite, Chrysotile, Crocidolite, and Nonfibrous Tremolite for Oral Ingestion Studies by the National Institute of Environmental Health Sciences." Report of Investigations 8452, National Library of Natural Resources, U.S. Department of the Interior. 1980.[3]

Case BW and Dufresne A; "Asbestos, Asbestosis, and Lung Cancer: Observations in Quebec Chrysotile Workers." Environmental Health Perspectives. Vol. 105, Supplement 5, pp. 1113-1120. September, 1997.newnew

Castranova, V, Vallyathan, V; Ramsey, DM; McLaurin, JL; Pack, D; Leonard, S; Barger, MW; Ma, JUC; Dalal, NS; and Teass, A; "Augmentation of Pulmonary Reactions to Quartz Inhalation by Trace Amounts of Iron-containing Particles." Environmental Health Perspectives. Vol. 105, Supplement 5, pp. 1319-1324. September, 1997.newnew

Chang, L-Y; Overby, LH; Broday, AR; and Crapo, JD; "Progressive Lung Cell Reactions and Extracellular Matrix Production After a Brief Exposure to Asbestos." Am J Path. Vol. 131, No. 1, Pp. 156-170. 1989. **OLD**

NEED CHAO ET AL. 1996

CHAP (Chronic Hazard Advisory Panel on Asbestos), "Report to the U.S. Consumer Product Safety Commission." July 1983.

Chatfield, E.J. and Berman, D.W.; *Interim Superfund Method for the Determination of Asbestos in Ambient Air. Part 1: Method,* Office of Solid Waste and Remedial Response, U.S. EPA, Washington, D.C., EPA/540/2-90/005a, May, 1990.

Chen, Y.K., Ph.D. Dissertation, Mechanical and Aerospace Engineering, State University of New York at Buffalo, 1992.

Chen, Y.K. and Yu, C.P., "Deposition of Charged Fiber in the Human Lung." Journal of Aerosol Science Vol 24, Suppl. 1, pp. 5459-5460, 1993.

Cherrie, J.W., Dodgson, J., Groat, S., and Carson, M., "Comparison of Optical and Electron Microscopy for Evaluating Airborne Asbestos." Institute of Occupational Medicine, Edinburgh, (U.S. Department of Commerce), 1979.

Chesson, J., Rench, J.D., Schultz, B.D. and K.L. Milne, "Interpretation of Airborne Asbestos Measurements." Submitted for publication, 1989.

Cherrie, J.W., Dodgson, J., Groat, S., Carson, M., "Comparison of Optical and Electron Microscopy for Evaluating Airborne Asbestos." Inst. Occupational Medicine, Edinburgh, U.S. Dept. of Commerce, 1987.

Choe, N; Zhang, J; Iwagaki, A; Tanaka, S; Hemenway, DR; and Kagan, E; "Asbestos Exposure Upregulates the Adhesion of Pleural Leukocites to Pleural Mesothelial Cells via VCAM-1." Am J Physiology Vol. 277, No. 2, Part 1, pp. L292-L300. 1999 newnew

Choe, N; Tanaka, S, Xia, W; Hemenway, DR; Roggli, VI; and Kagan, E; "Pleural Macrophage Recruitment and Activation in Asbestos-Induced Pleural Injury." Environmental Health Perspectives. Vol. 105, Supplement 5, pp. 1257-1260. September, 1997.newnew

Choe, N; Tanaka, S; Kagan, E; "Asbestos Fibers and Interleukin-1 Upregulate the Formation of Reactive Nitrogen Species in Rat Pleural Mesothelial Cells." American Journal of Resp Cell and Molecular Biology. Vol. 19, No. 2, pp. 226-236. 1998.

Churg, A., Wiggs, B., Depaoli, L. Kampe, B., Stevens, B., "Lung Asbestos Content in Chrysotile Workers with Mesothelioma." American Review of Respiratory Disease, Vol. 130, pp. 1042-1045, 1984.

Coin, PG; Roggli, VL; Brody, AR; "Deposition, Clearance, and Translocation of Chrysotile Asbestos from Peripheral and Central Regions of the Rat Lung." Environ Research. Vol. 58, pp. 970-116. 1992.newnew

Coin, PG; Roggli, VL; and Brody, AR; "Persistence of Long, Thin Chrysotile Asbestos Fibers in the Lungs of Rats" Environmental Health Perspectives Vol.102, Suppl.5, pp.197-199, 1994.newnew

Costa, DL; Dreher, KL; "Bioavailable Transition Metals in Particulate Matter Mediate Cardiopulmonary Injury in Healthy and Compromised Animal Models." Environmental Health Perspectives. Vol. 105, Supplement 5, pp. 1053-1060. September, 1997.newnew

Cox D. and Lindley, D., *Theoretical Statistics*. Chapman and Hall, London, 1974.

Cox and D. Oakes, *Analysis of Survival Data*. Chapman and Hall, London, 1984.

Crump et al. 1985 – ref description of exposures in textiles (grades of fibers) NEED

Davis, JMG; Cowie, HA; "The Relationship Between Fibrosis and Cancer in Experimental Animals Exposed to Asbestos and Other Fibers." Environmental Health Perspectives. Vol. 88, pp. 305-309. 1990.newnew

Davis, J.M.G., Beckett, S.T., Bolton, R.E., Collings, P., Middleton, A.P., "Mass and Number of Fibres in the Pathogenesis of Asbestos-Related Lung Disease in Rats." British Journal of Cancer, Vol. 37, pp. 673-688, 1978.

Davis, J.M.G., Beckett, S.T., Bolton, R.E., Donaldson, K., "A Comparison of the Pathological Effects in Rats of the UICC Reference Samples of Amosite and Chrysotile with Those of Amosite and Chrysotile Collected from the Factory Environment." *Biological Effects of Mineral Fibres*, Wagner, J.C., ed., IARC Scientific Publications, pp. 288-292, 1980.

Davis, J.M.G., Addison, J., Bolton, R.E., Donaldson, K., Jones, A.D., Miller, B.G., "Inhalation Studies on the Effects of Tremolite and Brucite Dust in Rats." Carcinogenesis, Vol. 6, No. 5, pp. 667-674, 1985.

Davis, J.M.G., Addison, J., Bolton, R., Donaldson, K., Jones, A.D., Smith, T., "The Pathogenicity of Long Versus Short Fibre Samples of Amosite Asbestos Administered to Rats by Inhalation and Intraperitoneal Injection." British Journal of Experimental Pathology, Vol. 67, pp. 415-430, 1986a.

Davis, J.M.G., Gylseth, G., Morgan, A., "Assessment of Mineral Fibres from Human Lung Tissue." Thorax, Vol. 41, pp. 167-175, 1986b.

Davis, J.M.G., Bolton, R.E., Brown, D., Tully, H.E., "Experimental Lesions in Rats Corresponding to Advanced Human Asbestosis." Exposure Molecular Pathology, Vol. 44, No. 2, pp, 207-221, 1986c.

Davis, J.M.G., Addison, J., Bolton, R.E., Donaldson, K., Jones, A.D., "Inhalation and Injection Studies in Rats Using Dust Samples from Chrysotile Asbestos Prepared by a Wet Dispersion Process." British Journal of Pathology, Vol. 67, pp. 113-129, 1986d.

Davis, J.M.G., Jones, A.D., Smith, T., "Comparisons of the Pathogenicity of Long and Short Fibres of Chrysotile Asbestos in Rats." Institute for Research and Development of Asbestos, Montreal, ed., Institute of Occupational Medicine, publ., Report No. TM-87/08, 1987.[2]

Davis, J.M.G., Bolton, R.E., Douglas, A.N., Jones, A.D., Smith, T., "Effects of Electrostatic Charge on the Pathogenicity of Chrysotile Asbestos." British Journal of Industrial Medicine, Vol. 45, No. 5, pp. 292-309, 1988a.

Davis, J.M.G., Jones, A.D., "Comparisons of the Pathogenicity of Long and Short Fibres of Chrysotile Asbestos in Rats." British Journal of Exposure Pathology, Vol. 69, No. 5, pp. 171-738, 1988b.

Davis, JMG; Addison, J; McIntosh, C; Miller, BG; Niven, K; "Variations in the Carcinogenicity of Tremolite Dust Samples of Differing Morphology." Annals New York Academy of Sciences." pp. 473-490.1991. newnew

DeKlerk, NH; Musk, AW; Armstrong, BK; and Hobbs, MST; "Diseases in Miners and Millers of Crocidolite from Wittenoom, Western Australia: A further Followup to December 1986." Annals of Occupational Hygiene, Vol. 38, Supplement 1, pp. 647-655. 1994.

Dement, J.M., "Estimation of dose and evaluation of dose-response in a retrospective cohort mortality study of chrysotile asbestos textile workers." Ph.D. Thesis, The University of North Carolina at Chapel Hill, 1980.

Dement, J.M. and Brown, D.P.; "Lung Cancer Mortality Among Asbestos Textile Workers: A Review and Update." *Annals of Occupational Hygiene,* Vol. 38, No. 4, pp. 525-532, 1994.

Dement, J.M., Brown, D.P., "Cohort Mortality and Case-Control Studies of White Male Chrysotile Asbestos Textile Workers", Journal of Clean Technology, Environmental Toxicology, and Occupational Medicine 7:1052-1062, 1998.

Dement, J.M.; Brown, D.P.; and Okun, A.; "Follow-up Study of Chrysotile Asbestos Textile Workers: Cohort Mortality and Case-Control Analysis." *American Journal of Industrial Medicine,* Vol 26, pp. 431-447, 1994.

Dement, J.M., Harris, R.L., "Estimates of Pulmonary and Gastrointestinal Deposition for Occupational Fiber Exposure." NTIS PB80-149644, U.S. HEW Contract #78-2438, 1979.

Dement, J.M., Harris, R.L., Symons, M.J., Shy, C.M., "Estimates of Dose-Response for Respiratory Cancer Among Chrysotile Asbestos Textile Workers." Annals Occupational Hygiene, Vol. 26, No. 1-4, pp. 869-887, 1982.

Dement, J.M., Harris, R.L., Symons, M.J., Shy, C.M., "Exposures and Mortality Among Chrysotile Workers. Part I: Exposure Estimates." American Journal of Industrial Medicine, Vol. 4, pp. 399-419, 1983a.

Dement, J.M., Harris, R.L., Symons, M.J., Shy, C.M., "Exposures and Mortality Among Chrysotile Workers. Part II: Mortality." American Journal of Industrial Medicine, Vol. 4, pp. 421-433, 1983b.

Doll R, and Peto R.; "Cigarette smoking and bronchial carcinoma: dose and time relationships among regular smokers and lifelong non-smokers." J Epidemiol Community Health Vol. 32, pp. 303-313. 1978.

Doll, R., Peto, J., "Asbestos: Effects on Health of Exposure to Asbestos." Health and Safety Commission, London, United Kingdom, 1985.

Dopp, E; Schiffmann, D; "Analysis of Chromosomal Alterations Induced by Asbestos and Ceramic Fibers." Toxicology Letters (Shannon). Vol. 96-97, No Spec. Issue. Pp. 155-162. 1998.newnew

Driscoll, KE; Carter, JM; Hassenbein, DG; Howard, B; "Cytokines and Particle-Induced Inflammatory Cell Recruitment." Environmental Health Perspectives. Vol. 105, Supplement 5, pp. 1159-1164. September, 1997.newnew

NEED EASTES AND HADLEY 1994

Eastes, W; Hadley, JG; "Dissolution of Fibers Inhaled by Rats" Inhalation Toxicology Vol.7, pp.179-196, 1995.newnew

Eastes, W; Hadley, JG; "A Mathematical Model of Fiber Carcinogenicity and Fibrous in Inhalation and Intraperitoneal Experiments in Rats" Inhalation Toxicology Vol.8, pp.323-343, 1996.newnew

Economou, P; Samet, JM; and Lechner, JF; "Familial and Genetic Factors i the Pathogenesis of Lung Cancer" In: Epidemiology of Lung Cancer; Samet, JM ed.; Marcel Dekker, Inc., New York., Chapter 14, 1994.

Enterline, P.E., Harley, J., Henderson, V., "Asbestos and Cancer – A Cohort Followed to Death." Graduate School of Public Health, University of Pittsburgh, 1986.

Everitt, JI; Gelzleichter, TR; Bermudez, E; Mangum, JB; Wong, BA; Janszen, DB; Moss, OR; "Comparison of Pleural Responses of Rats and Hamsters to Subchronic Inhalation of Refractory Ceramic Fibers." Environmental Health Perspectives. Vol. 105, Supplement 5, pp. 1209-1213. September, 1997.newnew

Finkelstein, M.M., "Mortality Among Long-Term Employees of an Ontario Asbestos-Cement Factory." British Journal of Industrial Medicine, Vol. 40, pp. 138-144, 1983.

Finkelstein, M.M., "Mortality Among Employees of an Ontario Asbestos-Cement Factory", American Review of Respiratory Disease 129:754-761, 1984.

Finkelstein, MM; and Dufresne, A; "Inferences on the Kinetics of Asbestos Deposition and Clearance Amoung Chrysotile Miners and Millers." American Journal Ind Med Vol. 35, No. 4, pp. 401-12. April 1999.newnew

Finkelstein, JN; Johnston, C; Barrett, T; Oberdorster, G; "Particulate-Cell Interactions and Pulmonary Cytokine Expression." Environmental Health Perspectives. Vol. 105, Supplement 5, pp. 1179-1182. September, 1997.newnew

Floyd, RA; "Role of Oxygen Free Radicals in Carcinogenesis and Brain Ischemia." The FASEB Journal. Vol. 4, pp. 2587-2597. June,1990.newnew

Fubini, B; "Surface Reactivity in the Pathogenic Response to Particulates." Environmental Health Perspectives. Vol. 105, Supplement 5, pp. 1013-1020. September, 1997.newnew

Gehr, P; Geiser, M; Stone, KC; and Crapo, JD; "Morphometric Analysis of the Gas Exchange Region of the Lung." In Toxicology of the Lung, 2nd edition, Gardner, DE; Crapo, JD; and McClellan, RO eds. Raven Press, New York. 1993. Newnew

Ghio, AJ; Kadiiska, MB; Xiang, Q-H; Mason, RP; "In Vivo Evidence of Free Radical Formation After Asbestos Instillation: An ESR Spin Trapping Investigation." Free Radical Biology and Medicine. Vol. 24, No. 1, pp. 11-17. 1998.newnew

Gibbs, G.W., Hwang, C.Y., "Physical Parameters of Airborne Asbestos Fibres in Various Work Environments - Preliminary Findings." American Industrial Hygiene Association Journal, Vol. 36, No. 6, pp. 459-466, 1975.

Gibbs, G.W. and Hwang, C.Y., "Dimensions of Airborne Asbestos Fibers." In *Biological Effects of Mineral Fibers*, Wagner, ed., IARC Scientific Publication, pp. 69-78, 1980.

Gilbert, O. *Statistical Method for Environmental Pollution Monitoring.* Van Nostrand Reinhold, New York. 1987.

Gold, J; Amandusson, H; Krozer, A; Kasemo, B; Ericsson, T; Zanetti, G; Fubini, B; "Chemical Characterization and Reactivity of Iron Chelator-Treated Amphibole Asbestos." Environmental Health Perspectives. Vol. 105, Supplement 5, pp. 1021-1030.1997 newnew

Goldstein, B., Rendall, R., Webster, I., "A Comparison of the Effects of Exposure of Baboons to Crocidolite and Fibrous-Glass Dusts." Environmental Research, Vol. 32, pp. 334-359, 1983.

Golladay, SA; Park, S-H; and Aust, AE; "Efflux of Reduced Glutathione after Exposure of Human Lung epithelial Cells to Crocidolite Asbestos." Environmental Health Perspectives. Vol. 105, Supplement 5, pp. 1273-1278.1997 newnew

Governa, M; Camilucci, L Amati, M; Visona, I; Valentino, M; Botta, GC; Campopiano, A; Fanizza, C; "Wollastonite Fibers In Vitro Generate Reactive Oxygen Species Able to Lyse Erythrocytes and Activate the Complement Alternate Pathway." Toxicological Sciences. Vol. 44, No. 1, pp. 32-38. 1998.newnew

Gross, TJ; Cobb, SM; Peterson, MW; "Asbestos Exposure Increases Paracellular Transport of Fibrin Degradation Products Across Human Airway Epithelium." Am J Physiol. Vol. 266, No. 3, pp. L287-95. Mar, 1994.newnew

Hammond, E.C., Selikoff, I.J., Seidman, H., 1979. "Asbestos Exposure, Cigarette Smoking and Death Rates." Annals New York Academy of Sciences, Vol. 330, pp. 473-490, 1979.

Harris, R.L., Timbrell, V., "The Influence of Fibre Shape in Lung Deposition - Mathematical Estimates." *Inhaled Particles IV*, Walton, W.H., ed., Pergamon Press, 1977.

Hart, GA; Kathman, LM; and Hesterberg, TW; "*In Vitro* Cytotoxicity of Asbestos and Man-Made Vitreous Fibers: Roles of Fiber Lenght, Diameter and Composition." Carcinogenesis. Vol. 15, No. 5, pp. 971-977. May, 1994.newnew

Health Effects Institute - Asbestos Research. *Asbestos in Public and Commercial Buildings: A Literature Review and Synthesis of Current Knowledge.* HEI-AR, 141 Portland St., Suite 7100, Cambridge, MA. 1991.

Hei, TK; Wu, LJ; Piao. CQ; "Malignant Transformation of Immortalized Human Bronchial Epithelial Cells by Asbestos Fibers." Environmental Health Perspectives. Vol. 105, Supplement 5, pp. 1085-1088. September, 1997.newnew

Heidenreich WF, Luebeck EG, and Moolgavkar SH; "Some properties of the hazard function of the two-mutation clonal expansion model." Risk Analysis Vol. 17, pp. 391-399. 1997.

Henderson, V.L., Enterline, P.E., "Asbestos Exposure: Factors Associated with Excess Cancer and Respiratory Disease Mortality." Annals New York Academy of Sciences, Vol. 330, pp. 117-126, 1979.

Hesterberg, TW; Chase, G; Axten, C; Miller, WC; Musselman, RP; Kamstrup, O; Hadley, J; Morscheidt, C; Bernstein, DM; Thevenaz, P; "Biopersistence of Synthetic Vitreous Fibers and Amosite Asbestos in the Rat Lung Following Inhalation" Toxicology and Applied Pharmacology Vol. 151, 262-275. 1998a.

Hesterberg, TW; Hart, GA; Chevalier, J; Miller, WC; Hamilton, RD; Bauer, J; Thevenaz, P; "The Importance of Fiber Biopersistence and Lung Dose in Determining the Chronic Inhalation Effects of X607, RCF1, and Chrysolite Asbestos in Rats." Toxicology and Applied Pharmacology. Vol. 153, No. 1, pp. 68-82. 1998b.newnew

NEED HESTERBERG ET AL. 1996, A REF IN HESTERBERG 1998A, WHICH HAS THE ANALYSIS FOR CROCIDOLITE.

Hesterberg, TW; Axtin, C; McConnell, EE; Oberdorster, G; Everitt, J; Miller, WC; Chevalier, J; Chase, GR; Thevenaz, P; "Chronic Inhalation Sutdy of Fiber Glass and Amosite Asbestos in Hamsters: Twelve-month Preliminary Results." Environmental Health Perspectives. Vol. 105, Supplement 5, pp. 1223-1230. September, 1997.newnew

Hesterberg, TW; Miiller, WC; McConnell, EE; Chevalier, J; Hadley, JG; Bernstein, DM; Thevenaz, P; Anderson, R; "Chronic Inhalation Toxicity of Size-Separated Glass Fibers in Fischer 344 Rats" Fundamental and Applied Toxicology Vol.20; pp.464-476, 1993.newnew

Hesterberg, TW; Miiller, WC; Thevenaz, P; Anderson, R; "Chronic Inhalation Studies of Man-Made Vitreous Fibres: Characterization of Fibres in the Exposure Aerosol and Lungs" Ann.Occup.Hyg. Vol.39, No.5, pp.637-653, 1995.newnew

Hodgson, A.A.; "Fibrous Silicates." *Lecture Series No. 4.* The Royal Institute of Chemistry, London, United Kingdom. 1965.

Hodgson, J and Darnton, A; "The Quantitative Risk of Mesothelioma and Lung Cancer in Relation to Asbestos Exposure." *Ann Occup Hyg* Vol. 44, No. 8, Pp. 565-601. 2000.

Holian, A; Uthman, MO; Goltsova, T; Brown, SD; Hamilton, RF; "Asbestos and Silica-Induced Changes in Human Alveolar Macroophage Phenotype." Environmental Health Perspectives. Vol. 105, Supplement 5, pp. 1139-1142. September, 1997.newnew

Hughes, J.M., Weill, H., "Asbestos Exposure: Quantitative Assessment of Risk." American Review of Respiratory Disease, Vol. 133, pp. 5-13, 1986.

Hughes, J.M., Weill, H., Hammad, Y.Y., "Mortality of Workers Employed at Two Asbestos Cement Plants." British Journal of Industrial Medicine 44:161-174, 1987.

Hume, LA and Rimstidt; "The Biodurability of Chrysotile Asbestos." Am Mineralogist Vol. 77, pp. 1125-1128. 1992. Newnew

Hwang, C.Y., Gibbs, G.W., "The Dimensions of Airborne Asbestos Fibres –I. Crocidolite from Kuruman Area, Cape Province, South Africa." Annals Occupational Hygiene, Vol. 24, No. 1, pp. 23-41, 1981.

Ilgren, E; Chatfield, E; "Coalinga Fibre: A Short, Amphibole-Free Chrysotile ." Part 3: Lack of Biopersistence. Indoor Built Environ. Vol. 7, pp. 98-100. 1998.newnew

International Agency for Research on Cancer (IARC). *Monographs on the Evaluation of Carcinogenic Risks to Man.* Vol 14. IARC, Lyon, France. 1977.

IRIS 1988 **FINISH THIS.**

Ishizaki, T; Yano, E; Evans, PH; "Cellular Mechanisms of Reactive Oxygen Metabolite Generation from Human Polymorphonuclear Leukocytes Induced by Crocidolite Asbestos." Environmental Research. Vol. 75, No. 2, pp. 135-140. 1997.newnew

ISO 10312: *Ambient Air - Determination of Asbestos Fibres - Direct-Transfer Transmission Electron Microscopy Method.* (Developed by Chatfield, E.J. 1993).

Jagirdar, J; Lee, TC; Reibman, J; Gold, LI; Aston, C; Begin, R; Rom, WN; "Immunohistochemical Localization of Tranforming Growth Factor Beta Isoforms in

Asbestos-Related Diseases." Environmental Health Perpsectives. Vol. 105, Supplement 5, pp. 1197-1203. September, 1997.newnew

Jaurand, M-C; "Mechanisms of Fiber-Induced Genotoxicity." Environmental Health Perspectives. Vol. 105, Supplement 5, pp. 1073-1084. September, 1997.newnew

NEED TO ADD JAURAND'S 1991 REVIEW OF MUTAGENICITY ASSAY TESTING OF ASBESTOS (GET REF FROM JAURAND 1997 OR KEANE ET AL. 1999)

Jesch, NK; Dorger, M; Enders, G; Rieder, G; Vogelmeier, C; Messmer, K; and Krombach, F; "Expression of the Inducible Nitroc Oxide Synthase and Formation of Nitric Oxide by Alveolar Macrophages." Environmental Health Perspectives. Vol. 105, Supplement 5, pp. 1297-1300. September, 1997.newnew

Johnson, N.F., "Asbestos-Induced Changes in Rat Lung Parenchyma." Journal of Toxicology and Environmental Health, Vol. 21, pp. 193-203, 1987.

Johnson, NF; Jaramillo, RJ; "P53, Cip 1, and Gadd 153 Expression Following Treatment of A549 Cells with Natural and Man-Made Vitreous Fibers." Environmental Health Perspectives. Vol. 105, Supplement 5, pp. 1143-1145. September, 1997.newnew

Jones, A.D., McMillan, C.H., Johnston, A.M., McIntosh, C., Cowie, H., Bolton, R.E., Borzuki, G., Vincent, J.H., "Pulmonary Clearance of UICC Amosite Fibres Inhaled by Rats During Chronic Exposure at Low Concentrations." British Journal of Industrial Medicine, Vol. 45, pp. 300-304, 1988.

Kaiglova, A; Hurbankova, M; Kovacikova, Z; "Impact of Acute and Subchronic Asbestos Exposure on Some Parameters of Antioxidant Defense System and Lung Tissue Injury." Industrial Health. Vol. 37, No. 3, pp. 348-351. July, 1999.newnew

Kamp, DW; Greenberger, MJ; Sbalchierro, JS; Preusen, SE; Weitzman, SA; "Cigarette Smoke Augments Asbestos-Induced Alveolar Epithelial Cell Injury: Role of Free Radicals." Free Radical Biology & Medicine. Vol. 25, No. 6, pp. 728-739. 1998.newnew

Kamp, DW; Dunne, M; Dykewicz, MS; Sbalchiero, JS; Weitzman, SA; and Dunn, MM; "Asbestos-Induced Injury to Cultured Human Pulmonary Epithelial-like Cells: Role of Neutroophil Elastase." J Leukocyte Biology. Vol. 54, July, 1993.newnew

Kamp, DW; Graceffa, P; Pryor, WA; Weitzman, SA; "The Role of Free Radicals in Asbestos-Induced Diseases." Free Radical Biology & Medicine. Vol. 12, pp. 293-315. 1992.newnew

Kane, AB; Macdonald, JL; "Mechanisms of Mesothelial Cell Injury, Proliferation, and Neoplasia Induced by Asbestos Fibers." Fiber Toxicology. Chapter 14, pp. 323-347. 1993.newnew

Kauffer, E., Vigneron, J.C., Hesbot, A., Lemonnier, M., "A Study of the Length and Diameter of Fibres, in Lung and in Broncho-Alveolar Lavage Fluid, Following Exposure of Rats to Chrysotile Asbestos." Annals of Occupational Hygiene, Vol. 31, No. 2, pp. 233-240, 1987.

Keane, MJ; Miller, WE; Ong, T; Stephens, JW; Wallace, WE; Zhong, B-Z; "A Study of the Effect of Chrysotile Fiber Surface Composition on Genotoxicity In Vitro." Journal of Toxicology and Environmental Health Part A. Vol. 57, No. 8, pp. 529-541. Aug, 1999.newnew

Kimizuka, G., Wang, N., Hayashi, Y., "Physical and Microchemical Alterations of Chrysotile and Amosite Asbestos in the Hamster Lung." Journal of Toxicology and Environmental Health, Vol. 21, pp. 251-264, 1987

Kodama, Y; Boreiko, CJ; Maness, SC; and Hesterberg, TW; "Cytotoxic and Cytogenetic Effects of Asbestos on Human Bronchial Epithelial Cells in Culture." Carcinogenesis Vol. 14, No. 4, pp. 691-697. 1993.

Kostyuk, VA; Potapovich, AI; "Antiradical and Chelating Effects in Flavonoid Protection Against Silica-Induced Cell Injury." Archives of Biochemistry and Biophysics." Vol. 355, No. 1, pp. 43-48. 1998.newnew

Kravchenko, IV; Furalyov, VA; Vasylieva, LA; and Pylev, LN; "Spontaneous and Asbestos-Induced Transformation of Mesothelial Cells in Vitro." Teratogenesis Carcinogenesis and Mutagenesis. Vol. 18, No. 3, pp. 141-151. 1998.newnew

Krombach, F.; Münzing, S.; Allmeling, A.M.; Gerlach, JT; Behr, J; and Dörger, M., "Cell Size of Alveolar Macrophages: An Interspecies Comparison.." Environmental Health Perspectives. Vol. 105, Supplement 5, pp. 1261-1263. September, 1997.

Lacquet, L.M., VanderLinden, L., Lepoutre, J., "Roentgenographic Lung Changes, Asbestosis and Mortality in a Belgian Asbestos-Cement Factory." *Biological Effects of Mineral Fibres*, Wagner, J.C., ed., IARC Sci Publ., pp. 783-793, 1980.

Law, BD; Bunn, WB; and Hesterberg, TW; "Dissolution of Natural Mineral and Man-Made Vitreous Fibers in Karnovsky's and Formalin Fixatives." Inh. Tox. Vol. 3, pp. 309-321, 1991.newnew

Law, BD; Bunn, WB; and Hesterberg, TW; "Solubility of Polymeric Organic Fibers and Manmade Vitreous Fibers in Gambles Solution." Inh. Tox. Vol. 2, pp. 321-339, 1990.newnew

Leanderson, P., Soderkvist, P., Tagesson, C., Axelson, O., "Formation of 8-hydroxydeoxyguanosine by Asbestos and Man-Made Mineral Fibres." British Journal of Industrial Medicine, Vol. 45, pp. 309-311, 1988.(2)

LeBouffant, L., Daniel, H., Heninn, J.P., Martin, J.C., Normand, C., Tichoux, G., Trolard, F., "Experimental Study on Long-Term Effects of Inhaled MMF on the Lungs of Rats." Annals of Occupational Hygiene, Vol. 31, No. 4B, pp. 765-790, 1987.

LeBouffant, L., "Physics and Chemistry of Asbestos Dust." *Biological Effects of Mineral Fibres*, Wagner, J.C., ed., IARC Scientific Publications, pp. 15-34, 1980.

Lee, K.P., Barras, C.E., Griffith, R.S., Waritz, R.S., Lapin, C.A., "Comparative Pulmonary Responses to Inhaled Inorganic Fibers with Asbestos and Fiberglass." Environmental Research, Vol. 24, pp. 167-191, 1981.

Leigh, J; Wang, H; Bonin, A; Peters, M; and Ruan, X; "Silica-induced Apoptosis in Alveolar and Granulomatous Cells in Vivo." Environmental Health Perspectives. Vol. 105, Supplement 5, pp. 1241-1246. September, 1997.newnew

Leikoff, G; and Driscoll, K; "Cellular Approaches in Respiratory Toxicology" In Toxicology of the Lung, 2nd edition, Gardner, DE; Crapo, JD; and McClellan, RO eds. Raven Press, New York. 1993. Newnew

Levin, J.L., McLarty, J.W., Hurst, G.A., Smith, A.N., Frank, A.L, "Tyler Asbestos Workers: Mortality Experience in a Cohort Exposed to Amosite." Occupptional and Environmental Medicine 55:155-160, 1998.

Levresse, V; Reiner, A; Fleury-Feith, J; Levy, F; Moritz, S; Vivo, C; Pilatte, Y; Jaurand, M-C; "Analysis of Cell Cycle Disruptions in Cultures of Rat Pleural Mesothelial Cells Exposed toAsbestos Fibers." Amer J Resp Cell and Molecular Biology. Vol. 17, No. 6, pp. 660-671. 1997.newnew

Li, XY; Gilmour, P.S.; Donaldson, K; and MacNee, W; "In Vivo and in Vitro Proinflammatory Effects of Particulate Air Pollution (PM10)." Environmental Health Perspectives. Vol. 105, Supplement 5, pp. 1279-1284. September, 1997.newnew

Liddell, F.D.K., McDonald, A.D., McDonald, J.C., "The 1891-1920 Birth Cohort of Quebec Chrysotile Miners and Millers: Development From 1904 and Mortality to 1992." Annals of Occupational Hygiene 41:13-36, 1997.

Lim, Y; Kim, S-H; Kim, K-A; Oh, M-W; and Lee, K-H; "Involvement of Protein Kinase C, Phospholipase C, and Protein Tyrosine Kinase Pathways in Oxygen Radical Generation by Asbestos-stimulated Alveolar Macrophage " Environmental Health Perspectives. Vol. 105, Supplement 5, pp. 1325-1328. September, 1997.newnew

Lippmann M; "Asbestos and Other Mineral and Vitreous Fibers." **NEED REST OF CITATION.** 2000

Lippmann, M; "Deposition and Retention of Inhaled Fibres: Effects on Incidence of Lung Cancer and Mesothelioma." Occupational and Environmental Medicine. Vol. 51, pp.793-798. 1994.newnew

Lippmann, M., Schlesinger, R.B., "Interspecies Comparisons of Particle Deposition and Mucociliary Clearance in Tracheobronchial Airways." J. Toxicol. Env. Health, Vol. 3, pp. 441[261]-469[289], 1984 (from old bib)

Luster, MI; Simeonova, PP; "Asbestos Induces Inflammatory Cytokines in the Lung Through Redox Sensitive Transcription Factors." Toxicology Letters (Shannon). Vol. 102-103, pp. 271-275. 1998.newnew

Lynch, J.R., Ayer, H.E., Johnson, D.J., "The Interrelationships of Selected Asbestos Exposure Indices." American Industrial Hygiene Association Journal, Vol. 31, No. 5, pp. 598-604, 1970.

Marconi, A., Menichini, E., Paoletti, L., "A Comparison of Light Microscopy and Transmission Electron Microscopy Results in the Evaluation of the Occupational

Exposure to Airborne Chrysotile Fibres." Annals of Occupational Hygiene, Vol. 28, No. 3, pp. 321-331, 1984.

Marsella, JM; Liu, BL; Vaslet, CA; Kane, AB; "Susceptibility of p53-Deficient Mice to Induction of Mesothelioma by Crocidolite Asbestos Fibers." Environmental Health Perspectives. Vol. 105, Supplement 5, pp. 1069-1072. September, 1997.newnew

Martin, LD; Krunkosky, TM; Dye, JA; Fischer, BM; Jiang, NF; Rochelle, LG; Akley, NJ; Dreher, KL: and Adler, KB; "The Role of Reactive Oxygen and Nitrogen Speices in the Response of Airway Epithelium to Particulates." Environmental Health Perspectives. Vol. 105, Supplement 5, pp. 11301-1308. September, 1997.newnew

Mattson, SM; "Glass Fiber Dissolution in Simulated Lung Fluid and Measures Needed to Improve Consistency and Correspondence in In-Vitro Studies." Presented at the IARC Conf. "Biopersistence of Respirable Synthetic Fibres and Minerals." Lyon, France, September 7-9, 1992. Envron Health Perspect. 1994.

McConnell, E., Wagner, J., Skidmore, J., Moore, J., "A Comparative Study of the Fibrogenic and Carcinogenic Effects of UICC Canadian Chrysotile B Asbestos and Glass Microfibre (JM 100)." Biological Effects of Man-made Fibres, Proceedings of a WHO/IARC Conference, pp. 234-252, 1982.

McConnell, EE; Rutter, HA; Ulland, BM; Moore, JA; "Chronic Effects of Dietary Exposure to Amosite Asbestos and Tremolite in F344 Rats." Environ Health Perspectives. Vol. 53, pp. 27-44. 1983.newnew

NEED TO ADD SECOND MCCONNELL 1983 (FROM ILGREN AND CHATFIELD 1998)

McConnell, E.E.; Mast, R.W.; Hesterberg, T.W.; Chevalier, J.; Kotin, P.; Bernstein, D.M.; Thevenez, P.; Glass, L.R.; and Anderson, R.; "Chronic Inhalation Toxicity of a Kaolin-Based Refractory Ceramic Fiber in Syrian Golden Hamsters." Inhalation Toxicity, Vol. 7, pp. 503-532, 1995.

McDonald, A.D., Fry, J.S., Wooley, A.J., McDonald, J.C., "Dust Exposure and Mortality in an American Chrysotile Textile Plant." British Journal of Industrial Medicine 39:361-367, 1983a.

McDonald, A.D., Fry, J.S., Woolley, A.J., McDonald, J.C., "Dust Exposure and Mortality in an American Factory Using Chrysotile, Amosite, and Crocidolite in Mainly Textile Manufacture." British Journal of Industrial Medicine 40:368-374, 1983b.

McDonald, A.D., Fry, J.S., Woolley, A.J., and McDonald, J.C., "Dust Exposure and Mortality in an American Chrysotile Asbestos Friction Products Plant." British Journal of Industrial Medicine, Vol. 41, pp. 151-157, 1984.

McDonald, JC; "Mineral Fibre Persistence and Carcinogenicity." Ind Health Vol.36, No.4, pp.372-375, October 1998a.newnew ***reviewed/to be filed.***

McDonald, JC; "Invited Editorial: Unfinished Business - The Asbestos Textiles Mystery." Annals of Occupational Hygiene. Vol. 42, No. 1, pp. 3-5. 1998b.newnew

McDonald, J.C., Gibbs, G.W., Liddell, F.D.K., "Chrysotile Fibre Concentration and Lung Cancer Mortality: A Preliminary Report." *Biological Effects of Mineral Fibres*, Wagner, J.C., ed., IARC Scientific Publications, pp. 811-817, 1980a.

McDonald, J.C., Liddell, F.D.K., Gibbs, G.W., Eyssen, G.E., McDonald, A.D., "Dust Exposure and Mortality in Chrysotile Mining, 1910-1975." British Journal of Industrial Medicine, Vol. 37, pp. 11-24, 1980b.

McDonald, J.C.; Liddell, F.D.K., Dufresne, A.; and McDonald, A.D.; "The 1891-1920 Birth Cohort of Quebec Chrysotile Miners and Millers: Mortality 1976-1988." *British Journal of Industrial Medicine,* Vol. 50, pp. 1073-1081, 1993.

McDonald J.C., McDonald, A.D., Armstrong, B., Sebastien, P., "Cohort Study of Mortality of Vermiculite Miners Exposed to Tremolite." British Journal of Industrial Medicine, Vol. 43, pp. 436-444, 1986.

McGavran, PD; Butterick, CJ; and Brody, AR; "Tritiated Thymidine Incorporation and the Development of an Interstitial Lesion in the Bronchiolar-Alveolar Regions of the Lungs of Normal and Complement Deficient Mice After Inhalation of Chrysotile Asbestos." J Environ Pathol Toxicol Oncol (United States) Vol. 9, No. 5-6, pp. 377-391. December, 1989.newnew

McGavran, PD; Moore, LB; and Brody, AR; "Inhalation of Chrysotile Asbestos Induces Rapid Cellular Proliferation in Small Pulmonary Vessels of Mice and Rats." Am J Path Vol. 136, No. 3, pp. 695-705, 1990.newnew.

Mercer RR and Crapo, JD; "Three-dimensional Analysis of Lung Structure and its Application to Pulmonary Dosimetry Models." In Toxicology of the Lung, 2nd edition, Gardner, DE; Crapo, JD; and McClellan, RO eds. Raven Press, New York. 1993. Newnew

Middleton, A.P., Beckett, S.T., Davis, J.M.G., "Further Observations on the Short-Term Retention and Clearance of Asbestos by Rats, Using UICC Reference Samples." Annals of Occupational Hygiene, Vol. 22, pp. 141-152, 1979.

Miller, FJ; Overton, JH; Kimbell, JS; and Russell, ML; "Regional Respiratory Tract Absorption of Inhaled Reactive Gases." In Toxicology of the Lung, 2nd edition, Gardner, DE; Crapo, JD; and McClellan, RO eds. Raven Press, New York. 1993. Newnew

Moolgavkar, SH; Dewanji, A; Venzon, DJ; "A Stochastic Two-Stage Model for Cancer Risk Assessment. 1: The Hazard Function and the Probability of Tumor." Risk Analysis. Vol. 8, No. 3, pp. 383-392. 1988.newnew

Moolgavkar, SH; Luebeck, EG; De Gunst, M; Port, RE; Schwarz, M; "Quantitative Analysis of Enzyme-Altered Foci in Rat Hepatocarginogenisis Experiments-I. Single Agent Regimen" Carcinogenisis Vol.11, No.8, pp.1271-1278, 1990.newnew

Moolgavkar SH, Luebeck EG, Krewski D, and Zielinski JM; "Radon, cigarette smoke, and lung cancer: a re-analysis of the Colorado plateau uranium miners' data." Epidemiology Vol. 4, pp. 204-217. 1993.

Morgan, A., Talbot, R.J., Holmes, A., "Significance of Fibre Length in the Clearance of Asbestos Fibres from the Lung." British Journal of Industrial Medicine, Vol. 35, pp. 146-153, 1978.

Morgan, A., Holmes, A., "Concentrations and Dimensions of Coated and Uncoated Asbestos Fibres in the Human Lung." British Journal of Industrial Medicine, Vol. 37, pp. 25-32, 1980.

Morgan, A., Black, A., Evans, N., Holmes, A., Pritchard, J.N., "Deposition of Sized Glass Fibres in the Respiratory Tract of the Rat." Annals of Occupational Hygiene, Vol. 23, pp. 353-366, 1980.

Morrow, PE; "Issues: Possible Mechanisms to Explain Dust Overloading of the Lungs." Fundamental and Applies Toxicology. Vol. 10, pp. 369-384. 1988.newnew

Mossman, B.T., "Mechanisms of Asbestos Carciongenesis and Toxicity: the Amphibole Hypothesis Revisited." British Journal of Industrial Medicine, Vol. 50, pp. 673-676, 1993.

Mossman, BT and Churg, A; "Mechanisms in the Pathogenesis of Asbestosis and Silicosis." Am J Crit Care Med. Vol. 157, pp. 1666-1680. 1998.newnew

Mossman, B.T., Marsh, J.P., "Role of Active Oxygen Species in Asbestos-induced Cytotoxicity, Cell Proliferation, and Carcinogenesis." Cellular and Molecular Aspects of Fiber Carcinogenesis, Cold Spring Harbor Laboratory Press, 0-87969-361-4/91, pp. 159-168, 1991.[3]

Mossman, B.T.; Bignon, J.; Corn, M.; Seaton, A.; and Gee, J.B.L., "Asbestos: Scientific Developments and Implications for Public Policy." Science, Vol. 247 (Jan 19), pp. 294-301, 1990.

Mossman, BT; Kamp, DW; Sigmund, A; and Weitzman, SA; "Mechanisms of Carcinogenesis and Clinical Features of Asbestos-Associated Cancers." Cancer Investigation. Vol. 14, No. 5, pp. 466-480. 1996.newnew

Mossman, BT; Faux, S; Janssen, Y; Jimenex, LA; Timblin, C; Zanella, C; Goldberg, J; Walsh, E; Barchowsky, A; Driscoll, K; "Cell Signaling Pathways Elicited by Asbestos." Environmental Health Perspectives. Vol. 105, Supplement 5, pp. 1121-1125. September, 1997.newnew

Muhle, H., Bellman, B., Takenata, S., Ziem, Y., "Inhalation and Injection in Rats to Test the Carcinogenicity of MMMF." Annals Occupational Hygiene, Vol. 31, No. 4B, pp. 755-764, 1987.

Nehls, P; Seiler, F; Rehn, B; Greferath, R; and Bruch, J; "Formation and Persistence of 8-Oxoguanine Rat Lung Cells as an Important Determinant for Tumor Formation following Particle Exposure." Environmental Health Perspectives. Vol. 105, Supplement 5, pp. 1231-1240. September, 1997.newnew

Nicholson, W.J., "Part III. Recent Approaches to the Control of Carcinogenic Exposures. Case Study 1: Asbestos - The TLV Approach." Annals New York Academy of Science 271:152-169, 1976.

Nicholson, W.J., Selikoff, I.J., Seidman, H., Lilis, R., Formby, P., "Long-Term Mortality Experience of Chrysotile Miners and Millers in Thetford Mines, Quebec." Annals New York Academy of Sciences, Vol. 330, pp. 11-21, 1979.

Nikula, KJ; Avila, KJ; Griffith, WC; and Mauderly, JL; "Sites of Particle Retention and Lung Tissue Responses to Chronically Inhaled Diesel Exhaust and Coal Dust in Rats and Cynomolgus Monkeys." Environmental Health Perspectives. Vol. 105, Supplement 5, pp. 1231-1240. September, 1997.newnew

Oberdorster, G; "Macrophage-Associated Responses to Chrysotyle" Annals of Occupational Hygiene Vol.38, No.4, pp.601-615, 1994.newnew

Oberdorster, G; Morrow, PE; and Spurny, K; "Size Dependent Lymphatic Short Term Clearance of Amosite Fibres in the Lung." Annals of Occupational Hygiene. Vol. 32, (Suppl 1). pp. 149-156. 1988.newnew

Ollikainen, T; Linnainmaa, K; and Kinnula, VL; "DNA Single Strand Breaks Induced by Asbestos Fibers in Human Pleural Mesothelial Cells In Vitro." Environmental and Molecular Mutagenesis. Vol. 33, No. 2, pp. 153-160. 1999.newnew

Ontario Royal Commission, "Report of the Royal Commission on Matters of Health and Safety Arising form the Use of Asbestos in Ontario." Vol. 3, 1984.

Palekar, LD; Spooner, CM; and Coffin, DL; "Influence of Crystallization Habit of Minerals on *In Vitro* Cytotoxicity." Annals New York Academy of Sciences. pp. 673-687. 1979.

Park, S-H; Aust, AE; "Regulation of Nitric Oxide Synthase Induction by Iron and Glutathione in Asbestos-Treated Human Lung Epithelial Cells." Archives of Biochemistry and Biophysics. Vol. 360, No. 1, pp. 47-52. 1998.newnew

Peto, J., "Lung Cancer Mortality in Relation to Measured Dust Levels in an Asbestos Textile Factory." *Biological Effects of Mineral Fibres*, Wagner, J.C., ed., IARC Scientific Publications, pp. 829-836, 1980a.

Peto, J., "The Incidence of Pleural Mesothelioma in Chrysotile Asbestos Textile Workers." *Biological Effects of Mineral Fibres*, Wagner, J.C., ed., IARC Scientific Publications, pp. 703-711, 1980b.

Peto, J., Doll, R., Howard, S.V., Kinlen, L.J., Lewinsohn, H.C., "A Mortality Study Among Workers in an English Asbestos Factory." British Journal of Industrial Medicine, Vol. 34, pp. 169-173, 1977.

Peto, J., Seidman, H., Selikoff, I.J., "Mesothelioma Mortality in Asbestos Workers: Implications for Models of Carcinogenesis and Risk Assessment." British Journal of Cancer, Vol. 45, pp. 124-135, 1982.

Peto, J., Doll, R., Hermon, C., Binns, W., Clayton, R., Goffe, T., "Relationship of Mortality to Measures of Environmental Asbestos Pollution in an Asbestos Textile Factory." Annals Occupational Hygiene, Vol. 29, No. 3, pp. 305-355, 1985.

Pinkerton, K.E., Brody, A.R., McLauren, D.A., Adkins, B., Jr., O'Connor, R.W., Pratt, P.C., Crapo, J.D., "Characterization of the Three Types of Chrysotile Asbestos After Aerosolization." Environmental Research, Vol. 31, pp. 32-35, 1983.

Pinkerton, K.E., Pratt, P.C., Brody, A.R., Crapo, J.D., "Fiber Localization and Its Relationship to Lung Reaction in Rats After Chronic Inhalation of Chrysotile Asbestos." American Journal of Pathology, Vol. 117, pp. 484-498, 1984.

Pinkerton, K.E., Plopper, C.G., Mercer, R.R., Rogli, V.L., Patra, A.L., Brody, A.R., Crap, J.D., "Airway Branching Patterns Influence Asbestos Fiber Location and the Extent of Tissue Injury in the Pulmonary Parenchyma." Laboratory Investigation, Vol. 55, No. 6, pp. 688-695, 1986.

Piolatto, G., Negri, E., LaVecchia, C., Pira, E., Decarli, A., Peto, J., "An Update of Cancer Mortality Among Chrysotile Asbestos Miners in Balangero, Northern Italy." British Journal of Industrial Medicine 47:810-814, 1990.

Platek, S.F., Groth, D.H., Ulrich, C.E., Stettler, L.E., Finnell, M.S., Stoll, M., "Chronic Inhalation of Short Asbestos Fibers." Fundamental and Applied Toxicology, Vol. 5, pp. 327-340. 1985.

Pooley, F.D., "An Examination of the Fiberous Mineral Content of Asbestos Lung Tissue from the Canadian Chrysotile Mining Industry." Environmental Research, Vol. 12, pp. 281-298, 1976.

Pooley, F.D., "Tissue Burden Studies." *Short and Thin Mineral Fibres: Identification, Exposure, and Health Effects*, Chatfield, E.J., ed., pp. 96-129, 1982.

Pott, F., Huth, F., Friedrichs, K.H., "Tumorigenic Effect of Fibrous Dust in Experimental Animals." Environmental Health Perspectives, Vol. 9, pp. 313-315, 1974.

Pott, F., Huth, F., Friedrichs, K.H., *Results of Animal Carcinogenesis Studies After Application of Fibrous Glass and Their Implications Regarding Human Exposure.*

Occupational Exposure to Fibrous Glass, U.S. HEW Publication No. 76-151, pp. 183-191, 1976.

Pott, F., "Some Aspects on the Dosimetry of the Carcinogenic Potency of Asbestos and Other Fibrous Dusts." Staub-Reinhalt, Vol. 38, No. 12, pp. 486-490, 1978.

Pott, F., "Animal Experiments with Mineral Fibers." *Short and Thin Mineral Fibers: Identification, Exposure, and Health Effects*, Chatfield, E.J., ed., pp. 133-161, 1982.

Pott, F., Ziem, U., Reiffer, R.J., Huth, F., Ernst, H., Mohr, U., "Carcinogencity Studies on Fibres, Metal Compounds, and Some Other Dusts in Rats." Experimental Pathology, Vol. 32, pp. 129-152, 1987.
Raabe, O., "Deposition and Clearance of Inhaled Particles." *Occupational Lung Diseases*, Gee, J.B., et al., eds., Raven Press, pp. 1047, 1984.

Quinlan, TR; Berube, KA; Hacker, MP; Taatjes, DJ; Timblin, CR; Goldberg, J; Kimberley, P; O'Shaughnessy, P; Hemenway, D; Torino, J; Jimenez, LA; Mossman, BT; "Mechanisms of Asbestos-Induced Nitric Oxide Production by Rat Alveolar Macrophages in Inhalation and In Vitro Models." Free Radical Biology & Medicine. Vol. 24, No. 5, pp. 778-788. 1998.newnew

Rahman, Q; Mahmood, N; Khan, SG; Arif, JM; Athar, M; "Mechanism of Asbestos-Mediated DNA Damage: Role of Heme and Heme Proteins." Environmental Health Perspectives. Vol. 105, Supplement 5, pp. 1109-1112. September, 1997.newnew

Roberts, D.R. and Zumwalde, R.D., *Industrial Hygiene Summary Report of Asbestos Exposure Assessment for Brake Mechanics*. NIOSH Reports No. IWS-32-4A, Industrial Hygiene Section, NTIS # PB 87-105433, 1982.

Robledo, R; and Mossman, B; "Cellular and Molecular Mechanisms of Asbestos-Induced Fibrosis" J of Cell Physiology Vol. 180:pp. 158-166. 1999. Newnew

Roggli, V.L., Brody, A.R., "Changes in Numbers and Dimensions of Chrysotile Asbestos Fibers in Lungs of Rats Following Short-Term Exposure." Experimental Lung Research, Vol. 7, pp. 133-147, 1984.

Roggli, V.L., George, M.H., Brody, A.R., "Clearance and Dimensional Changes of Crocidolite Asbestos Fibers Isolated from Lungs of Rats Following Short-Term Exposure." Environmental Research, Vol. 42, pp. 94-105, 1987.

NEED TO ADD ROOD AND SCOTT 1989

Rubino, G.F., Piolatto, G.W., Newhouse, M.L., Scansetti, G., Aresini, G.A., Murray, R., "Mortality of Chrysotile Asbestos Workers at the Balangero Mine, Northern Italy." British Journal of Industrial Medicine, Vol. 36, pp. 187-194, 1979.

St. George, JA; Harkema, JR; Hyde, DM; and Plopper, CG; "Cell Populations and Structure/Function Relationship of Cells in the Airways." In Toxicology of the Lung, 2nd edition, Gardner, DE; Crapo, JD; and McClellan, RO eds. Raven Press, New York. 1993. Newnew

Sanden, A; Jarvholm, B; Larsson, S; and Thiringer, G; "The Risk of Lung Cancer and Mesothelioma After Cessation of Asbestos Exposure: A Prospective Cohort Study of Shipyard Workers." Eur Respir J Vol. 5, pp. 281-285. 1992.newnew

Sebastien, P., Plourde, M., Robb, R., Ross, M., *Ambient Air Asbestos Survey in Quebec Mining Towns - Part 1, Methodological Study*. Environmental Protection Service, Quebec Region, 3/AP/RQ/1E, pp. 1-41, 1984.

Sebastien, P., Plourde, M., Robb, R., Ross, M., Nadon B., and Wypruk, T. *Ambient Air Asbestos Survey in Quebec Mining Towns. Part II: Main Study*. Environmental Protection Service, Environment, Canada. EPS 5/AP/RQ/2E, July 1986.

Sebastien, P; McDonald, JC; McDonald, AD; Case, B; and Harley, R; "Respiratory Cancer in Chrysotile Textile and Mining Industries: Exposure Inferences from Lung Analysis." Br J Ind Med, Vol. 46, pp. 180-187, 1989.

Seidman, H., "Short-Term Asbestos Work Exposure and Long-Term Observation – July 1984 Update." Department of Epidemiology, American Cancer Society, 1984.

Seidman, H., Selikoff, I.J. Hammond, E.C., "Short-Term Asbestos Work Exposure and Long-Term Observation." Annals New York Academy of Sciences, Vol. 330, pp. 61-89, 1979.

Seidman, H., Selikoff, I.J., Gelb, S.K., "Mortality Experience of Amosite Asbestos Factory Workers: Dose-Response Relationships 5 to 40 Years After Onset of Short-Term Work Exposure." American Journal of Industrial Medicine, Vol. 10, Nos. 5/6, pp. 479-514, 1986.

Selikoff, I.J. Hammond, E.C., Seidman, H., "Mortality Experience of Insulation Workers in the United States and Canada 1943-1976." Annals New York Academy of Sciences, Vol. 330, pp. 91-116, 1979.

Selikoff, I.J., Seidman, H., "Asbestos-Associated Deaths among Insulation Workers in the United States and Canada, 1967-1987." Annals of the New York Academy of Sciences 643:1-14, 1991.

Smith, D.M., Oritiz, L.W., Archuleta, R.F., Johnson, N.F., "Long-Term Health Effects in Hamsters and Rats Exposed Chronically to Man-Made Vitreous Fibres." Annals of Occupational Hygiene, Vol. 34, No. 4B, pp. 731-754, 1987.

Snyder, J., Virta, R., Segreti, J., "Evaluation of the Phase Contrast Microscopy Method for the Detection of Fibrous and Other Elongated Mineral Particulates by Comparison with a STEM Technique." American Industrial Hygiene Association Journal, Vol. 48, No. 5, pp. 471-477, 1987.

Stanton, M., Wrench, C. "Mechanisms of Mesothelioma Induction with Asbestos and Fibrous Glass." Journal of the National Cancer Institute, Vol. 48, pp. 797-821, 1972.

Stanton, M., Layard, M., Tegeris, A., Miller, E., May, M., Kent, E., "Carcinogenicity of Fibrous Glass: Pleural Response in the Rat in Relation to Fiber Dimension." Journal of the National Cancer Institute, Vol. 58, No. 3, pp. 587-597, 1977.

Stanton, M., Layard, M., Tegeris, A., Miller, E., May, M., Morgan, E., "Relation of Particle Dimension to Carcinogenicity in Amphibole Asbestos and Other Fibrous Minerals." Journal of the National Cancer Institute, Vol. 67, No. 5, pp. 965-975, 1981.

Stayner, LT; Dankovic, DA; Lemen, RA; "Occupational Exposure to Chrysotile Asbestos and Cancer Risk: A Review of the Amphibole Hypothesis." Am J Public Health. Vol. 86, No. 2, pp. 176-86. Feb. 1996.newnew

Stober, W; McClellen, RO; and Morrow, PE; "Approaches to Modeling Disposition of Inhaled Particles and Fibers i the Lung" In Toxicology of the Lung, 2nd edition, Gardner, DE; Crapo, JD; and McClellan, RO eds. Raven Press, New York. 1993. Newnew

Strom, K.A. and Yu, C.P., "Mathematical Modeling of Silicon-Carbide Whisker Deposition in the Lung - Comparison Between Rats and Humans." Aerosol Science and Technology, Vol. 24, No. 3. (Oct), pp. 193-209, 1994.

Sussman, RG; Cohen, BS; Lippmann, M; "Asbestos Fiber Deposition in a Human Tracheobronchial Cast. I. Experimental." Inhalation Toxicology. Vol. 3, pp. 145-160. 1991a.newnew

Sussman, RG; Cohen, BS; Lippmann, M; "Asbestos Fiber Deposition in a Human Trachebronchial Cast. II. Empirical Model." Inhalation Toxicology. Vol. 3, pp. 161-179. 1991b.newnew

Takeuchi, T; Nakajima, M; and Morimoto, K; "A Human Cell System for Detecting Asbestos Cytogenotoxicity In Vitro." Mutation Research. Vol. 438, No. 1, pp. 63-70. 1999.newnew

Tanaka, S; Choe, N; Hemenway, DR; Zhu, S; Matalon, S; Kagan, E; "Asbestos Inhalation Induces Reactive Nitrogen Species and Nitrotyrosine Formation in the Lungs and Pleura of the Rat." Journal of Clinical Investigation. Vol. 102, No. 2, pp. 445-454. 1998.newnew

Timblin, CR; Guthrie, GD; Janssen, YWM; Walsh, ES; Vacek, P; and Mossman, BT; "Patterns of C-Fos and C-Jun Proto-Oncogene Expression, Apoptosis, and Proliferation in Rat Pleural Mesothelial Cells Exposed to Erionite or Asbestos Fibers." Toxicology and Applied Pharmacology. Vol. 151, No. 1, pp. 88-97. 1998a.newnew

Timblin, CR; Janssen, YMW; Goldberg, JL; and Mossman, BT; "GRP78, HSP72/73, and CJUN Stress Protein Levels in Lung Epithelial Cells Exposed to Asbestos, Cadmium or H2O2." Free Radical Biology & Medicine. Vol. 24, No. 4, pp. 632-642. 1998b.newnew

Timbrell, V., Hyett, A.W., Skidmore, J.W., "A Simple Dispenser for Generating Dust Clouds From Standard Reference Samples of Asbestos." Annals of Occupational Hygiene, Vol. 11, pp. 273-281, 1968.

Timbrell, V., "Deposition and Retention of Fibres in the Human Lung." Annals of Occupational Hygiene, Vol 26, No. 1-4, pp. 347-369, 1982.

U.S. EPA (U.S. Environmental Protection Agency), *Airborne Asbestos Health Assessment Update*. Report 600/8-84-003F, U.S. EPA, 1986.

Venzon, D., Moolgavkar, S. "A method for computing profile-likelihood-based confidence intervals." Appl Stat 37:87-94, 1988.

Vincent, J.H., "On the Practical Significance of Electrostatic Lung Depositon of Isometric and Fibrous Aerosols." Journal Aerosol Science, Vol. 16, No. 6. pp. 511-519, 1985.

Vincent, JH; Johnston, AM; Jones, AD; Bolton, RE; and Addison, J; "Kinetics of Deposition and Clearance of Inhaled Mineral Dusts During Chronic Exposure." Br J Ind Med Vol. 42; pp. 707-715 (1985).

Wagner, J.C., Berry, G., Skidmore, J.W., Timbrell, V., "The Effects of the Inhalation of Asbestos in Rats." British Journal of Cancer, Vol. 29, pp. 252-269, 1974.

Wagner, J.C., Berry, G., Skidmore, J.W., "Studies of the Carcinogenic Effects of Fiber Glass of Different Diameters Following Intrapleural Innoculation in Experimental Animals." NIOSH 76-151, pp.193-197, 1976.

Wagner, J.C., "Opening Discussion -- Environmental and Occupational Exposure to Natural Mineral Fibres." *Biological Effects of Mineral Fibres*, Wagner, J.C., ed., IARC Scientific Publications, pp. 995-998, 1980.

Wagner, J.C., Berry, G., Hill, R., Munday, D., Skidmore, J., "Animal Experiments with MMM(V)F - Effects of Inhalation and Intrapleural Inoculation in Rats." *Biological Effects of Man-made Fibres – Proceedings of a WHO/IARC Conference*, Copenhagen, pp. 209-233, 1982.

Wagner, J.C., Skidmore, J.W., Hill, R.J., Griffith, D.M., "Erionite Exposure and Mesotheliomas in Rats." British Journal of Cancer, Vol, 51, pp. 727-730, 1985.

Wagner, J.C. Griffiths, D.M., Munday, D.E., "Experimental Studies with Palygorskite Dusts." British Journal of Industrial Medicine." Vol. 44, No. 11, pp. 749-763, 1987.

Walton, W.H., "The Nature, Hazards, and Assessment of Occupational Exposure to Airborne Asbestos Dust: A Review." Annals of Occupational Hygiene, Vol 25, pp. 117-247, 1982.

Warheit, DB; Snajdr, SI; Hartsky, MA; Frame, SR; "Lung Proliferative and Clearance Responses to Inhaled para-Aramid RFP in Exposed Hamsters and Rats: Comparisons with Chrysotiles Asbestos Fibers." Environmental Health Perspectives. Vol. 105, Supplement 5, pp. 1219-1222. September, 1997.newnew

Weill, H., Hughes, J., Waggenspack, C., "Influence of Dose and Fibre Type on Respiratory Malignancy Risk in Asbestos Cement Manufacturing." American Review of Respiratory Disease, Vol, 120, pp. 345-354, 1979.

Winer, A.A., Cossette, M., "The Effect of Aspect Ration on Fiber Counts: A Preliminary Study." Annals New York Academy of Sciences, Vol. 330, pp. 661-672, 1979.

Weitzman, SA and Graceffa, P; "Communication: Asbestos Catalyzes Hydroxyl and Superoxide Radical Generation from Hydrogen Peroxide." Archives of Biochemistry and Biophysics. Vol. 228, No. 1, pp. 373-376. 1984.newnew

World Health Organization; "Reference Methods for Measuring Airborne Man-Made Mineral Fibers (MMMF), 1985.newnew

Wright, G.W., Kuschner, M., "The Influence of Varying Lengths of Glass and Asbestos Fibres on Tissue Response in Guinea Pigs." *Inhaled Paricles: Part 2*, Walton, W.H., McGovern, B., Pergamon Press Oxford, pp. 455-474, 1975.

Wylie, A.G., Virta, R.L., Segretti, J.M., "Characterization of Mineral Population by Index Particle: Implications for the Stanton Hypothesis." Environmental Research, Vol, 43, pp. 427-439, 1987.

Wylie, A.G.; Bailey, K.F.; Kelse, J.W.; and Lee, R.J.; "The Importance of Width in Asbestos Fiber Carcinogenicity and its Implications for Public Policy." Am Ind Hyg Assoc J (54) 239-252, 1993.

Wylie, AG; Skinner, HCW; Marsh, J; Snyder, H; Garzione, C; Hodkinson, D; Winters, R; Mossman, BT; "Mineralogical Features Associated with Cytotoxic and Proliferative Effects of Fibrous Talc and Asbestos on Rodent Tracheal Epithelial and Pleural Mesothelial Cells." Toxicol and Applied Pharmacol. Vol. 147, pp. 143-150. 1997.newnew

Yamaguchi, R; Hirano, T; Ootsuyama, Y; Asami, S; Tsurudome, Y; Fukada, S; Yamato, H; Tsuda, T; Tanaka, I; and Kasai, H; "Increased 8-Hydroxyguanine in DNA and Its Repair Activity in Hamster and Rat Lung After Intratracheal Instillation of Crocidolite Asbestos." Japanese J of Cancer Research Vol. 90, No. 5, pp. 505-509, 1999. Newnew

Yeh, H-C and Harkema, JR; "Gross Morphometry of Airways." In Toxicology of the Lung, 2nd edition, Gardner, DE; Crapo, JD; and McClellan, RO eds. Raven Press, New York. 1993. Newnew

Yu, CP; Yoon, KJ; Investigator's Report: Retention Modeling of Diesel Exhaust Particles in Rats and Humans. 1991. **CHECK THIS**

Yu, C.P.; Asgharian, B; and Abraham, J.L.; "Mathematical Modeling of Alveolar Clearance of Chrysotile Asbestos Fibers from the Rat Lungs." Journal of Aerosol Science, Vol. 21, pp. 587-594, 1990a.

Yu, C.P. and Asgharian, B; "A Kinetic Model of Alveolar Clearance of Amosite Asbestos Fibers from the Rat Lung at High Lung Burdens." Journal of Aerosol Science, Vol. 21, pp. 21-27, 1990b.

Yu, C.P.; Asgharian, B; and Pinkerton, K.E.; "Intrapulmonary Deposition and Retention Modeling of Chrysotile Asbestos Fibers in Rats." Journal of Aerosol Science, Vol. 22, No. 6, pp. 757-761, 1991.

Yu, C.P.; Zhang, L.; Oberdoster, G.; Mast, R.W.; Glass, L.R..; and Utell, M.J., "Deposition Modeling of Refractory Ceramic Fibers in the Rat Lung" Journal of Aerosol Science, Vol. 25, No. 2 (Mar), pp. 407-417, 1994.

Yu, C.P.; Zhang, L.; Oberdoster, G.; Mast, R.W.; Maxim, D.; and Utell, M.J., "Deposition of Refractory Ceramic Fibers (RCF) in the Human Respiratory Tract and Comparison with Rodent Studies." Aerosol Science and Technology, Vol. 23, No. 3 (Oct), pp. 291-300, 1995a.

Yu, C.P.; Zhang, L.; Oberdoster, G.; Mast, R.W.; Glass, L.R.; and Utell, M.J., "Clearance of Refractory Ceramic Fibers (RCF) from the Rat Lung - Development of a Model." Environmental Research, Vol. 65, No. 2 (May), pp. 243-253, 1995b.

Zalma, R; Bonneau, L; Guignard, J; Pezerat, H; Jaurand, M-C; "Formation of Oxy Radicals by Oxygen Reduction Arising from the Surface Activity of Asbestos." Can J Chem. Vol. 65, pp. 2338-2341. 1987.newnew

Zanella, CL: Timblin, CR; Cummins, A; Jung, M; Goldberg, J; Raabe, R; Tritton, TR; and Mossman, BT; "Asbestos-induced Phosphorylation of Epidermal Growth Factor Receptor is Linked to c-fos and apoptosis." Am J of Physiology Vol. 277, No. 4, Part !, Pp. L684-L693. 1999 newnew.

Zhang, Y; Lee, TC; Guillemin, B; Yu, M-C; and Rom, WN; "Enhanced IL-1Beta and Tumor Necrosis Factor-Alpha Release and Messenger RNA Expression in Macrophages from Idiopathic Pulmonary Fibrosis or After Asbestos Exposure." J Immunol (United States). Vol. 150, No. 9, pp. 4188-4196. 1 May, 1993.newnew

Zhu, S; Manuel, M; Tanaka, S; Choe, N; Kagan, E; Matalon, S; "Contribution of Reactive Oxygen and Nitrogen Species to Particulate-Induced Lung Injury." Environmental Health Perspectives. Vol. 106, No. 5, pp. 1157-1163. 1998.newnew

Zoitus, BK; De Meringl, A; Rouyer, E; Thelohan, S; Bauer, J; Law, B; Boymel, PM; Olson, JR; Christensen, VR; Guldberg, M; Koenig, AR; and Perander, M; "In Vitro Measurement of Fiber Dissolution Rate Relevant to Biopersistence at Neutral pH: An Interlaboratory Round Robin." Inh Tox. Vol. 9, pp. 525-540. 1997.newnew